

Immobilised Homogeneous Catalysts for Sequential Fine Chemical Synthesis

Functionalised Organometallics for Nanotechnology

Geïmmobiliseerde Homogene Katalysatoren voor Stapsgewijze Chemische Synthese

Gefunctionaliseerde Organometaalverbindingen voor Nanotechnologische Toepassingen

(met een samenvatting in het Nederlands)

PROEFSCHRIFT

ter verkrijging van de graad van doctor aan de Universiteit Utrecht
op gezag van de rector magnificus, prof.dr. J. C. Stoof,
ingevolge het besluit van het college voor promoties
in het openbaar te verdedigen
op maandag 4 februari 2008, des middags te 2.30 uur

door

Aidan Richard McDonald

geboren op 30 mei 1980 te Dublin, Ierland

Promotor: Prof. dr. G. van Koten

Co-promotor: Dr. G. P. M. van Klink

McDonald, Aidan Richard

Title: Immobilised Homogeneous Catalysts for Sequential Fine Chemical Synthesis;
Functionalised Organometallics for Nanotechnology

Utrecht, Utrecht University, Faculty of Science

Thesis Utrecht University - with ref. - with summary in Dutch

ISBN: 978-90-393-4745-4

The work described in this thesis was carried out at the Organic Chemistry and Catalysis Group,
Faculty of Science, Utrecht University, The Netherlands

The work described in chapters 1 to 6 in this PhD thesis was financially supported by a Dutch
Technology Foundation grant (STW-05772).

CONTENTS

<i>Chapter 1</i>	Immobilised Homogeneous Catalysts for Asymmetric Hydrogenation and C-C Bond Forming Catalysis; Introduction to One-pot Sequential Catalysis	1
	Aim and Scope of this Thesis	44
<i>Chapter 2</i>	‘Click’ Immobilisation of Organometallic Catalysts for C-C Coupling Reactions	51
<i>Chapter 3</i>	‘Click’ Immobilisation of Metallo-Porphyrin Complexes and their Application in Epoxidation Catalysis	73
<i>Chapter 4</i>	BINAP-Ru and Rh Catalysts Covalently Immobilised on Silica and their Repeated Application in Asymmetric Hydrogenation	89
<i>Chapter 5</i>	Sequential Compartmentalised Tandem Catalysis; Iridium(III) Organometallics Bound to Silica for Alkane Activation	103
<i>Chapter 6</i>	Covalent Immobilisation of a Palladium Picolinate Complex for Hydroxycarbonylation: Silica Supported Synthesis and Catalysis	127
<i>Chapter 7</i>	Probing the <i>mer-</i> to <i>fac-</i> Isomerisation of Tris-Cyclometallated Homo- and Heteroleptic (C,N) ₃ Iridium(III) Complexes	143
<i>Graphical Abstract</i>		171
<i>Summary</i>		173
<i>Samenvatting</i>		181
<i>Acknowledgements</i>		189
<i>Curriculum Vitae</i>		193
<i>List of Publications</i>		195

CHAPTER 1

Introduction:

Immobilised Homogeneous Catalysts for Asymmetric Hydrogenation and C-C Coupling, an Overview

Metal Catalysed Sequential Reaction Systems, an Overview

An introduction to the field of homogeneous catalyst immobilisation is given by way of reporting a general overview of immobilised catalysts applied in two types of reactions, asymmetric hydrogenation and C-C bond forming reactions. The overview details the various methods for supporting homogeneous catalysts, and the effects, both positive and negative, that immobilisation causes. The second part of the report details the latest advances in the field of metal-catalysed sequential catalysis, and in particular tandem catalysis. The review details the various applications, in a wide range of reaction sequences, of homogeneous, heterogeneous and biocatalysts. It also opens the discussion as to why so few of these processes have been made truly green by not applying immobilised catalysts in them.

Based on a comprehensive review of immobilised catalysts for asymmetric hydrogenation: A. R. McDonald, R. Gossage, G. P. M. van Klink, G. van Koten; and a book chapter Immobilised Pincer Complexes Applied in Catalysis, A. R. McDonald, H. P. Dijkstra. Pincer Organometallics, editors G. van Koten, P. A. Chase

1.1 Introduction

A number of questions are being asked of the chemical industry due to the rise to prominence over recent years of a need for “green chemistry”. The process of manufacturing of fine chemicals has consistently been a co-producer of environmentally damaging waste. The reasons for this are many and varied.¹

Homogeneous catalysts are widely accepted to be more selective and easier to analyse and predict than heterogeneous catalysts. In homogeneous catalysis the active site is known, and much that is occurring in catalysis is discernable and modifiable. However, the bonuses of using heterogeneous catalytic systems (*e.g.* ease of separation and lower costs) far outweigh the positives that lie in the use of homogeneous catalytic systems. The major impedance in using homogeneous catalytic systems lies in our inability to separate like from like.

The continuous development of homogeneous catalysts as resources for the production of fine chemicals² (*e.g.* pharmaceuticals, agrochemicals, flavours and fragrances) has opened ways to develop new and better catalysts for clean synthesis. The complexes are generally the most expensive part of the catalytic process, when used in realistic quantities,³ and hence the loss of ligands/precious metals in homogeneous systems leads to high costs and hence often impedes industrial application.⁴

The sustained development of homogeneous catalysts for fine chemical production has led to the opinion that a method for heterogenising these homogeneous catalysts must be developed and brought to the industrial arena.⁵ Several methods for heterogenisation of catalysts have been explored which are mainly based on inorganic support systems,⁶ dendrimers,⁷ or functionalised organic polymers.⁸ In addition significant effort has been expended to develop catalysts for liquid multiphasic reaction systems.⁹

The various methods for the immobilisation of ligands and complexes on inorganic, polymeric, dendritic supports and in biphasic systems include the use of covalent or ionic bonding, applications of hydrophobic, hydrophilic and electrostatic interactions in addition to varying the solubility properties in a liquid biphasic system.¹⁰ The majority of these methods for immobilisation involve the functionalisation of ligands for the linking of a linker or solvator onto the support. It is observed that functionalisation or alteration of these species can modify their catalytic ability, *i.e.*, heterogenisation of a homogeneous catalyst can affect its activity and/or selectivity. Often a decrease in activity and selectivity is observed as a result of the lower number of available catalytic sites upon immobilisation. Recovery of these various forms of immobilised catalysts is carried out by a wide range of techniques. Simple filtration is the main technique used to isolate catalysts bound to inorganic supports and insoluble polymeric species. Considerable effort has been carried out on the development of polymeric membranes for the encapsulation and filtration of homogeneous catalysts.¹¹ Nanofiltration membrane techniques are commonly used in the case of dendritic systems.¹² When using biphasic systems, simple decantation techniques are often the best way of recovering the catalyst.

The ultimate challenge to modern catalysis is to develop efficient systems, where minimal intermediate product work-up or isolation is necessary, and to present catalysis as a sustainable alternative to the standard stoichiometric preparation of fine chemicals.¹³ Furthermore, catalysts which demonstrate high stability, and can thus survive multiple uses in reactions which are both high yielding and highly selective, are essential to future applications. Present trends for the development of a valuable organic end-product generally follow a route as depicted in figure 1. The diagram demonstrates that, for what would be considered a short three-step reaction sequence, at least three work-up steps are involved, all of which may require column chromatography, and recrystallisation steps. This results in large amounts of chemical (and solvent) waste, and likely the synthesis of undesired side products, which are discarded, thus producing more waste.

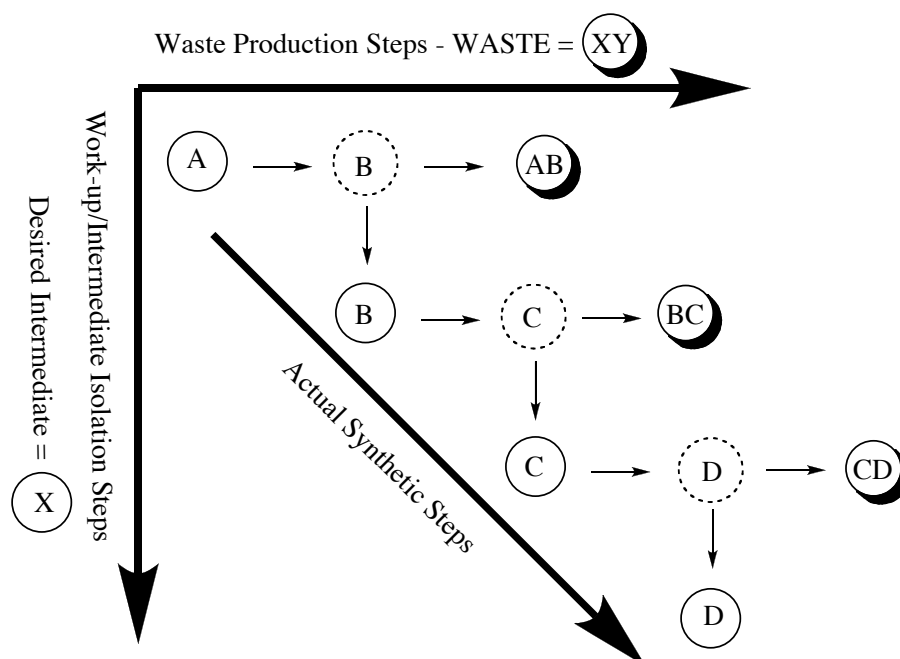


Figure 1. Present chemistry towards a fine chemical product.¹³

Multi-step, work-up free reaction sequences are commonplace in the natural world. Enzymes can be applied in sequences in single pots or separate pots (the cell) for the sequential synthesis of natural products, producing little side product 'waste', and requiring no intermediate product isolation. Any 'waste' that is produced is usually a secondary product, which is converted in a parallel reaction, with the ultimate result that any true side products inevitably amount to being only CO₂, ammonia and water. Nature's ability to compartmentalise its catalysts allows for this possibility, and allows for reaction sequences as depicted in figure 2. Ultimately the goal of the modern homogeneous catalysis exponent is to apply non-natural catalysts in a similar manner, thus reducing work-up or isolation steps, and reducing waste.

Heterogenised homogeneous catalysts could allow for such reaction sequences, where multiple steps are carried out in the presence of compartmentalised catalysts and/or substrates. This would involve the simple transfer of substrate solution between catalytic compartments, as opposed to multiple work-up steps. An essential point to this concept is catalyst stability, particularly because homogeneous catalysts are relatively unstable compared to their enzymatic and

heterogeneous counterparts. Nature has the ability to carry out self-repair and regeneration, which is not the case with the coordination complexes often applied in homogeneous catalysis. To date very, very few examples of heterogenised homogeneous catalysts maintain their high selectivity and activity levels over more than 3 cycles of a certain catalyst.

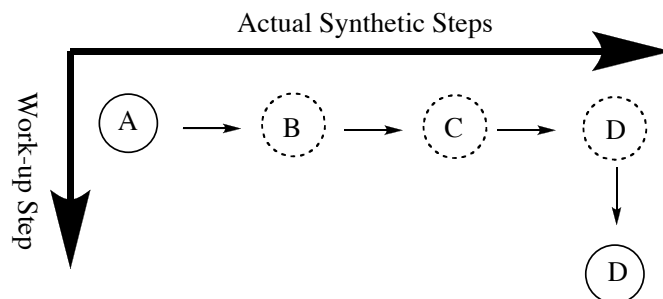


Figure 2. Compartmentalisation of catalysts by Nature results in multi-step syntheses with minimal waste.

This report is aimed at giving a review of the various methods and applications that are common for the heterogenisation of homogeneous catalysts. It is also designed as a brief overview of the techniques of, and examples from, multi-step catalytic chemistry, and an introduction to sequential multi-pot tandem catalysis.

1.2 Modern Trends in Homogeneous Catalyst Immobilisation

The key issues of the first section of this report will focus on the immobilisation and then the subsequent activity, selectivity and recyclability of heterogenised homogeneous catalysts. In this context *immobilisation* will be defined as ‘a form of a catalyst which can be easily separated from a reaction mixture/substrates, as a result of being in a different phase or through size exclusion techniques’.¹⁴ This topic is a very broad field, and thus to summarise and give a good overview of the field we have focussed on two classes of reactions (asymmetric hydrogenations, and C-C bond forming reactions) to give an introduction to the techniques used to immobilise homogeneous catalysts and their investigation. This report also includes an overview of some reports where immobilisation has revealed unexpected results, and has given a deeper insight into the mechanism of certain reactions.

1.2.1 Immobilised Homogeneous Catalysts for Asymmetric Hydrogenation

Table 1. Industrial use of catalysed asymmetric reactions.^a

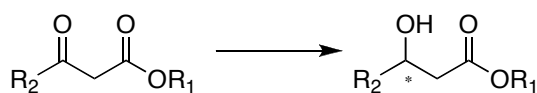
Transformation	Production		Pilot		Bench Scale
	>5 t/y	<5 t/y	>50 kg	<50 kg	
Hydrogenation of Enamides	1	1	2	6	4
Hydrogenation of acidic/alcoholic alkenes	2	0	3	4	6
Hydrogenation of Other alkenes	1	0	1	1	2
Hydrogenation of α and β functionalised ketones	2	3	3	2	4
Hydrogenation/reduction of other ketones	0	0	2	2	4
Hydrogenation of cyano group	1	0	1	0	0
Dihydroxylation of alkenes	0	1	0	0	4
Epoxidation of alkenes, oxidation of sulphides	2	2	1	0	2
Isomerisation, epoxide opening, addition reactions.	2	4	2	0	1
Total	11	11	15	15	27

^a Taken from Blaser *Chem. Commun.* 2003, 293-296.

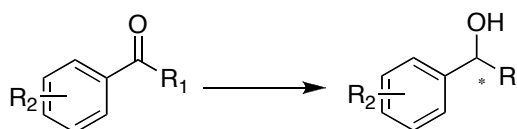
Blaser has recently stated that enantioselective hydrogenations are the most widely used asymmetric catalytic process in the industrial synthesis of fine chemicals. Table 1 gives a clear signal as to the extent that chiral hydrogenation catalysts are required.²

Chiral derivatives as a result of asymmetric hydrogenation are vitally important to the fine chemical, pharmaceutical and flavours and fragrances industries. It should be noted that the field of asymmetric (transfer) hydrogenation (AH/ATH) involves the modification of the most fundamentally basic of organic moieties. In general hydrogenation is an attractive operation as it follows easy construction steps, that is the formation of C=C, C=N, or C=O bonds (figure 1). What is also attractive is the fact that the introduction of chirality (thus AH) can be carried out in the final step of a reaction sequence. This alleviates the possibility of racemisation in subsequent reaction steps. Furthermore, it must be noted chiral drug sales are growing at an annual rate of 13%.

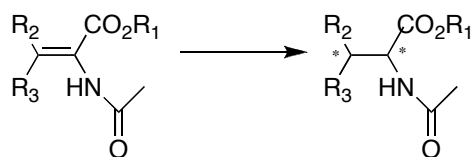
B-keto ester reduction



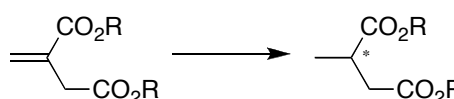
Aromatic ketone reduction



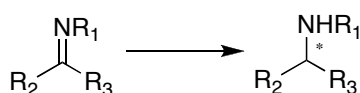
Enamide reduction



Itaconate reduction



Imine reduction



Arylpropenoic acid reduction

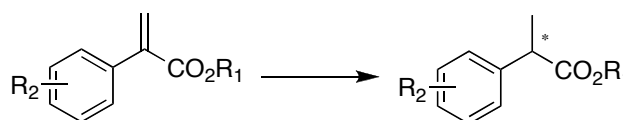


Figure 3. Standard Homogeneous Asymmetric hydrogenation catalysis.

Lin *et al.* have studied the immobilisation of chiral, phosphonate functionalised BINAP ligands in a zirconia mesoporous structure (figure 4).¹⁵ Some surprising results were obtained with the ruthenium catalysed enantioselective hydrogenation of several aromatic ketones, which showed a greater enantioselectivity than the parent homogeneous system developed by Noyori *et al.* In the hydrogenation of acetophenone, Noyori's homogeneous systems show ~80% *ee*, whereas the immobilised systems produced a >95% *ee* for the same reaction. The immobilised system was tested for recyclability and initially showed constant *ee*'s. However, the conversion decreased considerably after six runs. It is believed that the oxygen sensitive ruthenium complex has been affected by air. Hence in an air free system, the recycling would show better results. It is indicated that less than 0.2% of ruthenium has leached from the support. Subsequent to the work on aromatic ketones the AH of β -keto esters was tested using the above systems.¹⁶ However, the results were

not as promising with a slightly lower enantioselectivity than its homogeneous counterpart. The conversion did not drop over five cycles (recycled by filtration). However, the enantioselectivity did drop, for unspecified reasons, after the fifth cycle.

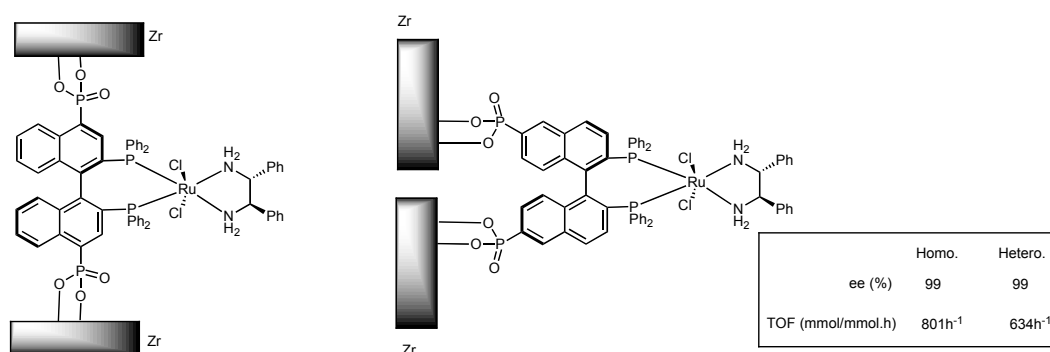


Figure 4. Phosphonate functionalised Noyori system, immobilised on Zirconia.

Lin has later used the same phosphonate functionalised BINAP complexes and covalently immobilised them on magnetite nanoparticles.¹⁷ These magnetically recoverable homogeneous catalysts are the latest breakthrough in attempts to facilitate the separation of homogeneous catalyst from reaction mixtures. Hydrogen bonding interactions apparently bind the catalyst to the magnetite surface. In solution the particles readily disperse, and can be attracted using a small magnet. The immobilised catalysts showed complete conversion with enantioselectivities as high as or higher than those of the homogeneous catalyst with a large range of substrates. Recycling of the catalyst was carried out by decantation of the reaction mixture while holding a magnet to the reaction vessel. Depending on how the catalyst is immobilised (best with co-precipitation techniques) the catalysts were recycled over 10 cycles without a loss in selectivity (see figure 5).

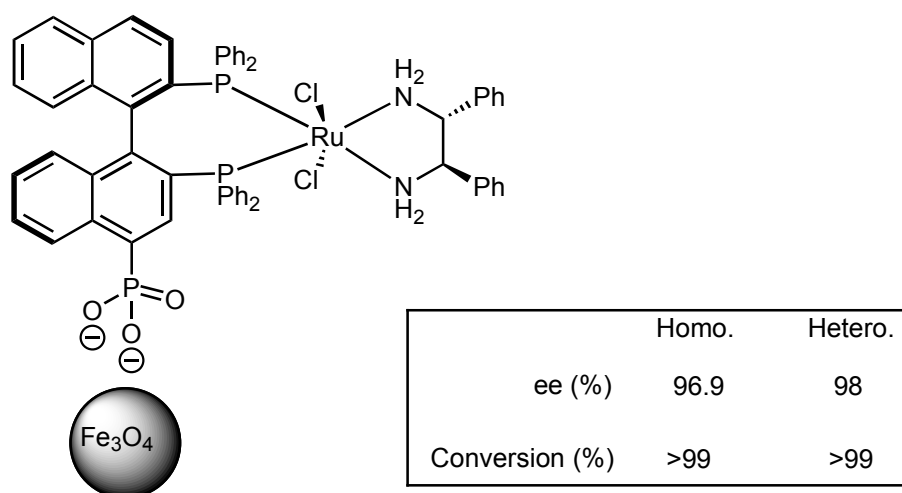


Figure 5. Phosphonate functionalised Noyori system, immobilised on Magnetite.

Recently a mono-substituted BINAP- has been developed and functionalised with a triethoxysilyl linker (see figure 6a).¹⁸ This precursor was coupled with SBA-15 yielding the immobilised ligand which was stirred with [RuCl₂(cymene)] in DMF to give the immobilised complex which was used in the AH of β -ketoesters. Alkyl ketoesters showed high conversion and

enantiomeric excess results, however the aryl derivatives were converted with lower activity and selectivity. Recycling tests were carried out using these catalysts and over three runs conversion and selectivity remained constant. On the fourth run, however, a notable decrease in both aspects was observed, and no comments on catalyst activity were given.

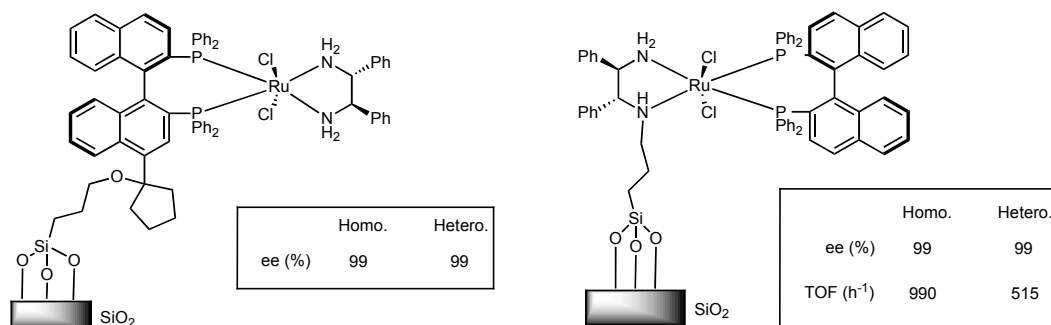


Figure 6 (a-left and b-right). BINAP-RuCl₂-DPEN complex via BINAP linkage, bound to silica and DPEN-RuCl₂-BINAP immobilised via the diamine on silica.

In contrast to the above-mentioned work, Kumar has covalently immobilised the other ligand present in the Noyori BINAP-MX₂-DPEN system (see figure 6b), viz. the DPEN ligand, on silica (specifically on well-ordered mesoporous MCM-41/48).¹⁹ TOF's in the range of 500 were observed, however complete substrate conversion was not achieved. *Ee*'s were consistently above 90% for a wide range of substrates, which in comparison with the homogeneous system is a lower value. Recycling of the catalyst was carried out with a notable decrease in catalytic activity in the case of normal SiO₂ as support; however, when MCM-41 or -48 was used, neither loss in conversion levels nor in enantioselectivity was observed over four catalytic cycles. Minimal amounts of ruthenium leaching were observed, $1 \times 10^{-3}\%$.

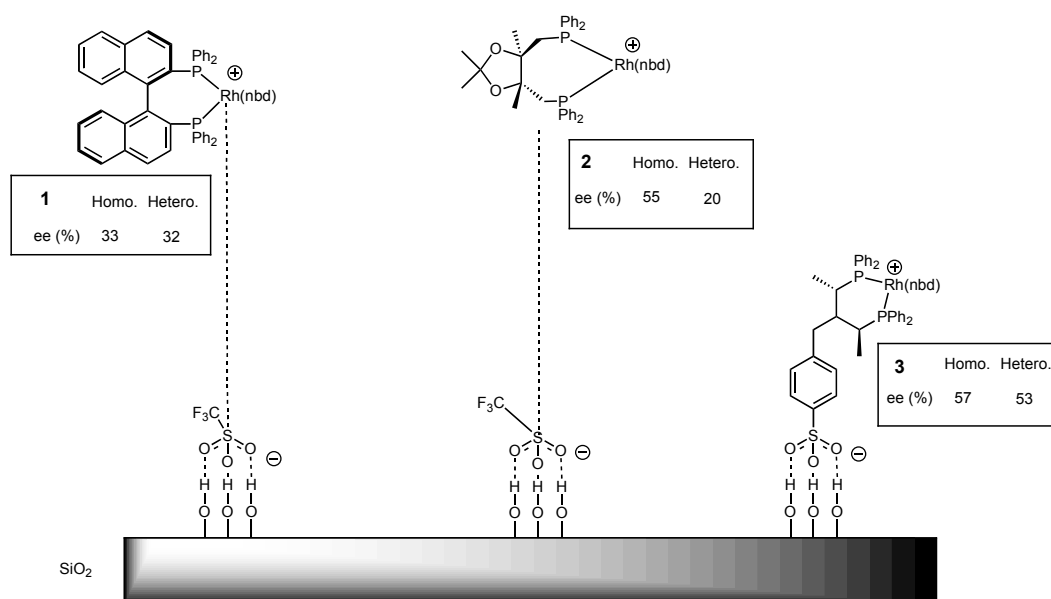


Figure 7. SHB rhodium catalysts.

Work by the Bianchini group has shown great promise for the immobilisation of certain important Rh-phosphine complexes (figure 7).²⁰ The procedure involves using a hydrogen bonding interaction between the silanol groups of silica and either a sulfonate group on a ligand or a triflate complex counter ion. These so-called SHB's (Supported Hydrogen Bonded catalysts) were tested in the AH of itaconate species and enamides, with mixed results. Complete conversion was achieved with several of the heterogeneous catalysts, however poor enantioselectivity was observed under all conditions that were examined.

The catalytic results show little change in terms of enantioselectivity for the BINAP (**1**) and BDPBz (**3**) complexes when compared with the analogous homogeneous systems. The supported DIOP (**2**) complex showed a decrease in enantioselectivity compared to its homogeneous counterpart. It was noted that no leaching of rhodium was observed in all three chiral systems.

The Blaser group, which has had considerable success in the development of immobilised diphosphine complexes, focussed on the development of immobilised Xyliphos (figure 8, SiO₂, polystyrene-PS, water soluble) complexes for the hydrogenation of the sterically hindered MEA-imine. The chiral product of this is a key intermediate in the synthesis of the herbicide (S)-Metalachlor (Syngenta Inc.).²¹ The measured TOF's for metal catalysed AH were on average found to be about one quarter of that of the homogeneous system with identical *ee* throughout. It is noted here that it is common for PS bound species to have very low activity, presumably due to slow mass transport within the polymeric material. Recycling of the various immobilised systems proved not to be possible. It was consistently observed that the systems ceased reacting before complete substrate conversion, thus making reuse impossible. Reasons for this can include side-reactions on functional groups on the ligands, a modified chemical environment (in relation to the homogeneous conditions) in close proximity to the reactive site and high local catalyst concentrations leading to dimeric/oligomeric formation.

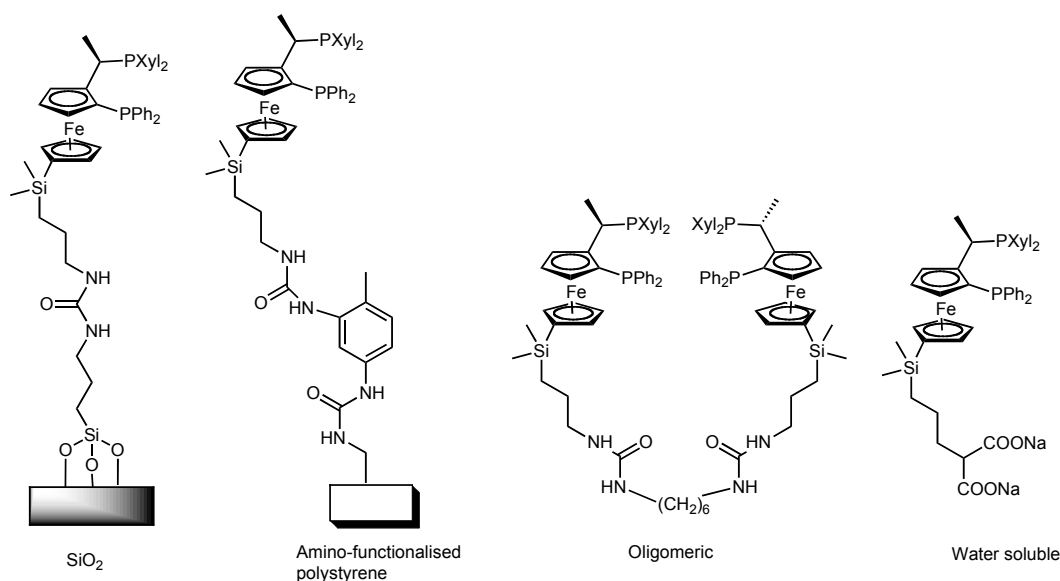


Figure 8. Various functionalised Xyliphos derivatives.

A positive effect of the immobilisation of homogeneous catalysts on the catalytic activity (and hence TOF) of Ir-BPPM complexes has been reported by the same researchers.²² In solution, it is believed that complex dimerisation occurs, and this aspect leads to a reduction in catalytic activity. This theory was convincingly demonstrated by the fact that an increase in the surface density of catalytic species (on silica) resulted in a likewise decrease in TOF. It was observed that no marked decrease in *ee* was recorded, indicating that there was no decomposition of the complexes. The site isolation phenomenon has been examined in detail by Pugin,²³ in an investigation of model systems (see figure 9) that demonstrate an increase in activity and enantioselectivity upon immobilisation of catalysts. The model reactions used for this expanded study were the rhodium and Ir catalysed hydrogenation of methoxymethylketimin (MEI) and methyl-acetamidocinnamate (MAC).

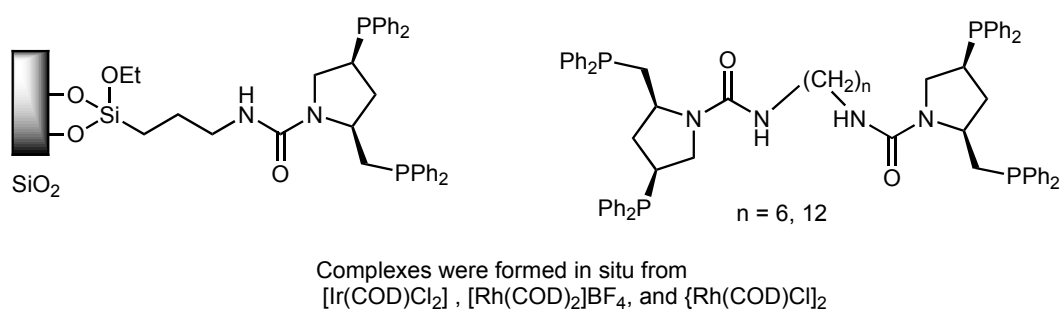


Figure 9. Ligand systems used for site isolation experiments.

The metallic complexes of the above species were used for the AH of MEI and MAC. With rhodium the AH of MAC showed no dependence on loading when the cationic complexes were used. When the neutral complexes were used activity decreased when loading was increased. The same can be said when the bis neutral complex was used, where higher local concentration ($n = 6$) is less active than when lower local concentrations are present ($n = 12$). This led to the conclusion that interactions between neutral complexes are detrimental to catalysis. Similar results were observed when Ir-BPPM catalysts were used for the AH of MEI. The report then continues in attempts to quantify the optimal loading/interaction dependence for immobilisation. It is argued that a certain fraction of sites will be in close enough proximity to another catalytic site to allow interactions, and similarly a certain number of sites are completely isolated and unable to interact. This means that with loading affecting the above properties, loading can be used to control the rate of reaction. Furthermore, the researchers appeared to be able to calculate the area of one catalytic site on a support from the reaction rate. Recent work has been done to verify this hypothesis by characterisation of the supported ligands and complexes using ^{31}P NMR and IR spectroscopic techniques.²⁴

A number of studies have been carried out on the immobilisation of BINAP onto dendritic and polymeric species.²⁵ The Chan/Deng group is to the fore in the dendritic immobilisation of BINAP species with several attempts being made to produce a highly active, recyclable system. They used Fréchet type dendrimers to immobilise the BINAP ligand at the core of the dendrimer (figure 10a).²⁶

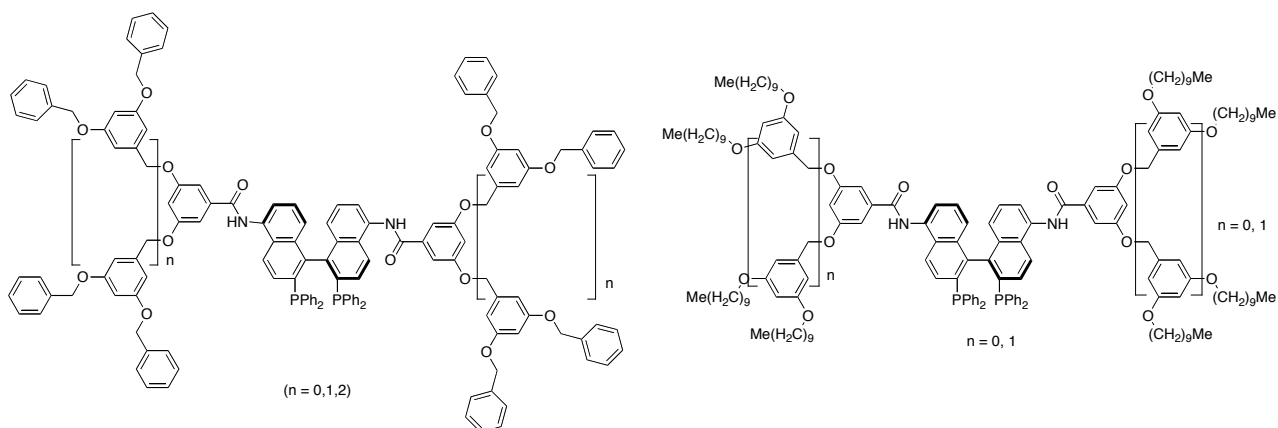


Figure 10. a) BINAP at core of a dendrimer. b) BINAP at core of a dendrimer, with alkyl units at periphery.

Synthesis of the system was relatively facile, with the 5,5-diamino-BINAP reacting with the carboxylic acid of the Fréchet dendrimer. This catalyst was tested initially for the AH of an Ibuprofen precursor and recently in the AH of various aryl ketones.²⁷ In the synthesis of Ibuprofen, the $n=2$ dendrimer was the only one that showed reasonable conversion (69%) with an *ee* of 91.6%. This was subsequently tested over four recycles and gave a constant optical purity, however, the conversion dropped by a total of 3% over the four cycles. The catalysts were recycled by addition of MeOH, which precipitated the catalyst. Work on the hydrogenation of aryl ketones showed that the catalysts are slightly less enantioselective than the non-dendritic catalyst, with a drop in *ee* of about 3-4%, however 100% conversion was observed. Only after the fourth cycle did the conversion drop below 100%; the *ee* dropping constantly from 75 to 68%.

Further work, by the same group, has led to the introduction of hydrocarbon “tails” introduced at the periphery of the dendrimer in an attempt to modify the solubility properties of the macromolecules (figure 10b).²⁸ The procedure used here brings into play the use of biphasic systems for catalyst recycling. This functionality ensures that the dendrimer is completely soluble in hydrocarbon solvents. On addition of small amounts of water, the completely immiscible system became biphasic. Consequently, this system provides for the advantages of homogeneous catalysis and the advantages of biphasic separation methods. The catalytic results (in hexane/MeOH) were not affected. All five systems (figure 10 a,b) showed equal conversion and *ee* compared with the free BINAP ligand in the AH of arylpropenoic acids. However, when using hexane/ethanol/water as media there was a dramatic decrease in the conversion (from quantitative to 38%) and a 10% decrease in the *ee*. Several runs were performed to evaluate phase separation and catalytic recycling by addition of water after catalysis had been carried out. A gradual loss of conversion (down by 4% after run four) but no loss in enantioselectivity was observed. It must be noted that in all of these examples no comments on the activity of the recycled catalysts were given.

The Deng group has shown the development of multimeric Fréchet functionalised dendrimers, involving two dendritic wedges coupled together.²⁹ On the periphery of one of the wedges are a number of catalytic sites, while the other half of the system is a common Fréchet wedge, and thus a hybrid system is formed (figure 11). These ligands were tested and compared to the above mentioned dendritic Ts-DPEN and the analogous homogeneous catalysts in the

ruthenium catalysed ATH of acetophenone. A general trend was observed in comparing solvent polarities; the more polar the solvent the lower the TOF, however no effect on the selectivity was observed. No considerable differences were observed when comparing the hybrid systems to the above-mentioned dendritic catalysts. Also no difference was observed between the homogeneous and hybrid systems, when the solubility issues were resolved. By evaporation of solvent (DCM) under vacuum and then introducing MeOH the dendritic species could be precipitated and thus recycled. The hybrid systems showed poor recyclability with an almost 30% decrease in conversion after one cycle of the catalyst. These results are similar to those of the polymer immobilised systems, and it is believed the proximity of the dendritic wedge plays a vital role in protecting/stabilising the catalytic site.

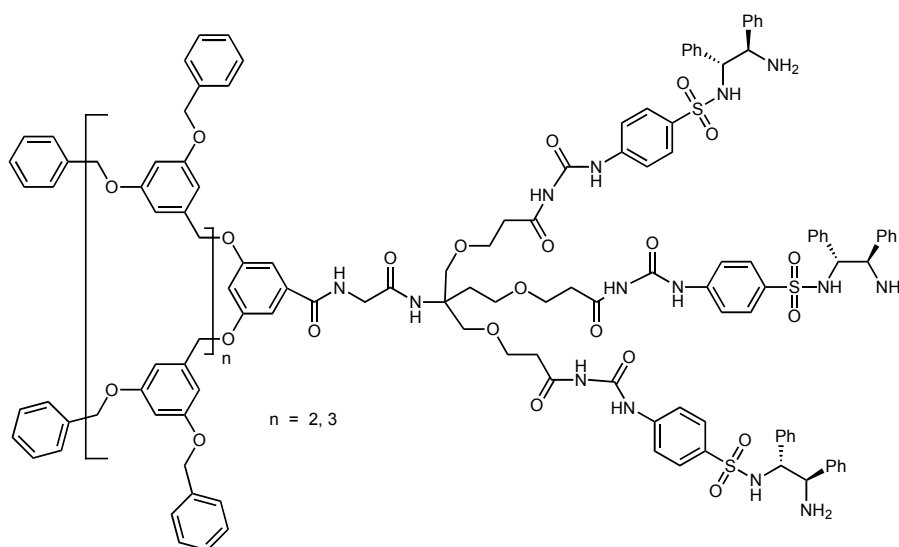


Figure 11. Hybrid multimeric-Ts-DPEN/Fréchet wedge ligand.

In an expansion on the above work, Deng and co-workers have developed another Fréchet-wedge system of TsDPEN ligand.³⁰ Phenol functionalised Ts-DPEN was coupled with a Fréchet wedge precursor to yield several ligands with differing dendritic generations. The core-functionalised dendrimers showed similar activities and selectivities to the monomeric analogue and could also be recycled over 4 runs with an approximate 20% loss in conversion levels (97%-83%) with no loss in *ee* levels.

Bergens has developed a polymeric diphosphine system for enantioselective hydrogenation of arylketones. This system is formed as a result of ruthenium catalysed ROMP.³¹ The catalyst has been synthesised using cyclooctene as a copolymerisation medium because the Norphos ligand itself does not readily polymerise using the catalysts employed and actually forms di-ruthenium organometallics which do not react further with Norphos (figure 12).

A ratio of 15,000 equivalents of cyclooctene to 3000 parts norphos was combined to make a long chain catalyst which was subsequently reacted with 3000 equivalents of dicyclopentadiene (to facilitate cross-linking). The resulting polymer was coated onto BaSO₄ as a thin film and was then tested as a catalyst in the AH of 1-acetonaphthone. The heterogeneous reaction rate was approximately 40% of that of the homogeneous system. The *ee* was 83%, which was an increase of

35% compared to the homogeneous system. The system was tested for recycling and was reused ten times without significant drops in *ee* or rates of substrate activation. Where this huge increase in *ee* comes from was not examined. However, it is likely that, as with inorganic silica, the BaSO₄ produces divots and hollows where the active catalyst is located, thus forcing the formation of single enantiomers as previously described.

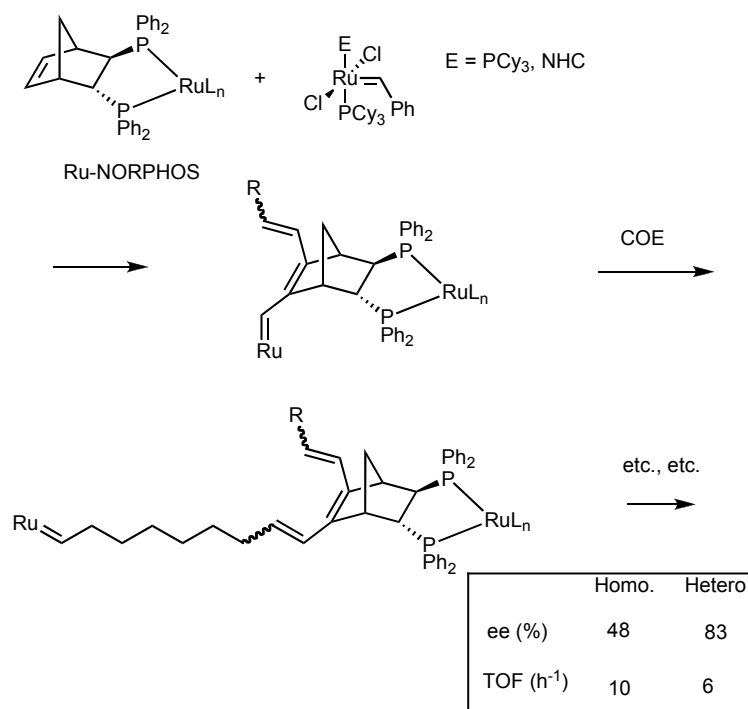


Figure 12. ROMP to form immobilised chiral diphosphine-Ru complex.

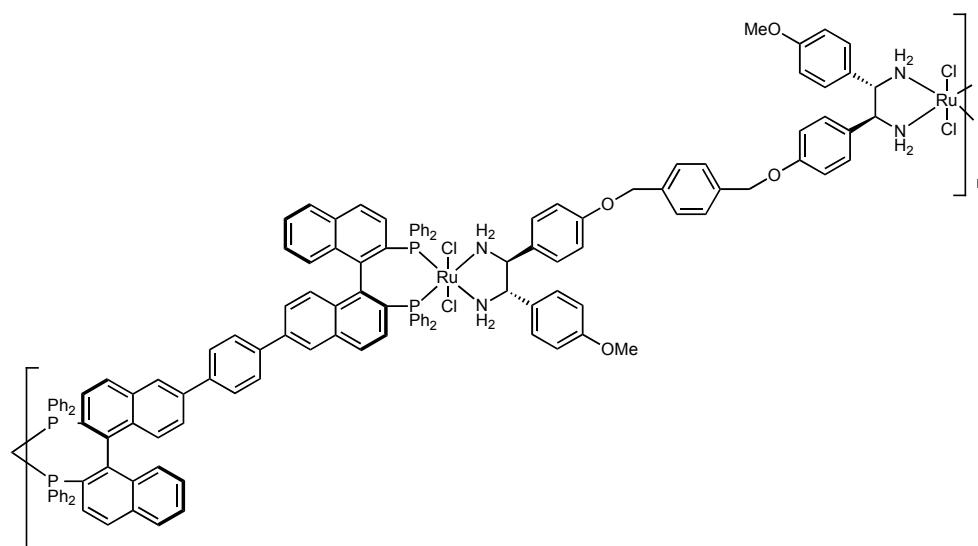


Figure 13. Noyori system as connectors in the formation of coordination polymer as studied by Deng *et al.*

Further work on the immobilisation of [BINAP-RuCl₂-DPEN] systems has shown the very attractive formation of heteroligand coordination polymers.³² Ding has outdone himself in utilising coordination polymers to immobilise catalysts (figure 13). The utilisation of the fact that the

Noyori BINAP/DPEN system preferentially forms has allowed these researchers to develop the system. SEM and powder X-ray diffraction techniques have confirmed that the polymeric Noyori system has formed. The immobilised catalyst showed similar results to those of the homogeneous system in the AH of various aryl-ketones, whilst keeping TOF values in the range of 500 h^{-1} . The catalyst could be filtered easily and reused 6 times with no drop in activity and a very small drop in enantioselectivity.

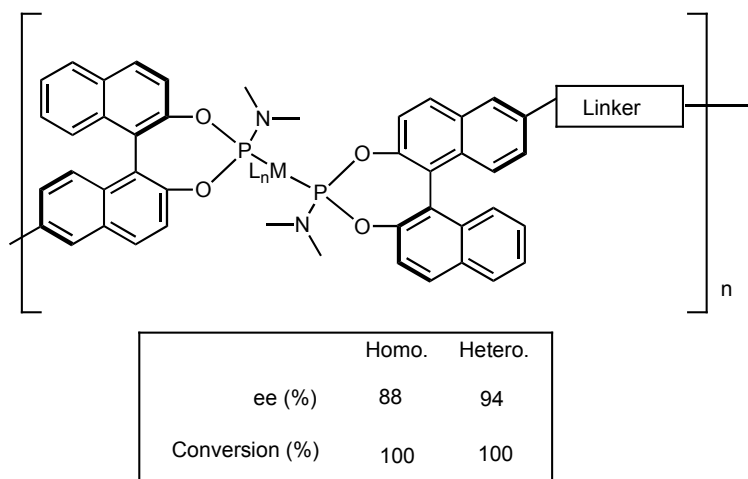


Figure 14. Co-ordination polymeric rhodium phosphoramidites.

The same technique has been applied for some amino-phosphites (figure 14).³³ A di-aminophosphite ligand is polymerised as a coordination polymer when $[\text{Rh}(\text{COD})_2]\text{BF}_4$ is introduced, with the aminophosphites coordinating to the metal centre leading to linear polymers. AH conversion rates in enamides reduction were consistently observed as 99% or higher, which is comparable to homogeneous systems with similar loading, and *ee* results were consistently in the range of 94-97%. In some cases the *ee* results were indeed higher than that of the homogeneous system. The reaction mixture with the insoluble polymer removed showed no activity, and no rhodium was observed in this solution. Upon recycling of the catalyst >99% conversion was observed over seven runs with an approximate drop of 5% in enantiomeric excess overall.

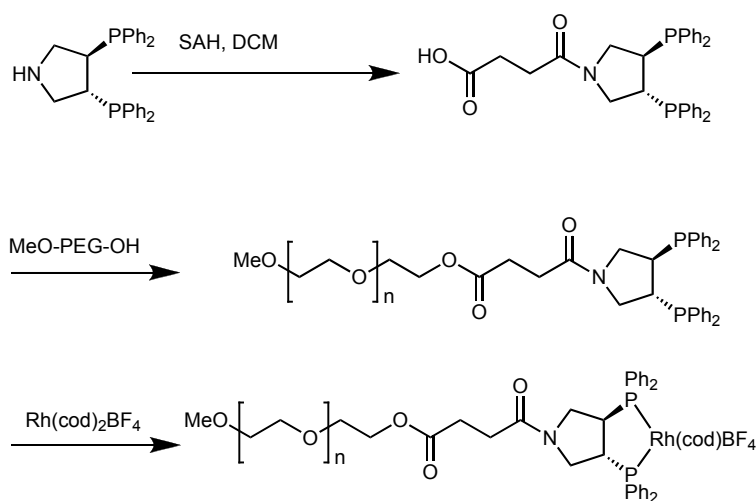


Figure 15. PEG supported pyrphos-Rh complex.

Pyrphos was incorporated into polymers with a PEG backbone by Chan *et al.*³⁴ The pyrphos ligand was coupled with succinic anhydride giving the linker bound ligand suitable for incorporation into the polymer. The polymer bound pyrphos (figure 15) was subsequently tested in the AH of prochiral enamides using rhodium as the metal centre. The enantioselectivities showed a very slight increase with respect to that of unbound complex (1%). Furthermore, this high enantioselectivity was retained through three cycles of the same catalyst. This is important because the insoluble PS supported analogue loses its activity dramatically after the first cycle, which implies substantial catalyst leaching upon recycling.

Immobilisation of phosphoramidite ligands for AH of various itaconates and enamides has been carried out by the Doherty group.³⁵ Two similar phosphoramidite ligands were synthesised and functionalised to allow for inclusion into PS copolymers. The ligand syntheses are carried out in three to four steps from 2,2'-bis(chlorophosphite)binaphthyl. The polymerised ligands were subsequently complexed with $[\text{Rh}(\text{cod})_2]\text{BF}_4$ in dichloromethane. The two immobilised catalysts (figure 16) were tested in the enantioselective hydrogenation of dimethylitaconate and dehydroacidic amides. The phenylamine derived polymeric catalyst showed a higher catalytic activity and consistently gave 100% conversion with all substrates used and showed *ee*'s superior to a couple of the homogeneous systems (increases of 2-3%). The quinoline derived polymeric catalyst showed lower activity towards dimethylitaconate and the enamides, however an exact comparison could not be made, because no homogeneous analogue was developed. The polymeric catalysts were recycled for the hydrogenation of a phenyldehydroaminoacid. The system lasted through four cycles of filtration and washing before a loss in activity was observed (100%-95%) but with constant *ee* values (80%). It was noted, however, that significant losses in activity were observed for the catalysis and thus requiring longer reaction times on sequential cycles.

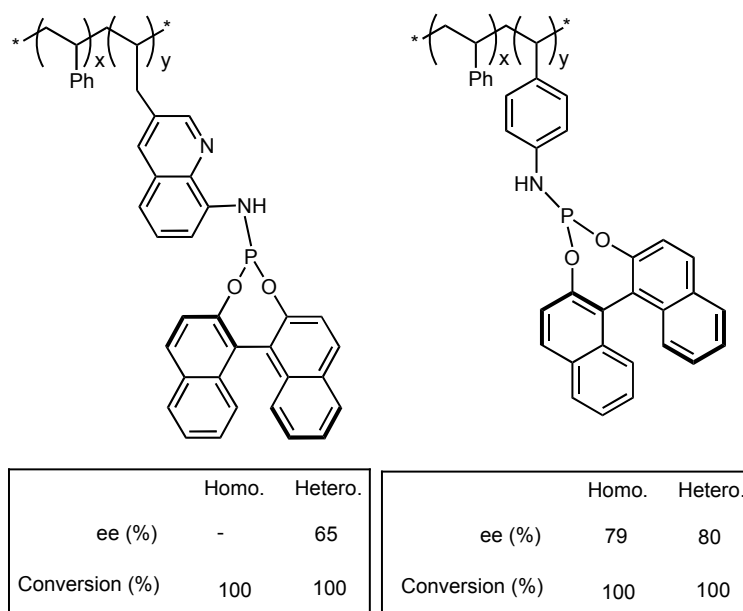


Figure 16. Polystyrenyl chiral phosphoramidites.

Lemaire has immobilised a chiral diamine (Ts-DPEN) in PS for ruthenium and iridium catalysed ATH's.³⁶ The vinyl functionalised ligands were polymerised with various amounts of

styrene and divinyl benzene so as to alter the cross-linking and loading of the catalyst (figure 17a). The materials were then tested in the ATH of acetophenone. Conversion of 94 and 96% for (Ir and ruthenium complexes, respectively) were the highest yields attained. The ruthenium compounds showed much lower enantioselectivity than the Ir systems. The cross-linked materials were slightly more active and enantioselective when compared with their linear counterparts. Recycling of the catalysts was carried out but a large deactivation occurred. An analogous *methyl*-amino ligand has been immobilised by the same research group, however in this case by incorporation within a polymer backbone.³⁷ Several polyureas were developed with various aryl isocyanates as precursor bridging linkers. A 100% level of substrate conversion was achieved on one occasion with a cross-linked polymer, however the maximum *ee* that was observed was only 70% (Rh catalysed ATH of acetophenone).

Bayston has developed an immobilised Ts-DPEN system for ATH using amino functionalised PS and PEG linked PS (figure 17b).³⁸ The [RuCl₂(cymene)] catalysed reduction of acetophenone was tested using these systems. The reaction was performed with and without solvent. The PS system showed the best results for enantioselectivity, but conversely the PEG/PS combination gave the best results for conversion under solvent free conditions. With solvent present (DCM), the PS system showed an increase in activity, and was more active than the PEG linked PS. Upon reuse, the systems showed a drop in activity but were constant in terms of *ee*.

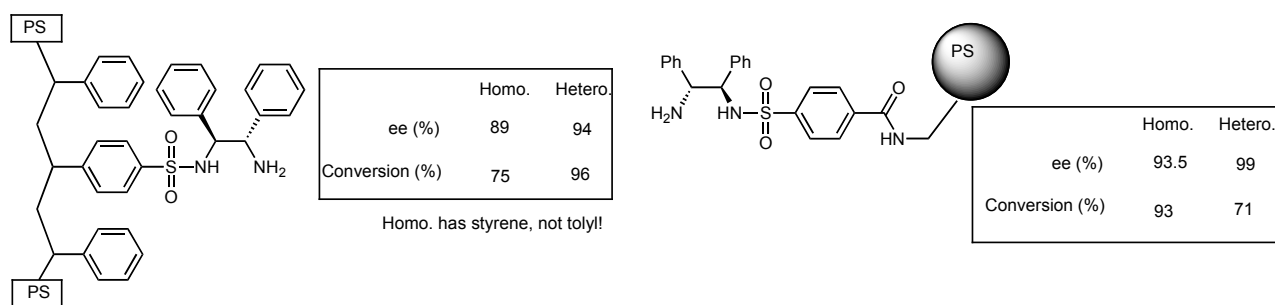


Figure 17. a-left) Lemaire's immobilised chiral amine ligand. b-right) Bayston's immobilised chiral ligand

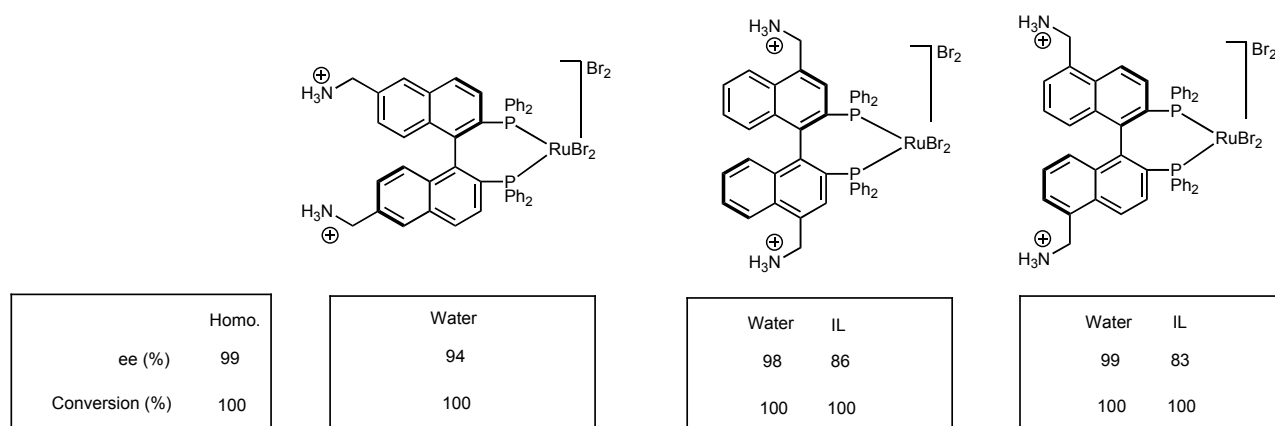


Figure 18. Water and ionic liquid soluble [RuBr₂BINAP].

As a follow-up to the extensive work done on immobilising BINAP ligands, Lemaire has made some water soluble BINAP species for the reduction of ethyl acetoacetate.³⁹ The previously

mentioned 6,6'-diamino BINAP ligand is protonated so as to make it water soluble (figure 18). The HBr salt was easily formed (96% yield) and the ruthenium was introduced thereafter. The catalyst led to good enantiomeric excess (94%) and complete conversion in pure water solutions. Extraction of the substrates was carried out using pentane. After the third use, the *ee* level began to drop (from 94% to 83%), however the conversion remained quantitative, however no mention of the activity of the recycled catalysts was given.

Lemaire has further developed two novel amino-BINAP species for water-soluble enantioselective hydrogenation and applied this technology to the same reaction as above.⁴⁰ The ligands 4,4'- and 5,5'-diamino-BINAP were developed (figure 18) in a similar manner to the 6,6'-diamino-BINAP. The new ligands showed the same activity as the previous system with complete substrate conversion and *ee*'s greater than 90% in pure water. Furthermore, it was shown that the catalysts could be recycled up to eight times without loss of activity or enantioselectivity. This recycling is performed after extraction of the products with pentane. The same catalysts were also used for the identical reaction in ionic liquids (IL's).⁴¹ Imidazolium, pyridinium, and phosphonium species with BF₄, PF₆, and aminoditrate counter ions were used as the ionic liquids. The phosphonium liquid did show good activity, but no selectivity, however, the other two gave complete substrate conversions and reasonably high *ee*'s which are dependent on the counter ion. It is believed solubility constraints in the phosphonium IL led to the low selectivity, but solvent coordination and thus poisoning on the catalyst cannot be ruled out. The inability of the catalysts to reach the high levels of selectivity and activity found in organic and aqueous systems is believed to be as a result of halide impurities in the IL's which can completely deactivate the catalyst. The catalysts were recycled by extraction of the substrates and products with pentane. The recycled materials showed no decrease in activity and a slight increase in selectivity.

Ionic liquids have been also used in biphasic AH catalysts for the reduction of enamides.⁴² A diphosphine was immobilised as part of a di-imidazolium salt, from which the rhodium complex was subsequently synthesised (figure 19). This complex was then tested in an ionic solution of 1-butyl-3-methylimidazolium with SbF₆ as the counter-anion and *iso*-propanol (IPA) as co-solvent. In the first run, in a biphasic system, the catalysts showed 100% conversion with the same activity as the non-functionalised ligand (which was constant over three runs in total) and a 95.8% *ee* level was obtained. After the first run, the *ee* dropped by a meagre 0.7% after each subsequent run. The activity of the catalyst did decrease after the third run, however. Similar results were acquired with the non-functionalised ligand in the same biphasic system, which leads to the point that with cationic catalysts it is quite possible to carry out catalysis in biphasic IL/organic solvent mixtures.

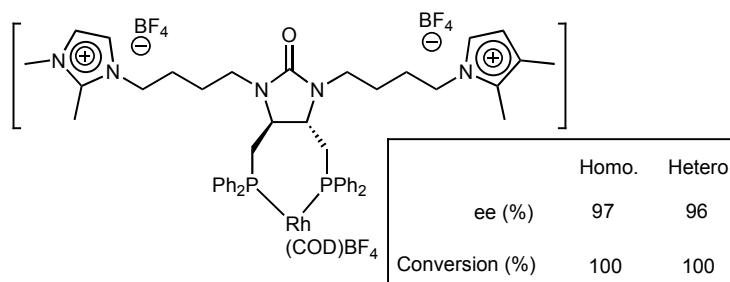


Figure 19. BMIIm derived bidentate chiral phosphine.

Sulphonated BINAP has been developed for water-soluble AH.⁴³ The AH of prochiral acylamino acid precursors was followed. Sulphonation of the phenyl groups of the diphenylphosphine moiety gave a tetra-sulphonated water soluble BINAP ligand which was subsequently metallated with [RuCl₂(benzene)]. The enantioselectivity results were improved in two cases in the hydrogenation of acetamidoacrylic acid and acetamidocinnamic acid in the aqueous system. However, a decrease in *ee* was observed in the hydrogenation of dimethylitaconic acid. Various alterations were made to the system (*e.g.* solvent ratios, temperature, pressure, catalyst/substrate ratios); however, little improvement in the catalytic results was noted. The same catalysts were tested in the AH of arylpropenoic acids.⁴⁴ In aqueous solvent mixtures, the catalytic results were not impressive as water was found to significantly hinder the formation of the enantiopure product. In MeOH, *ee*'s as high as 96.1% were observed. In subsequent publications, the systems were reported to have been immobilised in ethylene glycol (EG) coated on a glass porous support (*i.e.*, supported aqueous phase catalysis). No leaching of ruthenium was observed during immobilisation or catalysis. The AH of aryl-propenoic acids was monitored. *Ee*'s as high as 96% were observed with this new EG immobilised catalyst, however, no tests on reuse were carried out (figure 20).

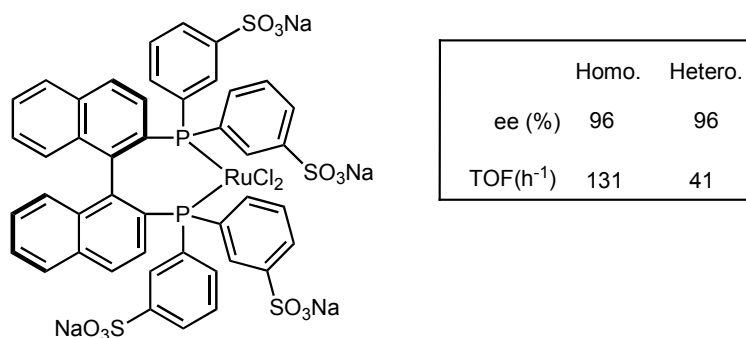


Figure 20. Sulphonated [RuCl₂(BINAP)].

Fluorinated BINAP ligands have been developed by Sinou for the rhodium catalysed AH of α -acetamidocinnamic methyl ester.⁴⁵ The phenyl groups of the BINAP ligand were functionalised with fluoro-alkyl ethers. The rhodium catalyst was used in a D-100 (fluorous solvent)/EtOH mixture and showed high conversion levels (100%), however with only 15% *ee*. In a previous reaction (Pd catalysed asymmetric alkylation) the same ligand was tested for recycling and showed that the complex was not recyclable, due to metal-ligand dissociation upon introduction of a fluorous solvent.

1.2.2 Immobilised Homogeneous Catalysts for C-C Coupling Reactions

Carbon-carbon bond forming reactions are an essential process. A wide range of metallic catalysts have been applied to carry out such reactions. In this report we gather together metal mediated Lewis acid catalysis, Heck-type catalysis, carbonylation catalysis and metathesis catalysis. These are all essential C-C bond formation fields and allow for the introduction of functionalities or the coupling of organic moieties to make a whole compound. Furthermore, all of these processes are widely used industrially. In this section we focus further on techniques used to

immobilise homogeneous catalysts, but also on the activation and deactivation pathways relating to Heck catalysis. Recent work in the field of immobilised catalysis has shown that any catalysis that involves a Pd(0)-Pd(II) catalytic cycle are probably catalysed by soluble Pd(0) clusters, and *not* single palladium sites with coordinated ligands as previously believed.⁴⁶ The proof for this is discussed herein.

1.2.2.1 Immobilised Catalysts for Heck Catalysis

Bergbreiter and co-workers are to the fore in immobilising homogeneous catalysts on soluble organic polymeric supports.⁴⁷ Initial work was directed towards single SCS-Pd complexes bound to linear poly(ethylene glycol) (PEG) tails with molecular weights of 5000.⁴⁸ Reaction of diethyl-5-hydroxyisophthalate with mesylate terminated PEG gave the ester PEG-isophthalate (figure 21). Reduction of the ester to the alcohol followed by halogenation and subsequent reaction with activated thiophenol yields the PEG-SCS ligand. Complexation was carried out using standard techniques.

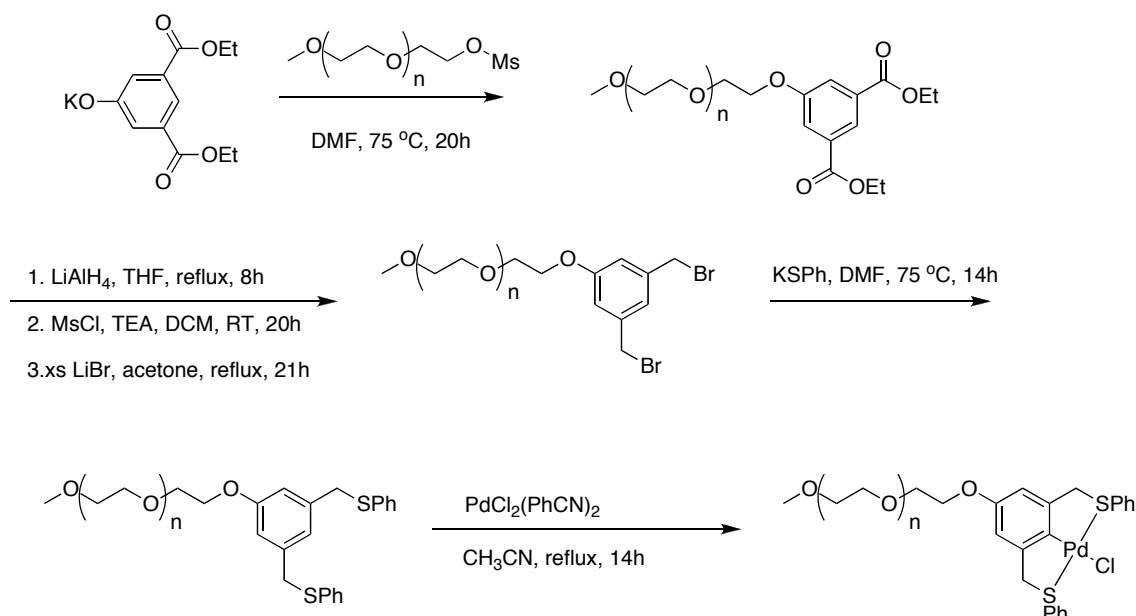


Figure 21. Synthesis of PEG-SCS-PdCl.

The PEG-bound catalyst was tested in the Heck coupling reaction and was found to be an active catalyst. It was observed that the catalyst slowly decomposed, as does its homogeneous analogue, and thus was *not tested in recycling experiments*. A *para*-amino functionalised SCS analogue was reacted with succinic anhydride yielding a carboxylate, which was then coupled with the PEG tail. This catalyst was also active, and did not show decomposition, and was used in recycling tests. The catalyst was recycled by adding the post-catalysis reaction mixture to diethyl ether solution which precipitated the catalyst. No loss in activity was observed upon recycling. The same group later published similar work with polyisobutylene oligomers bound to an SCS-Pd complex.⁴⁹

Later work showed multimetallic polymer supported SCS-Pd complexes used under thermomorphic conditions for Heck catalysis.⁵⁰ Poly(N-isopropylacrylamide) (PNIPAM) bound SCS-Pd complexes and the previously mentioned PEG-SCS-Pd were used in a type of biphasic catalysis. At room temperature substrate in heptanes and catalysts in ethanol or dimethylacetamide are immiscible. However, upon heating formation of a homogeneous solution and product formation is observed. Re-cooling creates a biphasic system again, and allows for catalyst recycling. PEG-SCS-Pd showed activity in the thermomorphic mixture and was recycled three times, with increasing conversion levels (run one 53%, run three >99%). PNIPAM bound SCS-Pd showed improved catalytic activity, and also a similar pattern of increased yields upon recycling (up to 4 cycles!). This unusual increase in conversion levels is unexplained in the publications. However, after the work of Jones and co-workers, which explains that ECE-Pd complexes are precatalysts to soluble Pd(0) particles, one could presume that recycling of the catalyst just leads to increased levels of Pd(0) particles which are sticking to and possibly being stabilised by the polymeric supports. Similar work has been shown by Kobayashi and co-workers.⁵¹

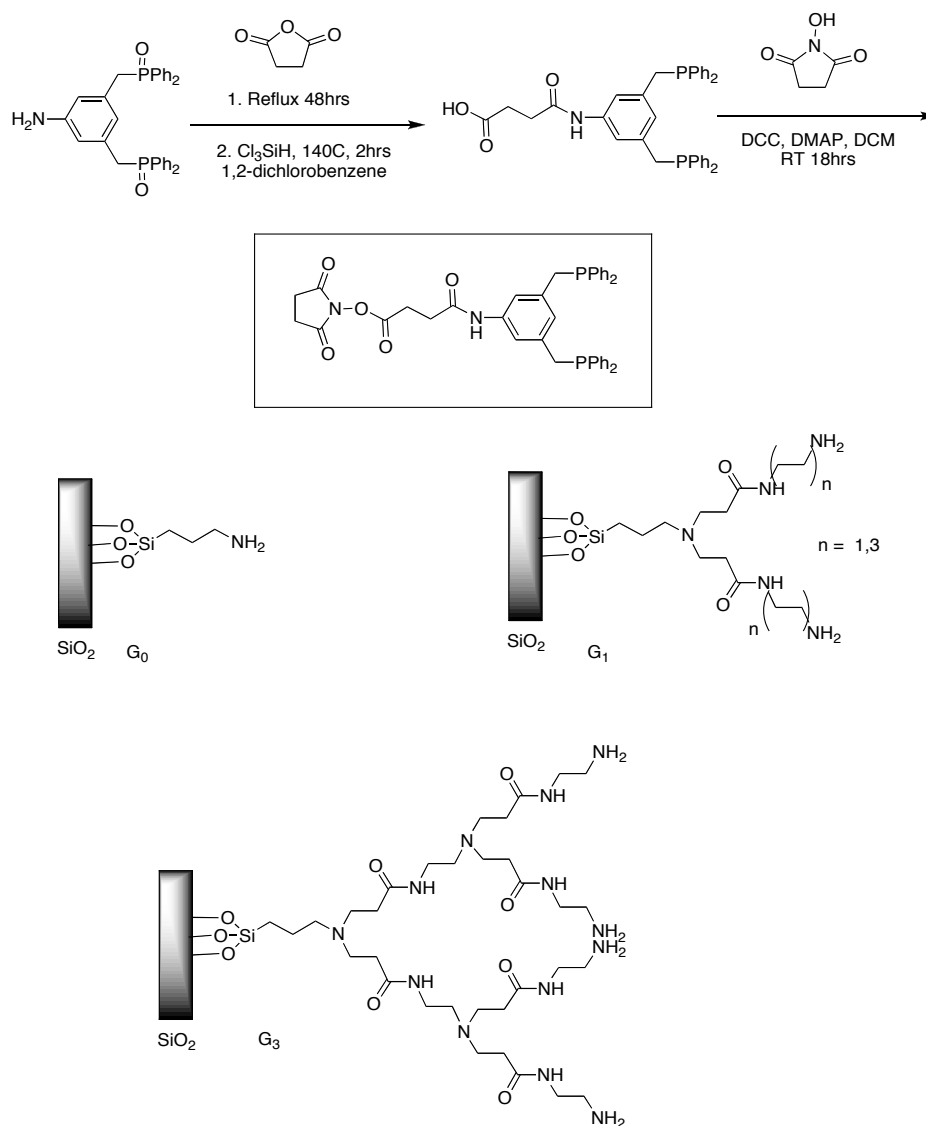


Figure 22. Various generation dendritic PCP ligands on Silica.

Alper has been to the fore in immobilising PCP-Pd type complexes on silica.⁵² Protected *para*-amino-functionalised PCP ligand was reacted with succinic anhydride and deprotected. Activation of the resulting carboxylic acid was carried out, and the resulting active ester was subsequently reacted with amino-functionalised silica yielding the immobilised ligand. Similarly, PAMAM functionalised silica was reacted with the activated acid yielding dendronised silica supported ligands of various generation (figure 22). Complexation was carried out using palladium bistrifluoroacetate.

CNC-Pd bis-carbene complexes have been immobilised on clay for use in the Heck reaction.⁵³ Using activated clays cationic palladium complexes were immobilised either by hydrogen bonding interaction (montmorillonite) or counterion exchange (bentonite). The immobilised catalysts were active and yields were both counterion and support dependent. Upon recycling, substantial decreases in activity were observed, which was believed to be as a result of sodium acetate (a substrate) blocking the active sites on the clay support.

Subsequent to all of the aforementioned work, Jones and co-workers have recently thoroughly investigated whether or not pincer alkyl-palladium complexes are in fact stable under catalytic reaction conditions by immobilisation of several pincer palladium complexes.⁵⁴ SCS- and PCP-palladium complexes were immobilised on both silica and organic polymeric supports using either hydroxyl- or amino-functionalities at the *para*-position of the pincer complex. For silica immobilisation the *para*-hydroxy SCS- and PCP-complexes were coupled with iodopropyltrimethoxysilane and the resulting compound could be easily grafted onto a silica support. For immobilisation of organic polymeric supports both amino- and hydroxyl-functionalised pincers were reacted with activated polymer precursors or polymers themselves. A Merrifield resin and ROMP formed polynorbornene were used as supports. Both insoluble (silica and Merrifield) and soluble (polynorbornene) catalysts (figure 23) were tested in the Heck reaction of iodoarenes and various acrylates.

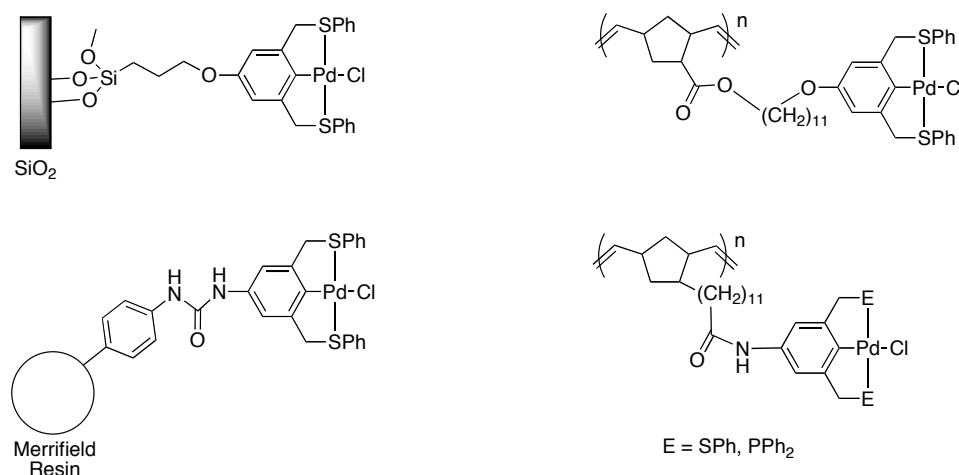


Figure 23. ECE-pincer palladium complexes immobilised on silica, Merrifield resin, and polynorbornene.

With all catalysts used, high yields were observed, with impressive activity. Furthermore, no Pd-black was observed, which is often the case when homogeneous catalysts are used under

Heck conditions. The heterogenised catalysts all behaved similarly to their homogeneous counterparts. However, recycling of the catalysts (biphasic separation for norbornene, filtration for silica/Merrifield) showed that gradual decreases in activity were occurring over successive cycles. It was also observed that approximately 20% of palladium on the support was lost per catalytic cycle. Leaching of palladium species was only occurring under catalytic conditions, and not all pincer palladium complexes were leaching palladium, as post catalytic spectroscopy showed. When Hg(0) was added to the catalytic solution of both the multimetallic heterogeneous and multimetallic homogeneous catalysts, complete deactivation was observed. Hg(0) forms an amalgam with Pd(0) particles, and stops them from being catalytically active. When polyvinylpyridine (PVPY) was added to the multimetallic species no activity was observed. It is unlikely that the PVPY could block all active sites on the supported materials, nevertheless no activity was observed, suggesting that Heck activity comes from dissolved palladium species. Because no observation of palladium black was observed, and the filtrate of the catalysed solution is active when further substrates are added, it is presumed that soluble palladium(0) clusters are forming from the ECE-pincer Pd(II) complexes. These soluble palladium clusters are the active catalysts in the reaction. This theory is further backed up by when iodobenzene was immobilised on an inorganic support and was placed under Heck reaction conditions with silica immobilised SCS-Pd. It was observed that the supported iodobenzene reacted with butylacrylate. This work has shown that pincer palladium complexes are in fact pre-catalysts to soluble palladium(0) species, and are themselves not active catalysts in the Heck reaction. This particular topic has now been expanded to all homogeneous palladium catalysts in Heck and Suzuki type reactions.⁵⁵

1.2.2.2 Immobilised Homogeneous Catalysts for Lewis Acid Catalysis

Various Lewis acids have been immobilised on inorganic supports for recyclable and environmentally friendly catalysis.⁵⁶ It must be noted that inorganic materials as such can also be applied as Lewis acid catalysts, with the possibility to tune their acidity by making slight alterations to the inorganic material (*e.g.* silica, alumina, other oxide and mixed oxide materials). However, herein we will focus on material that have been altered or functionalised with organic or organometallic groups so as to apply them in Lewis acid catalysed C-C bond forming reactions.

Luis and Mayoral have tethered chiral amino-alcohols to a polystyrene support.⁵⁷ The tethered amino-alcohols were treated with ethyl-aluminium dichloride yielding an immobilised Lewis acid catalyst for asymmetric Diels-Alder reactions. In the reaction of methacrolein with cyclopentadiene a dramatic *increase* in the reaction rate was observed with the immobilised catalyst. The endo/exo ratio was comparable to that found with homogeneous system, however there was also some enantioselection when using the heterogenised catalyst, which was not observed in the homogeneous system. The observed rate increase is believed to be as a result of site isolation which prevents inter-catalytic site interactions. These interactions retard the catalytic reaction.

The same group showed in a later report a similar system, however with a tethered TADDOL ligand system while titanium was used as the Lewis acid site.⁵⁸ The TADDOL ligand was functionalised with a phenolic group which was coupled with a styrenyl benzyl halide. The

resulting functionalised ligand was polymerised, or the phenol-functionalised ligand was directly coupled with chloromethyl-functionalised polystyrene yielding immobilised TADDOL (figure 24). Titanium was introduced and the resulting Ti-TADDOL complex was applied again in an asymmetric Diels-Alder reaction. Quantitative conversion levels were observed throughout, however the enantioselection levels were lower using tethered TADDOL complexes compared to homogeneous complexes. The endo/exo selection levels were comparable between the homogeneous and heterogenised catalysts. In a continuous flow coated-column set-up the TADDOL-Ti tethered complex could be applied for extended periods of time with little loss in enantioselection values.

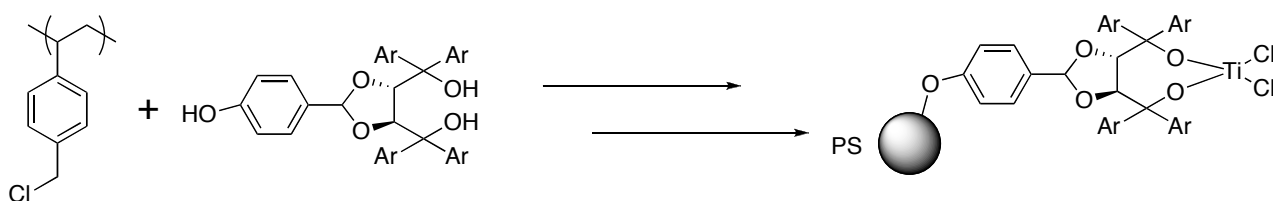


Figure 24. Polystyrene immobilised TADDOL-titanium complex for Lewis acid catalysis.

Tin halide catalysts for Prins condensation of isobutene with formaldehyde have been bound to functionalised silica materials using ionic interactions.⁵⁹ Ammonium or pyridinium functionalised silica supports were reacted with SnCl_4 facilitating the immobilisation of the Lewis acid catalyst as the SnCl_5^- anion (figure 25). The rate and extent of formaldehyde conversion levels were diminished compared to using just SnCl_4 . However, selectivity for the desired product, an unsaturated alcohol, was much improved. A substantial decrease in the formation of undesired dioxane and saturated diol products was observed when using the immobilised homogeneous catalyst. No explanation for the improved selectivity was given. The catalytic material could be recycled without any decrease in selectivity, and more importantly activity.

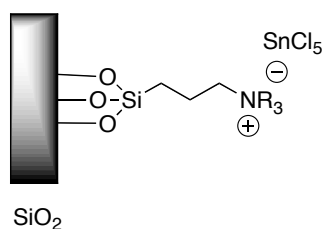


Figure 25. Silica supported tin halide species for Lewis acid catalysed Prins condensation reaction.

The van Koten group has immobilised ECE-Pd type pincers for the Lewis catalysed aldol reaction ($\text{E} = \text{SPh}, \text{PPh}_2, \text{NMe}_2$).⁶⁰ *para*-Hydroxy functionalised ECE-Pd pincer complexes were reacted with an activated tether. The resulting triethoxysilane-tethered complex was immobilised on silica using both grafting and sol gel techniques (figure 26). Due to the stability of the pincer complex it is possible to immobilise the complex itself on the support, thus alleviating the possibility of untoward interactions between the silica and the metal centre while introducing the metal to the already supported ligand. This is, in fact, the case with most pincer complexes immobilised on insoluble supports, and is a rarity in immobilisation chemistry, however when

sustainable catalysts are a necessity this is a much more desirable technique. Most often, the metal complex has to be constructed on the support, due to the harsh reaction conditions required to induce covalent binding of an organic moiety to an inorganic compound. However, the stability of the metal-carbon sigma bond,⁶¹ flanked by the dative bonds of the two arms of the pincer ligand, mean that a wide range of immobilisation techniques can be availed of without developing new synthetic procedures.

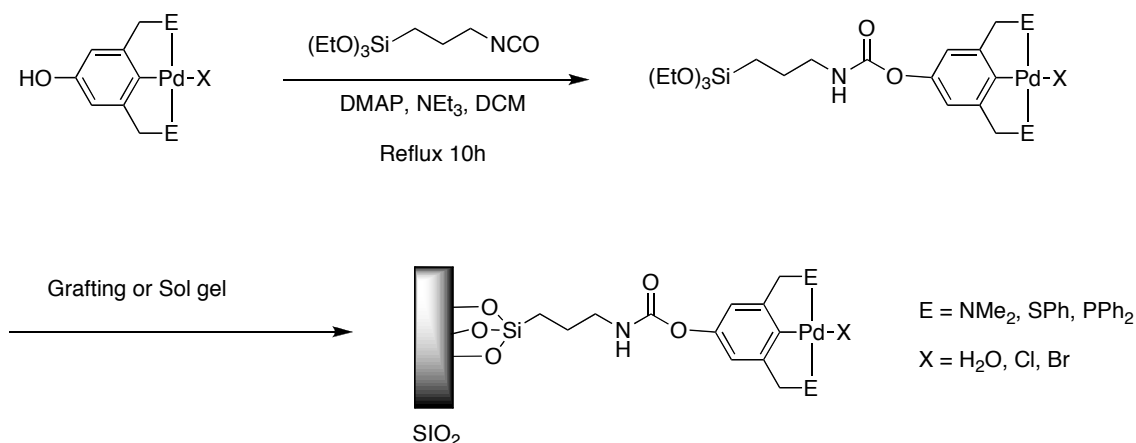


Figure 26. Immobilised NCN-Pd pincer complex.

The depicted complexes were converted to the aqua form of the complex and tested in the aldol reaction of benzaldehyde with methyl isocyanoacetate. Catalytic results showed the immobilised catalysts to be active as both aqua salts and as the metal halide complexes. It was also found that silver salts used to convert the metal halide to the aqua salt were active catalysts in this reaction. Recycling of the catalytic materials was carried out by centrifugation and subsequent decantation. Substantial losses in activity were observed over consecutive recycles when NCN and SCS complexes were used. The PCP complex was shown to be active over 5 recycles of the catalyst, with minimum leaching of palladium species into the reaction mixture. The decreased activity in SCS and NCN complexes is assigned to the low stability of the active catalyst, which is not as depicted in figure 26. Insertion of isocyanate into the NCN and SCS- σ -aryl-palladium bond, yields what is believed to be the active material.⁶² This insertion reaction does not occur when the PCP-pincer palladium complex is used. It is believed that surface reconstitution led to loss of and inaccessibility to catalytic material and hence a decrease in activity upon recycling of the heterogenised catalyst.

1.2.2.3 Immobilised Catalysts for Carbonylation Catalysis

A recent review describing ‘green techniques’ for alkoxy-carbonylation describes the most interesting advances in the field.⁶³ Herein we describe immobilisation techniques for alkoxy-/hydroxy-carbonylation catalysis, but also for hydroformylation. The carbonylation of alkenes is an essential fundamental process which is used widely industrially.

Van Leeuwen has developed a water-soluble form of the Xantphos ligand (figure 27), and applied the palladium complex thereof in biphasic catalysis for the hydroxycarbonylation of

ethene, styrene, and propene.⁶⁴ The sulphonated ligand was complexed with PdCl₂ yielding a charged chloro-intermediate which was immediately converted to the ditosylate salt. The formed complex was applied initially in the hydroxycarbonylation of ethene showing TOF's of up to 300h⁻¹. Subsequently propene and styrene were used as substrates, showing on average linear to branched ratios of approximately 2:1 with similar TOF values to the ethene hydroxycarbonylation. No recycling work was carried out in this work.

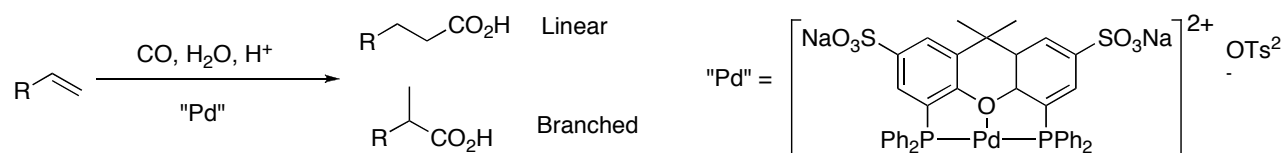


Figure 27. Xantphos-palladium catalysed hydroxycarbonylation in water.

Doherty and Knight have developed polystyrene bound 2-pyridyldiphenylphosphine for the alkoxy carbonylation of phenylacetylene.⁶⁵ Two methods were used for the tethering of the ligand to the polymeric support; a styrene functionalised form of the ligand was developed and copolymerised with styrene or methylacrylate; and a phenol functionalised form of the ligand was developed being coupled with acrylic acid, and the resulting acrylate ester was polymerised (figure 28). Catalysis with the various heterogeneous ligand was carried out with the introduction of Pd(OAc)₂. The ligand to metal ratio was high. Interestingly the ligand has a dual role in the alkoxy carbonylation of alkynes. On the one hand the ligand coordinates to the metal centre, while the excess, unbound ligands act as proton transfer agents. The immobilised catalysts performed very similarly to their homogeneous analogue (TOF ~260 vs. 300 h⁻¹). No metal leaching into the catalytic solution was observed.

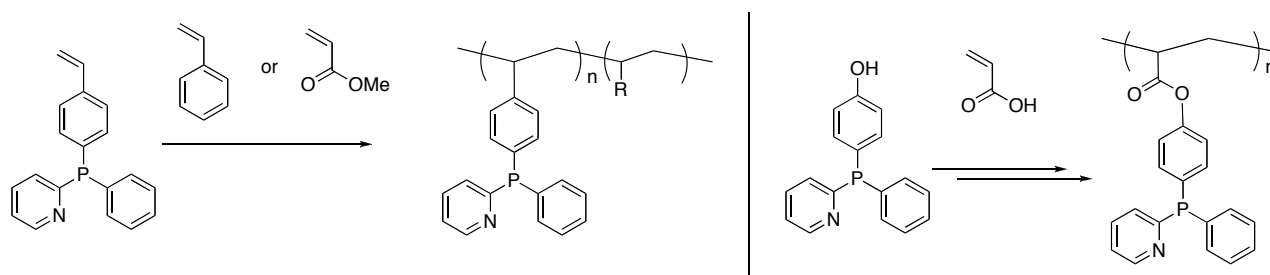


Figure 28. Polystyrene bound 2-pyridyldiphenylphosphine ligands for alkoxy carbonylation catalysis.

Alper developed dendrimer functionalised silica, with peripheral chelating phosphine groups for alkoxy carbonylation catalysis.⁶⁶ Polyamide dendrons functionalised with diphenylphosphine at their periphery were coupled with amino-functionalised silica. Various palladium salts were introduced to the tethered ligands and the resulting complexes were tested in the alkoxy carbonylation of 1-decene. The acid present played a key role in the reactions in terms of both conversion levels and linear/branched levels. The ratio of palladium to acid was also key, with nearly 40 equivalents of acid to palladium necessary to get reasonable yields. The catalysts were recycled by simple filtration, however, they showed significant drops in activity after each recycle. Furthermore, extra triphenylphosphine was added to the reaction mixture to 'stabilise' the catalysts.

This, in our view, suggests occurrence of a homogeneous catalytic reaction, in the presence of heterogenised ligands.

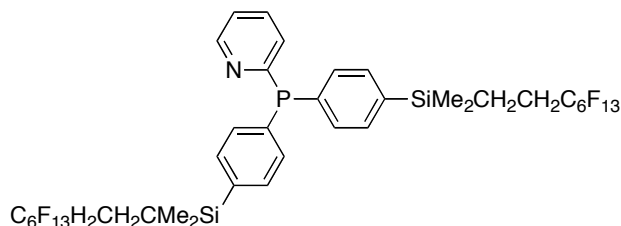


Figure 29. Fluorinated 2-pyridyldiphenylphosphine ligand for alkoxy carbonylation of acetylenes.

The van Koten/Elsevier groups have developed fluorinated functionalised 2-pyridyldiphenylphosphine ligands (figure 29) for palladium catalysed alkoxy carbonylation in supercritical CO_2 .⁶⁷ Coupling of a fluorinated tail with bromo-functionalised 2-pyridyldiphenylphosphine yielded the functionalised ligand which could be applied in the palladium catalysed methoxy carbonylation of phenyl acetylene in both biphasic solutions and in scCO_2 . In $\text{MeOH/BTF}(\text{C}_6\text{H}_5\text{CF}_3)$ conversion levels are slightly diminished compared to straight MeOH , however the linear/branched ratios were comparable. The fluorinated ligands were then applied in scCO_2 and showed >50% conversion levels, with improved l/b ratios compared to the methanolic solutions (>99% cf. 97%). It was also found that ligand used with no fluorinated tail present in scCO_2 showed low conversion levels, demonstrating the effectiveness of fluorinating the ligand for recyclable catalysts.

Catalytic intramolecular cyclocarbonylation was carried out using these catalysts. A range of allylphenols was tested. Overall selectivity was found not to be generation dependent, but CO/H_2 pressure and temperature dependent. Activity was indeed generation and tail length dependent, with the highest generation dendrimer giving the best reactivity. Similarly the extended tailed G1 system showed greater activity than the shorter G1 and the G0. The G0 catalyst was recycled, and depending on the substrates could be reused up to 5 times. However, in most cases, recycling led to a loss in activity and/or selectivity. Interestingly, throughout a co-ligand DPPB (1,4-diphenylphosphinebutane) is added to the reaction mixture. Without this additive the reaction is very slow to non-existent. This would suggest that there is decomposition of the pincer palladium unit, and that it is not the active catalyst, but rather a pre-catalyst. This is backed up by the poor recyclability results, which suggest the catalyst is in the filtrate and not the filter. Other work had focussed on the G0 dendritic silica and its application in the Heck reaction. The homogeneous catalyst, used in the reaction of phenyl iodide with butylacrylate has a TOF of 1983 h^{-1} , which is about four times that of the heterogenised catalyst (505 h^{-1}). Recycling tests were carried out and showed no loss in yield over five cycles in particular reactions. There is no mention of changes in activity. A silica immobilised palladium trifluoroacetate was synthesised, however palladium black was observed and this system could not be recycled without loss in activity, and thus the authors believe the active catalyst to be PCP-Pd catalyst. They believe that the PCP-Pd complex is decomposing, and thus becomes inactive. They do not believe that the formed 'Pd' from decomposition can be an active catalyst.

1.2.2.4 Immobilised Homogeneous Catalysts for Metathesis Catalysis

The immobilisation of both Grubbs/Hoveyda-type and Schrock-type complexes for metathesis catalysts has developed into a major field in recent years with several techniques used to immobilise the catalysts in a number of support media.⁶⁸ Initial attempts focussed on the Grubbs and Hoveyda systems and were based on tethering of the complex to an organic polymeric support via the alkylidene unit.⁶⁹ The so-called ‘Boomerang’ principle was utilised to the extent that the ruthenium alkylidene bond inevitably breaks (between support and Ru), but is expected to catch the ruthenium centre once all other alkene groups (from substrate) have reacted (figure 30a). This principle is unreliable, and is demonstrated so, when the catalyst can only be recycled three times before it loses all of its activity. The immobilised catalyst shows the high yields expected of Grubbs alkylidene ruthenium catalysts for ring closing metathesis.



Figure 30. a) Polystyrene bound ruthenium benzylidene complex; b) PEG bound benzylidene complex.

Similar ‘Boomerang’ concepts were applied for PEG functionalised benzylidene ligands bound to ruthenium centres in both Grubbs and Hoveyda systems (figure 30b).⁷⁰ Again ring closing metathesis was the reaction in which the functionalised catalyst was tested. In the first use the catalysts demonstrated the expected high yields, however upon recycling the catalyst generally lost activity after the first cycle (condition dependent), and in all cases was showing greatly diminished conversion levels by the third cycle. Furthermore, very little was mentioned about the kinetics of the recycled catalyst, and the rate of reaction which would be a more revealing description of the recyclability of the catalyst.

A more reliable approach has been taken to immobilise similar systems, ensuring better recyclability by tethering one of the coordinating ligands which are believed to remain bound to the catalytic centre throughout the catalytic cycle. Verpoort⁷¹ has demonstrated that by immobilising the phosphine ligand of the complex one can easily immobilise Grubbs metathesis catalysts. He covalently tethered a biscyclohexylphosphine ligand to a mesostructured silica support and introduced a Grubbs-I system to the phosphine functionalised silica. By phosphine ligand exchange the ruthenium catalyst was immobilised. The formed material was applied in ring opening polymerisation metathesis and ring closing metathesis. In ROMP 70% yield was achieved in the polymerisation of norbornene. In RCM high yields were achieved (100%), however these results were both substrate and solvent dependent.

Recent work has focussed on the functionalisation of N-heterocyclic carbene ligands which are present in the Grubbs II and Hoveyda systems. Buchmeiser has used alcohol functionalised imidazolium groups and coupled them with norbornene and applied ROMP to immobilise the

carbene precursor on a monolithic support (figure 31a).⁷² The carbene was subsequently generated in situ, and a ruthenium alkylidene complex was introduced to synthesise immobilised Grubbs-II type complexes. The immobilised catalyst was applied in both ROMP and RCM. The catalytic material shows selectivity (cis/trans) comparable to the homogeneous catalyst. In a similar piece of work Blechert has constructed a carbene on polystyrene and complexes in the same manner to Buchmeiser.⁷³ The polystyrene immobilised Grubbs II catalysts (figure 31b) were applied in both RCM and cross metathesis giving quantitative yields.

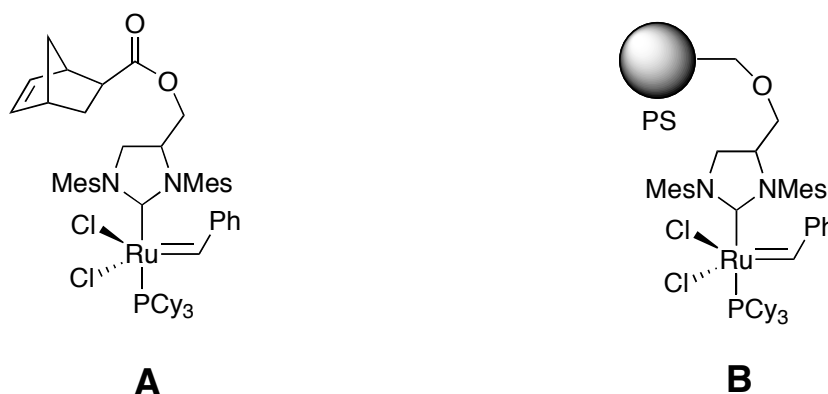


Figure 31. Functionalised carbene ligands to immobilise Grubbs-II catalysts to support materials a) ROMP for immobilisation; b) covalent link to polystyrene.

1.2.3 Conclusions to take from the Immobilisation of Homogeneous Catalysts

As was stated previously, the primary goal in attaching (heterogenising) any homogeneous catalyst is to combine the advantages of the homogeneous system, *viz.* high selectivity, high activity and ease of mechanistic probing, with the huge advantages in terms of separation, recyclability and cost effectiveness of a heterogeneous one. The details provided herein have described the numerous methods and techniques that can be applied to effectively immobilise a homogeneous catalyst for applications in enantioselective hydrogenation and carbon-carbon bond forming reactions. However, the process of immobilisation invariably leads to a number of *modified* aspects of the reactive system. These effects have been described in the many examples above and can be classified into four main areas:

(i) Since functionalisation of the ligand is pre-requisite to covalent or non-covalent binding of the catalyst, this may alter (as an advantage *or* disadvantage) the nucleophilic properties of the ligand and hence the interaction of the active metal centre with the substrate (*i.e.*, active-site modification).

(ii) Entrapment or enclosure of the complex may occur with the linker backbone or the support matrix which can result in a kind of “hide and seek chemistry” in which substrate transport to the active site is affected.

(iii) Contrary to intuition, the supports seem to play an enormous role in the chemistry. This is likely due to modification of the accessibility of the catalytic sites (*vide supra*) or effects of the

support on the solvent cage that is in close proximity to the metal complex (wettability properties of the surface).

And. (iv) In the case of substrate or reagent molecules which are *gases* (usually CO, H₂) at standard temperature and pressure, the effect of gas (vessel) pressure seems to be negligible but the *solubility* of the gas (*i.e.*, the actual concentration of the gas in the same phase as the catalyst) in the reaction medium can be very important. Particularly because any system is likely to be triphasic, and thus rate of dissolution of a gas to a certain substrate containing phase, has to be faster than with the rate of dissolution into the catalyst phase.

In light of the systems that directly mimic (or improve) product yields and enantioselectivity, have the extreme efforts to develop these systems been effective? As mentioned throughout this review, there can be an increase in enantioselectivity observed upon immobilisation of ruthenium, rhodium, and iridium based AH catalysts. Certainly, the early attempts at *immobilising* DIOP type ligands were aimed purely at increasing enantioselectivity, and it is this goal, along with recycling possibilities, that make the immobilisation of homogeneous catalysts key to the industrial observer. It is disappointingly, catalyst recycling where this topic apparently falls down. Innumerable reports have demonstrated ingenious methods for the immobilisation of homogeneous catalysts, however when it comes to the performance of the ultimate goal, quite often it is not even done, and if it is done recycling is not examined in depth. Kinetic measurements are essential to the catalysis field, and are regularly ignored in the catalysts immobilisation area with the preference to comment on yield and selectivity levels. Quite often *only* selectivity levels are reported for recycling experiments, with absolutely no mention of catalyst activity upon recycling. We have taken this as a guise for apparent catalyst deactivation, which the authors have chosen not to mention. It is apparent that the systems developed to date have not got the stability and robustness to be used repetitively, and this maybe a major weakness in the field. The general conclusion must therefore be that catalyst stability is essential when immobilising homogeneous catalysts, and kinetic measurements are a must when applying immobilised catalysts repetitively.

This review leads one to believe that the field has been thoroughly covered, so what is the next step? Novel polymeric membranes, and organic supports are continually being developed and the challenge now is to continue these studies with *optimisation* of results and indeed to attempt to make the whole area of catalyst immobilisation more “green”. In addition, it still seems difficult to quantify exactly what factors should be adjusted to engender more effective systems, and hence this kind of work will continue. The take-home message is that catalyst stability is essential. Novel catalyst systems which demonstrate recyclability, have higher stability and have long-term reliable total turnover number per catalyst use must be developed. These catalysts may not need to be the fastest, but selectivity and stability are key.

1.3 Multi-step Metal-catalysed Green Catalysis

Present trends in homogeneous catalysis are moving towards the so-called Tandem/Domino/Cascade reactions. These reactions fall under the general heading of multi-step, catalysed synthesis, however each has a specific difference;⁷⁴ Domino Catalysis⁷⁵ is defined as (Tietze) ‘Two or more bond forming reactions which take place under the same reaction conditions without adding additional reagents and catalysts, and in which the subsequent reactions result as a consequence of the functionality formed in the previous step’, Cascade Catalysis is shipped in the same basket as Domino, however there are other interpretations of this term. Tandem catalysis is defined as (Fogg) ‘Coupled Catalyses in which sequential transformation of a substrate occurs via two or more mechanistically distinct processes’. Tandem catalysis obviously can have various sub-headings dependent on whether only one catalyst is used or multiple catalysts are used and the introduction of ‘additives’ during a reaction sequence or the introduction of a trigger point where a certain reaction in a sequence needs to be initiated.

What follows is a brief report on the present stage on metal-catalysed multi-step one-pot tandem catalysis and the scope for expanding the field to include Sequential Compartmentalised Tandem Catalysis (SCTC). Domino catalysis, where intermediates spontaneously react, and are thus not isolatable, is not discussed here. Nature is of course the ultimate model for multi-step compartmentalised catalysis. Many examples using Nature’s catalysts to carry out multi-step procedures have been demonstrated,⁷⁶ however we choose here to focus on non-natural catalysis, or the use of non-natural catalysis in sequence with natural catalysts.

1.3.1 Multi-step One-Pot Catalysed Reactions Involving C-C coupling Catalysis

Burka has presented a simple manner to develop highly enantiopure functionalised amino acids by applying an asymmetric hydrogenation in sequence with a Suzuki coupling reaction (figure 32).⁷⁷ This involved the application of a rhodium-DuPHOS catalyst for the asymmetric hydrogenation of a bromo-aryl functionalised enamide. This reaction generally gave complete conversion with enantiomeric excess yields in the high 90’s%. The palladium catalysed cross-coupling reaction was demonstrated with a number of aryl boronic acids using Pd(OAc)₂ tris-(ortho-tolyl)phosphine as a co-ligand. It is not clear in this work whether the reactions were carried out in one pot, or whether there was a work-up step involved.

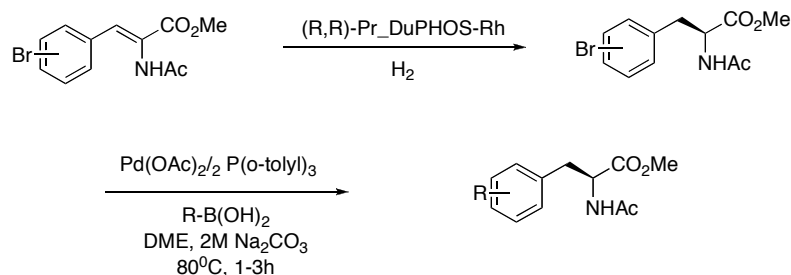


Figure 32. Tandem asymmetric hydrogenation/Suzuki cross-coupling reaction for functionalised enantiopure amino acid synthesis.

Heck catalysis has been used in tandem with oxidation catalysis for the synthesis of chiral diols using several heterogeneous catalysts in sequence.⁷⁸ A functionalised material containing three different catalysts was applied to mediate Heck cross coupling, Sharpless asymmetric dihydroxylation, and oxidant activation (figure 33). A so-called layered double hydroxide material is reacted with PdCl_2^{2-} , OsO_4^{2-} , and WO_4^{2-} yielding a trifunctional heterogeneous catalyst. It was demonstrated that the novel material was active in the various separate reactions showing high conversion levels and selectivity for the desired products. The material was then tested in a Heck/N-oxidation/asymmetric dihydroxylation multi-component one-pot reaction. Phenyl iodide, styrene, and triethylamine were mixed together in the presence of the catalytic material for several hours. N-methylmorpholine, (DHQD)₂PHAL, in ^tBuOH/H₂O was added, followed by slow constant addition of H₂O₂. The desired diols were observed in high yields (80-90%) with *ee*'s in the high 90's%. The catalytic material could be easily removed from the reaction mixture by simple filtration, and could be re-applied. This is in essence a two-step system, however no work-up is required. The Heck reaction⁷⁹ provides the prochiral alkene for the dihydroxylation, but obviously the Heck reaction is sensitive to the presence of oxidant.

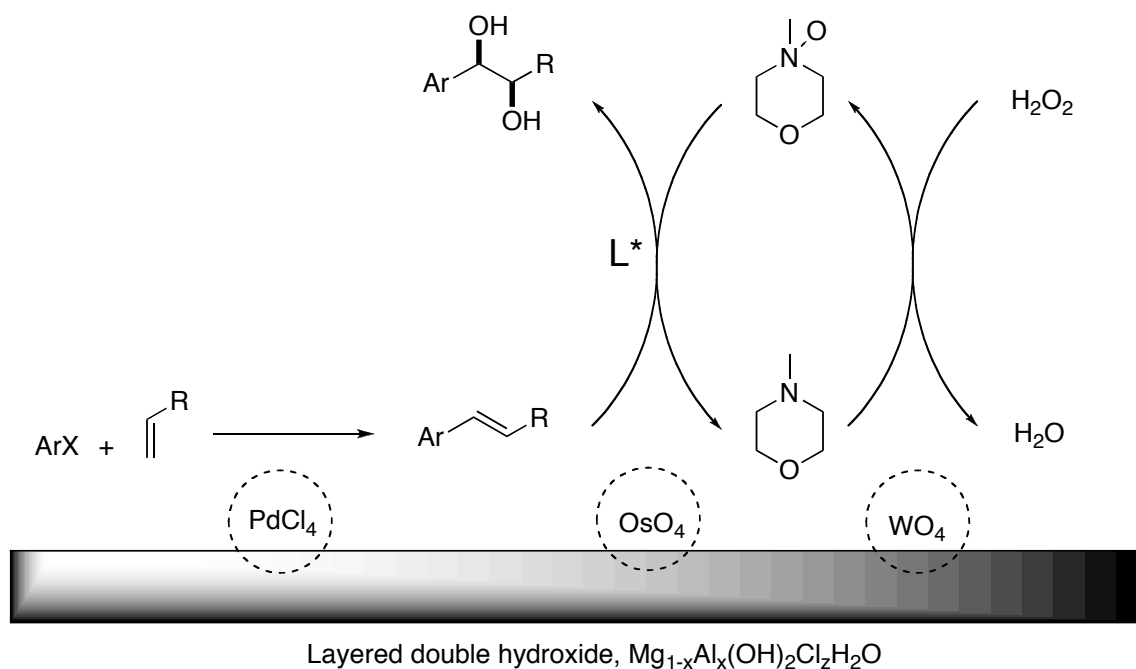


Figure 33. Trifunctional catalysts for tandem Heck/N-oxidation/asymmetric dihydroxylation catalysis.

Stille coupling reactions could essentially be catalytic in tin, however, most reports demonstrate stoichiometric amounts of tin activated alkene (*e.g.* $\text{RCH}=\text{CHSnBu}_3$) in reaction with substrate organic halides ($\text{R}'\text{X}$) in the presence of catalytic amounts of a palladium complex. Maleczka and co-workers have demonstrated the tandem, one-pot application of tin and palladium catalysts for cross-coupling reactions.⁸⁰ The sequence involves a hydrostannylation/Stille cross coupling process, where an activating agent is used to convert any stannyl by-products back to a tin hydride which allows for the palladium catalysed stannylation of halo-alkenes. Alkynyl compounds are stannylated using palladium-stannanes. This results in the formation of an alkenylstannane and $\text{Pd}(0)$. The $\text{Pd}(0)$ reacts with an alkenyl bromide which then reacts with the formed alkenyl

stannane resulting in cross-coupling, stannyl halide formation, and Pd(0) formation. The formed stannylchloride is converted back to a stannyl hydride via reaction with sodium carbonate. The resulting tin carbamate is converted using polymethylhydrosiloxane (PMHS) to a tin hydride. The tin hydride re-reacts with the Pd(0) catalyst, thus starting the catalytic cycle again (figure 34).

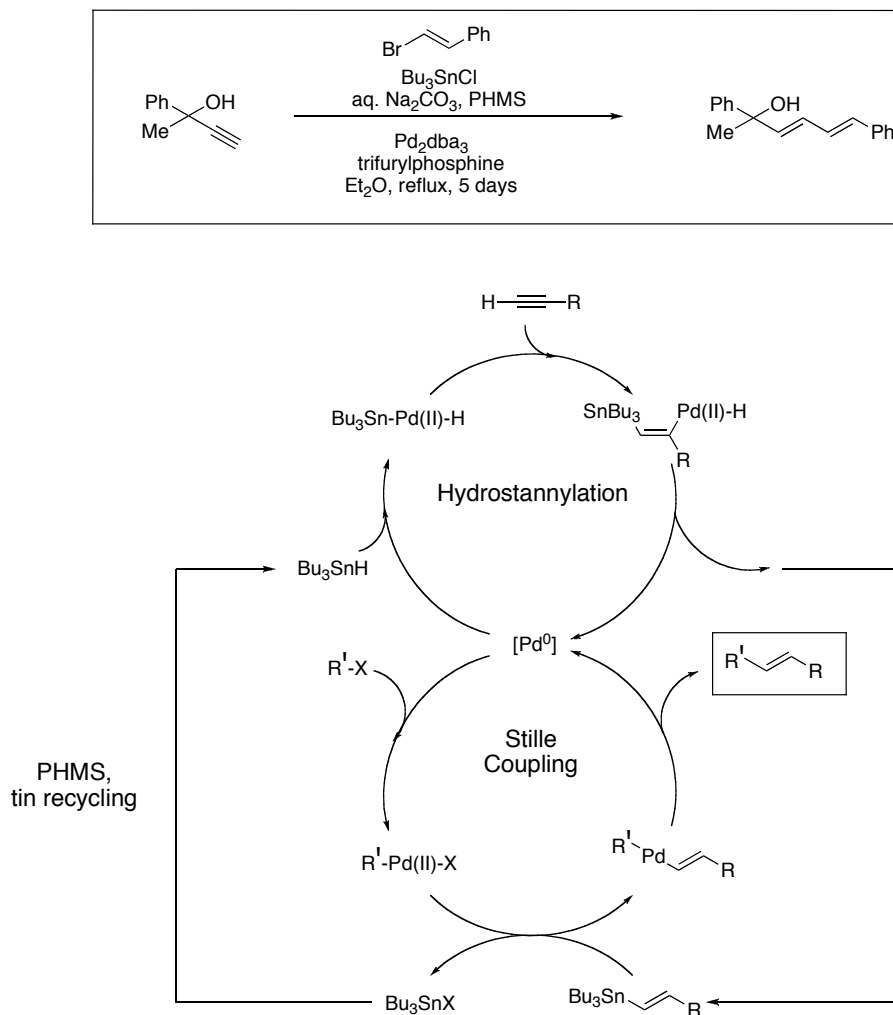


Figure 34. Tandem catalysed stannylation, Stille coupling reaction.

In a similar piece of work, Szabo and co-workers have developed systems which demonstrate sequential allylic stannylation/allylic alkylation catalysed by pincer-palladium complexes.⁸¹ However, stoichiometric amounts of stannylating reagent are used in the reported reaction sequence.

Functionalised heterocycles and fused polycyclic compounds have been synthesised in a multi-step, one pot procedure using ruthenium and platinum complexes in tandem.⁸² Ruthenium catalysed nucleophilic attack on a secondary alcohol is followed by platinum catalysed hydration of a propargyl group and subsequent platinum catalysed ring closing dehydration yields a functionalised furan (figure 35). If carried out in the presence of a primary amine, a pyrrole is synthesised. The same concept was applied for the synthesis of fused heterocycles using functionalised aromatics. Importantly, these reaction sequences do not, in principle, produce any carbonaceous side-products, with water being the only by-product. The yields observed are

reasonable (50-70% on average), and in the case of the fused polycyclic species the syn/anti selectivity levels are quite impressive (all >90%).

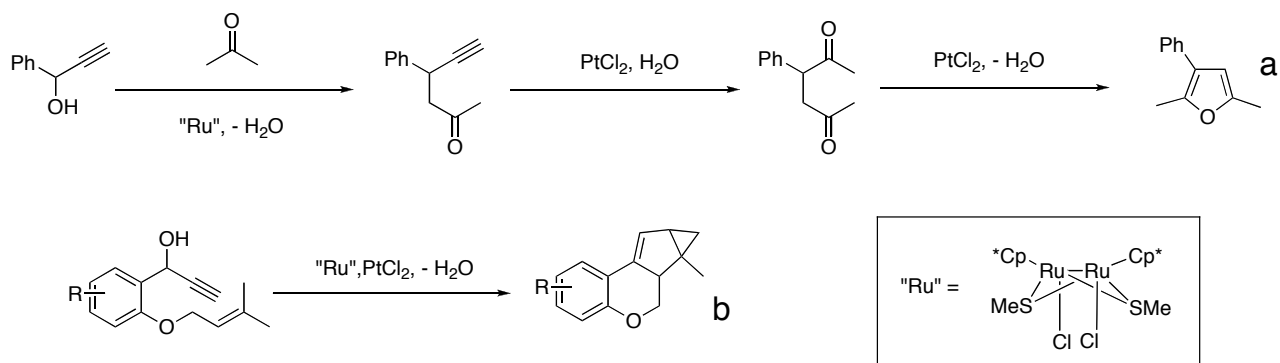


Figure 35. Sequential synthesis of functionalised heterocycles (a), and polycyclic fused heterocycles (b) using ruthenium/platinum catalysts.

1.3.2 Multi-Step One-Pot Catalysed Reactions Involving Carbonylation Catalysis

Hydroformylation catalysis is a standard technique for the introduction of functional groups to alkyl chains. It is often the first step in a complex synthetic procedure. Castillon has demonstrated the application of rhodium catalysts for the sequential hydroformylation/acetylation of terminal alkenes.⁸³ As a typical example furan was stirred in the presence of triethylorthoformate and pyridinium *p*-toluenesulphonate (PPTS) and under 50 bar CO/H₂. The desired diacetal was acquired in high yields, without any aldehyde formation observed. PPTS acts as the acetalisation catalyst, and does not inhibit the rhodium catalyst. This one-pot, two-step process shows a conversion to high value products which would otherwise require large amounts of solvent for purification. It also shows high selectivity for the desired product.

The Eilbracht group expanded upon this concept by applying hydroformylation in sequence with hydrogenation and Schiff-base chemistry allowing for the sequential synthesis of secondary and tertiary amines from alkenes and nitroso functionalised aromatics.⁸⁴ The reaction of methyl styrene with nitrobenzene in the presence of [Rh(COD)Cl]₂ and CO/H₂ yields the expected tertiary amine if an excess of methylstyrene is used. The sequential reaction involves the hydroformylation of the styrene resulting in an aldehyde. The nitrobenzene is simultaneously reduced to aniline which reacts with the formed aldehyde. By playing with reaction conditions, and substrate ratios it is possible to selectively synthesise either the mono-alkylated secondary amine, or bis-alkylated tertiary amine (figure 36).

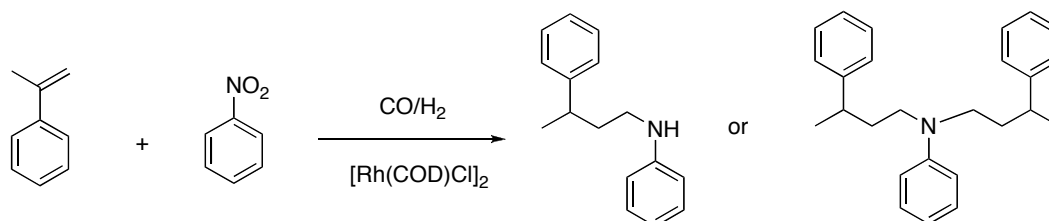


Figure 36. Sequential hydroformylation/hydrogenation/Schiff base catalysis for secondary and tertiary amines.

Carbonylation is also used in a mixed palladium/ruthenium mediated ester synthesis from aryl halides and formate functionalised species.⁸⁵ $[\text{Ru}_3(\text{CO})_{12}]$ was used simultaneously with PdCl_2 to synthesise benzoate esters from iodobenzene and 2-pyridinemethyl formate. The ruthenium complex catalyses the decarbonylation of formate resulting in the formation of free CO. The CO is believed to react with an aryl halide, mediated by palladium, resulting in a species that readily reacts with the carbonyl that is formed when decarbonylation occurs, providing the desired ester. It was found that the presence of a chelating substrate was essential for this reaction to occur. This reaction sequence contains an *in situ* ‘hydroformylation’ step that alleviates the necessity for high pressure CO, and also demonstrates a two-step sequence in high yields for the desired product with little side product formation.

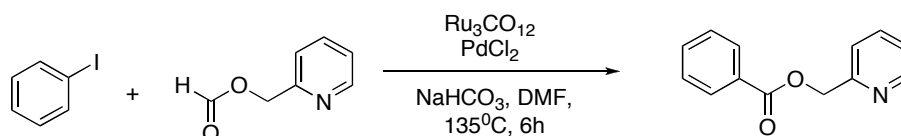


Figure 37. Sequential decarbonylation/hydroformylation for benzoate ester synthesis.

1.3.3 Multi-Step One-Pot Catalysed Reactions Involving Metathesis Catalysis

Brookhart and Goldman have recently demonstrated a beautiful sequential/tandem catalysed system for the up-conversion of lower alkanes to high value, higher alkanes.⁸⁶ The process involves using a dehydrogenation catalyst in sequence with a metathesis catalyst. An organometallic iridium pincer complex, which is a highly active transfer dehydrogenation catalyst, was applied in one-pot in sequence with a molybdenum ‘Schrock’ metathesis catalyst, in the presence of a small amount of dihydrogen accepting ethene. n-Hexane was added to the reaction mixture and the solution was heated. Initial transfer dehydrogenation of n-hexane yielding hexene and ethane is followed by cross-metathesis between formed hexene, yielding extra ethene in the process. The formed higher alkenes can subsequently act as dihydrogen acceptors as can the formed ethene. Internal isomerisation of any terminal alkene formed means that a wide range of metathesis products is possible, however the process shows yields for C_8 - C_{12} alkanes with very low amounts of lower alkanes (C_2 - C_5) observed.

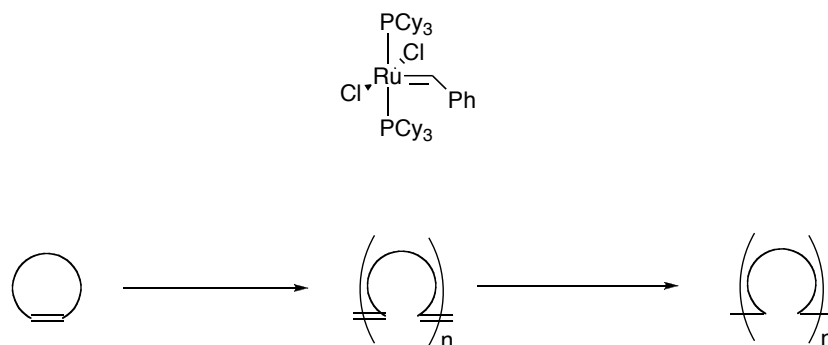


Figure 38. Sequential ROMP/Hydrogenation using ruthenium alkyldiene complex.

Fogg has demonstrated the application of ruthenium alkylidene Ring-Opening Metathesis Polymerisation (ROMP) catalysts for cyclized polymerisation/hydrogenation, one-pot catalysis.⁸⁷ ROMP of norbornenyl substrate using a ruthenium alkylidene complex was followed by the application of hydrogen pressure (1 atm) and base (NEt_3) to the reaction solution. This resulted in complete conversion of all double bonds (figure 38).

Ruthenium metathesis catalysts have shown to be tremendously stable and versatile, and thus have a large scope for application in multi-step catalytic sequences. This has been demonstrated in particular where the Grubbs ruthenium alkylidene catalysts have been applied for both metathesis and hydrogenation in one pot. Grubbs applied both his first and second generation ruthenium alkylidene complexes in the sequential ring closing, hydrogenation of diallylic substrates.⁸⁸ This involved a simple metathesis reaction mixture of substrate and catalyst (5 mol%) in halogenated solvent being stirred at 40°C until all starting material (e.g. diethyl diallyl malonate) had been consumed. Dihydrogen pressure (1 atm.) was then applied to the reaction vessel that was then heated to 70°C resulting in complete conversion of the intermediate alkene to the desired cycloalkane (figure 39).

In the same report, it was also shown that this concept could be applied for cross-metathesis reactions followed by either hydrogenation, or transfer hydrogenation, where ethylene diamine is added, to selectively hydrogenate either the formed metathesis product's C-C double bond, or transfer hydrogenate a ketone functionality that was introduced (figure 39). The cross metathesis reaction of styrene with methyl vinyl ketone yields an enone. The functionalities of the enone can be selectively addressed depending on whether hydrogen pressure is applied, or a diamine coligand and hydrogen transfer reagent is introduced. This procedure was demonstrated for the synthesis of a valuable fine chemical, Muscone, where ring-closing metathesis was followed by a transfer hydrogenation step, and then a hydrogenation step to yield the desired product in three steps without work-up.

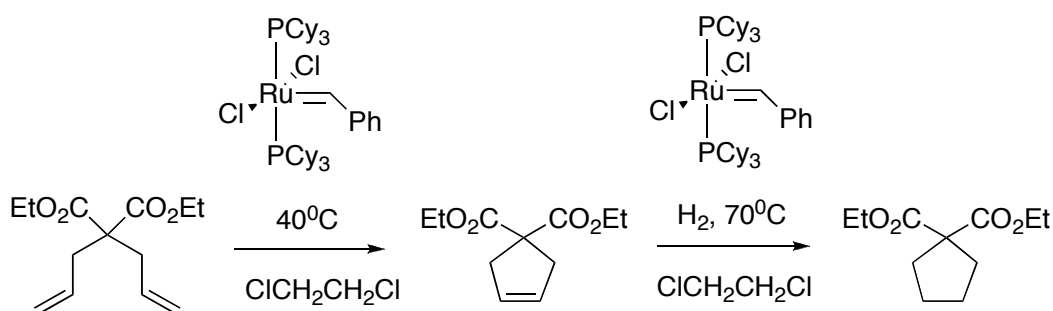


Figure 39. Tandem, single catalyst metathesis/hydrogenation sequences.

Similar to the aforementioned work, Cossy and co-workers have developed a system which has two catalysts working sequentially in cross-metathesis/hydrogenation reactions.⁸⁹ The cross metathesis reaction of ethyl acrylate with allyl triphenylsilane in the presence of Grubbs-II catalyst *and* under 1 bar H₂ showed a mixture of the expected reduced metathesis product (6% yield), the metathesis product and propyl triphenylsilane. However, upon the introduction of PtO₂ complete conversion of any formed metathesis product to the desired saturated ester was observed, with a

small amount of propyl silane side-product. It was mentioned that catalyst compatibility was key to the success of this sequence, with the ruthenium Grubbs-II catalyst being sensitive to the type of hydrogenation catalysis that was used. The same group later expanded upon this work demonstrating the application of the same system for cross-metathesis reactions followed by reduction of the formed unsaturated bond which results in a cyclisation reaction.⁹⁰ The one-pot, three step synthesis of lactones and lactols was demonstrated. In both cases it was observed that neither catalyst showed the desired activity/conversion levels in the respective catalysts reactions, demonstrating that the multi-catalyst route was essential. This work shows the facile combination of both homogeneous and heterogeneous catalysts in sequence giving high yielding selection for the desired product.

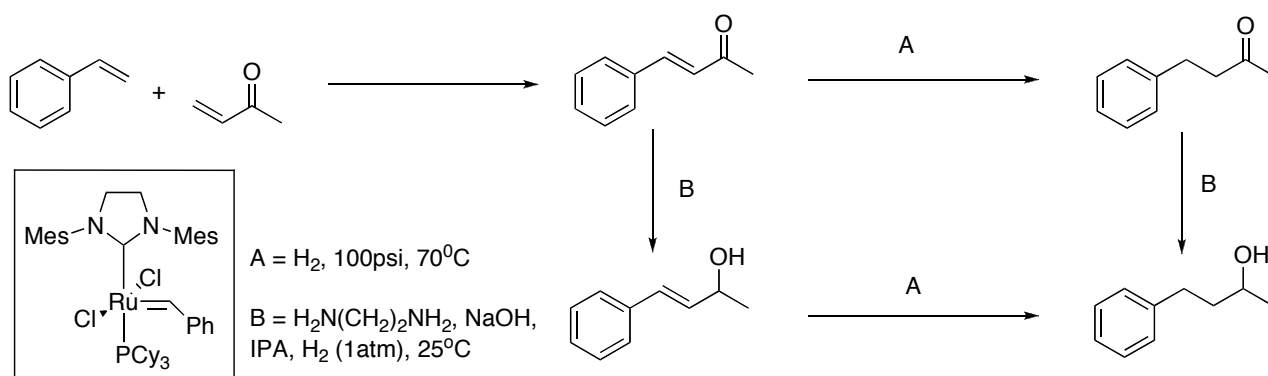


Figure 40. Sequential metathesis/ double hydrogenation yielding a secondary alcohol product.

Applying the catalysts that have taken his name, Grubbs and co-workers, have applied ruthenium alkylidene catalysts simultaneously for the synthesis of block copolymers (figure 41).⁹¹ It was found that a Grubbs I type catalyst was both active in ROMP and atom-transfer radical polymerisation (ATRP). The use of the ruthenium alkylidene complex as a catalyst for the one-pot simultaneous ATRP and ROMP yielded polymeric material containing both linear and branched polyalkene units bridged by an ester linker. Dihydrogen pressure was subsequently applied to the reaction mixture to reduce the double bonds using the remnant ruthenium complex yielding ester bridged polyalkane materials.

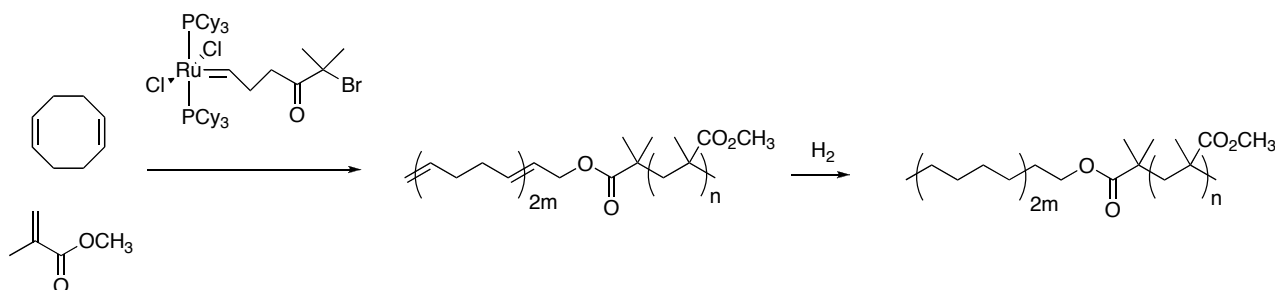


Figure 41. One-pot simultaneous ROMP/ATRP with sequential hydrogenation.

The Grubbs alkylidene catalysts have further shown to be highly versatile catalysts with recent work showing their application in sequential metathesis/Kharasch addition reaction sequences.⁹² The sequential ring closing metathesis of a diene is followed by the reaction of the

formed alkene with a perhalogenated carbon centre. This sequential procedure has been applied for both intra and inter molecular metathesis/Kharasch addition reactions. In the intermolecular reactions the reacting styrene is introduced after a certain period of time to allow the ring closing metathesis reaction to occur, and to ensure no undesired cross metathesis. In general, the reactions are high yielding, and demonstrate the synthesis of highly functionalised polycyclic molecules from acyclic precursors.

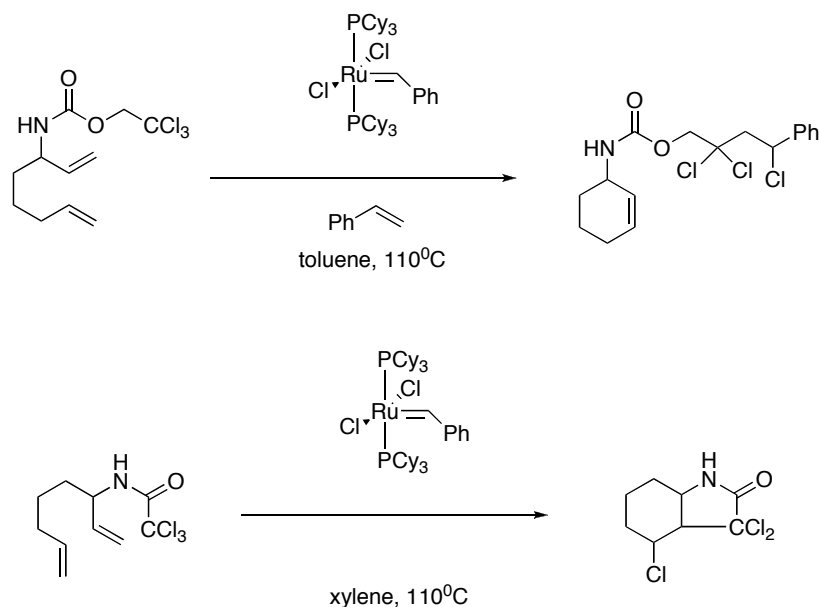


Figure 42. Sequential inter and intramolecular RCM/Kharasch addition reactions using Grubbs metathesis catalysts.

Several examples of metathesis catalysts being used in tandem with other catalysts have shown the importance of the metathesis catalysts to organic synthesis. One-pot olefin metathesis/Heck catalysis has demonstrated the effective synthesis of compounds containing multiple rings.⁹³ The Grubbs-I catalyst was applied in a ring-closing metathesis reaction yielding a substrate which favours intramolecular Heck catalysis in the presence of a Pd(0) source. Addition of Pd(OAc)₂, base and triphenylphosphine to the reaction mixture, post metathesis, allowed the formation of the Heck product (figure 43). The metathesis reaction was high yielding, as was the Heck coupling reaction, and overall yields in the two step, work-up free, reaction were generally around 80%. The downside to this work is the obvious incompatibility of the catalysts/ligands/promoters to the respective reactions. Adding both catalysts at the start and allowing the reaction to take place showed a very slow conversion to the desired final product, however yields were as high as 54%.

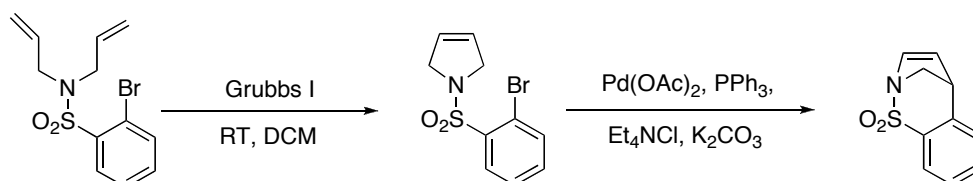


Figure 43. Sequential metathesis/Heck catalysis for polycyclic compounds.

1.3.4 Multi-Step One-Pot Catalysed Reactions Involving Enzymes and Organometallics in Sequence for Alcohol Deracemisation

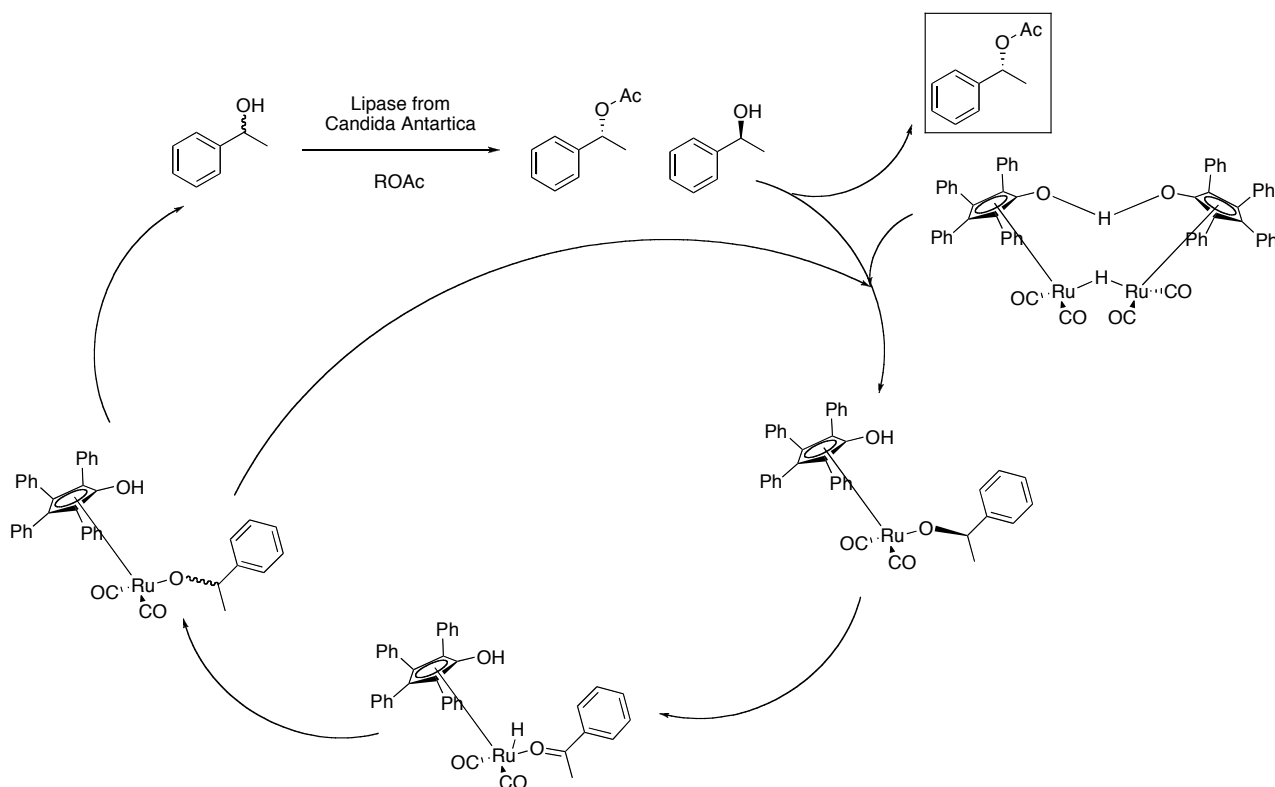


Figure 44. Dynamic kinetic resolution by sequential racemisation/enantioselective acylation of secondary alcohols.

Bäckvall has been to the fore in demonstrating the application of homogeneous catalysts in parallel with enzymes for the dynamic kinetic resolution of various substrates, in particular secondary alcohols.⁹⁴ The concept is based on the principle of selective acylation of a certain enantiomer of a secondary alcohol. Fundamentally the maximum yield from this reaction is 50%. However, what Bäckvall has ingeniously demonstrated is the application of a ruthenium complex in sequence with the acylating enzyme as an alcohol racemisation catalyst (figure 44).⁹⁵ An immobilised lipase from *Candida antarctica* was applied in the presence of a ruthenium catalyst showing high yields, and enantiomeric excess values of greater than 99% for a large range of substrates. The ruthenium catalyst racemises any alcohol that is present in the reaction pot by what is equivalent to dihydrogen abstraction yielding a ketone. The ketone is essentially *in equilibrium* with the formed ruthenium dihydride species and thus any secondary alcohol is inevitably racemised. The lipase present acylates, in the presence of acylating agents such as isopropenyl acetate, only one enantiomer of the secondary alcohol, and thus provides a mixture of enantiopure ester and a single (opposite) enantiomer of the secondary alcohol. The alcoholic single enantiomer is again racemised by the ruthenium catalyst. The entire process is carried out in toluene at 70°C, thus the conditions are not ideal, but relatively mild. However, the concept demonstrates the simple application of sequential catalysis for the synthesis of a high value product, the isolation of which, using standard techniques, would incur high costs both monetary and environmentally. Later work showed that the ruthenium catalyst was essential for the racemisation step, and that the

racemisation occurred in the coordination sphere of the ruthenium complex.⁹⁶ It was also found that ketone formation from the acylating substrate was detrimental to the process because the ketone formed (from esterification of the secondary alcohol) competes with the formed ketone from the deracemisation process, for the ruthenium dihydride. Later work from the same group has demonstrated the same principle for a wide range of systems, most notably for diols.⁹⁷

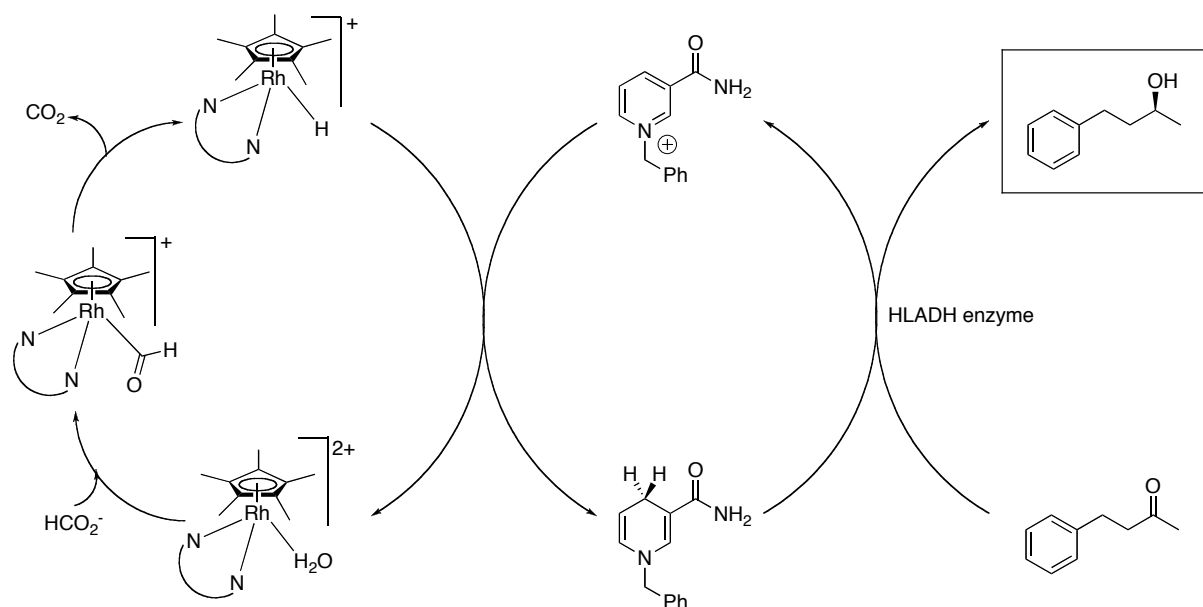


Figure 45. Tandem rhodium catalysed hydrogenation, and enzyme catalysed cofactor transfer hydrogenation.

Fish and co-workers have developed a similar system where an organometallic hydride source is used as a catalyst for the regeneration of a cofactor which is a dihydrogen source for an enzyme which in turn catalyses the asymmetric reduction of a ketone.⁹⁸ A rhodium hydride generated by the reaction of sodium formate with a rhodium(II) precursor reacts with a biomimetic co-factor yielding a hydrogenated pyridinium. This co-factor then reacts in the presence of an enzyme with an alkyl ketone, resulting in the asymmetric reduction of said ketone with high enantioselection. This process is carried out in one pot, with constant pH. Furthermore, no triggers were necessary to initiate any of the steps in the sequence, with every reaction occurring spontaneously. The same work demonstrates the use of simple model cofactor species as the ‘dihydrogen storage’ materials.

1.3.5 Miscellaneous Multi-Step Catalysed Reactions

Similar to the work by Chaudhari previously mentioned, Backvall has demonstrated the selective dihydroxylation of alkenes using homogeneous osmium catalysts in sequence with an organic catalyst for the oxidation of N-methylmorpholine (NMM).⁹⁹ NMM formed post activation of OsO₃ is reoxidised by catalytic flavin/H₂O₂. This means only catalytic amounts of NMM are necessary (figure 46). This is in essence a triply catalysed reaction and has been demonstrated for a range of *trans*-alkenes showing yields in the 90%’s. It was also demonstrated for *cis*-stilbene, however with lower yields. Replacements for NMM were also tried, however none showed comparable yields.

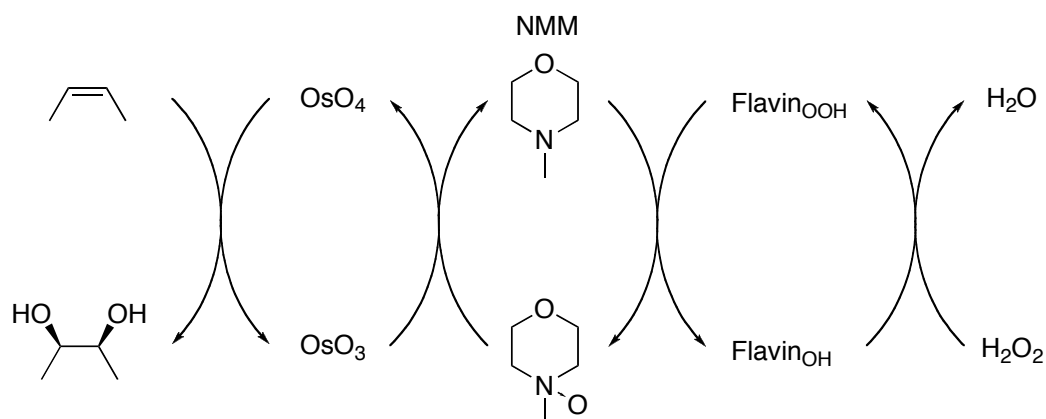


Figure 46. Sequential activation of NMM, OsO_3 , and dihydroxylation of olefins.

Incorporation of BINAP into polymeric chains has been carried out by Pu via Suzuki coupling reaction with a bisbrominated triaryl linker and 6,6'-bisboronate-BINAP (figure 47).¹⁰⁰ A protected BINOL species acts as a second “corner” to the polymer. It is in fact a bifunctional catalyst, which could be used in tandem reactions. Ruthenium introduction from $[\text{RuCl}_2(\text{benzene})]_2$ and subsequent addition of chiral DPEN gave the immobilised Noyori asymmetric hydrogenation catalyst.

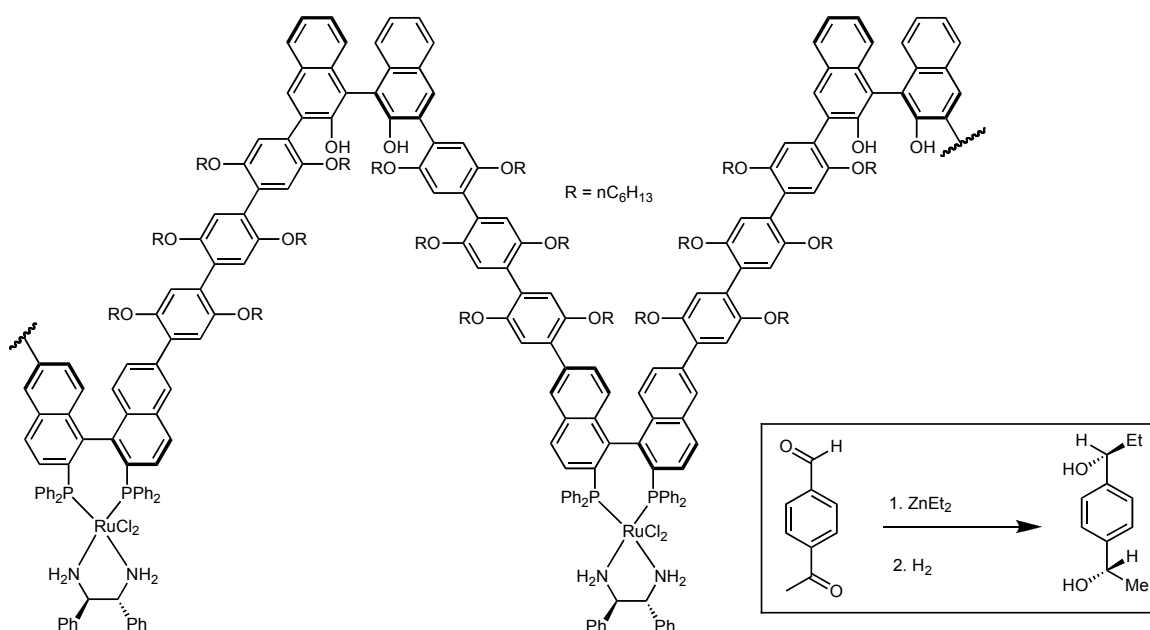


Figure 47. Bifunctional $[\text{BINAP-RuCl}_2\text{-DPEN}]\text{-BINOL}$ hybrid, for use in bifunctional catalysis.

This catalyst was tested in a tandem asymmetric addition and hydrogenation, and showed $>99\%$ conversion throughout the catalytic runs on *meta*- and *para*- acetyl substituted benzaldehyde substrates as seen in figure 47. The reaction involved a trigger point, after the diethylzinc addition was believed to be complete, dihydrogen pressure was applied and transfer hydrogenation substrates were added. The enantiomeric excess was consistently high (94%) for all substrates in the diethylzinc addition, however the diastereomeric excess was lower for the hydrogenation, at around 87%. In terms of the *meta*-acetyl benzaldehyde, the *de* value was as low as 75%. All of

these results are similar to the monomeric catalysts under the same conditions. The catalyst has also been shown to be active in the AH of acetophenone, where it showed similar *ee*'s to that of the monomeric system, but also very high catalytic turnover numbers. The great benefit of this catalyst is the ability to recycle the catalyst, and remove the catalyst from the reaction mixture by simple precipitation and filtration.

Shibasaki has demonstrated the one-pot two-step synthesis of chiral alcohols from α,β -unsaturated amides using a samarium epoxidation catalyst in sequence with palladium on charcoal.¹⁰¹ A samarium BINOL derivative is used for the asymmetric epoxidation (TBHP oxidant) of said alkenes in almost quantitative yields and *ee*'s for most substrates exceeding 99%. It was also demonstrated that the formed epoxides could be opened using H₂ over Pd/C yielding a chiral alcohol. Depending on the substrate, selectivity for the desired alcohol was quantitative (no dehydration or ketone products observed). The tandem reaction was performed by addition of Pd/C and MeOH to the post epoxidation mixture and applying hydrogen pressure. Yields were in the 90%'s and *ee* values for the formed secondary alcohol were generally >97%. This tandem process was furthermore demonstrated for a commercially valuable peptide sequence precursor, showing high yield and *ee* values of 99%.

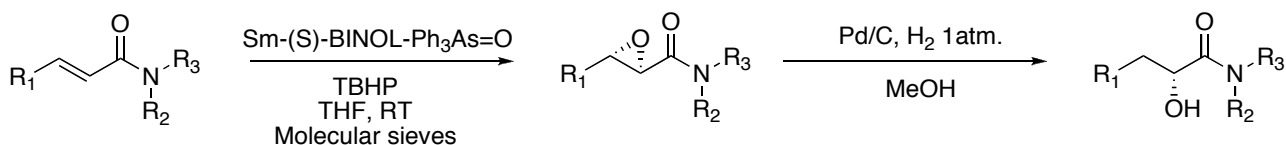


Figure 48. Sequential asymmetric epoxidation/hydrogenation for chiral alcohol synthesis.

Titanium and palladium catalysed C-heteroatom bond formation has been applied for multi-step synthetic procedures for the synthesis of indoles.¹⁰² A titanium catalysed intramolecular hydroamination results in an imine, which, in the presence of base, is in equilibrium with an enamine. The formed enamine reacts intramolecularly via a palladium catalysed aromatic carbon-heteroatom coupling reaction yielding an indole. A range of *ortho*-chlorosubstituted 1-phenyl-2-alkyl alkynes has been reacted with a range of primary amines, resulting in a library of indoles derived from simple precursors. Practically the reaction is in principle a two-step reaction. The reaction mixture is charged with the titanium catalyst, and the hydroamination reaction is allowed to proceed. After that reaction is complete Pd₂(dba)₃, base and dioxane are added to allow the N-arylation reaction to proceed. The yields in the reaction are in general high (60-80%), and this reaction should, in principle, have no side products because all atoms are used in the product.

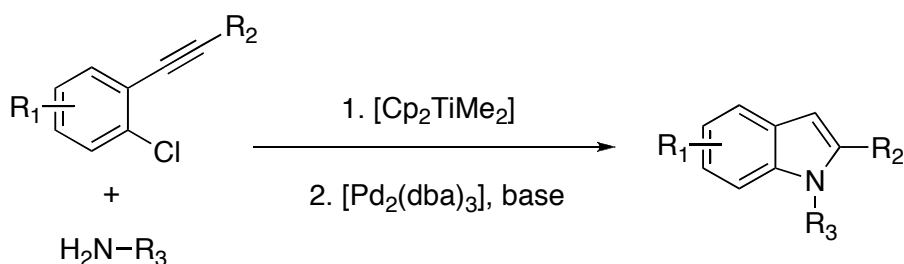


Figure 49. Sequential C-N bond forming reactions for indole synthesis.

1.3.6 Tandem Catalysis with Immobilised Catalysts

Sheldon and co-workers are to the fore in using immobilised enzymes, and enzymes in multi-step reactions for organic synthesis.¹⁰³ A cationic rhodium phosphoramidite complex has been immobilised on a charged anionic alumina and applied in the asymmetric hydrogenation of an enamide.¹⁰⁴ *Ee* levels in the high 90's% were observed, and were found to be highly solvent dependent. The immobilised catalyst was found to be recyclable over four cycles without a loss in *ee* or yields. A later piece of work has demonstrated the application in sequence of an enzyme after the hydrogenation of the enamide (figure 50).¹⁰⁵ Post-hydrogenation filtration of the catalysts gives an aqueous solution containing the formed chiral protected amino acid which is directly transferred to a pot containing an acylase and buffer solution. The acylase carries out the hydrolysis of the amide bond, and cleaves the ester group yielding enantiopure (*ee* = 98%) amino acid in high overall yield (>95%).

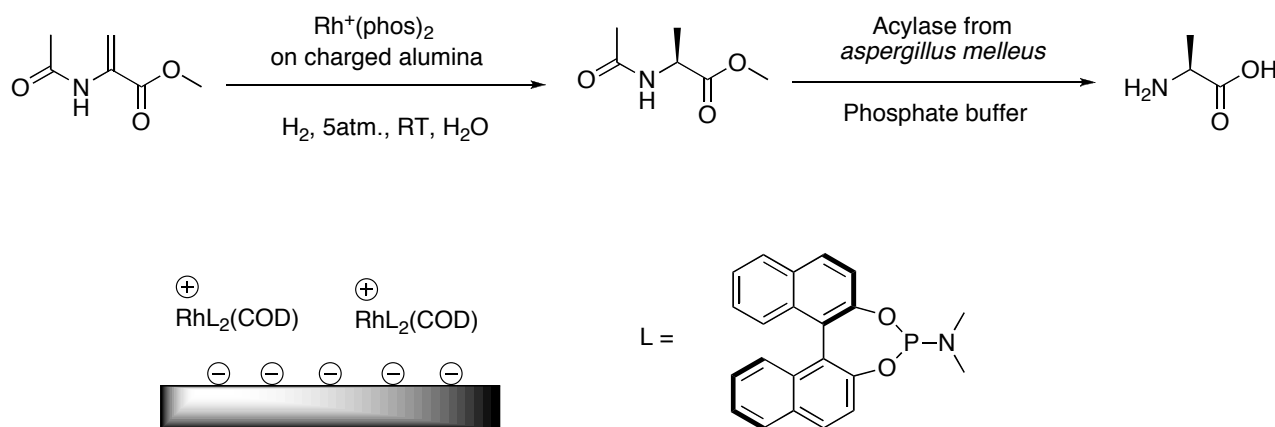


Figure 50. Sequential hydrogenation, deprotection steps using immobilised rhodium catalyst and an acylase.

1.3.7 Conclusions to be taken from Multi-pot Catalysis Section

Although multi-step one-pot catalysis is a field with a strong foothold in homogeneous catalysis one feels that there are still goals to be reached to develop systems that can be reliably used on an industrial scale. Quite often, it seems, the reaction sequences described are dependent on a specific substrate and are not applicable in a broad sense. Solvent compatibility is not a controlling factor, which was often not believed to be the case, however catalyst compatibility is certainly the governing factor in determining whether a certain reaction sequence is plausible.

Catalyst separation has not been addressed at all in this field, which claims to be fundamentally green. In our opinion the application of sequential catalysis is useless without the proviso that the separation of the various reactants, catalysts and products is also an efficient, environmentally benign process. Solvent waste reduction, which is the goal here, is not addressed when the catalysts are not easily separated from the products, no matter how many work-up steps have been alleviated. Compartmentalisation of catalysts by immobilisation could open this field. A catalyst could be placed (compartmentalised) in a certain time frame in a continuous flow system,

resulting in certain reactions in a sequence occurring at a precise time, and then moving on to the next catalytic site in the next time frame.

1.4 Aims and Scope of this Thesis

One of the inherent problems with all of the previously mentioned sequential catalysed syntheses is catalyst stability to other reactions, and catalyst recovery. Firstly, catalyst stability limits the field of one-pot tandem catalysis because catalyst compatibility is essential for a successful system. All catalysts present in the system must be stable/reactive in the presence of the reacting functionalities in preceding/subsequent reactions, the conditions of the other reactions, and the solvent. To overcome this problem several attempts have been made at applying a single catalyst in different catalytic reactions in one reaction sequence. This topic has recently been reviewed elsewhere.¹⁰⁶ Secondly, to carry out multiple steps in a reaction sequence without work-up is only half the story when the catalysts still need to be recovered after the multi-step reaction. The process of homogeneous catalyst recovery, whether the complex is intact or not, results in solvent waste and the connected high costs. By performing multi-step, one-pot processes it has been demonstrated that intricate organic fine chemicals can be synthesised with minimal work-up and intermediate isolation. However, the final hurdle to make the entire process an efficient and 'green' process has not been taken, and to date we have found few examples of any domino or tandem catalytic processes using immobilised catalysts.

An as of now undefined process, that we wish to introduce here, is sequential compartmentalised tandem catalysis (SCTC), defined as "*a multi-step reaction sequence involving no intermediate isolation steps, and no work-up at any point in the reaction sequence, in a catalyst-compartmentalised system*". Both Domino and Tandem catalysis have similarities with SCTC, however catalyst compartmentalisation allows for a much broader scope. This is because sequential catalysis does not necessarily have to be a one-pot process as the other processes are. SCTC can be described as a reciprocal of concurrent tandem catalysis (CTC). CTC is defined as (Bazan)¹⁰⁷ '*a sequence which contains two or more catalytic reactions in one pot, where all catalysts and reagents are compatible*'.

The aims of the research described in this thesis are simply put 'to combine the fields of homogeneous catalyst immobilisation and multi-step catalysis'. We wish to develop a range of immobilised homogeneous catalysts for a broad range of the most important reactions to the modern industrial organic chemist. We wish to apply the developed heterogenised homogeneous catalysts in a sequential manner for the synthesis of fine chemicals/fine chemical precursors. If successful this work will demonstrate the compartmentalisation of catalysts, as Nature does, for multi-step reaction sequences with non-natural catalysts. This process will ultimately be a Green process as described by the '12 principles of Green chemistry':

- Principle 1, Waste Prevention: Less work-up steps mean less solvent waste.
- Principle 2, Atom Economy: System will be designed to be highly efficient.
- Principle 6, Design for Energy Efficiency: Less waste, and less work-up means high energy conservation.
- Principle 9, Catalysis: as described herein.

The SCTC concept is schematically demonstrated in figure 51. Theoretical reactants ‘A’ and ‘B’ can react to yield product ‘AB’ in the presence of catalyst ‘X’. The reaction mixture containing ‘AB’ can then be transferred to a new reaction vessel with the removal of catalyst ‘X’ by simple decantation/filtration. Substrate ‘C’ could be introduced with a different catalyst, ‘Y’, which catalyses the reaction of ‘AB’ with ‘C’ yielding ‘ABC’, which can be isolated by simple filtration of catalyst ‘Y’.

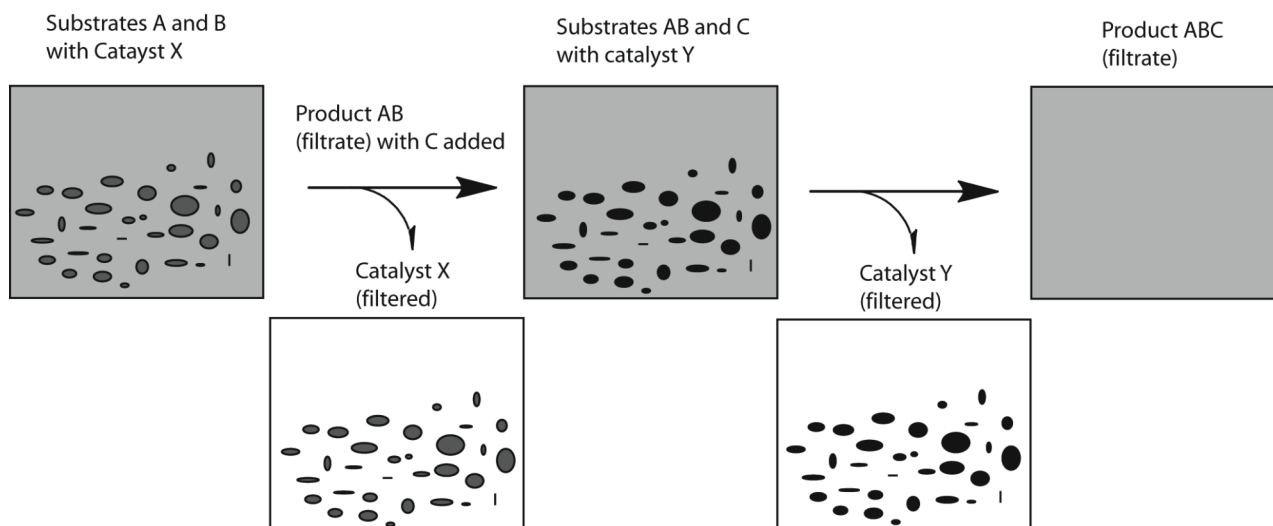


Figure 51. Schematic depiction of sequential compartmentalised tandem catalysis, SCTC.

To facilitate the immobilisation of homogeneous catalysts the development of materials and functionalised homogeneous catalysts (in this study organometallic complexes), which can easily be coupled with each other, is essential. In this thesis several techniques for the simple, atom efficient immobilisation of organometallic complexes on inorganic silica are presented (chapter 2). This involves the synthesis of silica materials with functionalities for simple reaction with organometallic catalysts. Likewise the development of organometallics with functionalities allowing anchoring via standard, atom efficient, synthetic methods is presented.

Organometallic complexes functionalised with nucleophilic groups (amino- or alcoholic groups) for immobilisation on silica via reaction with isocyanate groups bound to the silica surface are developed (chapters 2 and 5 for alcohol, chapter 4 for amine). Furthermore, ethynyl functionalised organometallics are presented for reaction with azide functionalised silica in a copper(I) catalysed 1,3-Huisgens cycloaddition reaction (chapters 2 and 3). These so-called click immobilisation techniques demonstrate facile immobilisation of homogeneous catalysts for immediate use.

A range of catalytic materials that can be applied in Lewis acid catalysis, allylic stannylations/alkylations (chapter 2), dehydrogenation and metathesis (chapter 5), epoxidation (chapters 3 and 5), asymmetric hydrogenation (chapters 4 and 5), and hydroxycarbonylation (chapter 6), are developed. The materials all consist of an inorganic support with a tethered organometallic unit bound to the surface of the support. All materials are insoluble in standard organic solvents. All novel materials were applied in their respective reactions, demonstrating an –

off-the shelf ease of catalyst immobilisation and application. All the catalytic materials have been applied in their respective ‘heterogeneously’ catalysed reactions, some showing activity and selectivity comparable to their homogeneous analogues. The developed catalytic materials, because of their heterogeneous nature, can be easily separated from reaction solutions using simple decantation or filtration techniques. The separated catalysts have also been applied repetitively to demonstrate their recyclability, and stability. In the cases where the catalytic material was not recycled or recyclable an investigation was carried out to discover why this was so, and in some cases has given enlightenment as to the catalytic reaction mechanism, and to the stability of the organometallic species.

Sequential Compartmentalised Tandem Catalysis is presented (chapters 2 and 5), where multi-pot work-up free reaction sequences are carried out for the multi-step synthesis of valuable fine chemicals. Transfer dehydrogenation catalytic material has been applied in sequence with three separate catalytic materials. A reaction mixture, post-dehydrogenation of an alkane (thus mixture contains alkene and alkane, catalytic material has been filtered away) has been introduced to a separate reaction ‘compartment’ containing a Grubbs-II catalyst tethered to silica and a functionalised alkene. Cross-metathesis occurs, resulting in a bis-ester functionalised alkene, formed in two-steps, without work-up, from an unreactive alkane. Likewise the post-dehydrogenation solution is transferred to a reaction vessel containing an epoxidation catalyst and oxidant, resulting in the synthesis of an epoxide, formed in two-steps, without work-up, from an unreactive alkane. Finally, a reaction solution from the dehydrogenation of a racemic secondary alcohol, is introduced to a vessel containing an asymmetric hydrogenation catalyst, resulting in the quantitative deracemisation of the secondary alcohol.

1.5 References

- ¹D. E. De Vos, I. F. J. Vankelecom, P. A. Jacobs [Eds. Weinheim]; Chiral Catalyst Immobilization and Recycling, **2000**. Wiley-VCH.
- ²H.-U. Blaser. *Chem. Commun.* **2003**, 293-296.
- ³This statement applies to the field of fine chemical synthesis, however in polymerisation catalysis, this is not often the case. However, in the polymerisation case the homogeneous catalyst is often *not* removed from the reaction mixture post-catalysis.
- ⁴B. Cornils, W. A. Herrmann, *J. Catal.* **2003**, 216, 23-31.
- ⁵(a) D. J. Cole-Hamilton, *Science* **2003**, 299, 1702-1706. (b) K. Fodor, S. G. A. Kolmschot, R. A. Sheldon, *Enantiomer* **1999**, 4, 497-511.
- ⁶(a) C. E. Song, S. Lee, *Chem. Rev.* **2002**, 102, 3495-3524. (b) J. M. Notestein, A. Katz, *Chem. Eur. J.* **2006**, 12, 3954-3965. (c) A. Corma, H. Garcia, *Adv. Synth. Catal.* **2006**, 348, 191-1412.
- ⁷(a) G. R. Newkome, H. He, C. N. Moorefield, *Chem. Rev.* **1999**, 99, 1689-1746. (b) L. J. Twyman, A. S. H. King, I. K. Martin, *Chem. Soc. Rev.* **2002**, 31, 69-82. (c) R. van Heerbeek, P. C. J. Kamer, P. W. N. M. van Leeuwen, J. N. H. Reek, *Chem. Rev.* **2002**, 102, 3717-3756. (d) G. P. M. van Klink, G. van Koten, *C.R. Chimie* **2003**, 6(8-10), 1079-1085. (e) Y. Ribourbouille, G. D. Engel, L. H. Gade, *C.R. Chimie* **2003**, 6, 1087-1096. (f) P. A. Chase, R. J. M. Klein Gebbink, G. van Koten, *J. Organometallic Chem.* **2004**, 689, 4016-4054. (g) R. van de Coevering, R.J.M. Klein Gebbink, G. van Koten, *Prog. Polym. Sci.* **2005**, 30, 474-490. (h) A. Berger, R. J. M. Klein Gebbink, G. van Koten, *Topics in Organometallic Chemistry* **2006**, 20(Dendrimer Catalysis), 1-38. (i) R. Andres, E. De Jesus, J.-C. Flores, *New J. Chem.* **2007**, 31, 1161-1191. (j) S.-H. Hwang, C. D. Shreiner, C. N. Moorefield, G. R. Newkome, *New J. Chem.* **2007**, 31, 1192-1217.
- ⁸(a) S. J. Shuttleworth, S. M. Allin, P. K. Sharma, *Synthesis* **1997**, 1217-1239. (b) D. E. Bergbreiter, *Catal. Today* **1998**, 42, 389-397. (c) S. J. Shuttleworth, S. M. Allin, R. D. Wilson, D. Nasturica, *Synthesis* **2000**, 8, 1035-1074. (d) B. Clapham, T. S. Reger, K. D. Janda, *Tetrahedron* **2001**, 57, 4637-4662. (e) T. J. Dickerson, N. N. Reed, K. D. Janda, *Chem. Rev.* **2002**, 102, 3325-3344. (f) S. Kobayashi, R. Akiyama, *Chem. Commun.* **2003**, 449-460. (g) P. Mastrolilli, C. F. Nobile, *Coord. Chem. Rev.* **2004**, 248, 377-395.
- ⁹(a) W. A. Herrmann, C. W. Kohlpaintner, *Angew. Chem. Int. Ed. Engl.* **1993**, 32, 1524-1544. (b) P. G. Jessop, T. Ikariya, R. Noyori, *Chem. Rev.* **1999**, 99, 475-493. (c) E. de Wolf, G. van Koten, B.-J. Deelman, *Chem. Soc. Rev.* **1999**, 28, 37-41. (d) R. H. Fish, *Chem. Eur. J.* **1999**, 5, 6, 1677-1680. D. Sinou, *Adv. Synth. Catal.* **2002**, 344, 221-237. (e) G. Pozzi, I. Shepperson, *Coord. Chem. Rev.* **2003**, 242, 115-124. (f) C. Baudequin, J. Baudoux, J. Levillain, D. Cahard, A. -C. Gaumont, J. -C. Plaquevent, *Tetrahedron; Asymm.* **2003**, 14, 3081-3093. (g) C. Eui Song, *Chem. Commun.* **2004**, 1033-1043. (h) F. Fache, *New J. Chem.* **2004**, 28, 1277-1283. (i) B. Cornils, W. A. Herrmann, I. T. Horvath, W. Leitner, S. Mecking, H. Olivier-Bourbigou, D. Vogt, *Multiphase Homogeneous Catalysis* **2005**, Wiley-VCH.
- ¹⁰Q.-H. Fan, Y.-M. Li, A. S. C. Chan, *Chem. Rev.* **2002**, 102, 3385-3466.
- ¹¹I. F. J. Vankelecom, *Chem. Rev.* **2002**, 102, 3779-3810.
- ¹²(a) H. P. Dijkstra, G. P. M. van Klink, G. van Koten, *Acc. Chem. Res.* **2002**, 35, 798-810. (b) C. Müller, M. G. Nijkamp, D. Vogt, *Eur. J. Inorg. Chem.* **2005**, 4011-4021.
- ¹³A. Bruggink, R. Schoevaart, T. Kieboom, *Org. Proc. R & D* **2003**, 7, 622-640.
- ¹⁴M. Studer, H.-U. Blaser, C. Exner, *Adv. Synth. Catal.* **2003**, 345, 45-65.
- ¹⁵(a) A. Hu, H. L. Ngo, W. Lin, *J. Am. Chem. Soc.* **2003**, 125, 11490-11491. (b) L.-X. Dai, *Angew. Chem. Int. Ed.* **2004**, 43, 5726-5729.
- ¹⁶A. Hu, H. L. Ngo, W. Lin, *Angew. Chem. Int. Ed.* **2003**, 42, 6000-6003.
- ¹⁷A. Hu, G. T. Yee, W. Lin, *J. Am. Chem. Soc.* **2005**, 127, 12486-12487.
- ¹⁸B. Kesanli, W. Lin, *Chem. Commun.* **2004**, 2284-2285.

- ¹⁹ A. Ghosh, R. Kumar, *J. Catal.* **2004**, *228*, 386-396.
- ²⁰ (a) C. Bianchini, D. G. Burnaby, J. Evans, P. Frediani, A. Meli, W. Oberhauser, R. Psaro, L. Sordelli, F. Vizza, *J. Am. Chem. Soc.* **1999**, *121*, 5961-5971. (b) C. Bianchini, V. dal Santo, A. Meli, W. Oberhauser, R. Pisaro, F. Vizza, *Organometallics* **2000**, *19*, 2433-2444. (c) C. Bianchini, P. Barbaro, V. Dal Santo, R. Gobetto, A. Meli, W. Oberhauser, R. Psaro, F. Vizza, *Adv. Synth. Catal.* **2001**, *343*, 41-45.
- ²¹ B. Pugin, H. Landert, F. Spindler, H.-U. Blaser, *Adv. Synth. Catal.* **2002**, *344*, 974-979.
- ²² H.-U. Blaser, B. Pugin, F. Spindler, A. Togni, *C.R. Chemie* **2002**, *5*, 379-385.
- ²³ (a) B. Pugin, *J. Mol. Catal. A: Chemical* **1996**, *107*, 273-279. (b) B. Pugin, M. Muller, *Stud. Surf. Sci. Catal.* **1993**, *78*, 107-114.
- ²⁴ K. J. Stanger, J. W. Wiench, M. Pruski, R. J. Angelici, *J. Mol. Catal. A: Chemical* **2003**, *195*, 63-82.
- ²⁵ C. Saluzzo, M. Lemaire, *Adv. Synth. Catal.* **2002**, *344*, 915-927.
- ²⁶ Q.-H. Fan, Y.-M. Chen, X.-M. Chen, D.-Z. Jiang, F. Xi, A. S. C. Chan, *Chem. Commun.* **2000**, 789-790.
- ²⁷ (a) G.-J. Deng, Q.-H. Fan, X.-M. Chen, G.-H. Liu, *J. Mol. Catal. A: Chemical* **2003**, *193*, 21-25. (b) G.-J. Deng, B. Yi, Y.-Y. Huang, W.-J. Tang, Y.-M. He, Q.-H. Fan, *Adv. Synth. Catal.* **2004**, *346*, 1440-1444.
- ²⁸ G.-J. Deng, Q.-H. Fan, X.-M. Chen, D.-S. Liu, A. S. C. Chan, *Chem. Commun.* **2002**, 1570-1571.
- ²⁹ Y. -C. Chen, T. -F. Wu, L. Jiang, J. -G. Deng, H. Liu, J. Zhu, Y. -Z. Jiang, *J. Org. Chem.* **2005**, *70*, 1006.
- ³⁰ (a) W. Liu, C. Chi, L. Cun, J. Zhu, J. Deng, *Tetrahedron: Asymm.* **2005**, *16*, 2525-2530. (b) W. Liu, J. Wu, J. Zhu, J. Deng, Q. Fan, *Synlett* **2005**, 1591-1595.
- ³¹ C. K. Ralph, O. M. Akotsi, S. H. Bergens, *Organometallics* **2004**, *23*, 1484-1486.
- ³² Y. Liang, Q. Jing, X. Li, L. Shi, K. Ding, *J. Am. Chem. Soc.* **2005**, *127*, 7694-7695.
- ³³ X. Wang, K. Ding, *J. Am. Chem. Soc.* **2004**, *126*, 10524-10525.
- ³⁴ Q.-H. Fan, G.-J. Deng, C.-C. Lin, A. S. C. Chan, *Tetrahedron Asymm.* **2001**, *12*, 1241-1247.
- ³⁵ S. Doherty, E. G. Robins, I. Pál, C. R. Newman, C. Hardacre, D. Rooney, D. A. Mooney, *Tetrahedron Asymm.* **2003**, *14*, 1517-1527.
- ³⁶ R. ter Halle, E. Schulz, M. Lemaire, *Synlett* **1997**, 1257-1258.
- ³⁷ F. Locatelli, P. Gamez, M. Lemaire, *J. Mol. Catal. A: Chemical* **1998**, *135*, 89-98.
- ³⁸ D. J. Bayston, C. B. Travers, M. E. C. Polywka, *Tetrahedron Asymm.* **1998**, *9*, 2015-2018.
- ³⁹ T. Lamouille, C. Saluzzo, R. ter Halle, F. Le Guyader, M. Lemaire, *Tetrahedron Lett.* **2001**, *42*, 663-664.
- ⁴⁰ M. Berthod, C. Saluzzo, G. Mignani, M. Lemaire, *Tetrahedron Asymm.* **2004**, *15*, 639-645.
- ⁴¹ M. Berthod, J. -M. Joerger, G. Mignani, M. Vaultier, M. Lemaire, *Tetrahedron Asymm.* **2004**, *15*, 2219-2221.
- ⁴² S. -G. Lee, Y. J. Zhang, J. Y. Piao, H. Yoon, C. E. Song, J. H. Choi, J. Hong, *Chem. Commun.* **2003**, 2624-2625.
- ⁴³ K. T. Wan, M. E. Davis, *Tetrahedron Asymm.* **1993**, *4*, 2461-2468.
- ⁴⁴ (a) K.T. Wan, M. E. Davis, *J. Catal.* **1994**, *148*, 1-8. (b) K. T. Wan, M. E. Davis, *Nature* **1994**, *370*, 449-450. (c) K. T. Wan, M. E. Davis, *J. Catal.* **1995**, *152*, 25-30.
- ⁴⁵ J. Bayardon, M. Cavazzini, D. Maillard, G. Pozzi, S. Quici, D. Sinou, *Tetrahedron: Asymm.* **2003**, *14*, 2215-2224.
- ⁴⁶ M. Weck, C. W. Jones, *Inorg. Chem* **2007**, *46*, 1865-1875.
- ⁴⁷ D. E. Bergbreiter, *Chem. Rev.* **2002**, *101*, 3345-3384.
- ⁴⁸ D. E. Bergbreiter, P. L. Osborn, Y.-S. Liu, *J. Am. Chem. Soc.* **1999**, *121*, 9531-9538.
- ⁴⁹ D. E. Bergbreiter, J. Li, *Chem. Commun.* **2004**, 42-43.

- ⁵⁰ (a) D. E. Bergbreiter, P. L. Osborn, A. Wilson, E. M. Sink, *J. Am. Chem. Soc.* **2000**, *122*, 9058-9064. (b) D. E. Bergbreiter, P. L. Osborn, J. D. Frels, *J. Am. Chem. Soc.* **2001**, *123*, 11105-11106.
- ⁵¹ K. Okamoto, R. Akiyama, H. Yoshida, T. Yoshida, S. Kobayashi, *J. Am. Chem. Soc.* **2005**, *127*, 2125-2135.
- ⁵² (a) R. Chanthateyanonth, H. Alper, *J. Mol. Catal. A: Chemical* **2003**, *201*, 23-31. (b) R. Chanthateyanonth, H. Alper, *Adv. Synth. Catal.* **2004**, *346*, 1375-1384.
- ⁵³ M. Poyatos, F. Márquez, E. Peris, C. Claver, E. Fernandez, *New J. Chem.* **2003**, *27*, 425-431.
- ⁵⁴ (a) K. Yu, W. Sommer, M. Weck, C. W. Jones, *J. Catalysis* **2004**, *226*, 101-110. (b) W. J. Sommer, K. Yu, J. S. Sears, Y. Ji, X. Zheng, R. J. Davis, C. D. Sherrill, C. W. Jones, M. Weck, *Organometallics* **2005**, *24*, 4351-4361. (c) K. Yu, W. Sommer, J. M. Richardson, M. Weck, C. W. Jones, *Adv. Synth. Catal.* **2005**, *347*, 161-171.
- ⁵⁵ N. T. S. Phan, M. van der Sluys, C. W. Jones, *Adv. Synth. Catal.* **2006**, *348*, 609-679.
- ⁵⁶ A. Corma, H. Garcia, *Chem. Rev.* **2003**, *103*, 4307-4365.
- ⁵⁷ J. M. Fraile, J. A. Mayoral, A. J. Royo, R. V. Salvador, B. Altava, S. V. Luis, M. I. Burguete, *Tetrahedron* **1996**, *52*, 9853-9862.
- ⁵⁸ B. Altava, M. I. Burguete, J. M. Fraile, J. I. Garcia, S. V. Luis, J. A. Mayoral, M. J. Vicent, *Angew. Chem. Int. Ed.* **2000**, *39*, 1503-1506.
- ⁵⁹ T. M. Jyothi, M. L. Kaliya, M. V. Landau, *Angew. Chem. Int. Ed.* **2001**, *40*, 2881-2884.
- ⁶⁰ (a) N. C. Mehendale, C. Bezemer, C. A. van Walree, R. J. M. Klein Gebbink, G. van Koten, *J. Mol. Catal. A: Chemical* **2006**, *257*, 167-175. (b) N. C. Mehendale, J. R. A. Sietsma, K. P. de Jong, C. A. van Walree, R. J. M. Klein Gebbink, G. van Koten. Chapter 4, PhD. thesis, Utrecht University, (2007).
- ⁶¹ M. Gagliardo, D. J. M. Snelders, P. A. Chase, R. J. M. Klein Gebbink, G. P. M. van Klink, G. van Koten, *Angew. Chem. Int. Ed.* **2007**, ASAP.
- ⁶² N. C. Mehendale, R. J. M. Klein Gebbink, G. van Koten. PhD. thesis, Utrecht University, (2007).
- ⁶³ J. J. M. de Pater, B.-J. Deelman, C. J. Elsevier, G. van Koten, *Adv. Synth. Catal.* **2006**, *348*, 1447-1458.
- ⁶⁴ M. Schreuder, J. N. H. Reek, P. C. J. Kamer, P. W. N. M. van Leeuwen, *Chem. Commun.* **1998**, 2431-2432.
- ⁶⁵ S. Doherty, J. G. Knight, M. Betham, *Chem. Commun.* **2006**, 88-90.
- ⁶⁶ J. P. K. Reynhardt, H. Alper, *J. Org. Chem.* **2003**, *68*, 8353-8360.
- ⁶⁷ J. J. M. de Pater, C. E. P. Maljaars, E. de Wolf, M. Lutz, A. L. Spek, B.-J. Deelman, C. J. Elsevier, G. van Koten, *Organometallics* **2005**, *22*, 5299-5310.
- ⁶⁸ (a) C. Coperet, J.-M. Basset, *Adv. Synth. Catal.* **2007**, *349*, 78-92. (b) H. Clavier, K. GRela, A. Kirschning, M. Mauduit, S. P. Nola, *Angew. Chem. Int. Ed.* **2007**, *46*, 6786-6801.
- ⁶⁹ M. Ahmed, A. G. M. Barrett, D. C. Braddock, S. M. Cramp, P. A. Procopiou, *Tetrahedron Lett.* **1999**, *40*, 8657-8662.
- ⁷⁰ S. Varray, R. Lazaro, J. Martinez, F. Lamaty, *Organometallics* **2003**, *22*, 2426-2435.
- ⁷¹ K. Melis, D. de Vos, P. Jacobs, F. Verpoort, *J. Mol. Catal. A: Chemical* **2001**, *169*, 47-56.
- ⁷² S. C. Schurer, S. Gessler, N. Buschmann, S. Blechert, *Angew. Chem. Int. Ed.* **2000**, *39*, 3898-3901.
- ⁷³ M. Mayr, B. Mayr, M. R. Buchmeiser, *Angew. Chem. Int. Ed.* **2001**, *40*, 3839-3842.
- ⁷⁴ D. E. Fogg, E. N. dos Santos, *Coord. Chem. Rev.* **2004**, *248*, 2365-2379.
- ⁷⁵ L. F. Tietze, *Chem. Rev.* **1996**, *96*, 115-136.
- ⁷⁶ (a) For example: R. Schoevaart, F. van Rantwijk, R. A. Sheldon, *J. Org. Chem.* **2000**, *65*, 6940-6943. (b) S. F. Meyer, W. Kroutil, K. Faber, *Chem. Soc. Rev.* **2001**, *30*, 332-339.
- ⁷⁷ M. J. Burk, J. R. Lee, J. P. Martinez, *J. Am. Chem. Soc.* **1994**, *116*, 10847-10848.

- ⁷⁸ B. M. Choudary, N. S. Chowdari, S. Madhi, M. L. Kantam, *Angew. Chem. Int. Ed.* **2001**, *40*, 4619-4623.
- ⁷⁹ It must be noted that this reaction involves the formation of active Pd(0) aggregates.
- ⁸⁰ (a) R. E. Maleczka, W. P. Gallagher, I. Terstiege, *J. Am. Chem. Soc.* **2000**, *122*, 384-385. (b) W. P. Gallagher, I. Terstiege, R. E. Maleczka, *J. Am. Chem. Soc.* **2001**, *123*, 3194-3204.
- ⁸¹ (a) O. A. Wallner, K. J. Szabo, *Org. Lett.* **2002**, *4*, 1563-1566. (b) O. A. Wallner, K. J. Szabo, *Org. Lett.* **2004**, *6*, 1829-1831.
- ⁸² (a) Y. Nishibayashi, M. Yoshikawa, Y. Inada, M. D. Milton, M. Hidai, S. Uemura, *Angew. Chem. Int. Ed.* **2003**, *42*, 2681-2684. (b) Y. Nishibayashi, M. Yoshikawa, Y. Inada, M. Hidai, S. Uemura, *J. Am. Chem. Soc.* **2004**, *126*, 16066-16072.
- ⁸³ E. Fernandez, S. Castillon, *Tet. Lett.* **1994**, *35*, 2361-2364.
- ⁸⁴ T. Rische, P. Eilbracht, *Tetrahedron* **1998**, *54*, 8441-8450.
- ⁸⁵ S. Ko, C. Lee, M-G. Choi, Y. Na, S. Chang, *J. Org. Chem.* **2003**, *68*, 1607-1610.
- ⁸⁶ A. S. Goldman, A. H. Roy, Z. Huang, R. Ahuja, W. Schinski, M. Brookhart, *Science* **2006**, *312*, 257-261.
- ⁸⁷ S. D. Drouin, F. Zamanian, D. E. Fogg, *Organometallics* **2001**, *20*, 5495-5497.
- ⁸⁸ J. Louise, C. W. Bielawski, R. H. Grubbs, *J. Am. Chem. Soc.* **2001**, *123*, 11312-11313.
- ⁸⁹ J. Cossy, F. C. Bargiggia, S. BouzBouz, *Tet. Lett.* **2002**, *43*, 6715-6717.
- ⁹⁰ J. Cossy, F. Bargiggia, S. BouzBouz, *Org. Lett.* **2003**, *5*, 459-462.
- ⁹¹ C. Bielawski, J. Louie, R. H. Grubbs, *J. Am. Chem. Soc.* **2000**, *122*, 12872-12873.
- ⁹² B. A. Seigal, C. Fajardo, M. L. Snapper, *J. Am. Chem. Soc.* **2005**, *127*, 16329-16332.
- ⁹³ R. Grigg, V. Sridharan, M. York, *Tetrahedron Lett.* **1998**, *39*, 4139-4142.
- ⁹⁴ O. Pamies, J-E. Backvall, *Chem. Rev.* **2003**, *103*, 3247-3261.
- ⁹⁵ B. A. Persson, A. L. E. Larsson, M. Le Ray, J-E. Backvall, *J. Am. Chem. Soc.* **1999**, *121*, 1645-1650.
- ⁹⁶ B. Martin-Matute, M. Edin, K. Bogar, F. B. Kaynak, J-E. Backvall, *J. Am. Chem. Soc.* **2005**, *127*, 8817-8825.
- ⁹⁷ B. A. Persson, F. F. Huerta, J-E. Backvall, *J. Org. Chem.* **1999**, *64*, 5237-5240.
- ⁹⁸ H. C. Lo, R. H. Fish, *Angew. Chem. Int. Ed.* **2002**, *41*, 478-481.
- ⁹⁹ (a) K. Bergstad, S. Y. Jonsson, J-E. Backvall, *J. Am. Chem. Soc.* **1999**, *121*, 10424-10425. (b) S. Y. Jonsson, K. Farnegardh, J-E. Backvall, *J. Am. Chem. Soc.* **2001**, *123*, 1365-1371.
- ¹⁰⁰ (a) H.-B. Yu, Q.-S. Hu, L. Pu, *J. Am. Chem. Soc.* **2000**, *122*, 6500-6501. (b) H.-B. Yu, Q.-S. Hu, L. Pu, *Tetrahedron Lett.* **2000**, *41*, 1681-1685. (c) W. S. Huang, Q. S. Hu, L. Pu, *J. Org. Chem.* **1999**, *64*, 7940-7956.
- ¹⁰¹ T. Nemoto, H. Kakei, V. Gnanadesikan, S-Y. Tosaki, T. Ohshima, M. Shibasaki, *J. Am. Chem. Soc.* **2002**, *124*, 14544-14545.
- ¹⁰² H. Siebeneicher, I. Bytschkov, S. Doye, *Angew. Chem. Int. Ed.* **2003**, *42*, 3042-3044.
- ¹⁰³ L. Veum, U. Hanefeld, *Chem. Commun.* **2006**, 825-831.
- ¹⁰⁴ C. Simons, U. Hanefeld, I. W. C. E. Arends, A. J. Minnaard, T. Maschmeyer, R. A. Sheldon, *Chem. Commun.* **2004**, 2830-2831.
- ¹⁰⁵ C. Simons, U. Hanefeld, I. W. C. E. Arends, T. Maschmeyer, R. A. Sheldon, *Topics in Catal.* **2006**, *40*, 35-44.
- ¹⁰⁶ A. Ajamian, J. L. Gleason, *Angew. Chem. Int. Ed.* **2004**, *43*, 3754-3760.
- ¹⁰⁷ J-C. Wasilke, S. J. Obrey, R. T. Baker, G. C. Bazan, *Chem. Rev.* **2005**, *105*, 1001-1020.

CHAPTER 2

‘Click’ Immobilisation of Organometallic Catalysts for C-C Coupling Reactions

Model systems for the simple, high yielding, efficient ‘click’ immobilisation of homogeneous catalysts are demonstrated. The synthesis of azide and isocyanate functionalised high-density silica materials which react readily with ethynyl and nucleophile functionalities is reported. Both *para*-ethynyl functionalised palladium and platinum pincer organometallics (pincer = [C₆H₃(CH₂NMe₂)_{2-2,6-}]), were coupled with azide-functionalised silica material yielding the corresponding tethered complexes in high yields with no complex degradation. Furthermore, analogous *para*-alcohol functionalised palladium and platinum pincer complexes were coupled with isocyanate functionalised silica material to yield immobilised organometallics in high yields. The acquired immobilised organometallic pincer complexes were characterised using various techniques (solid state IR, solid state NMR, elemental content analysis, surface area measurements) which confirmed the covalent nature of the immobilisation, and also the retention of the structural integrity of the pincer metal complexes. Palladium containing materials were applied as Lewis acid catalysts in the double Michael addition reaction between ethyl-cyanoacetate and methylvinyl ketone and were found to be active catalysts. When measured on a per-palladium site basis the novel materials were found to be as active as the homogeneous forms of the catalyst. This led to the discovery that one of the support materials, with no palladium organometallic units, however with linker triazole groups present, was also an active catalyst, with slightly diminished activity compared to the palladium-containing material. It was found that localised triazole sites on the silica surface act as pseudo-Lewis acid catalysts. The palladium containing materials were also applied in allylic stannylation catalysis, and were found to be active catalysts, approximately three times slower than the homogeneous catalysts when measured on a per-palladium site basis. The support material was not found to be an active catalyst in this reaction, however the triazole linkers were believed to play a role. The immobilised palladium catalysts have been applied sequentially for the conversion of an allyl chloride to an allylic alkylation product.

2.1 Introduction

The process of manufacturing of fine chemicals has consistently been a co-producer of environmentally damaging solvent and non-natural chemical waste.¹ Interest in the sustained development of homogeneous catalysts for fine chemical production has led to the opinion that a method for heterogenising these catalysts must be developed and brought to the industrial arena.^{2,3} Several methods for heterogenisation of homogeneous catalysts have been explored which are mainly based on inorganic support systems,⁴ dendrimers,⁵ or functionalised organic polymers.⁶ In addition, significant effort has been expended to develop catalysts for biphasic reaction systems.⁷ It is generally acknowledged that covalent immobilisation of ligands and complexes on an inorganic support gives the best recycling results. However, covalent immobilisation of any organic species on an inorganic support requires multi-step reaction procedures that often fail at the last hurdle, *i.e.* the reaction of functionalised ligand or complex with the inorganic support. Failure comes through either ligand/complex decomposition due to the properties of the inorganic support, or due to the relatively extreme conditions required to immobilise. A simple manner to couple a functionalised inorganic material with a functionalised catalyst has, to the best of our knowledge, not yet been demonstrated.

An area of organic chemistry that has gained precedence in recent years is the so-called 'Click' reaction chemistry.⁸ This broad area of organic synthesis incorporates any reaction which has high atom efficiency, low by-product levels, and high yields. The ultimate 'Click' reaction is defined by a complete conversion of all starting materials, no side-product formation and relatively mild reaction conditions. The most widely used reaction under the 'click' heading is the copper(I) catalysed Huisgens 1,3-dipolar cycloaddition reaction between an alkyne and an azide yielding a single isomer of a 1,2,3-triazole, the 1,4-isomer.⁸ Recent work has shown the application of 'click' chemistry for the tethering of molecules to both organic and inorganic polymeric supports. Bio-functionalisation of silica supports by 'click' tethering has been demonstrated.⁹ Similarly biotin has been 'clicked' to an organic polymeric support to demonstrate the use of tethered 'click' precursors for biosensing.¹⁰ Azide functionalised amino acids have been immobilised on glass surfaces for protein immobilisation by 'click' reaction.¹¹ 'Click' chemistry has also been applied for the immobilisation of Cinchona alkaloid derivatives on silica¹² and also to immobilise coordination complexes on SAM coated gold surfaces,¹³ as well as to organic polymeric supports.¹⁴ The latter has shown the application of the formed functionalised triazole bound to a dendritic support as a ligand in copper catalysed benzylation reactions. Chiral pyrrole derivatives have been 'click' immobilised on polystyrene for organic catalysis in water.¹⁵

The so-called pincer organometallic complexes have been utilised by our group to demonstrate a range of techniques for catalyst recycling. A pincer organometallic is generally described as a terdentate ligand bound to a metal centre via one sigma and two dative bonds.¹⁶ The sigma bond is a direct aromatic carbon-metal bond, and the dative bonds are from lone pair donating groups binding the metal as a tweezers would. Previous work has demonstrated the application of pincer metal complexes of the general formula $[M(C_6H_3(CH_2E)_2-2,6-)]$ ($E = SR$),¹⁷

NR₂,¹⁶ PR₂¹⁸) immobilised on dendritic,¹⁹ organic polymeric²⁰ and inorganic supports.²¹ Pincer metal complexes have been applied in a wide range of catalytic reactions; Aldol condensation,²² double Michael addition (the application of pincer palladium complexes as Lewis acid catalysts is high yielding, and this reaction is often used to demonstrate the feasibility of a certain immobilisation technique),²³ Kharasch addition,²⁴ transfer hydrogenation,²⁵ transfer dehydrogenation²⁶ and recently allylic stannylation²⁷ and allylic alkylation reactions.²⁸ This latest discovery, where pincer palladium and platinum complexes can be applied in the activation and coupling of allylic substrates, is one of the most promising catalytic applications of pincer palladium species because of the high yields observed. Furthermore, this work has demonstrated the ability of various forms of the pincer ligand with palladium to be active catalysts in cascade processes. For example, the conversion of cinnamyl chloride to cinnamyl stannane followed by reaction with an aldehyde shows a simple one-pot process for allylic alkylation of otherwise unreactive substrates.

In this paper we demonstrate the development of novel functionalised silica materials for facile immobilisation of organometallics. Azide and isocyanate functionalised silica materials are presented. These functionalised materials react with ethynyl groups or nucleophiles, respectively, yielding tethered organic moieties with no side products, and complete conversion of the respective silica bound functionality. This so-called 'Click' immobilisation has been demonstrated for a range of organometallic palladium and platinum pincer complexes. The developed materials have been applied in the double Michael addition and allylic stannylation reactions showing high yields and activities which are, unexpectedly, not substantially diminished compared to the homogeneous catalysts. The roles of the support material and linkers have been investigated and it was found that the support/tether can have a significant effect on the catalytic reactions. The recycling of the catalytic materials has been studied. The immobilised catalysts have been applied sequentially for the conversion of an allyl chloride to an allylic alkylation product. It is demonstrated that catalyst immobilisation can be a simple, high yielding process, without complex degradation, and that catalysts immobilised using 'click' techniques can be recycled.

2.2 Results and Discussion

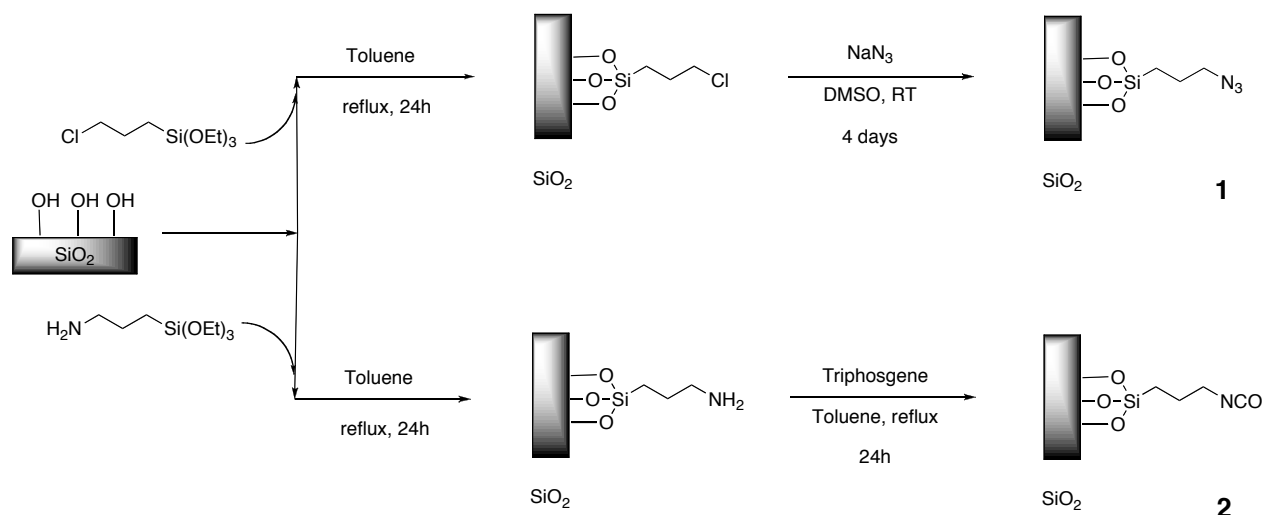
2.2.1 Synthesis

Novel materials for high yielding, highly atom efficient 'click' immobilisation of homogeneous catalysts were synthesised. Reaction of a high-density silica with either 3-chloro- or 3-amino-propyl-1-triethoxysilane in refluxing toluene yielded 3-chloro- and 3-amino-propyl functionalised silica (figure 1). These conditions are the standard conditions used to functionalise silica with organic or organometallic moieties. The conditions are relatively harsh, with relatively high temperatures required, in the presence of a large concentration of acidic silanol groups. Obviously these conditions could be too extreme for the immobilisation of a labile coordination complex, or an acid sensitive species. Therefore one would prefer to be able to react a functionalised complex with an appropriate support under mild conditions, which are compatible

with the precious complex and do not result in the decomposition thereof. High-density silica was used because we wish to focus on organic moieties bound only at easily accessible sites in the silica. We hope to avoid mass transport limitations, and effects on the kinetics of catalytic reactions that come as a result of highly porous silica.

The conversion of chloro- and amino-propyl groups bound to silica, to active functionalities was successful using standard practices for the synthesis of azides²⁹ and isocyanates.³⁰ The reaction of alkyl halides with sodium azide is a high yielding reaction with only NaCl as a by-product. Chloro-propyl functionalised silica was reacted with a large excess of NaN₃ (w.r.t Cl) yielding material **1**, which could be isolated and purified by simple filtration and washing with water and acetone. Likewise, the synthesis of isocyanates from alkyl amines is a high yielding reaction with by-products that can easily be removed. Material **2** was synthesised by reaction of amino-functionalised silica with a large excess of triphosgene (w.r.t. NH₂) and subsequently isolated and purified by simple filtration and washing with (nucleophile free) organic solvents. The synthetic techniques have been chosen because they ensure all chloro- or amino-functionalities are converted to the desired azide and isocyanate, respectively.

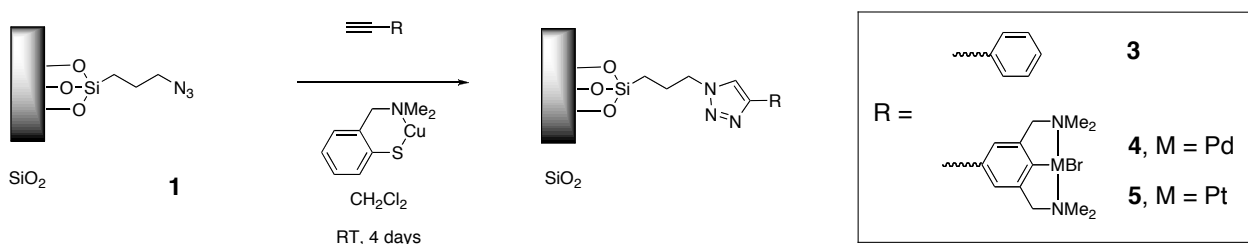
Scheme 1. Synthesis of azide and isocyanate functionalised materials **1** and **2**.



Reaction of **1** with an excess of ethynylbenzene in the presence of a catalytic amount of [Cu(MeCN)₄]PF₆ led to complete conversion of all azide groups. However, after several washing steps, and a Soxhlet extraction, the isolated material was blue in colour. This suggests the presence of remnant copper(II) species on the material. Several attempts to remove these species from the silica surface were made using aqueous ammonium halide solutions, highly acidic/basic solutions, and solutions containing EDTA. However, none of these procedures showed complete removal of the copper from the material. Recent work in our group has shown the application of a Cu(I) thiolate catalyst [CuSC₆H₄CH₂NMe₂-2-]₃ (5 mol%) for the Huisgens 1,3-dipolar cycloaddition of an alkyne with an azide.³¹ When this catalyst was used for the reaction of **1** with ethynylbenzene, the silica material showed no visual signs of copper remnants. Furthermore, elemental content analysis showed there was no copper present. Material **1** was subsequently reacted with ethynyl functionalised palladium and platinum organometallic pincer species³² yielding immobilised

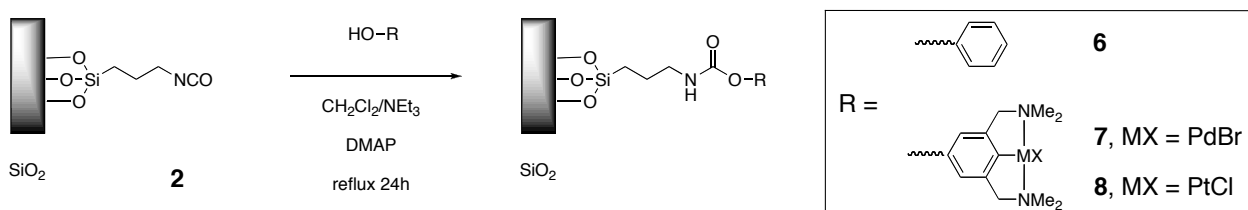
complexes that could be applied in catalysis. The Cu(I) thiolate catalyst (5 mol% w.r.t ethynyl compound) was used again in this immobilisation procedure. In both cases no signs of palladium or platinum complex decomposition were observed. It was also found that the palladium and platinum complexes did *not* catalyse the Huisgens 1,3-dipolar cycloaddition reaction themselves, and that the Cu(I) thiolate catalyst was essential for the reaction to occur at an efficient rate. Upon the completion of the reactions, it was sometimes observed that not all azide had reacted (IR spectroscopy), so fresh solvent and Cu(I) thiolate catalyst were added with ethynylbenzene to ‘cap’ any remaining azide groups.

Scheme 2. ‘Click’ Huisgens 1,3-dipolar cycloaddition of an alkyne and an azide for the immobilisation of Pd and Pt pincer organometallics.



The reaction of material **2** with various nucleophile functionalised organic species was also analysed. The reaction of **2** with hydroxymethylbenzene in benzene proceeds at room temperature with complete conversion of all isocyanate groups. The reaction of hydroxyl functionalised organometallics with isocyanate groups, as previously shown in our group,³³ requires a large excess of NEt_3 , with a catalytic amount of *N,N*-dimethyl-4-pyridine amine (DMAP) in refluxing dichloromethane to ensure conversion of all isocyanate groups. Materials **7** and **8** were produced under these conditions. The fact that more forcing conditions (excess NEt_3 , higher temperatures) were required is very important for any future work. Much less extreme conditions are required to couple alkyl nucleophiles than to couple aromatic nucleophiles and hence the ‘click’ coupling is a step easier and more efficient. Any remaining isocyanate groups on the silica surface, were capped by addition of hydroxymethylbenzene to the solution. The quantity of remnant isocyanate groups for materials **7** and **8**, and azide groups for materials **4** and **5** could not be quantified easily, and thus after any immobilisation procedure excess hydroxymethylbenzene or ethynylbenzene were always added to ensure capping of all remnant functionalities.

Scheme 3. ‘Click’ nucleophilic attack of an alcohol on isocyanate for immobilisation of Pd and Pt pincer organometallics.



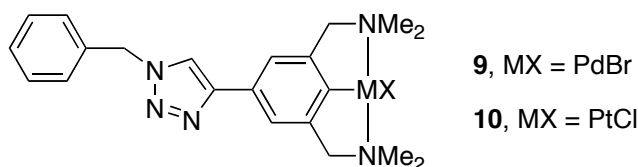


Figure 1. Triazole-functionalised pincer palladium (**9**) and platinum (**10**) complexes as model compounds for materials **4** and **5**.

Previous work in our group has shown models for materials **7** and **8**.³³ Here we report the synthesis of compounds **9** and **10**, *para*-triazole-functionalised pincer palladium and platinum organometallics (figure 1). These compounds are synthesised in a similar manner to materials **4** and **5**, however azidomethyl-benzene (benzyl azide) is the coupling agent instead of silica bound propyl azide. In both cases the reactions are high yielding. Single crystals, suitable for X-ray structural determination of **10**, were acquired by slow evaporation of a concentrated solution of a CH₂Cl₂/hexanes mixture. Figure 2 depicts the ORTEP diagram of the X-ray diffraction measurement of **10**. All bond distances are within the range expected for NCN-Pt pincer complexes. Coordination around the metal centre is distorted square planar. The plane of the triazole group is slightly rotated with respect to the pincer backbone. The two five-membered metallocycles are puckered in opposite directions, as expected with such platinum species.

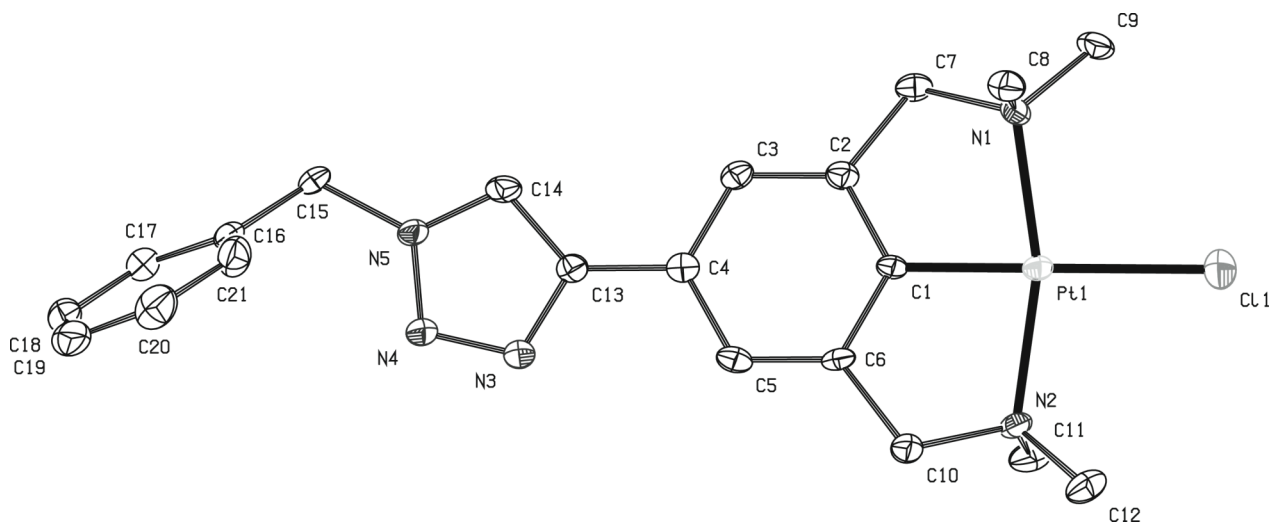


Figure 2. Molecular structure, from X-ray diffraction measurements, of *para*-triazolo-NCN-PtCl (**10**), as model compound for immobilised complex. Hydrogen atoms removed for clarity.

2.2.2 Elemental Analysis

Elemental content analysis has been used to characterise materials **3** - **8**. Nitrogen content analysis gives us indications how the synthetic procedures that have been carried out on the materials affect the substituents present. Carbon, silicon, and oxygen analysis gives little information because they are present in large excess with respect to the organometallic species (C as TMS capping groups, Si and O as polymeric support). Material **1** shows no Cl content suggesting that all chloropropyl groups have been substituted by azide. The nitrogen loading is

1.39% of all material. Reaction of **1** with ethynylbenzene (for **3**) showed little change in the nitrogen content (1.35%) and a marked increase in carbon content, as expected (3.49 to 5.56%). Reaction of ethynyl functionalised palladium and platinum complexes showed an increase in nitrogen content, as would be expected (ligands contain N). The ‘loading’ of catalytic sites was determined by measuring the palladium and platinum elemental content (**4**, Pd = 0.52%, **5**, Pt = 0.45%). The metal to nitrogen content comparisons show that not all surface triazole groups are tethered to a metal pincer complex, and in fact there is a quantity of ‘free’ triazole groups present as a result of capping any remnant azide functionalities. The nitrogen loading is in fact five times as much as would be expected if all azide groups had reacted to yield an immobilised pincer complex (expected N:Pd 5:1, observed is 26:1).

Isocyanate functionalised material **2** gave similar results. The nitrogen loading was found to be 0.77% of the total mass. The introduction of a pincer organometallic functionality showed a marked increase in nitrogen content, as would be expected for NCN-pincer metal complexes. Again the loading of catalytic material was measured using metal content analysis (Pd **6**, 0.26%, Pt **7**, 0.79%).

2.2.3 Surface Area Measurements

Table 1. BET surface area, pore volume and size measurements of materials **1** and **2**.

Material	Surface area (m ² /g)	Pore Volume (cm ³ /g)	Pore size (nm)
Starting SiO ₂	218.40	1.13	20.61
1	208.20	0.92	17.62
2	208.09	0.86	16.47

BET surface area measurements were used to analyse the effects of carrying out organic synthetic techniques on the high-density silica material used for the preparation of materials **1** and **2**.³⁴ Both materials showed similar results, demonstrating that there is little difference in the effect of the organic synthesis on the nature of the support material. The surface area of the starting material was approximately 218 m²/g which compares favourably with the data obtained for materials **1** and **2**. Both materials showed a surface area of 208 m²/g. This is an expected decrease, which comes with the coupling of organic moieties to the silica surface, thus decreasing the surface area. The pore diameter and volume measurements also gave valuable information about catalyst site accessibility. We set out to immobilise catalysts without having influences from the support material. This is reflected in the observed pore volumes for materials **1** and **2** versus the starting material. On loading the silica material with the tethering functionality, the pore volume drops minimally. The observed large pore volumes (~1 cm³/g) and the observed pore size (16-17nm)

means it is highly unlikely that the support has much influence on the kinetics (mass transport) of the catalytic reactions.

By combining the nitrogen content analysis results of materials **1** and **2** with the BET surface area results we can get an indication of the 'area' *per* a single catalytic site, and the proximity of catalytic sites to each other. This relies on the assumption that all azide/isocyanate sites are available for reaction with functionalised organometallic species, and the entire surface of the material is accessible to the organic moieties used to functionalise the material. With material **1** the nitrogen content is 1.39% of the total loading, which gives 4.76×10^{-6} mol/m² nitrogen loading. This can be converted to functionality loading by dividing by three (three nitrogen's for every azide) which gives 1.59×10^{-6} mol/m² (1.59×10^{-26} mol/Å²) azide loading. Using Avogadro's constant this gives an approximation that every azide group sits on 104.4 Å². In the case of material **2** (isocyanate) the nitrogen content is 0.77% of the total material content. This gives 2.64×10^{-26} mol/Å² of nitrogen (and thus isocyanate), leading to an approximation that every isocyanate group sits on 63.0 Å². Simplifying the calculations even further, we can estimate the 'ideal situation' distance between catalytic sites. Assuming that all catalytic sites are equally deposited on the silica surface, we treat every functionality site as a cylinder lying perpendicular to the silica surface. The estimated radius (*r*) of the area around a catalytic site could be acquired from $\pi r^2 = \text{area}$. Therefore, in material **1**, the average distance between catalytic sites is equal to $2r$, and thus is 11.3Å, and in material **2** it is 9.0Å. This appears to be quite a short distance, and would suggest interactions between functionalities (and thus catalytic sites) in materials **1** and **2** are likely (and also materials **3-8**).

2.2.4 Infra-Red Analysis

DRIFT³⁵ and ATR³⁶ IR spectroscopy has been utilised to analyse materials **1 - 8** and complexes **9** and **10**. In particular DRIFT difference spectroscopy has been used to analyse what has been 'added' and 'subtracted' from the materials **1 - 8**. DRIFT difference spectra of materials **1** and **2** are depicted in figure 3 (spectrum of material minus spectrum of unfunctionalised silica).

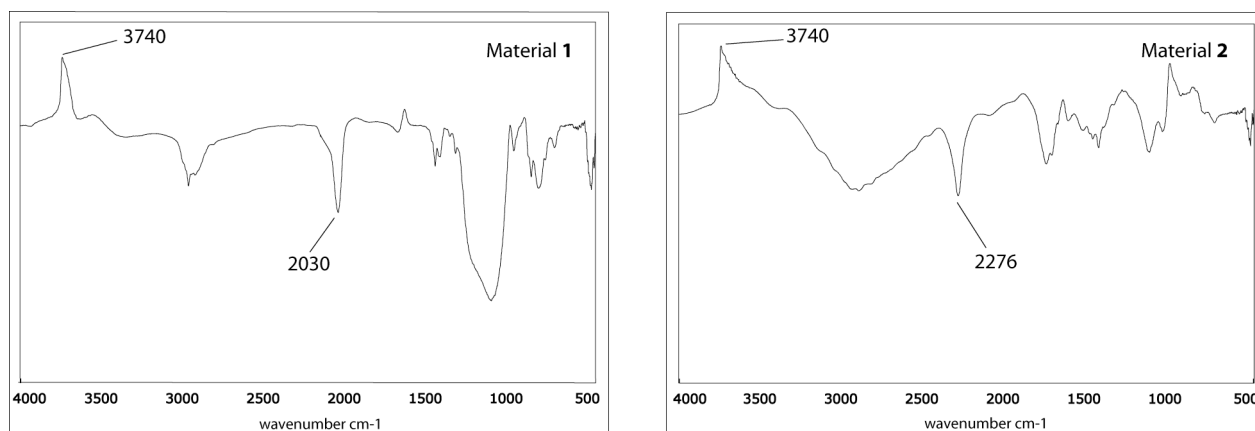


Figure 3. IR DRIFT difference spectra of **1** (azide) and **2** (isocyanate) minus SiO₂.

Azide functionalised material **1** shows a characteristic $\nu_{\text{N-N-N}}$ at $\sim 2030\text{cm}^{-1}$ while isocyanate functionalised material **2** shows a characteristic ν_{NCO} at $\sim 2276\text{cm}^{-1}$. The intensity of the resonances is a valuable characteristic of these materials. Furthermore, the stretches lie in a region of the spectrum which is unlikely to have resonances from other functional groups. This means that reaction of the functionalities can be easily monitored with IR spectroscopy. Both difference spectra show a trough at $\sim 3740\text{cm}^{-1}$. This corresponds to where $\nu_{\text{Si-O-H}}$ is expected. This means that Si-OH groups have been consumed in the process of converting silica to functionalised materials **1** and **2**. This confirms that triethoxysilyl groups have reacted with surface silanol groups yielding covalently functionalised materials.

The IR DRIFT difference spectra of materials **3**, **4**, and **5** showed agreeing results (figure 4, **5**). In all cases the azide resonance was consumed (trough at 2030cm^{-1}), and new resonances were observed at $\sim 1450\text{cm}^{-1}$. These resonances are not very intense, however, they are the only characteristic resonances of a triazole group. The pincer complex unit itself has no strong IR stretches. The ATR IR spectra of **9** and **10** show the similarities between materials **4** and **5** and their untethered analogues (see supplementary information).

The synthesis of materials **6** - **8** showed likewise a consumption of isocyanate groups upon reaction of **2** with nucleophile functionalised moieties. The formed carbamate group has characteristic stretches at ~ 1650 and 1550cm^{-1} . Figure 4 also shows the IR DRIFT difference spectrum of **8**, which clearly depicts the above-mentioned characteristics. The features of this spectrum are comparable to previous reports on carbamate tethered silica species.³⁷ As mentioned previously any remnant isocyanate or azide groups on the silica surface are capped by hydroxymethylbenzene or ethynylbenzene, respectively. The depicted spectra are difference spectra, however the normal DRIFT spectra of materials **3** - **8** show no azide or isocyanate resonances indicating all functionalities have reacted.

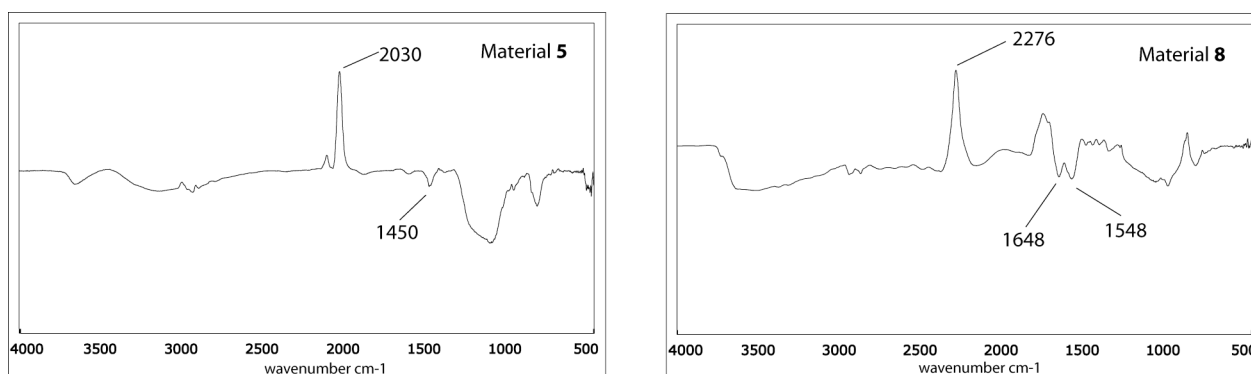


Figure 4. IR DRIFT difference spectra of materials **5** and **8**, minus starting material **1** and **2**, respectively.

2.2.5 NMR Analysis

^{29}Si CP-MAS NMR was applied to analyse the effects of carrying out organic synthetic techniques on silica (^{29}Si spectra of materials **1**, **2**, **5**, and **8** are available as supplementary information, they all look similar to those depicted in figure 5). The ^{29}Si spectrum of

organometallic containing materials **4** and **7** shows us several peaks that indicate different forms of silicon species (figure 5). Peaks at ~ -101 and -111 ppm are characteristic of Q type ($Si(O)_4$) silicates, which are in the bulk material. Peaks at ~ -58 and -66 ppm are typical of T-type ($R_1Si(O)_3$) silicates, that is, the silicon bound to the propyl group at the surface of the support. This is a clear indication that the catalyst is covalently bound to the support. The presence of double peaks in the -60 ppm (T^2 at 58 ppm, T^3 at 66 ppm) region indicates that not all ethoxy groups of 3-chloro- or 3-aminopropyl-1-triethoxysilane have reacted in the grafting process, and in some cases only two (thus nomenclature T^2) of the three have reacted. The single peak at ~ 13 ppm is typical of M-type ($R_3Si(O)_-$) silicates (where R is the methyl groups of the trimethylsilyl capped silanol groups).

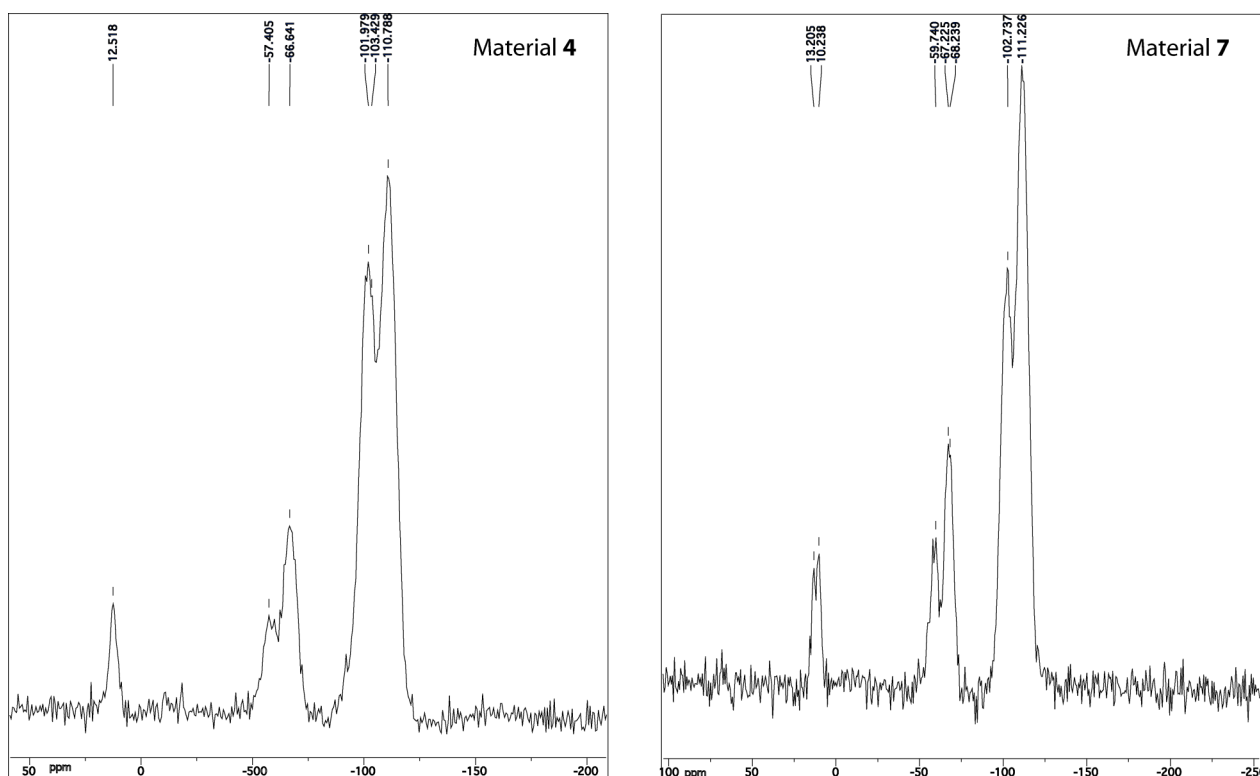


Figure 5. ^{29}Si CP-MAS NMR spectra of materials **4** and **7**.

2.2.6 Catalysis

Palladium complexes **9** (*para*-triazole) and **11** (*para*-H, parent compound) and palladium containing materials **4** (*para*-triazole link to SiO_2) and **7** (*para*-carbamate linker to SiO_2) were applied as Lewis acid catalysts in the double Michael addition between ethyl-cyanoacetate (ECA, cyano-acetic acid ethyl ester) and methyl vinyl ketone (MVK, 3-buten-2-one). Previous work has demonstrated the application of aquo-salts of ECE-pincer palladium complexes ($E = SR, NR_2, PR_2$) as catalysts for this reaction.³⁸ It was believed that the metal-halide complexes were not active catalysts. In this report we show this not to be true. This alleviates the necessity to use silver salts to convert metal halide complexes into aquo-complexes before catalysis. With materials **4** and **7** this is very important, because removal of any formed (insoluble) silver salts from the support

would be difficult. Recent work in our group has also demonstrated that silver salts are active catalysts in the Lewis acid catalysed aldol addition reaction.³⁹ This means, to demonstrate the application of immobilised pincer palladium complexes, one should ensure no remnant silver salts are present. Therefore using the metal-halo complex as the pre-catalyst is an excellent alternative. Table 2 shows the observed rate constants, k , for both the aquo- and bromo- pincer complexes **9** and **11**, and catalytic materials **4** and **7**, as well as functionalised support materials **3** and **6**. In all cases 100% conversion was observed.

Scheme 4. Double Michael addition between ECA and MVK with pincer palladium complexes.

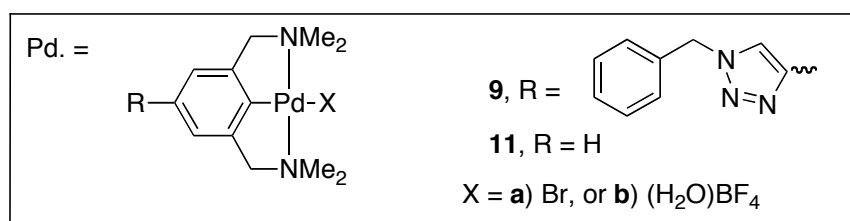
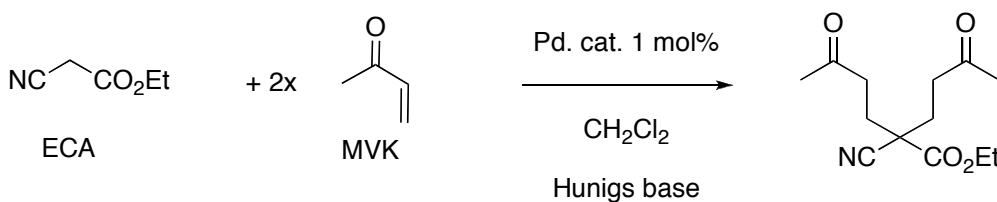


Table 2. Reaction rate constants, and half-lives of homogeneous bromo- and aquo-pincer palladium complexes **9** and **11** (**a** and **b**), and NCN-pincer palladium containing materials **4**, and **7**, and organic functionalised materials **3** and **6** in the double Michael addition.

		Homogeneous Catalysts				Heterogeneous Catalytic Materials			
Complex/ Material	blank	9(a)	11(a)	9(b)	11(b)	4	7	3	6
k	0.60	5.10	3.75	25	28	-	-	-	-
$(\times 10^{-5}, \text{s}^{-1})^{\text{a}}$									
$t_{1/2}$ (min.) ^{a,b}	1925	226	308	46	41	200	380	370	2000

^aAs measured by plotting $\ln\{[\text{ECA}]/[\text{ECA}]_0\}$ vs. time. ^bWhen $[\text{ECA}] = [\text{ECA}]_0/2$

Both types of precursor (bromo- or aquo-) showed first order kinetics. The blank reaction, thus substrates, base and solvent showed $t_{1/2} = 1925$ min. ($k = 6 \times 10^{-6}$). With the homogeneous catalysts, **9** and **11**, the bromo-species is an order of magnitude slower in catalytic reactivity than

the corresponding aquo-complex. This suggests that in the reactions catalysed by **9(a)** and **11(a)** competition between the bromide ligand, and substrate ligands, is resulting in a slower reaction. We did not observe an activation period for either bromo- or aquo- catalytic precursors.

Materials **4** and **7** were found to be active catalysts in the double Michael addition. Both were applied as the neutral NCN-pincer palladium bromide complex. The activity of the catalytic material (**4**, $t_{1/2} = 200$ min.; **7**, $t_{1/2} = 380$ min., table 2) was not diminished when compared to the corresponding homogeneous pincer palladium bromide species, **9(a)** and **11(a)** respectively. This is a remarkable discovery, because in most instances the covalent immobilisation of homogeneous catalysts on inorganic supports results in a substantial decrease in catalytic activity. However, when we investigated the reaction kinetics we found that the reaction did not follow zeroth, first or second order kinetics in the ECA substrate (MVK was always used in excess). In fact the organometallic functionalised silica was expected to demonstrate first order kinetics, as the homogeneous catalyst does. Figure 6 depicts the plot, for both materials **4** and **7**, of the natural log of starting material (ECA, from ^1H NMR) concentration against time (a straight line plot would be expected for a first order system). It appears that there is an initial high conversion level which then slows at a certain point and a slower, constant reaction rate is observed. Apparently the support, or heterogenisation is having an effect on the reaction rate.

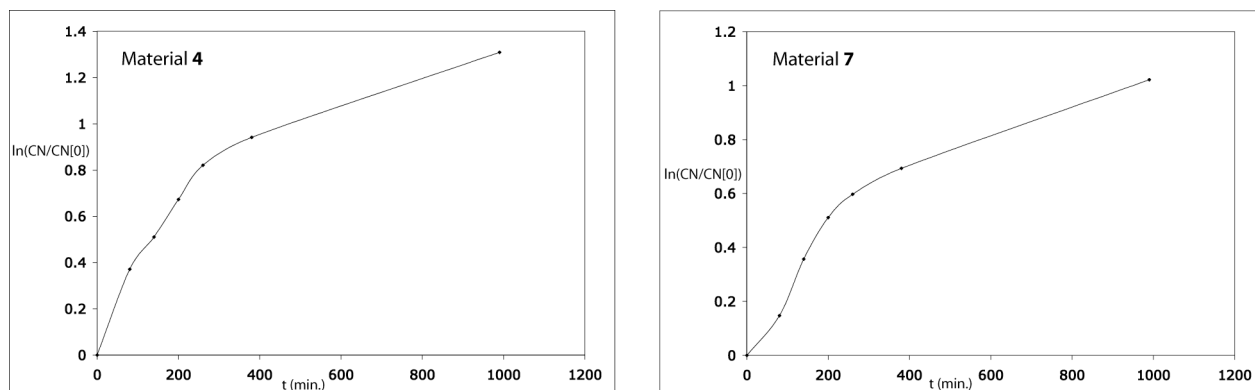


Figure 6. Plot of $\ln(\text{CN}/\text{CN}[0])$ (concentration of ECA over initial concentration) versus time for materials **4** and **7**.

To investigate the effects of the support material, and the linker groups to the support, on the Lewis acid catalysis, we synthesised materials **3** (*triazole* functionalised silica) and **6** (*carbamate* functionalised silica) to mimic the immobilised catalysts **4** and **7**, respectively. Neither material contains an organometallic pincer catalyst unit, but have a phenyl end group instead. The source of the surprising catalytic results could arise either from Si-O-Si surface species or from either the triazole or carbamate linkers. Surprisingly, material **3** was found to be an active catalyst in the double Michael addition reaction, when used in the same quantities as materials **4** and **7** (**3**, $t_{1/2} = 370$ min.; **6**, $t_{1/2} = 2000$ min., table 2). Material **3** showed a slightly diminished (factor of 2) activity compared to the homogeneous organometallic catalyst **9(a)**, whilst material **6** showed activity similar to the blank reaction ($t_{1/2} = 1925$ min.). These data suggest material **6** is thus not a catalyst in the double Michael reaction. Because material **6** is not an active catalyst, the obvious conclusion to be drawn is that the triazole functionalised silica material is an active catalyst, and

more importantly, the tethered triazole groups themselves are the likely source of catalytic activity. The triazole ring may act as a basic site, with N's -2 and -3 possible bases. The 'catalytic' loading of triazole groups in this reaction is calculated to be 7mol% (50mg of **3** used, comparable to quantities of materials **4** and **7** in previous experiments, however, materials **4** and **7** are accompanied by 1 mol% Pd loading as well). With this loading, one could also propose that if the triazole group acts as a base, then there are possibly multiple extra basic sites present in the reaction mixture. No reports on the pKa of the triazole group have been reported to date, so the relative strength of the triazole basic sites cannot be commented upon. As material **4** is a better catalyst than material **3** it can be concluded that the palladium organometallic *does* play a role in the catalysed reaction. It is possible that a cooperative effect between triazole groups and the pincer palladium unit is allowing for this increase in activity. It must be noted here that catalysts **9(a)** and **11(a)** show comparable activities. The BET surface area studies in this report show that the organometallic/triazole groups (vide infra azide) on the silica surface are all relatively close to each other, and are more than likely able to interact with or assist each other. Previous work in our lab has also found that coordination between a triazole group and an organometallic pincer complex yield stable coordination complexes.⁴⁰ Whether these types of interactions are playing a role is uncertain.⁴¹

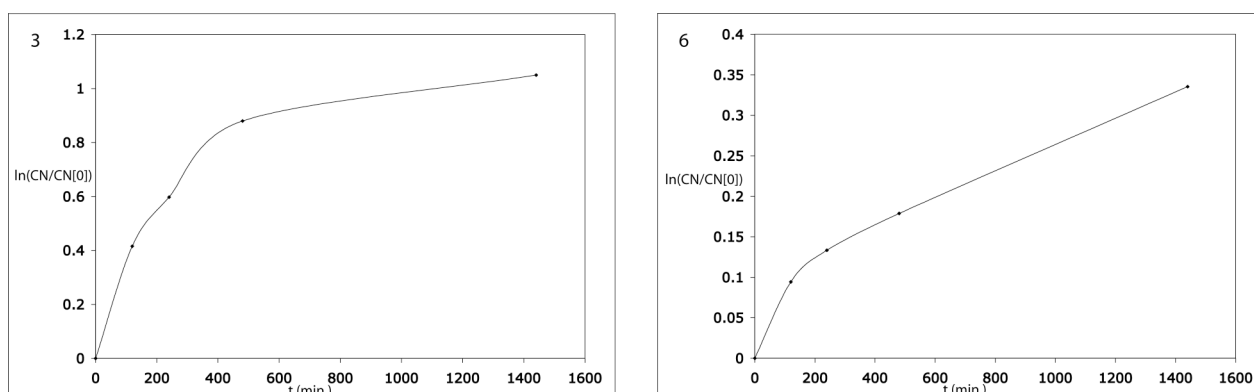


Figure 7. Plot of $\ln(\text{CN}/\text{CN}[0])$ (concentration of starting ECA over initial concentration) versus time for materials **3** and **6**.

Materials **4** and **7** could be recycled by simple filtration of the catalytic mixture and then washing with dichloromethane, and subsequent recharging with substrates and base. Material **4** was found to gradually lose catalytic activity over 3 cycles. With material **7** all three cycles showed half lives of ~400 mins. with quantitative yields. No palladium leaching was observed in either material (table 3). All three recycles showed the same reaction kinetic profile of the first catalysis test (figure 8). These results clearly indicate that material **7** is the more stable catalytic material, and something is killing the catalytically active species in material **4**. The nature of the catalyst deactivation could both be as a result of triazole coordination to any palladium sites on the surface thus deactivating both possible active sites. Another likely explanation is that product is blocking the active site (triazole) on the silica surface, and is not easily washed away in the recycling of the catalytic material.

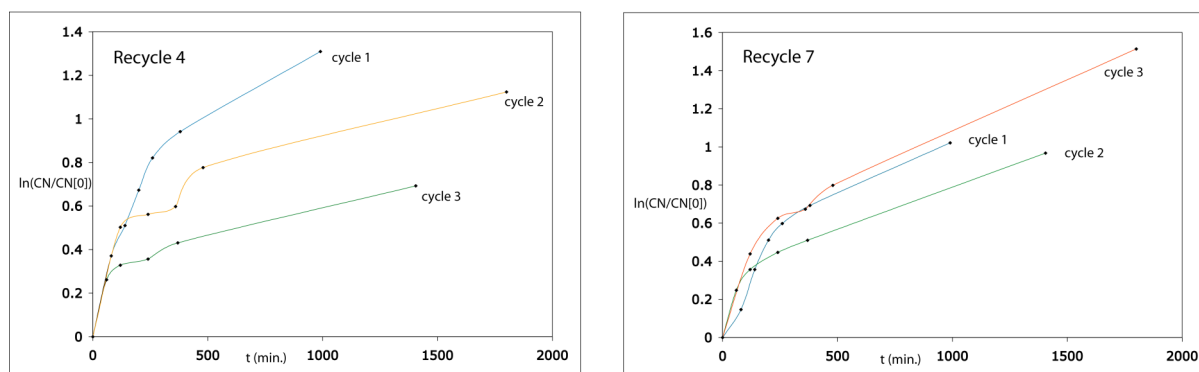
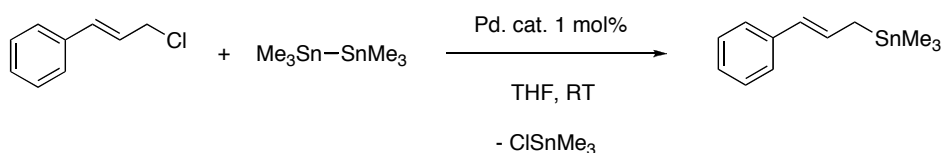


Figure 8. Kinetic plots of recycled catalysts **4** and **7**.

Scheme 5. Palladium pincer catalysed allylic-stannylation reaction.



In order to further test the immobilised NCN-pincer palladium complexes, a catalytic reaction was chosen in which any involvement of the support and linker would be unlikely. Accordingly, we selected the allylic stannylation reaction of allyl chloride with hexamethylditin yielding an allyl-stannane (scheme 5). ECE-pincer metal complexes have recently been shown to be highly active catalysts in this reaction (ECE = NCN, SCS).²⁷ Material **4** (triazole linker) showed diminished activity compared to its homogeneous counterpart **9(a)** (complete conversion within 1 hour, material **4** complete conversion in 6 hours) while material **7** showed very slow reaction rates (20% conversion after 72 hours). Szabo *et al* showed that the *para*-substituent plays a significant role in the activity of the catalyst, with previous work showing the *para*-nitro NCN-pincer palladium species being the most active catalyst for this reaction. In our opinion, the differences in the electron withdrawing/donating properties of a triazole group compared to that of a carbamate group are not great enough to cause such a large difference in reaction rates. Material **3** did not catalyse the reaction of cinnamyl chloride with hexamethylditin, showing that the NCN-pincer palladium unit was the active catalyst in the allylic stannylation reaction. However, the triazole group is not likely to be innocent in this reaction either. The reaction taking place on the palladium centre may well be affected by the ability of the triazole group to coordinate any tin-containing compounds. It may also be affected by the ability of the triazole group to intermolecularly coordinate with neighbouring palladium centres.

Elemental content analysis of catalytic materials **4** and **7** was analysed *post*-catalysis to measure how much palladium had leached into the reaction mixture. Minimal changes (within experimental error) were observed in the palladium content of the various catalytic materials (table 3). This demonstrates that no soluble palladium species are leaching from the silica surface during the catalytic reactions. Furthermore, it emphasises the stability of the pincer organometallic unit when acting as a Lewis acid catalyst. The tin content was measured for the *post*-catalysis material **4**

and was found to be 7.64%, this corresponds to 3.2×10^{-5} mol present post catalysis. In a typical catalytic reaction material **4** contains 4.8×10^{-5} mol triazole and 2.3×10^{-5} mol of pincer complex units. It is likely that both palladium stannane and triazole stannane complexes are on the silica surface after allylic stannylation catalysis. The question this leads to is can triazole ligands achieve stannylation catalysis. The answer is no, material **3** does not catalyse the reactions, neither does an organic molecule containing triazole groups.

Table 3. Palladium content of recycled catalytic material.

Reaction	Material 4	Material 7
Pd		
Michael	0.58%	0.40%
Sn		
Stannylation	7.64%	-

Material **4** showed the best catalytic activity in the allylic stannylation reaction and thus was tested in a recycling study (figure 9). Material **4** could be recycled by centrifugation and decantation of the reaction solution resulting in isolation of the solid catalytic material. No loss in activity was observed over three recycles of the catalytic material. Quantitative yields were also observed over three cycles and no Pd(0) was observed.

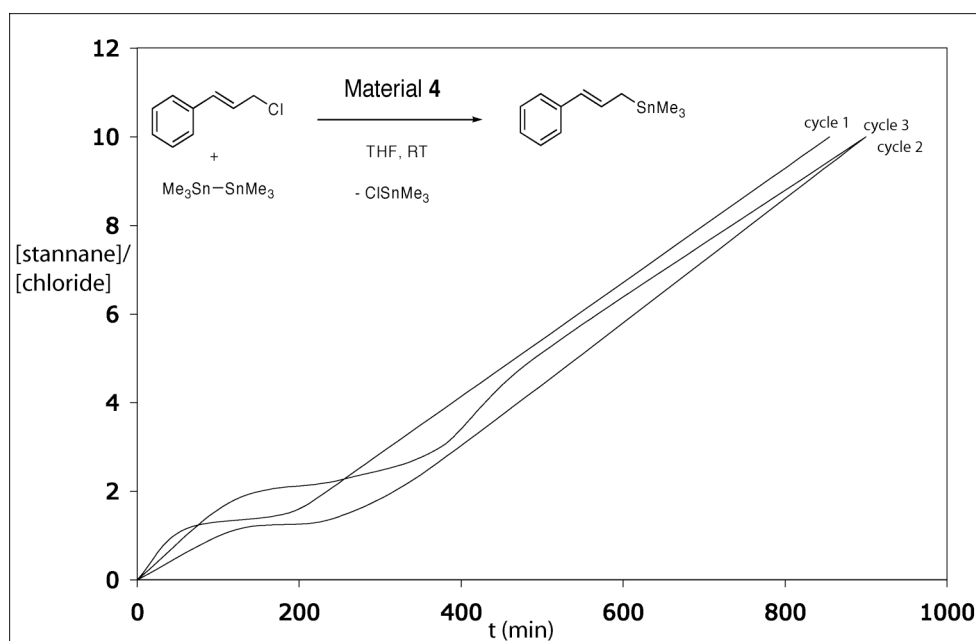
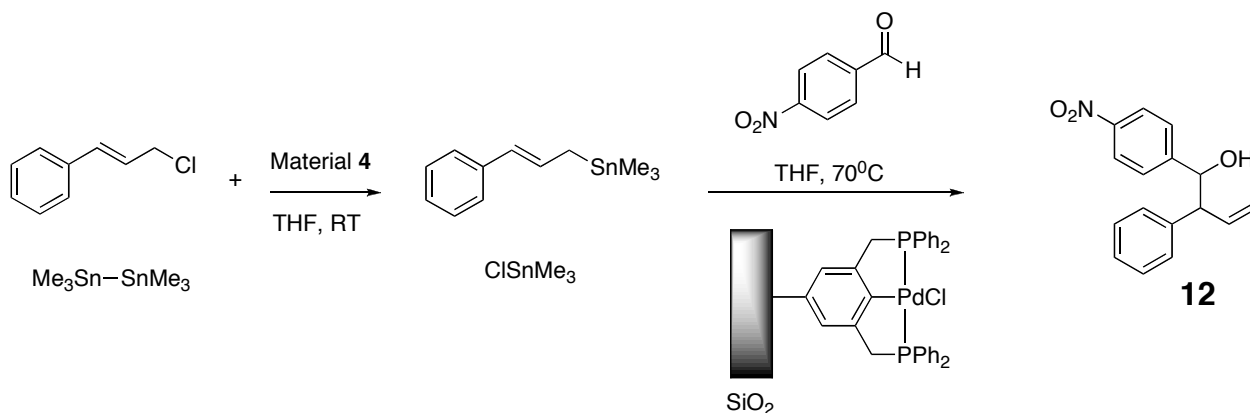


Figure 9. Recycled material **4** in the allylic stannylation reaction.

2.2.7 Sequential Catalysis

Scheme 6. Sequential allylic-stannylation/allylic-alkylation using immobilised NCN-Pd and PCP-Pd organometallic complexes.



The filtrate from the allylic stannylation reaction was subsequently immediately used (scheme 6), *without work-up*, in an allylic alkylation reaction, using a PCP-pincer palladium chloride catalyst immobilised on silica made previously in our group (carbamate linker to the support, $\text{P} = \text{PPh}_2$).³³ The *in situ* formed stannane from the first catalytic reaction was reacted with 4-nitrobenzaldehyde giving quantitative conversion to the C-C coupled product **12** as a mixture of diastereoisomers. This result gives a proof of principle of cascade catalysis with immobilised catalysts. For example, in the case that two catalysts are incompatible under certain reaction conditions, catalyst immobilisation allows one to simply transfer reaction solutions between reaction vessels containing a specific catalytic material. This approach does not require separation of catalysts (economy of solvent use) while the conditions required for catalysis can be optimised for most operations. A key point in this concept is catalyst stability, which is excellent for many ECE-pincer metal catalysts, as demonstrated for NCN-pincer palladium complexes in this report.

2.3 Conclusions

Copper(I) catalysed 1,3-Huisgens cycloaddition and nucleophilic reaction of an alcohol with an isocyanate have been applied to demonstrate ‘click’ immobilisation of pincer palladium and platinum organometallics on silica. Novel material for this ‘click’ immobilisation have been developed containing both azide or isocyanate functionalities. The copper(I) catalyst used for Huisgens 1,3-cycloaddition is an areneaminothiolate complex. Use of this copper catalyst ensures no remnant copper compounds are on the silica surface after immobilisation, which is not the case with other copper(I) catalysts.

The synthesised materials were thoroughly characterised using solid-state IR, NMR spectroscopic techniques and elemental content analysis and surface area measurements demonstrating that the pincer-palladium/platinum complexes remain intact and are inert during the immobilisation procedures. The acquired palladium containing materials were applied in two types

of C-C bond forming reactions. In the Lewis acid catalysed double Michael addition reaction of methylvinyl ketone with ethyl-cyanoacetate the developed materials showed activity comparable to the homogeneous catalyst. Furthermore, a model system containing only the linkers which connect the organometallic to the support was found to be almost as active as the homogeneous palladium catalyst. This demonstrates the non-innocent role that the linkers play in the 'heterogeneously' catalysed reaction. Furthermore in allylic stannylation reactions the triazole linker was again found to be non-innocent.

Catalyst stability is an important point in the developed systems. Recycling of the immobilised organometallics resulted in no complex decompositions. This is demonstrated in the recycling experiments in the stannylation catalysis section, where there are minimal differences in the kinetic profile of the three recycling reactions. This report shows that simple one-step lab-shelf to reaction vessel procedures can be applied for the application of homogeneous catalysts in a heterogeneous manner. Simple mixing of a support material with a functionalised organometallic yields a ready-to-use catalytic material that can be removed from the reaction vessel post-catalysis, allowing simple work-up of products, and for reapplication of the catalytic material.

2.4 Experimental Section

General Considerations. Standard Schlenk procedures under N₂ were carried out throughout. Reagents were used as supplied from Acros BV or Sigma-Aldrich, unless otherwise stated. ¹H, ¹³C and ³¹P solution NMR was carried out on a Varian Inova 300 spectrometer or a Varian Oxford AS400. CP-MAS NMR was carried out using a Bruker AV 750. Elemental analyses were performed by Dornis und Kölbe, Mikroanalytisches Laboratorium, Mülheim a. d. Ruhr, Germany. MS measurements were carried out on an Applied Biosystems Voyager DE-STR MALDI-TOF MS. IR spectra were recorded on a Perkin-Elmer SpectrumOne FT-IR Spectrometer. GC analyses were performed on a Perkin-Elmer AutosystemXL Gas Chromatograph.

3-Chloropropyl-1-silica.

Silica (10g, BASF bv Nederland, C500-383) and 3-chloropropyl-1-(triethoxy)silane (10mL, 0.041mol) were placed in dry toluene (100mL) and heated at reflux for 24h. The mixture was filtered hot and then washed with toluene (2x), boiling EtOH (2x), CH₂Cl₂ (2x), and pentane (2x), and subsequently dried under vacuum. White powder. IR (DRIFT, difference); $\nu_{\text{SiO-H}}$ 3740 cm⁻¹ (trough).

TMS-capped-3-chloropropyl-1-silica.

3-Chloropropyl-1-silica (5g) was placed in dry hexanes (50mL) with hexamethyldisilazane (5mL, 3.87g, 0.024mol) and the mixture was heated at reflux for 24h. The mixture was filtered hot and then washed with pentane (2x), boiling EtOH (2x), CH₂Cl₂ (2x), and pentane (2x), and subsequently dried under vacuum. White powder. IR (DRIFT, difference); $\nu_{\text{SiO-H}}$ 3740 cm⁻¹ (trough). Elemental analysis found; C 5.90, H 1.31, Cl 4.02.

TMS-capped-3-azidopropyl-1-silica, 1.

TMS-capped-3-chloropropyl-1-silica (5g) was placed in DMSO (50mL) with NaN₃ (5g, 0.077mol) and stirred at RT for 96h. The mixture was filtered and then washed with DMSO (2x), water (4x) and then acetone (2x) and subsequently dried under vacuum. White powder. IR (DRIFT, difference); $\nu_{\text{N-N}}$ 2037 cm⁻¹, $\nu_{\text{SiO-H}}$ 3740 cm⁻¹ (trough). Elemental analysis found; C 3.49, H 1.10, N, 1.39, Cl 0.

TMS-capped-3-(4-phenyl-1H-1,2,3-triazole)-propyl-1-silica, 3.

TMS-capped-3-azidopropyl-1-silica (1g) was placed in dry degassed toluene with ethynylbenzene (1mL, 0.009mol) and 2-[(dimethylamino)methyl]phenylthiolato-copper(I) (0.025g, 1.1mmol) and stirred at RT under inert conditions for 72h. The mixture was filtered and then washed with toluene (2x), EtOH (4X) CH₂Cl₂ (2x), and pentane (2x), and subsequently dried under vacuum. Light brown powder. IR (DRIFT, difference); ν_{triazole} 1450 - 1430cm⁻¹, ν_{NNN} 2025 cm⁻¹(trough), $\nu_{\text{SiO-H}}$ 3740 cm⁻¹ (trough). Elemental analysis found; C 5.56, H 1.15, N, 1.35, Cu not detected.

TMS-capped-3-[(4-[2,6-bis[(dimethylamino)methyl]-1-palladium(II)bromide-benzene]-1H-1,2,3-triazole)]-propyl-1-silica, 4.

TMS-capped-3-azidopropyl-1-silica (1g) and 4-ethynyl-2,6-bis[(dimethylamino)methyl]-1-palladium(II)bromide-benzene (0.052g, 1.3mmol) and 2-[(dimethylamino)methyl]phenylthiolato-copper(I) (0.005g, 0.02mmol) were placed in a CH₂Cl₂/CH₃CN (1:1 30mL) solution and stirred at RT for 72h. The mixture was filtered and then washed with CH₂Cl₂ (2x), and CH₃CN (2x), and pentane (2x), and subsequently dried under vacuum. Light brown powder. IR (DRIFT, difference); ν_{triazole} 1450 - 1430cm⁻¹, ν_{NNN} 2027 cm⁻¹(trough), $\nu_{\text{SiO-H}}$ 3740 cm⁻¹ (trough). Elemental analysis found; C 4.60, H 1.10, N, 1.78, Pd 0.52.

TMS-capped-3-[(4-[2,6-bis[(dimethylamino)methyl]-1-platinum(II)bromide-benzene]-1H-1,2,3-triazole)]-propyl-1-silica, 5.

TMS-capped-3-azidopropyl-1-silica (1g) and 4-ethynyl-2,6-bis[(dimethylamino)methyl]-1-platinum(II)bromide-benzene (0.05g, 1mmol) and 2-[(dimethylamino)methyl]phenylthiolato-copper(I) (0.005g, 0.02mmol) were placed in a CH₂Cl₂/CH₃CN (1:1 30mL) solution and stirred at RT for 72h. The mixture was filtered and then washed with CH₂Cl₂ (2x), CH₃CN (2x), and pentane (2x), and subsequently dried under vacuum. Light yellow powder. IR (DRIFT, difference); ν_{triazole} 1450 - 1430cm⁻¹, ν_{NNN} 2030 cm⁻¹(trough), $\nu_{\text{SiO-H}}$ 3740 cm⁻¹ (trough). Elemental analysis found; C 7.75, H 1.50, N, 1.08, Pt 0.45.

Typical click reaction conditions for synthesis of 9 and 10:

Azidomethyl-benzene (90 mg, 0.68 mmol) and 4-ethynyl-2,6-bis[(dimethylamino)methyl]-platinum(II)chloride-benzene (0.20 g, 0.45 mmol) were dissolved in a 1:1 mixture CH₃CN:CH₂Cl₂ (2 mL) and 2,6-lutidine (78 μ L, 0.68 mmol) and [Cu(MeCN)₄](PF₆) were added. The resulting mixture was stirred at room temperature for 24 h. Next, Et₂O (~2 mL) was added resulting in a yellow precipitate. This precipitate was collected, washed with Et₂O (2 x 2 mL) and dried *in vacuo*.

1-Benzyl-4-[2,6-bis[(dimethylamino)methyl]-1-palladium(II)bromide-benzene]-1H-1,2,3-triazole, 9.

Brown powder, 82% yield. ¹H NMR (400 MHz, DMSO-d₆): δ 2.71 (s, 12H, N(CH₃)₂), 4.10 (s, 4H, CH₂N), 5.62 (s, 2H, CH₂Ph), 7.31 – 7.39 (m, 7H, ArH), 8.53 (s, 1H, H-Triazole); ¹³C NMR (100 MHz, DMSO-d₆): δ 52.55, 53.87, 73.60, 117.88, 121.11, 128.20, 128.57, 128.91, 129.51, 136.58, 145.56, 146.51, 148.03; MALDI-TOF (9-nitroanthracene, MeCN) (m/z): 542.14 (calcd. M - Br : 454.12). Anal. Calcd. for C₂₁H₂₆ClN₅Pt•4H₂O: C, 41.56; H, 5.65; N, 11.54; found: C, 41.80; H, 5.12; N, 11.35. IR; ν_{triazole} 1450 - 1430cm⁻¹. IR (ATR); ν_{triazole} 1450 - 1430cm⁻¹.

1-Benzyl-4-[2,6-bis[(dimethylamino)methyl]-1-platinum(II)bromide-benzene]-1H-1,2,3-triazole, 10.

Off-yellow powder, 96% yield. ¹H NMR (400 MHz, DMSO-d₆): δ 2.92 (s, 12H, N(CH₃)₂), 4.07 (s, 4H, CH₂N), 5.58 (s, 2H, CH₂Ph), 7.25 (s, 2H, ArH), 7.30 – 7.37 (m, 5H, ArH), 8.43 (s, 1H, H-Triazole); ¹³C NMR (100 MHz, DMSO-d₆): δ 53.63, 55.60, 77.27, 116.89, 120.84, 126.12, 128.53, 128.80, 129.46, 138.82, 144.84, 146.70, 148.99; MALDI-TOF (9-nitroanthracene, MeCN) (m/z): 578.15 (calcd.: 578.15), 542.17 (calcd. M - Cl : 542.64). Anal. Calcd. for C₂₁H₂₆ClN₅Pt: C, 43.56; H, 4.53; N, 12.10; found: C, 43.67; H, 4.50; N, 12.06. IR (ATR); ν_{triazole} 1450 - 1430cm⁻¹.

3-Aminopropyl-1-silica.

Silica (5g, BASF bv nederland, C500-383) and 3-aminopropyl-1-(triethoxy)silane (5mL, 0.021mol) were placed in dry toluene (100mL) and heated at reflux for 24h. The mixture was filtered hot and then washed with toluene (2x), boiling EtOH (2x), acetone (2x), CH₂Cl₂ (2x), and pentane (2x), and subsequently dried under vacuum. White powder. IR (DRIFT, difference); $\nu_{\text{SiO-H}}$ 3740 cm⁻¹ (trough).

TMS-capped-3-aminopropyl-1-silica.

3-aminopropyl-1-silica (5g) was placed in dry hexanes (50mL) with hexamethyldisilazane (5mL, 3.87g, 0.024mol) and the mixture was heated at reflux for 24h. The mixture was filtered hot and then washed with pentane (2x), boiling EtOH (2x), CH₂Cl₂ (2x), and pentane (2x), and subsequently dried under vacuum. White powder. IR (DRIFT, difference); $\nu_{\text{SiO-H}}$ 3740 cm⁻¹ (trough).

TMS-capped-3-isocyanatopropyl-1-silica, 2.

TMS-capped-3-aminopropyl-1-silica (5g) was placed in a schlenk with toluene (30mL, dry degassed). Triphosgene (2.03g, 6.8mmol) was added and the resulting mixture was heated at reflux for 24h. The mixture was filtered hot and then washed with toluene (2x), acetone (2x), CH₂Cl₂ (2x), and pentane (2x), and subsequently dried under vacuum. White powder. IR (DRIFT, difference); ν_{CNO} 2276 cm⁻¹, $\nu_{\text{SiO-H}}$ 3740 cm⁻¹ (trough). Elemental analysis found; C 7.47, H 2.20, N, 0.77.

TMS-capped-3-(benzylcarbamato)propyl-1-silica, 6.

TMS-capped-3-isocyanatopropyl-1-silica (1g) was placed in dry toluene (5mL) with benzylalcohol (1mL, 9.7mmol) and stirred at reflux for 24h. The mixture was filtered hot and then washed with toluene (2x), boiling EtOH (2x), acetone (2x), CH₂Cl₂ (2x), and pentane (2x), and subsequently dried under vacuum. White powder. IR (DRIFT, difference); $\nu_{\text{carbamate}}$ 1700 & 1530 cm⁻¹ ν_{CNO} 2276 cm⁻¹(trough), $\nu_{\text{SiO-H}}$ 3740 cm⁻¹ (trough).

TMS-capped-3-[4-(N-carbamato)-2,6-bis[(dimethylamino)methyl]-1-palladium(II)bromide-benzene]propyl-1-silica, 7.

4-(tert-Butyldimethylsiloxy)-2,6-bis[(dimethylamino)methyl]-1-palladium(II)bromide-benzene (0.05g, 0.11mmol) was dissolved in a CH₂Cl₂/MeOH mixture (1:1, 10mL) and stirred over an ion exchange resin (DOWEX 50WX8) for 6h (small amount Pd black observed). The resulting solution was filtered and solvent was removed. The resulting solid was dissolved in CH₂Cl₂ (20mL) with NEt₃ (3mL, large excess) and 4-dimethylaminopyridine (0.005g, cat., 0.04mmol) and TMS-capped-3-isocyanatopropyl-1-silica (1g) and was stirred at reflux for 24h. The mixture was filtered hot and then washed EtOH (2x), acetone (2x), CH₂Cl₂ (2x), and pentane (2x), and subsequently dried under vacuum. Light yellow powder. IR (DRIFT, difference); $\nu_{\text{carbamate}}$ 1641 & 1562 cm⁻¹ ν_{CNO} 2276 cm⁻¹(trough), $\nu_{\text{SiO-H}}$ 3740 cm⁻¹ (trough). Elemental analysis found; C 6.45, H 1.81, N, 2.12, Pd 0.26.

TMS-capped-3-[4-(N-carbamato)-2,6-bis[(dimethylamino)methyl]-1-platinum(II)chloride-benzene]propyl-1-silica, 8.

4-(tert-Butyldimethylsiloxy)-2,6-bis[(dimethylamino)methyl]-1-platinum(II)chloride-benzene (0.054g, 0.1mmol) was dissolved in a CH₂Cl₂/MeOH mixture (1:1, 10mL) and stirred over an ion exchange resin (DOWEX 50WX8) for 24h. The resulting solution was filtered and solvent was removed. The resulting solid was dissolved in CH₂Cl₂ (20mL) with NEt₃ (3mL, large excess) and 4-dimethylaminopyridine (0.005g, cat., 0.04mmol) and TMS-capped-3-isocyanatopropyl-1-silica (1g) and was stirred at reflux for 24h. The mixture was filtered hot and then washed EtOH (2x), acetone (2x), CH₂Cl₂ (2x), and pentane (2x), and subsequently dried under vacuum. Yellow powder. IR (DRIFT, difference); $\nu_{\text{carbamate}}$ 1648 & 1548 cm⁻¹ ν_{CNO} 2276 cm⁻¹(trough), $\nu_{\text{SiO-H}}$ 3740 cm⁻¹ (trough). Elemental analysis found; C 11.62, H 2.53, N, 2.17, Pt 0.79.

Standard conditions for double Michael addition:

Catalyst (0.0025 mmol active cat.), cyano-acetic acid ethyl ester (0.03g, 0.25mmol, ethyl-cyanoacetate), 3-buten-2-one (0.056, 0.79mmol, methylvinyl ketone) and diisopropylethylamine (Hünigs base, 0.005g, 0.025mmol) were placed in CH₂Cl₂ (1mL, dry degassed). The mixture was stirred at room temperature until the reaction was complete. Aliquots of 10µl were taken at regular time intervals (varied depending on whether homo. or hetero. cat.). All volatiles were then removed under a steady stream of nitrogen, and the remaining oil was dissolved in CDCl₃ for ¹H NMR analysis.

Standard Conditions for allylic stannylation:

Catalyst (0.0026 mmol active cat.), hexamethyldistannane (0.082g, 0.25mmol), 3-chloro-1-propenylbenzene (0.38g, 0.25mmol, cinnamyl chloride) were placed in dry, degassed THF (1mL). The mixture was stirred at room temperature until the reaction was complete. Aliquots of 10µl were taken at regular time intervals (varied depending on whether homo. or hetero. cat.). All volatiles were then removed under a steady stream on nitrogen, and the remaining oil was dissolved in CDCl₃ for ¹H NMR analysis.

Standard conditions for allylic alkylation:

Catalyst (0.0026 mmol active cat.), 3-(trimethylstannyl)-1-propenylbenzene (0.070g, 0.25mmol, cinnamyl trimethylstannane), 4-nitrobenzaldehyde (0.038g, 0.25mmol) were placed in dry, degassed THF (1mL). The mixture was stirred at room temperature until the reaction was complete. All volatiles were then removed under a steady stream on nitrogen, and the remaining oil was dissolved in CDCl₃ for ¹H NMR analysis.

Recycling:

Catalytic mixtures were poured over a glass frit (#4) and subsequently washed with the solvent used during the catalytic experiment (CH₂Cl₂ for Michael, THF for both stannylation and allylic alkylation). This method led to loss of some catalytic material, which could not be removed from the frit. Another technique is to centrifuge the reaction mixture to separate the insoluble catalytic material.

Sequential Experiments:

The mixture from the stannylation reaction was placed in a centrifugation vessel and the catalyst and substrates were separated from each other. The substrate was immediately placed onto the new catalysts, without addition of solvent, and the benzaldehyde was added to the solution.

2.5 References

¹ D. E. De Vos, I. F. J. Vankelecom, P. A. Jacobs [Eds. Weinheim]; Chiral Catalyst Immobilization and Recycling, **2000**. Wiley-VCH.

² D. J. Cole-Hamilton, *Science* **2003**, *299*, 1702-1706.

³ K. Fodor, S. G. A. Kolmschot, R. A. Sheldon, *Enantiomer* **1999**, *4*, 497-511.

⁴ (a) C. E. Song, S. Lee, *Chem. Rev.* **2002**, *102*, 3495-3524. (b) J. M. Notestein, A. Katz, *Chem. Eur. J.* **2006**, *12*, 3954-3965. (c) A. Corma, H. Garcia, *Adv. Synth. Catal.* **2006**, *348*, 191-1412.

⁵ (a) G. R. Newkome, H. He, C. N. Moorefield, *Chem. Rev.* **1999**, *99*, 1689-1746. (b) L. J. Twyman, A. S. H. King, I. K. Martin, *Chem. Soc. Rev.* **2002**, *31*, 69-82. (c) R. van Heerbeek, P. C. J. Kamer, P. W. N. M. van Leeuwen, J. N. H. Reek, *Chem. Rev.* **2002**, *102*, 3717-3756. (d) G. P. M. van Klink, H. P. Dijkstra, G. van Koten, *C.R. Chimie* **2003**, *6(8-10)*, 1079-1085. (e) Y. Ribourbouille,

- G. D. Engel, L. H. Gade, *C.R. Chemie* **2003**, *6*, 1087-1096. (f) P. A. Chase, R. J. M. Klein Gebbink, G. van Koten, *J. Organometallic Chem.* **2004**, *689*, 4016-4054. (g) R. van de Coevering, R.J.M. Klein Gebbink, G. van Koten, *Prog. Polym. Sci.* **2005**, *30*, 474-490. (h) A. Berger, R. J. M. Klein Gebbink, G. van Koten, *Topics in Organometallic Chemistry* **2006**, *20*(Dendrimer Catalysis), 1-38. (i) R. Andres, E. De Jesus, J-C. Flores, *New J. Chem.* **2007**, *31*, 1161-1191. (j) S-H. Hwang, C. D. Shreiner, C. N. Moorefield, G. R. Newkome, *New J. Chem.* **2007**, *31*, 1192-1217.
- ⁶ (a) S. J. Shuttleworth, S. M. Allin, P. K. Sharma, *Synthesis* **1997**, 1217-1239. (b) D. E. Bergbreiter, *Catal. Today* **1998**, *42*, 389-397. (c) S. J. Shuttleworth, S. M. Allin, R. D. Wilson, D. Nasturica, *Synthesis* **2000**, *8*, 1035-1074. (d) B. Clapham, T. S. Reger, K. D. Janda, *Tetrahedron* **2001**, *57*, 4637-4662. (e) T. J. Dickerson, N. N. Reed, K. D. Janda, *Chem. Rev.* **2002**, *102*, 3325-3344. (f) S. Kobayashi, R. Akiyama, *Chem. Commun.* **2003**, 449-460. (g) P. Mastrorilli, C. F. Nobile, *Coord. Chem. Rev.* **2004**, *248*, 377-395.
- ⁷ (a) W. A. Herrmann, C. W. Kohlpaintner, *Angew. Chem. Int. Ed. Engl.* **1993**, *32*, 1524-1544. (b) P. G. Jessop, T. Ikariya, R. Noyori, *Chem. Rev.* **1999**, *99*, 475-493. (c) E. de Wolf, G. van Koten, B-J. Deelman, *Chem. Soc. Rev.* **1999**, *28*, 37-41. (d) R. H. Fish, *Chem. Eur. J.* **1999**, *5*, 6, 1677-1680. D. Sinou, *Adv. Synth. Catal.* **2002**, *344*, 221-237. (e) G. Pozzi, I. Shepperson, *Coord. Chem. Rev.* **2003**, *242*, 115-124. (f) C. Baudequin, J. Baudoux, J. Levillain, D. Cahard, A. -C. Gaumont, J. -C. Plaquevent, *Tetrahedron; Asymm.* **2003**, *14*, 3081-3093. (g) C. Eui Song, *Chem. Commun.* **2004**, 1033-1043. (h) F. Fache, *New J. Chem.* **2004**, *28*, 1277-1283. (i) B. Cornils, W. A. Herrmann, I. T. Horvath, W. Leitner, S. Mecking, H. Olivier-Bourbigou, D. Vogt, *Multiphase Homogeneous Catalysis* **2005**, Wiley-VCH.
- ⁸ H. C. Kolb, M. G. Finn, K. B. Sharpless, *Angew. Chem. Int. Ed.* **2001**, *40*, 2004-2021.
- ⁹ N. D. Gallant, K. A. Lavery, E. J. Amis, M. L. Becker, *Adv. Mater.* **2007**, *19*, 965-969.
- ¹⁰ H. Nandivada, H-Y. Chen, L. Bondarenko, J. Lahann, *Angew. Chem. Int. Ed.* **2006**, *45*, 3360-3363.
- ¹¹ C. Gauchet, G. R. Labadie, C. D. Poulter *J. Am. Chem. Soc.* **2006**, *128*, 9274-9275.
- ¹² K. M. Kacprzak, N. M. Maier, W. Linder, *Tet. Lett.* **2006**, *47*, 8721-8726.
- ¹³ R. A. Decreau, J. P. Collman, Y. Yang, Y. Yan, N. K. Devaraj, *J. Org. Chem.* **2007**, *72*, 2794-2802.
- ¹⁴ A. Gissibl, C. Padie, M. Hager, F. Jaroschik, R. Rasappan, E. Cuevas-Yanez, C-O. Turrin, A-M. Caminade, J-P. Majoral, O. Reiser, *Org. Lett.* **2007**, *9*, 2895-2898.
- ¹⁵ E. Alza, X. C. Cambeiro, C. Jimeno, M. A. Pericas, *Org. Lett.* **2007**, *9*, 3717-3720.
- ¹⁶ M. Albrecht, G. van Koten, *Angew. Chem. Int. Ed.* **2001**, *40*, 3750-3781.
- ¹⁷ a) W. T. S. Huck, R. Hulst, P. Timmerman, F. C. J. M. van Veggel, D. N. Reinhoudt, *Angew. Chem. Int. Ed.* **1997**, *36*, 1006; b) W. T. S. Huck, F. C. J. M. van Veggel, D. N. Reinhoudt, *New J. Chem.* **1998**, *22*, 165.
- ¹⁸ M. E. van der Boom, D. Milstein, *Chem. Rev.* **2003**, *103*, 1759-1792.
- ¹⁹ J. W. J. Knapen, A. W. van der Made, J. C. de Wilde, P. W. N. M. van Leeuwen, P. Wijkens, D. M. Grove, G. van Koten, *Nature* **1994**, *372*, 659
- ²⁰ a) D. E. Bergbreiter, P. L. Osborn, A. Wilson, E. M. Sink, *J. Am. Chem. Soc.* **2000**, *122*, 9058-9064. b) D. E. Bergbreiter, P. L. Osborn, J. D. Frels, *J. Am. Chem. Soc.* **2001**, *123*, 11105-11106.
- ²¹ N. C. Mehendale, C. Bezemer, C. A. van Walree, R. J. M. Klein Gebbink, G. van Koten, *J. Mol. Catal. A: Chemical*, (2006), *257*, 167-175.
- ²² F. Gorla, A. Togni, L. M. Venanzi, A. Albinati, F. Lianza *Organometallics* **1994**, *13*, 1607-1616.
- ²³ H. P. Dijkstra, M. D. Meijer, J. Patel, R. Kreiter, G. P. M. van Klink, M. Lutz, A. J. Canty, G. van Koten, *Organometallics* **2001**, *20*, 3159-3168.
- ²⁴ L. A. van de Kuil, H. Luitjes, D. M. Grove, J. W. Zwikker, J. G. M. van der Linden, A. M. Roelofson, L. W. Jenneskens, W. Drenth, G. van Koten, *Organometallics* **1994**, *13*, 468-477.
- ²⁵ M. Gagliardo, P. A. Chase, S. Brouwer, G. P. M. Van Klink, G. Van Koten, *Organometallics* **2007**, *26*, 2219-2227.
- ²⁶ C. M. Jensen, *Chem. Commun.* **1999**, *24*, 2443-2449.

- ²⁷ a) O. A. Wallner, K. J. Szabo, *Org. Lett.* **2004**, *6*, 1829-1831. b) J. Kjellgren, H. Sunden, K. J. Szabo, *J. Am. Chem. Soc.* **2004**, *126*, 474-475.
- ²⁸ a) N. Solin, J. Kjellgren, K. J. Szabo *Angew. Chem. Int. Ed.* **2003**, *42*, 3656-3658. b) N. Solin, J. Kjellgren, K. Szabo, *J. Am. Chem. Soc.* **2004**, *126*, 7026-7033. c) S. Sebelius, V. J. Olsson, K. J. Szabo, *J. Am. Chem. Soc.* **2005**, *127*, 10478-10479. d) V. J. Olsson, S. Sebelius, N. Selander, K. J. Szabo, *J. Am. Chem. Soc.* **2006**, *128*, 4588-4589.
- ²⁹ S. Diez-Gonzalez, A. Correa, L. Cavallo, S. P. Nolan, *Chem. Eur. J.* **2006**, *12*, 7558-7564.
- ³⁰ Y. C. Charalambides, S. C. Moratti, *Synthetic Commun.* **2007**, *37*, 1037-1044.
- ³¹ H. P. Dijkstra, R. J. M. Klein Gebbink, G. van Koten, unpublished work. This is as a result of the better coordination properties of the aminearenehitato ligand compared to those of the triazole ligand.
- ³² G. Rodriguez, M. Albrecht, J. Schoenmaker, A. Ford, M. Lutz, A. L. Spek, G. van Koten, *J. Am. Chem. Soc.* **2002**, *124*, 5127-5138.
- ³³ N. C. Mehendale, C. Bezemer, C. A. van Walree, R. J. M. Klein Gebbink, G. van Koten, *J. Mol. Catal. A: Chemical*, **2006**, *257*, 167-175.
- ³⁴ S. Brunauer, P. H. Emmett, E. J. Teller, *J. Am. Chem. Soc.* **1938**, *60*, 309-319.
- ³⁵ DRIFT-IR (diffuse reflectance fourier transform) is a surface technique which analyses reflected IR beam from the surface/near surface of the material.
- ³⁶ ATR-IR (attenuated total reflection) is a technique whereby transmission of an IR beam through a sample is measured.
- ³⁷ A. R. McDonald, G. P. M. van Klink, G. van Koten, submitted work.
- ³⁸ H. P. Dijkstra, M. Q. Slagt, A. R. McDonald, C. A. Kruithof, R. Kreiter, A. M. Mills, M. Lutz, A. L. Spek, W. Klopper, G. P. M. van Klink, G. van Koten, *Eur J. Inorg. Chem.* **2003**, *5*, 830-838.
- ³⁹ N. Mehendale, R. J. M. Klein Gebbink, G. van Koten. *N. Mehendale Ph.D. thesis UU 2007*, chapter 8.
- ⁴⁰ B. M. J. M. Suijkerbuijk, B. N. H. Aerts, H. P. Dijkstra, M. Lutz, A. L. Spek, G. van Koten, R. J. M. Klein Gebbink, *Dalton Trans.* **2007**, *13*, 1273-1276.
- ⁴¹ An alternative explanation for the high catalytic activity of materials **3**, **4**, and **7** could be that capped silanol groups have become deprotected. Recent work has demonstrated that functionalised amines have been tethered to a silica/zeolite support and the resulting materials were applied in the double Michael addition reaction.⁴¹ However, that work requires that remnant acid sites (uncapped silanol groups) play a role in the catalysis. We have capped all silanol groups to the best of our knowledge, with the hope of avoiding effects from the inorganic support, and therefore we believe this option to be unlikely. Furthermore, post catalysis DRIFT-IR of the supported catalytic material shows minimal changes in the SiOH region of the spectrum, suggesting the silanol group capping has not been affected. See: K. Motokura, M. Tada, Y. Iwasawa, *J. Am. Chem. Soc.* **2007**, *129*, 9540-9541.

CHAPTER 3

‘Click’ Silica Immobilisation of Metallo-Porphyrin Complexes and their Application in Epoxidation Catalysis

We present the synthesis, via Adler condensation reactions, of mono- and tetrakis-4-(ethynyl-phenyl)porphyrin ligands and the zinc and manganese complexes thereof. The formed complexes were immobilised on silica by reacting the ethynyl groups with azide functionalised silica in a copper(I) catalysed Huisgens 1,3-dipolar cycloaddition reaction. The synthesised metallo-porphyrin containing materials were thoroughly characterised using various solid-state techniques (NMR, IR, UV-vis, elemental content analysis). The manganese containing materials were applied as catalysts in the epoxidation of various alkenes (cyclooctene, cyclohexene, styrene) with various oxidants (iodosylbenzene, tert-butyperoxide). The heterogenised homogeneous catalysts show diminished activity and yields compared to the analogous homogeneous catalysts (71% yield *cf* 92% for cyclooctene epoxidation, TOF 82h⁻¹ *cf* 230h⁻¹). Upon recycling, the heterogenised catalysts become gradually less active over 5 cycles until they are catalytically inactive. The deactivation process is discussed, with the conclusion that the catalysts themselves are stable to the reaction conditions and recycling, however the oxidants undergo side-reactions and the resulting product accumulates on the insoluble catalytic material surface thus blocking the active site.

3.1 Introduction

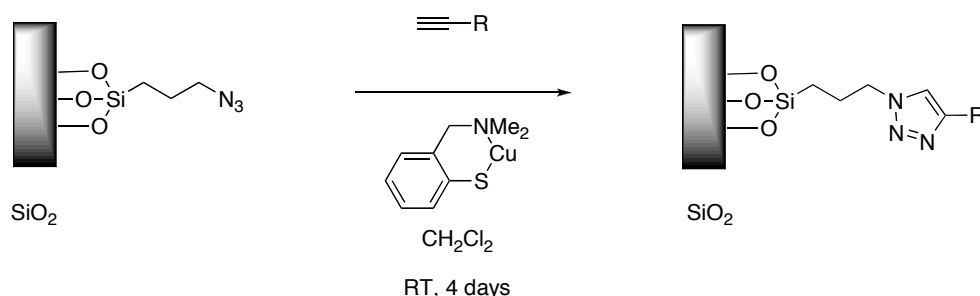
The immobilisation of homogeneous catalysts, and the stability of the catalyst itself, are important issues in the development of homogeneous catalytic systems for industrial application.¹ The immobilisation of homogeneous catalysts allows for ease of separation of catalyst from reactants and products, while catalyst stability is essential to recycling procedures and for the recovery of precious metal complexes. The synthesis of many of the fine chemicals essential for life and leisure involve at least one or more steps that involve the use of homogeneous catalysis.² The reason for this is relatively simple, selectivity. Homogeneous catalysts provide the required selectivity for certain end-products, that heterogeneous catalysts cannot offer. Thus the benefits of using heterogeneous catalysts, high stability and recyclability, are outweighed by the necessity to have selective syntheses using homogeneous catalysts. However, the cost of synthesis and recovery of homogeneous catalysts or their derivatives mean they are not widely applied. One manner to overcome this would be to immobilise homogeneous catalysts such that they can be treated in the same manner as heterogeneous catalysts, i.e. they can be recycled.

According to a recent report asymmetric epoxidation is the second most widely used asymmetric process in industry.³ Chiral epoxides and their derivatives are extremely high value products and are the basis of many enantiopure compounds. For this reason the immobilisation of chiral epoxidation catalysts has been investigated thoroughly in recent times.⁴ The field of supported metalloporphyrins for epoxidation catalysis⁵ and in particular the immobilisation of porphyrin complexes on inorganic supports and their application in alkane/alkene oxidation have been investigated.⁶ What comes from these previous reports and is a general trend in the field of homogeneous catalyst immobilisation, is that *covalent* immobilisation of catalysts on *inorganic* supports is essential for good catalyst recycling results, and minimal influences on the catalytic site by the support. It is also apparent that a simple manner for the immobilisation of such homogeneous catalysts on inorganic supports is necessary. A key point to add to this is that catalyst stability should be taken into account before any attempts are made to covalently immobilise a homogeneous catalyst. Previous work has shown that highly stable coordination complexes should be used, because labile coordination complexes do not withstand the relatively harsh conditions used for catalyst immobilisation, and subsequently for the recycling of the heterogenised catalyst. The conditions for immobilisation in some systems can be detrimental to the most stable of complexes, and ideally a modular system, comprising support, linker and catalyst would be a goal, in which mixing, under mild conditions, of the various components together resulted in the immobilised catalyst.

We have recently demonstrated such a system in which the immobilisation of homogeneous catalysts on an inorganic support is mediated using 'click' immobilisation techniques involving an azide linked to a high density silica support (figure 1).⁷ 'Click' immobilisation is defined by high yielding, highly atom efficient reactions for the tethering of an organic or organometallic moiety to an inorganic support. Azide functionalised silica has been used to couple ethynyl-functionalised compounds to high density silica using a copper(I) catalysed 1,3-Huisgens dipolar cycloaddition

reaction. The Huisgens dipolar cycloaddition is very prominent in organic chemistry presently, because of its high yielding, high atom efficiency and selectivity. The reaction has been classified as a ‘Click’ reaction, because of its high yielding, efficient nature, and its low by-product production.⁸

Scheme 1. Copper(I) thiolate catalysed ‘Click’ coupling of ethynyl organic moieties to silica support.



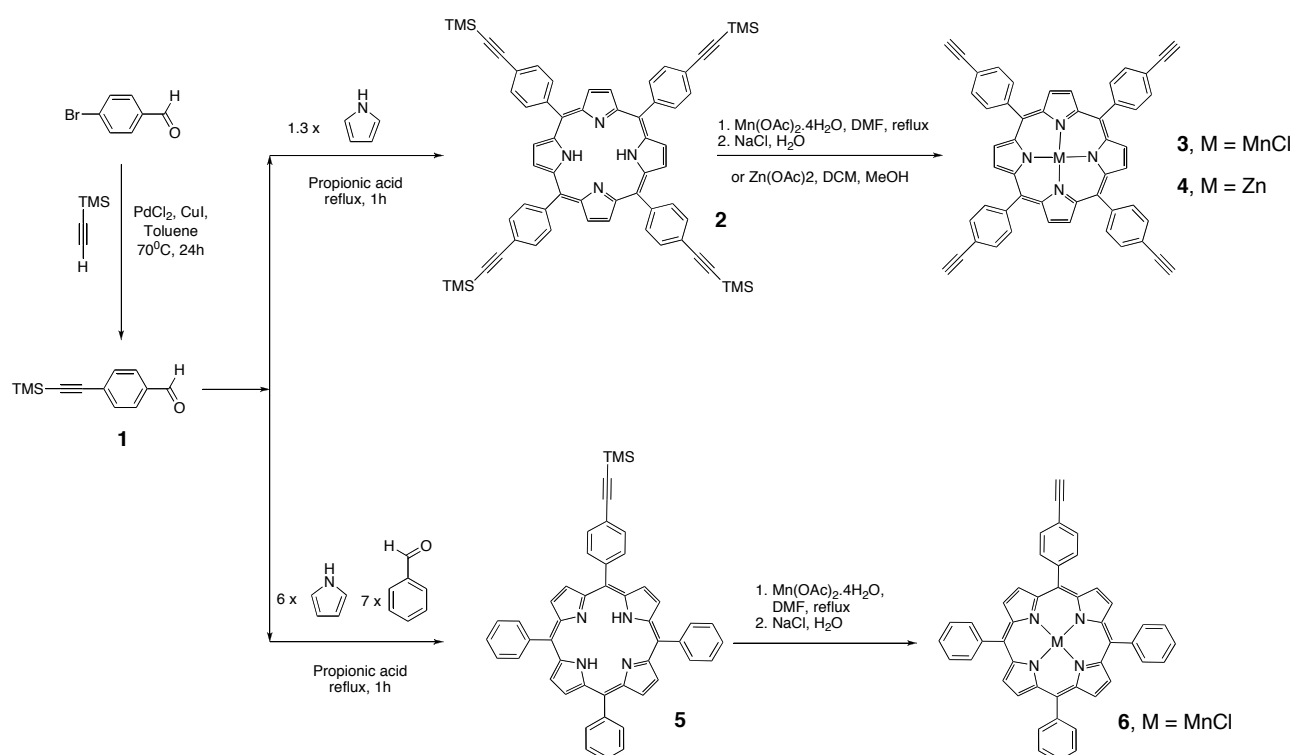
In this report immobilisation of manganese and zinc porphyrin complexes was mediated through the copper(I) thiolate catalysed reaction of an acetylene-functionalised porphyrin complex with the aforementioned azide-functionalised silica support. The novel materials were fully characterised using solid-state spectroscopic techniques. The synthesised manganese materials were applied as catalysts in the epoxidation of various alkenes showing results comparable to the homogeneous catalyst system. However, upon recycling the catalytic material showed considerably diminished activity. The porphyrin ligand system is acknowledged to be highly stable and rigid, however, the epoxidation reactions that metal porphyrin complexes catalyse use oxidants that can have great effects on complex stability, but also that give side products and we believe this is the source of the deactivation of the catalytic manganese materials.

3.2 Results and Discussion

3.2.1 Synthesis of Silica-Bound Porphyrin Complexes

For ethynyl-functionalised porphyrin synthesis (scheme 2), mono-trimethylsilyl (mono-TMS) protected ethyne was coupled with 4-bromo-benzaldehyde yielding 4-[(trimethylsilyl)ethynyl]benzaldehyde, **1**, in a palladium catalysed Sonigashira coupling reaction (79% yield). Aldehyde **1** was applied in an Adler porphyrin synthesis in two manners.⁹ Similar compounds have been previously synthesised.¹⁰ Firstly, it was mixed in a 1:1 ratio with pyrrole in refluxing propionic acid yielding 5,10,15,20-tetrakis-(4-[(trimethylsilyl)ethynyl]phenyl)-porphyrin, **2**. Compound **2** was reacted with both manganese(II) and zinc(II) acetates to yield complexes **3** and **4**, respectively, in relatively high yields. Secondly compound **1** was reacted with pyrrole and benzaldehyde (1:6:7 molar ratio, respectively) to synthesise 5-(4-[(trimethylsilyl)ethynyl]phenyl)-10,15,20-trisphenylporphyrin, **5**.

Scheme 2. Synthesis of mono- and tetra functionalised porphyrin complexes for tethering to silica support material.

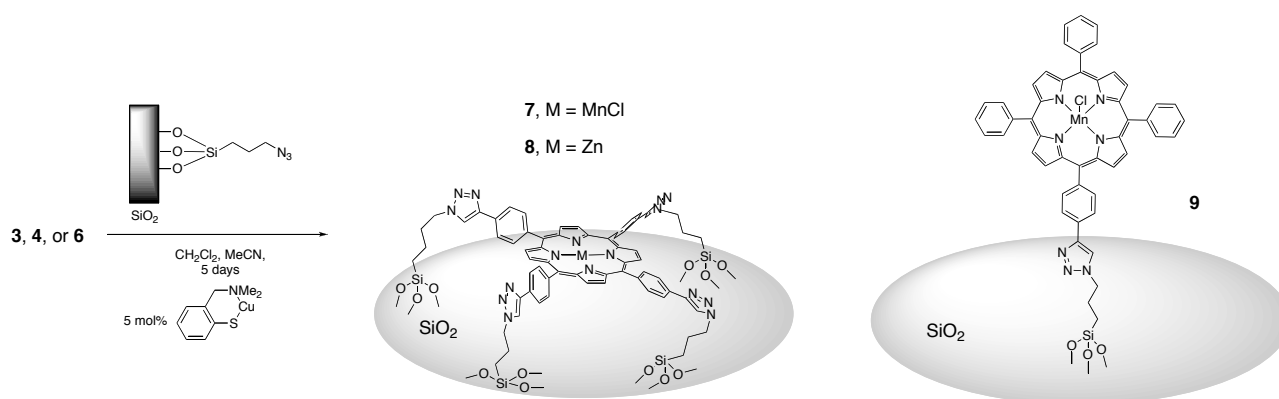


Compound **5** could not be completely purified (TPP, with small amounts of bis-, tris- and tetrakis- substituted porphyrins were also formed in the synthetic process) and complexation with $\text{Mn}(\text{OAc})_2$ was carried out on the mixture of functionalised ligands. Column chromatography was used to isolate the mono-ethynyl porphyrin manganese complex from the other products. However, it was not possible to separate **6** and $[\text{MnCl}(\text{TPP})]$ (TPP = 5,10,15,20-tetrakisphenylporphyrin). Nevertheless, for the immobilisation of **6** on silica, the **6**/ $[\text{MnCl}(\text{TPP})]$ mixture could be used, because the $[\text{MnCl}(\text{TPP})]$ could be washed off the silica support after **6** had been tethered to the support. In all three complexation reactions almost all TMS-protecting groups were cleaved during the reaction. Tetrabutylammonium fluoride (TBAF) was added to the reaction mixtures to ensure cleavage of all TMS groups, but in most instances was not necessary.

Ethynyl-functionalised porphyrin ligand **2** and metalloporphyrins **3**, **4**, and **6** were reacted with azide functionalised silica in the presence of a copper catalyst (2-[dimethylamino)methyl]-1-thiophenolato-copper(I)) at room temperature in MeCN for several days. With free-base porphyrin **2** (TMS groups cleaved using TBAF) several attempts to immobilise on silica using 'click' techniques were made. However, we were unsuccessful with both the aforementioned copper(I) thiolate complex and also $[\text{Cu}(\text{MeCN})_4]\text{PF}_6$ as catalyst. We found that transmetallation occurs between the copper(I) catalysts and the porphyrin ligand, thus deactivating the copper catalyst which resulted in very low yields of immobilised porphyrin ligand **2**. This led us to synthesise the 'protected' porphyrin material **4**, because, contrary to the copper porphyrin complexes, zinc containing porphyrins are known to be relatively labile and can be applied in demetallation and transmetallation reactions. Material **4** was reacted with azide functionalised silica yielding material **8**. We attempted to demetallate the zinc containing material **8** using trifluoro-acetic acid (TFA).

Spectroscopic studies (UV-vis) of the resulting material confirmed that the demetallation process to yield immobilised free-base porphyrin material **11** was successful. However, we found it very difficult to remove all the formed non-porphyrin zinc(II) salts from the silica material. The zinc elemental content only dropped from 0.24 to 0.14% even after carrying out several thorough washing techniques, and IR spectroscopy gives indications of acetates on the silica surface.

Scheme 3. Immobilisation of functionalised porphyrin complexes on silica support using copper(I) thiolate catalysed click chemistry.



Materials **7**, **8**, and **9** were successfully synthesised (scheme 3). Ethynylbenzene was subsequently added to the reaction mixture to ensure ‘capping’ of any remnant azide groups on the silica surface. In the case of materials **7** and **8** it was difficult to gather experimental proof that all ethynyl groups had reacted with surface azide groups. Therefore, extra free hexylazide was added to the reaction mixture to ensure any remnant ethynyl groups were ‘capped’ to ensure they did not influence any future applications of the materials. The obtained materials were either dark green in colour (manganese containing materials **7** and **9**) or light pink (zinc containing material **8**). Model system **10** was also synthesised for spectroscopic purposes, to monitor both the electronic effects of having triazole-substituents bound to the porphyrin backbone and to study the influence of the support material on the porphyrin metal complex itself.

It is important to note that test reactions were carried out to monitor if transmetallation between the copper(I) thiolate complex (‘click’ catalyst) and the porphyrin-manganese/zinc complexes had occurred during the immobilisation procedure. This was found not to be the case, demonstrating the effectiveness of using the copper catalysed coupling reaction for high yielding, clean, side-productless immobilisation. No signs of transmetallation were observed (MALDI-ToF mass analysis) when a stoichiometric 1:1 molar mixture of copper(I) thiolate and metallo-porphyrins **3**, **4** or **6**, were mixed together under standard ‘click’ reaction conditions. No signals pointing to copper porphyrin formation were observed, and likewise no manganese or zinc thiolate signals were observed. Furthermore, it was found that neither complexes **3**, **4**, or **6** catalyse the 1,3-Huisgens dipolar cycloaddition reaction.

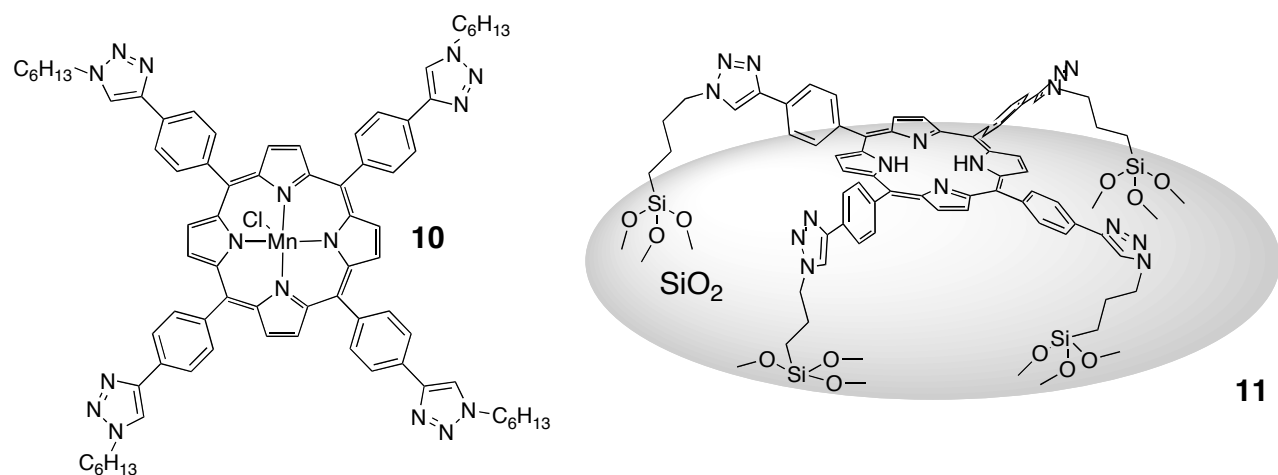


Figure 1. Soluble model system for immobilised manganese complexes, **10**, and insoluble immobilised free-base porphyrin material **11**.

3.2.2 Elemental Content Analysis of Mn-Porphyrin Materials

The manganese loading of materials **7** and **9** was found to be approximately 0.1% per weight of the total silica mass (1.8×10^{-5} mol/g Mn on SiO_2). The nitrogen loading of materials **7**, **8**, and **9** is less than the azide-functionalised silica material. However, the decrease in nitrogen loading is to be expected because the ethynyl-phenyl functionalised manganese porphyrin is a large macromolecule with a large carbon content, which would be expected to result in diminished nitrogen content measurement (even though it contains 4 nitrogen's itself). This is backed up by the relatively large carbon content (18% for material **7**). Previous results have also shown that no copper species remain on the silica surface when the copper thiolate catalyst is used during the immobilisation procedure.⁷

3.2.3 UV-vis Analysis of Mn- and Zn-Porphyrin Materials

Solid-state diffuse reflectance UV-vis spectroscopy was used to analyse materials **7**, **8**, and **9**. The acquired spectra for **7** and **9** were compared to solution-state transmission spectra of compound **10** and $[\text{MnCl}(\text{TPP})]$ respectively (figure 2). The solid-state spectra confirm that metallo-porphyrin species have been immobilised on the silica surface, with minimal changes in the photophysical properties of the coordination complexes bound to the support. Material **7** shows a Soret band at 479nm, which is comparable with both reference complexes **10** and $[\text{MnCl}(\text{TPP})]$. Similarly, the Q-band region of the spectrum shows results comparable to those of the untethered complexes. Material **9** shows contrasting results to material **7** with a considerable blue shift in both the Soret band and the Q-bands compared to the reference compounds. The strong blue shifts observed upon immobilization indicate aggregation of porphyrins by π -stacking on the silica surface.¹¹ This observation can tell us a lot about *both* materials **7** and **9**. It appears that with only one site for tethering of the porphyrin ring to the inorganic support (material **9**), high levels of interporphyrin interaction on the surface are possible. Because no blue shift is observed in the spectrum of **7** we assume the multiple anchoring of the porphyrin prevents this stacking. From surface area studies we have carried out on the starting azide material we have found that the

average distance between azide sites is 11.3\AA .⁷ This would suggest that inter-porphyrin interactions are highly likely when there is a single appendage between the porphyrin ring and the silica surface, because the porphyrin lies perpendicular to the silica surface, and is relatively mobile. In material **7**, because there are four possible appendages between the porphyrin ring and the silica surface, the porphyrin is probably forced to be parallel to the silica surface, and thus inter-porphyrin interactions are unlikely. This is backed up by the UV-vis spectrum of **7** which suggests no interactions.

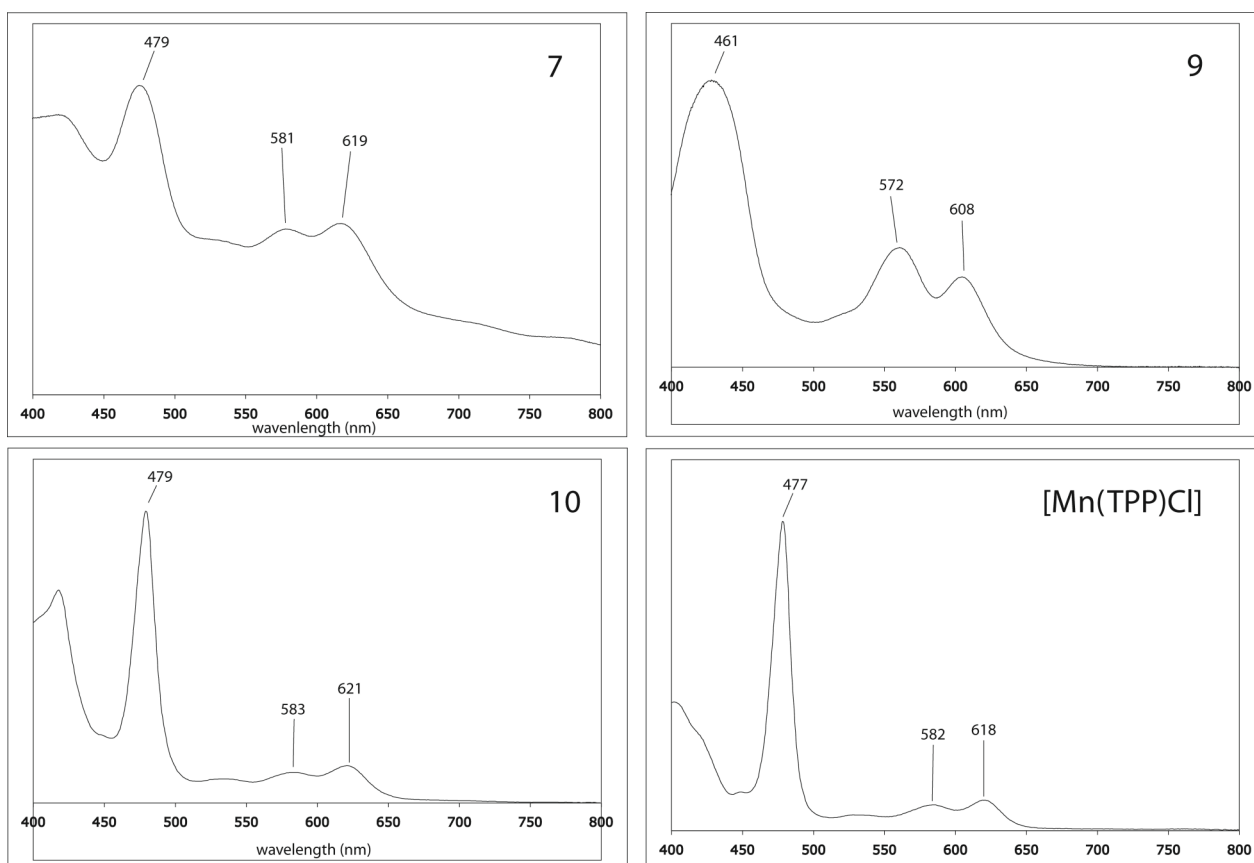


Figure 2. Solid- and solution-state UV-vis spectra of materials **7**, **9**, **10** and $[\text{MnCl}(\text{TPP})]$ respectively.

Material **8** was also characterised using solid-state UV-vis spectroscopy and the subsequent demetallation of material **8** was monitored. Figure 3 depicts the solid-state UV-vis reflectance spectrum of material **8** and the solid-state spectrum of material **11**, which is formed after demetallation of material **8**. The latter material shows characteristic absorptions of free base porphyrin species. The fact that positioning of the Soret band and the Q-bands have shifted considerably with respect to **8** is characteristic of an uncoordinated porphyrin ligand.

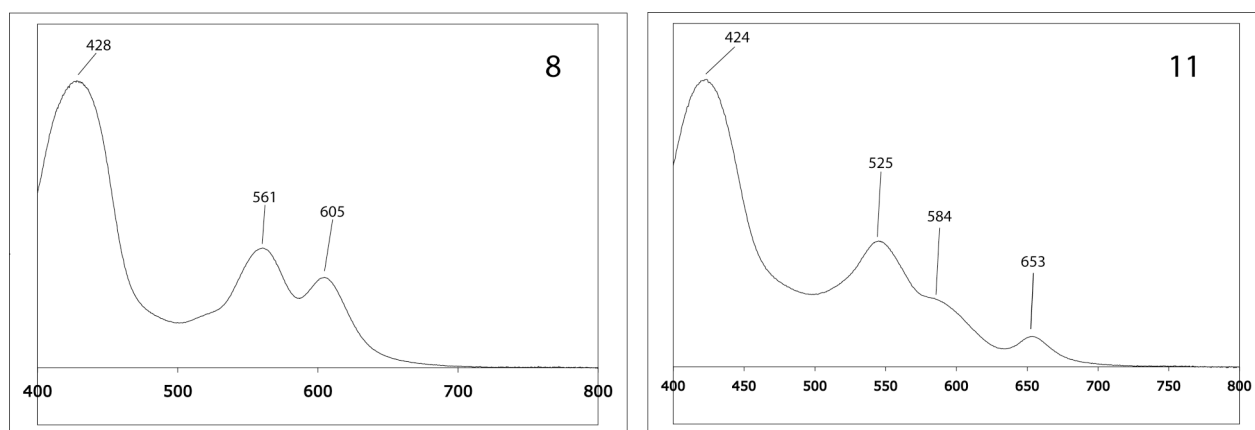


Figure 3. UV-vis solid-state reflectance spectra of materials 8 and 11.

3.2.4 Infra-Red Analysis of Porphyrin Materials

Porphyrin containing materials were also studied with ATR-IR¹² and DRIFT¹³ techniques. Figure 4 depicts the DRIFT difference spectra pertaining to material 7. The results observed are indicative for all porphyrin bound materials synthesised (7-11). The DRIFT spectrum of the starting silica is subtracted from the spectrum of 7 giving an indication of what has been 'added' to the silica (figure 4a). The spectra show that a trough in the difference spectrum is observed at 3738cm^{-1} which corresponds to a clear decrease in the intensity of silanol stretches demonstrating that all linker groups are covalently bound to the silica support. The decrease in silanol groups is a result of the synthesis of azide functionalised material (figure 1). It demonstrates a covalent linkage between the silica support and the propyl-triazole linker is present. Figure 4b confirms the reaction of ethynyl groups of the porphyrin complex with the azide group on the silica surface. The trough at 2037cm^{-1} is the azide stretch of the starting material which has disappeared in material 7. In both spectra a less intense resonance peak is observed at 1450cm^{-1} which corresponds to the triazole groups of the 'clicked' final product (confirmed by ATR spectrum of 10). These resonances are not observed in the starting material spectra. Due to the low amount of characteristic, intense IR resonances of metallo-porphyrin complexes, it was difficult to assign the remainder of the observed peaks. However, the broad resonances observed in the $3000\text{-}3500\text{cm}^{-1}$ and $900\text{-}1300\text{cm}^{-1}$ range are characteristic of the silica support material.

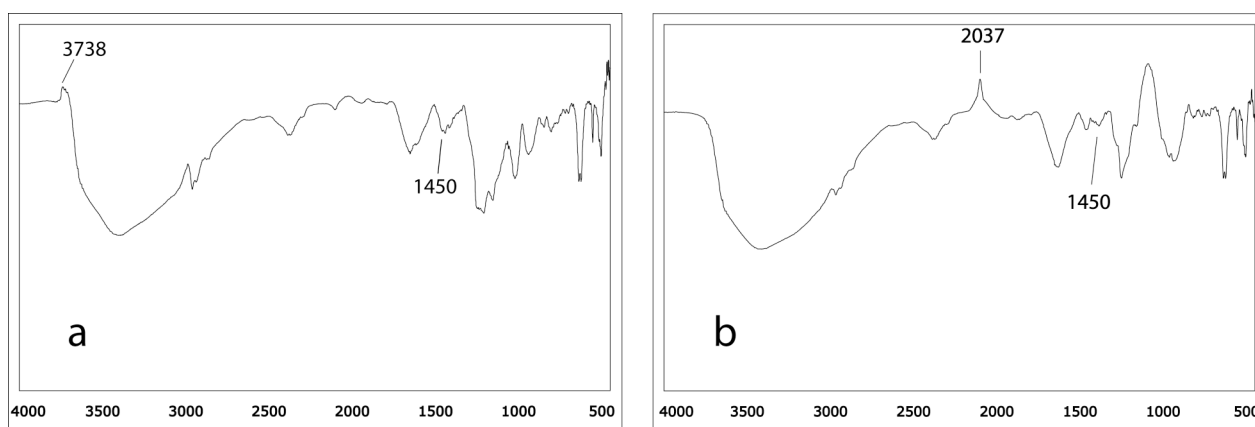


Figure 4. IR DRIFT difference spectra of material 7: a) 7 minus SiO_2 , b) 7 minus azide functionalised material.

3.2.5 NMR Analysis

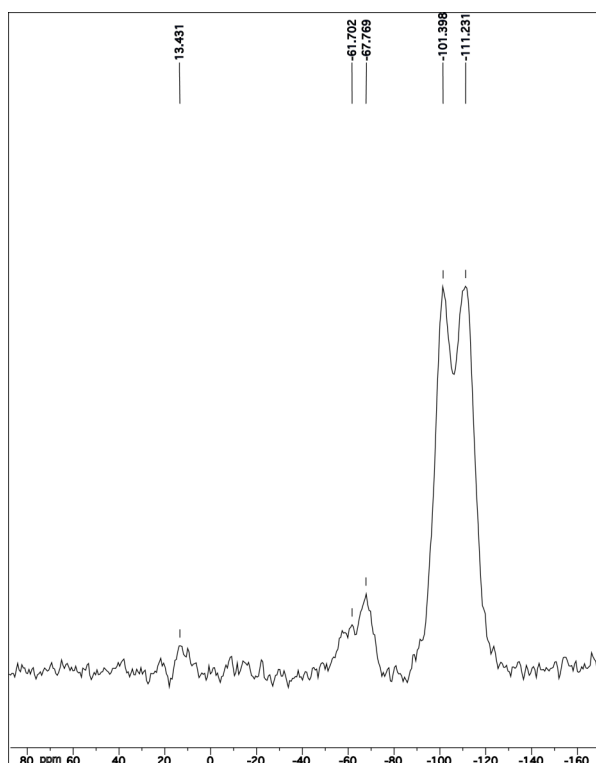


Figure 5. Solid-state CP-MAS ^{29}Si NMR spectrum of material **7**.

^{29}Si CP-MAS NMR spectroscopy was applied to analyse the effects of carrying out organic synthetic techniques on the silica support. The ^{29}Si spectrum of organometallic containing material **7** showed several peaks that indicated the presence of different forms of silicon species at the surface and in the bulk of the material (figure 5).¹⁴

3.2.6 ‘Heterogeneous’ Oxidation Catalysis with Mn-Porphyrin Materials **7** and **9**

Materials **7** and **9** were applied as heterogenised catalysts in the epoxidation of various substrates. Various oxidants were used to monitor the effects of the oxidant properties on the stability and reusability of the heterogenised catalysts. Materials **7** and **9** were initially applied in the epoxidation of cyclooctene (COE) using iodosylbenzene (PhIO) as oxidant, and with imidazole introduced as a catalytic co-ligand (table 1). Material **7** showed diminished activity compared to its homogeneous analogue, $[\text{MnCl}(\text{TPP})]$ (230 cf. 82 turnovers h^{-1}). The observed decrease in catalyst activity (on a per Mn site basis) is to be expected with the heterogenisation of homogeneous catalysts. However, the yield observed was 71% compared to 92% yield for the homogeneous system, which was unexpected (based on conversion of oxidant, alkene in excess). Material **9** showed low conversion levels and activity in the epoxidation of COE. This is surprising when compared to material **7**, however we believe it to be as a result of inter-porphyrin site interactions, resulting in intermolecular μ -oxo-bridged dimer formation (see following section). In all cases the kinetic profile of the catalysed epoxidation reaction is the same as the kinetic profile of the homogeneous catalyst, $[\text{MnCl}(\text{TPP})]$.

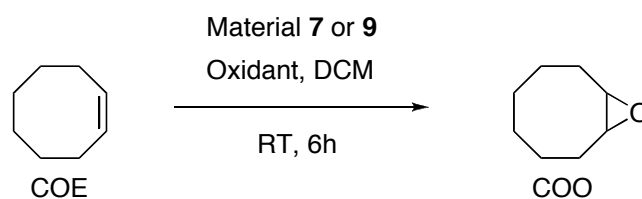


Figure 6. Epoxidation of COE using catalytic materials 7 or 9.

Table 1. Application of materials 7 and 9 in the epoxidation of COE.

Catalyst	Yield epoxide (%) ^a	TOF ^b
[MnCl(TPP)]	92	230
7	71	82
9	13	8.5

^aBased on iodosylbenzene consumed. ^bBased on rate of epoxide formation (h^{-1}).

Material 7 was applied as an epoxidation catalyst using other substrates to demonstrate the general applicability of these catalytic materials. Cyclohexene (CHE) and styrene (STE), which are less reactive substrates to manganese porphyrin catalysed epoxidation, were both tested using iodosylbenzene as oxidant. CHE was converted to cyclohexene epoxide (CHO) in very ordinary yields ($\sim 10\%$) with a TOF of 7.5 h^{-1} . Likewise STE was converted to styrene-epoxide (STO) in average yield (47%), however with a much higher TOF (58 h^{-1}).

Table 2. Application of materials 7 and 9 in the epoxidation of cyclooctene

Cycle # ^a	PhIO TOF ^b	BPO TOF ^c
1	76	3.4
2	66	2.9
3	40	1.7
4	20	1.0
5	-	0.4

^aCatalyst recycled by simple filtration and washing. ^bBased on rate of iodosylbenzene consumption (h^{-1}). ^cBased on rate of *t*-butylperoxide consumption (h^{-1}).

After the epoxidation of COE material 7 was recycled by simple filtration of the catalyst and subsequent washing of the solid remnants with CH_2Cl_2 and MeOH. A fresh solution of substrate and oxidant was then introduced to the catalytic material, and the catalysed reaction was restarted. In the epoxidation of COE catalyst recycling was carried out over four cycles. After every cycle the TOF decreased slightly and the yield decreased considerably, such that by the fourth cycle the TOF was under 20 h^{-1} and the yield was below 10% (table 2). The post-catalysis filtrate was charged with extra alkene and oxidant, however showed no extra turnovers. This

demonstrated that no Mn-porphyrin was leaching into the reaction solution. The observed gradual decrease in TOF and yields was a cause for concern, and thus we investigated the effects of other oxidants on the stability and durability of the catalytic material **7**. The milder oxidising agent *t*-butylperoxide (BPO) was applied in the epoxidation of COE using material **7** as a catalyst. The initial reaction using BPO showed considerably lower conversion levels and TOF's compared to PhIO (table 2). This is to be expected and is due to the better oxidising powers of PhIO compared to BPO. Material **7** was recycled in the same manner and fresh substrate and BPO were added to the separated catalytic material. However, a similar deactivation trend was observed.

The properties of material **7** after application as a catalyst in the epoxidation of COE were investigated to gain insights into the deactivation pathways. The elemental content of the post-catalysis material showed that the Mn loading had not changed at all, even after 5 catalyst cycles (0.1% Mn before catalysis, 0.1% after catalysis). Solid-state UV-vis and DRIFT IR spectroscopy were used to analyse the material as well (figure 7). Both spectra suggest that the integrity of the manganese porphyrin complex has been retained. In particular the UV-vis spectrum is perfectly comparable to that of material **7** and [MnCl(TPP)]. The DRIFT IR difference spectrum show that nothing new has been added to the silica surface, and that the triazole species remains intact.

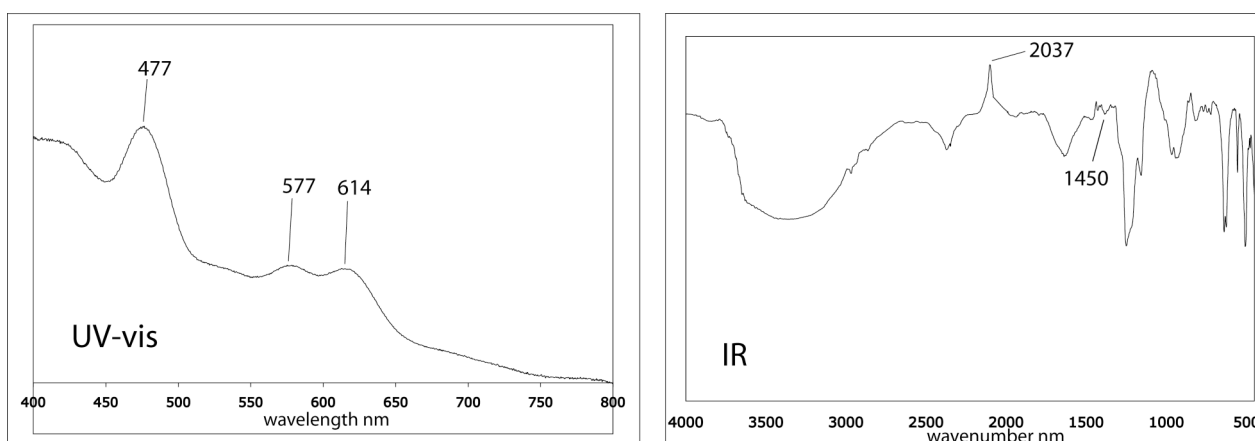


Figure 7. Post-catalysis solid-state UV-vis and IR spectra of material **7**.

3.2.7 Catalysts Deactivation Discussion

Supported Mn-complex deactivation is a very common occurrence in epoxidation catalysis. Several reports have commented on Mn-salen systems bound to supports which show gradual deactivation upon recycling of the catalytic materials.¹⁵ In these systems, the deactivation was believed to be as a result of decomplexation of the Mn-salen complexes bound to the silica support. Likewise Mn-porphyrins supported on polymeric supports have shown deactivation upon recycling in epoxidation catalysis.¹⁶ In some cases the deactivation is put down to bleaching of the manganese porphyrin complexes by intermolecular oxidation, resulting in decomplexation. The precursor to the decomplexation is a μ -oxo-bridged dimer which is also inactive in epoxidation catalysis. In other cases a convincing reason for deactivation is *not* given.

In the case of material **7**, as stated previously, we do not believe that any intermolecular interactions between porphyrin complexes on the silica surface are occurring. Firstly no UV-vis

evidence for this was observed, and secondly, the multi-dentate manner in which the complex is bound to the surface probably means the porphyrin ring lies in such a position that inter-porphyrin site interactions are unlikely. Post-catalytic UV-vis spectra are very similar to pre-catalytic spectra, showing no change in the electronic characteristics of the tethered Mn-porphyrin complexes. Obviously this does not tell us about all porphyrin sites on the silica surface, but gives an indication that the majority have retained their structural integrity. Previous reports have commented on the effects of using PhIO with supported manganese porphyrin catalysts. Accumulation of by-products was believed to deactivate the catalyst. PhIO reacts with itself giving iodobenzene (PhI) and iodoxybenzene (PhIO₂). It is believed that PhIO₂, having low solubility in the reaction solvent, accumulates on the support surface and blocks access to the active site.¹⁷ This is probably the reason for deactivation of material **7** over several cycles in the epoxidation of COE using PhIO. We have no spectroscopic evidence for this accumulation, however we have no other explanation for the deactivation of the catalytic material. In the case when BPO is used as oxidant we cannot give a reasonable explanation for the deactivation of the catalytic material over several cycles.

Another important point is imidazole accessibility to the manganese porphyrin site, and the role imidazole plays in activating *or* deactivating the immobilised catalysts. Particularly in the case of material **7**, activation of the active site by imidazole coordinating to the manganese centre is possibly inhibited by the manner by which the complex is bound to the silica support. The active catalyst contains axial imidazole and oxygen ligands, however if accessibility to either axial porphyrin positions is blocked then oxidation of the manganese(III) core is not possible, and thus the catalyst is not formed. Both sides of the porphyrin complex should be accessible to imidazole or oxidant.

In the case of material **9** we believe the deactivation to be as a result of inter-porphyrin interactions that are resulting in active site blockage and eventual decomplexation. This interaction acts to allow interactions between oxidised manganese complexes (the active catalyst) resulting in intermolecular degradation of the porphyrin complex. Whether the low activity observed is as a result of immediate degradation of the catalytic sites, or as a result of blockage of the active sites due to the proximity of the porphyrin sites to each other is debatable.

3.3 Conclusions

Metalloporphyrins have been immobilised on silica using 'click' techniques. The 'click' immobilisation procedure is highly efficient, and demonstrates a simple lab shelf to reaction vessel procedure for the application of heterogenised homogeneous catalysts. No side products are formed in the immobilisation procedure, no activating reagents are required, and there are no traces of the copper catalyst used in the coupling reaction. This click immobilisation alleviates the necessity for extreme reaction conditions, or even the use of base or acid to allow coupling between complex and support. The developed materials contain complexes bound to silica in both a monodentate and polydentate manner, and a notable difference is observed between the two. Monodentate appendage to the support allows freedom of movement of the porphyrin complexes, resulting in interporphyrin interactions, and deactivation. Polydentate immobilisation of porphyrin complexes

yields active catalytic materials. The catalytic materials become deactivated over a number of catalyst recycles, and this is as a result of side-product accumulation on the silica surface. The polydentate immobilisation may enhance the deactivation of the immobilised catalysts because the active site may be trapped between the silica surface and the porphyrin ring system.

3.4 Experimental Section

General Considerations. Standard Schlenk procedures under N₂ were carried out throughout. Reagents were used as supplied from Acros BV or Sigma-Aldrich, unless otherwise stated. ¹H, ¹³C and ³¹P solution NMR was carried out on a Varian Inova 300 spectrometer or a Varian Oxford AS400. CP-MAS NMR was carried out using a Bruker AV 750. Elemental analyses were performed by Dornis und Kölbe, Mikroanalytisches Laboratorium, Mülheim a. d. Ruhr, Germany. MS measurements were carried out on an Applied Biosystems Voyager DE-STR MALDI-TOF MS. IR spectra were recorded on a Perkin-Elmer SpectrumOne FT-IR Spectrometer. GC analyses were performed on a Perkin-Elmer AutosystemXL Gas Chromatograph. Solution UV-VIS spectra were recorded on a Varian Cay 50 Scan UV-Visible spectrophotometer and diffuse-reflectance UV-VIS spectra were recorded on a Cary 5 UV-Vis – NIR spectrophotometer.

5,10,15,20-Tetrakis-(4-[(trimethylsilyl)ethynyl]phenyl)porphyrin, 2.

A solution of 4-[(trimethylsilyl)ethynyl]-benzaldehyde (8.0 g, 39.5 mmol) in propionic acid (ca. 180 mL) was brought to reflux temperature. Pyrrole (3.2 mL, 49 mmol) was added and the mixture turned immediately black. The mixture was stirred at reflux for 1h after which it was allowed to cool to room temperature. A black solid precipitated and the suspension was allowed to settle overnight. The black liquid was removed by filtration and the remaining black solid was washed with methanol until the filtrate was colourless. The remaining purple solid was recrystallised from CH₂Cl₂ and MeOH (yield: 4.7-8.2%). ¹H NMR (CDCl₃, ppm): δ -2.84 (NH, s, 2H), 0.372 (Si-CH₃, s, 36H), 7.86 (*m*-ArH, d, ³J=7.80 Hz, 8H); 8.14 (*o*-ArH, d, ³J=7.80 Hz, 8H); 8.81 (*β*-H, s, 8H). ¹³C NMR (CDCl₃, ppm): 0.253(Si-CH₃); 40 ((CH₃)₃Si-C≡C); 51 ((CH₃)₃Si-C≡C); 120 (C_{meso}); 127 (ArC_{3,5}); 128 (ArC₄); 131 (C_β); 135 (ArC_{2,6}); 139 (ArC₁); 142 (C_α); UV-Vis (CH₂Cl₂): λ_{max/nm} (log ε): 422 (5.78); 517 (4.38); 553 (4.17); 592 (3.87); 648 (3.87). MALDI-TOF (m/z): 1000.02 (calc. 999.55).

5,10,15,20-Tetrakis-(4-(ethynyl-phenyl)porphyrin)manganese(III) chloride, 3.

To a purple solution of 5,10,15,20-tetrakis-(4-[(trimethylsilyl)ethynyl]phenyl)porphyrin (50 mg 0.05 mmol) in DMF (ca. 30 mL), Mn(OAc)₂·4 H₂O (250 mg, 1 mmol) was added and the mixture was stirred at reflux temperature overnight, during which it turned dark green. The solution was allowed to cool to room temperature. It was added to an ice cooled NaCl-solution (10g/40 mL) and a precipitate a dark green precipitate formed that was recovered by filtration. The green solid was dissolved in dichloromethane and saturated NaCl-solution was added. After stirring at room temperature for 3 hours the organic layer was separated dried over MgSO₄. Cleavage of the TMS-groups was checked using MALDI-TOF. If the cleavage was not complete, an extra reaction step was performed in which the dichloromethane was removed in vacuo and the remaining green solid was dissolved in THF (ca. 10 mL). A solution of tetra-butylammonium fluoride (TBAF) in THF (1M, 0.5 mL, 0.5 mmol) was added. The reaction was quenched by the addition of water and a precipitate formed. The liquid was removed by filtration after which the green solid was dissolved in dichloromethane and dried over MgSO₄. The green solution was concentrated in vacuo before it was loaded on a column containing dry, neutral alumina. After elution with 5 % MeOH in CHCl₃ a small purple fraction was collected, followed by a green product fraction. The solvent was removed in vacuo, yielding 44 % of a dark green solid. UV-VIS (CH₂Cl₂): λ_{max/nm} (log ε): 376 (4.44); 403 (4.39); 421 (4.39); 478 (4.72); 526 (3.52); 585 (3.68); 619 (3.75). MALDI-TOF (m/z): 763.75 (calc. 799.20; without Cl 763.75).

5,10,15,20-Tetrakis-(1-hexyl-4-phenyl-1,2,3-triazolo)porphyrin-manganese(III) chloride, 10.

To a solution of 5,10,15,20-tetrakis-(4-(ethynyl-phenyl)porphyrin)manganese(III) chloride (50 mg, 0.075 mmol) in dry and degassed CH₃CN was added hexylazide (65 μ L, 0.45 mmol), followed by addition of 2,6-lutidine (8.5 μ L, 0.075 mmol) and a spatula tip of [Cu(MeCN)₄]PF₆. The mixture was stirred at room temperature for 3 days, after which the CH₃CN was removed in vacuo. The remaining green oil was dissolved in dichloromethane and washed with water (2x). After drying over MgSO₄ the dichloromethane was removed in vacuo, yielding a green oily solid. 30%. UV-VIS (CH₂Cl₂): $\lambda_{\text{max/nm}}$ (log ϵ): 381 (5.32); 418 (5.40); 479 (5.56); 528 (3.59); 583 (3.65); 621 (3.72). MALDI-TOF (m/z): 1272.35 (calc. 1307.95, -Cl 1272.50).

5,10,15,20-Tetrakis-(4-[(trimethylsilyl)ethynyl]phenyl)porphyrin-zinc(II).

5,10,15,20-tetrakis-(4-[(trimethylsilyl)ethynyl]phenyl)porphyrin (63 mg, 0.08 mmol) was dissolved in CH₂Cl₂ (ca. 50 mL) and a solution of Zn(OAc)₂·2 H₂O (365 mg, 1.66 mmol, 20 eq.) in MeOH (ca. 5 mL) was added. After two hours stirring at room temperature, the solvent was removed in vacuo and the remaining purple-pink solid was dissolved in CH₂Cl₂ (5mL) and eluted through a silica column with CH₂Cl₂ as eluent. A pink fraction was collected. The pink solution was concentrated in vacuo and recrystallized from CH₂Cl₂/hexanes (yield: 34.4 %). ¹H NMR (CDCl₃, ppm): δ 0.378 (Si-CH₃, s, 36H), 7.88 (*m*-ArH, d, ³*J*=7.50 Hz, 8H); 8.16 (*o*-ArH, d, ³*J*=7.20 Hz, 8H); 8.93 (β -H, s, 8H). UV-VIS (CH₂Cl₂): $\lambda_{\text{max/nm}}$: 423; 550; 589.

5,10,15,20-Tetrakis-(4-(ethynyl)phenyl)porphyrin-zinc(II), 4.

TBAF (1M in THF, 120 μ L, 0.12 mmol) was added to a solution of (5,10,15,20-tetrakis-(4-ethynylphenyl)porphyrin-Zn(II) (29.3 mg, 0.03 mmol) in dry THF (ca. 20 mL). After stirring at room temperature for 30 minutes, the reaction was quenched with water and a pink solid precipitated. The solvent was removed by filtration, yielding a pink solid (yield: 95%). ¹H NMR (DMSO, ppm): δ 4.46 (acetyleneH, s, 4 H); 7.92 (*m*-ArH, d, ³*J*=7.80 Hz, 8H); 8.20 (*o*-ArH, d, ³*J*=8.10 Hz, 8H); 8.81 (β -H, s, 8H). UV-VIS (CH₂Cl₂): $\lambda_{\text{max/nm}}$ (log ϵ): 422 (5.74); 548 (4.35); 587 (3.70). MALDI-TOF (m/z): 772.41 (calc. 772.16).

5-(4-[(Trimethylsilyl)ethynyl]phenyl)-10,15,20-trisphenylporphyrin, 5.

A solution containing 4-[(trimethylsilyl)ethynyl]-benzaldehyde (296 mg, 1.34 mmol, 1 eq) and benzaldehyde (0.8 mL, 7.8 mmol, 5.8 eq) in propionic acid (ca. 40 mL) was brought to reflux temperature. Pyrrole (0.7 mL, 9.1 mmol, 6.8 eq) was added and the mixture turned immediately black. The mixture was stirred for 1 hour after which it was allowed to cool to room temperature. A black solid precipitated and the suspension was allowed to settle overnight. The black liquid was removed by filtration and the remaining black solid was washed with methanol until the filtrate was colorless. The crude product was used in further reaction steps.

(5-(4-[(Trimethylsilyl)ethynyl]phenyl)-10,15,20-trisphenylporphyrin)manganese(III)chloride, 6.

The remaining solid (from porphyrin synthesis reaction) was dissolved in DMF (ca. 40 mL) and Mn(OAc)₂·4 H₂O (250 mg, 1 mmol) was added. The mixture was refluxed overnight. The formed green solution was allowed to cool to room temperature. It was added to an ice cooled NaCl-solution (10g/40 mL) and a precipitate was formed that was removed by filtration. The green solid was dissolved in CH₂Cl₂ and saturated NaCl-solution was added. After stirring at room temperature for 3 hours the organic layer was separated dried with MgSO₄. The green solution was concentrated in vacuo before it was loaded on a silica column prepared with a mixture of hexanes and CH₂Cl₂ (3:1 v/v). First, a purple fraction was eluted followed by a small green fraction. Methanol (5%) was added to the eluent and a green product fraction was eluted, followed by a dark green band. The presence, in one of the fractions, (5-(*p*-acetylenophenyl)-10,15,20-triphenylporphyrin)Mn(III)Cl was confirmed by MALDI-TOF. However the same fraction also contained [Mn(III)(TPP)Cl]. This could not be separated from the other compound. The liquid was removed and the green solid

was dried in *vacuo*. The mixture of functionalised and unfunctionalised porphyrin was used in the immobilisation process. MALDI-TOF (m/z): 667.70 ([MnCl(TPP)]), 691.36 (calc. 727.13; without Cl 691.68).

Procedure for porphyrin immobilisation.

A porphyrin bearing free acetylene groups (50 mg) was dissolved in dry, degassed CH₃CN (10 mL). TMS-capped-3-azidopropyl-1-silica (500 mg) was added, together with a spatula tip of 2-[dimethylamino)methyl]-1-thiophenolato-copper(I) catalyst. After 5 days stirring under N₂ at room temperature, the solvent was removed by filtration and the green solid was washed with CH₂Cl₂ (2x), water and hot MeOH (2x) and dried in *vacuo*. The immobilised porphyrin was then again suspended in dry toluene and degassed for 15 min. ethynylbenzene (0.5 mL) was added as well as a spatula tip of copper(I) aminoarenethiolate catalyst and the mixture was stirred for 3 days under N₂ at room temperature. The liquid was removed by filtration, followed by washing with CH₂Cl₂ (2x), hot MeOH (2x) and water. The remaining solid was dried in *vacuo*. The solid was once again suspended in toluene and degassed for 15 min. Hexylazide (1 mL) was added together with a small amount of copper(I) aminoarenethiolate catalyst and the mixture was stirred for 3 days under N₂ at room temperature. The liquid was removed by filtration and the solid was washed with CH₂Cl₂ (2x), hot MeOH (2x) and hexanes. Drying in *vacuo* yielded the final product. The loadings of the different catalysts were quantified by elemental analysis.

Material 7

²⁹Si MAS CP (ppm): δ -111 (Q⁴ silica); -101 (Q³ silica); -61 (T², T³ RSi(O-)₃); 16 (-CH₂SiO-). UV-VIS: λ_{max/nm}: 479; 526 (sh); 581; 619. IR (DRIFT, difference, cm⁻¹): ν_{CH} 2967; ν_{triazole} 1460-1440. Elemental analysis found: C 18.03, H 0.95, N 0.50, Mn 0.10.

Material 8

UV-VIS: λ_{max/nm}: 428; 561; 605. IR (DRIFT, difference, cm⁻¹): ν_{CH} 2961; ν_{triazole} 1460-1440. Elemental analysis found: C 9.49, H 2.06, N 0.96, Zn 0.24.

Demetalation of 8, material 11.

TFA (30 μL, 0.42 mmol) was added to a suspension of X in CH₂Cl₂ (ca. 5 mL) upon which the mixture turned green immediately. After stirring for 1 hour at room temperature the mixture was poured in saturated NaHCO₃ (50 mL) solution. The mixture turned pink again upon stirring and a pink solid precipitated. The liquid was removed by filtration and the solid was dried in *vacuo*. UV-VIS: λ_{max/nm}: 424; 545; 584 (sh); 653. IR (DRIFT, difference, cm⁻¹): ν_{NH} 3449; ν_{CH} 2951. Elemental analysis found: C 10.50, H 2.62, N 0.61, Zn 0.14.

Material 9

UV-VIS (CH₂Cl₂): λ_{max/nm}: 461; 529; 572; 608. IR (DRIFT, difference, cm⁻¹): ν_{arCH} 3057; ν_{CH} 2964; ν_{triazole} 1440-1420. Elemental analysis found: C 17.71, H 1.59, N 0.69, Mn 0.05.

Standard alkene epoxidation catalysis conditions.

Cyclooctene, cyclohexene and styrene were distilled prior to use. Cyclooctene and cyclohexene were filtered over neutral alumina prior to every catalytic reaction to remove trace amounts of epoxide. Iodosylbenzene was synthesized according to literature procedure and *t*-butylperoxide was used as solution in decane. **Iodosylbenzene:** All experiments were performed at room temperature in small GC-vessels with magnetic stirring. All reagents were added as solutions in CH₂Cl₂, except iodosylbenzene and the supported catalysts. Catalyst (0.25 μmol active species) was stirred with the desired substrate (0.5 mmol), imidazole (5 μmol) and iodosylbenzene (0.03 mmol) in CH₂Cl₂. Product formation was monitored by taking small aliquots for GC analysis with 1,2-dibromobenzene as internal standard. ***t*-Butylperoxide:**

All experiments were performed at room temperature in small GC-vessels with magnetic stirring. All reagents were added as solutions in MeCN except the supported catalysts. Substrate (0.3 mmol), catalyst (1 μ mol), imidazole (0.02 mmol) and *t*-butylperoxide (0.02 mmol) were stirred in dichloromethane (2 mL). Product formation was checked by taking small aliquots for GC analysis with phenylbromide as internal standard.

Catalyst Recycling:

After each oxidation step, the reaction solution was removed by simple filtration and the catalytic material (solid) was washed with methanol. Fresh reagents were added and a subsequent catalytic experiment was performed.

3.5 References

- ¹ B. Cornils, W. A. Herrmann, *J. Catal.* **2003**, 216, 23-31.
- ² D. E. De Vos, I. F. J. Vankelecom, P. A. Jacobs [Eds. Weinheim]; *Chiral Catalyst Immobilization and Recycling*, **2000**. Wiley-VCH.
- ³ H.-U. Blaser. *Chem. Commun.* **2003**, 293-296.
- ⁴ C. Baleizao, H. Garcia, *Chem. Rev.* **2006**, 106, 3987-4043.
- ⁵ E. Brule, Y. R. de Miguel, *Org. Biomol. Chem.* **2006**, 4, 599-609.
- ⁶ (a) P Battioni, J-P. Lallier, L. Barloy, D. Mansuy, *Chem. Commun.* **1989**, 1149-1151. (b) J. R. Lindsay Smith, Y. Iamamoto, F. S. Vinhado, *J. Mol. Catal. A: Chemical* **2006**, 252, 23-30.
- ⁷ A. R. McDonald, H. P. Dijkstra, B. M. J. M. Suijkerbuijk, M. Lutz, A. L. Spek, G. P. M. van Klink, G. van Koten, Chapter 2 of this thesis.
- ⁸ H. C. Kolb, M. G. Finn, K. B. Sharpless, *Angew. Chem. Int. Ed.* **2001**, 40, 2004-2021.
- ⁹ A. D. Adler, F. R. Longo, J. D. Finarelli, J. Goldmacher, J. Assour, L. Korsakoff, *J. Org. Chem.* **1967**, 32, 476-476.
- ¹⁰ J. Rochford, D. Chu, A. Hagfeldt, E. Galoppini, *J. Am. Chem. Soc.* **2007**, 129, 4655-4665.
- ¹¹ F. Odobel, E. Blart, M. Lagr e, M. Villieras, H. Boujtita, N. El Mur, S. Caramori, C. A. Bignozzi, *J. Mater. Chem.*, **2003**, 13, 502.
- ¹² ATR-IR (attenuated total reflection) is a technique whereby transmission of an IR beam through a sample is measured.
- ¹³ DRIFT-IR (diffuse reflectance fourier transform) is a surface technique which analyses reflected IR beam from the surface/near surface of the material.
- ¹⁴ See chapter 2 of this thesis for in-depth discussion.
- ¹⁵ (a) M. D. Angelino, P. E. Laibinis, *Macromolecules* **1998**, 31, 7581-7587. (b) T. S. Reger, K. D. Janda, *J. Am. Chem. Soc.* **2000**, 122, 6929-6934.
- ¹⁶ (a) P. R. Cooke, J. R. Lindsay Smith, *J. Chem. Soc. Perkin Trans. 1*, **1994**, 1913-1923. (b) F. G. Doro, J. R. Lindsay Smith, A. G. Ferreira, M. D. Assis, *J. Mol. Catal. A: Chemical* **2000**, 164, 97-108.
- ¹⁷ (a) S. Camperstrini, B. Meunier, *Inorg. Chem.* **1992**, 31, 1999. (b) H. C. Sacco, Y. Iamamoto, J. R. Lindsay Smith, *J. Chem. Soc. Perkin Trans. 2*, **2001**, 181-190. (c) M. Bonnet, L. Schmid, A. Baiker, F. Diederich, *Adv. Funct. Mater.* **2002**, 12, 39-42.

CHAPTER 4

BINAP-Ru/Rh Catalysts Covalently Immobilised on Silica and their Repeated Application in Asymmetric Hydrogenation Catalysis

The facile immobilisation of a chiral diphosphine ligand, BINAP, on high-density silica is presented. The protected ligand has been immobilised and deprotected on the surface to prevent side reactions. The novel materials were characterised using various solid-state techniques. Ruthenium and rhodium catalysed asymmetric hydrogenation of various pro-chiral substrates is presented using immobilised BINAP ligands. The repeated use of the immobilised catalyst in five recycles demonstrates ‘homogeneous’ catalysis with ‘heterogeneous’ catalysts, thus reducing solvent waste, and loss of precious metal/ligand.

4.1 Introduction

Recent years have seen a resurgence in the development of immobilised homogeneous catalysts. Initial attempts at the immobilisation of asymmetric hydrogenation catalysts were aimed at improving enantioselectivity by altering reaction rates and decreasing metal-metal interactions.¹ Present work is directed towards the modern trend of cutting down on solvent use and catalyst costs. Separation of homogeneous catalysts from reaction mixtures is now key to industrial processes due to high costs of ligands and metals, and metal toxicities. From this perspective, the goal is to mimic the ease of separation of heterogeneous catalysts while keeping the high selectivity and predictability of homogeneous catalysts.

Asymmetric hydrogenation is the most widely used industrial homogeneously catalysed asymmetric reaction.² The production of a wide range of pharmaceutical and fine chemical products on a large scale relies on the asymmetric hydrogenation of precursors such as enamides, itaconates, arylketones, propenoic acids, and β -ketoesters. These hydrogenations are mediated through platinum group metal catalysed reaction with a chiral ligand bound to the metal. This chiral ligand can be diphosphine, diamine or ephedrine-type molecules which are mostly coordinated in a bidentate manner to the metal centre. Of the diphosphine ligands, the BINAP (2,2'-bis(diphenylphosphino)-1,1'-binaphthyl) ligand developed by the Noyori group has proven to give some of the highest activities and selectivities.³

As stated earlier initial attempts at immobilising homogeneous hydrogenation catalysts was directed towards influencing reaction kinetics so as to positively effect enantiomeric excess yields. Recent trends have seen immobilisation as a tool for ease of separation of catalyst from substrate/product.⁴ This is mediated mostly through phase differences, with organic⁵ and inorganic polymeric⁶ supports used widely as solid-state supports. Liquid biphasic systems are now commonly used with aqueous/organic or fluorous/organic solvent mixtures being used during catalysis, and allowing for easy decantation after catalysis.⁷ Our group has shown that phase differences are not necessary to separate catalysts with dendritic systems being separated from reaction mixtures using nanofiltration membranes, or even by altering the polarity of a reaction mixture.⁸

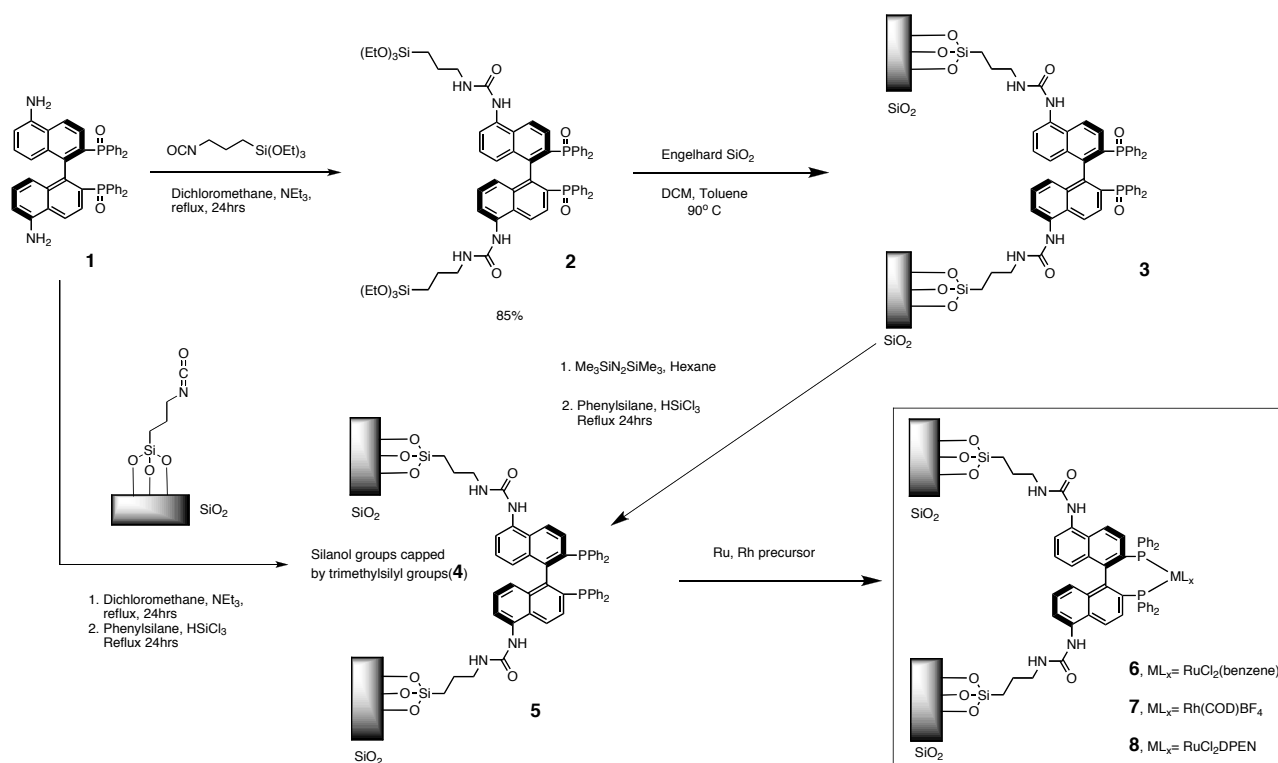
The BINAP ligand has been immobilised in various forms using all of these techniques. Water soluble BINAP derivatives have been used in liquid biphasic systems,⁹ and ionic liquids,¹⁰ BINAP has been incorporated at the core of several dendritic systems,¹¹ and both as a polymeric backbone,¹² as well as a functionality on a polystyrene support¹³ and entrapment within polymers.¹⁴ Non-covalent interactions have been used to immobilise BINAP on various inorganic supports; clays,¹⁵ silica,¹⁶ and zirconium phosphonate hybrids.¹⁷ At the assumption of this work BINAP had not yet been immobilised covalently on an inorganic support, however that was achieved recently by Lin et al where a mono-functionalised BINAP was covalently tethered to silica via an ethereal linker amongst others.¹⁸ Covalent immobilisation generally leads to the best results in terms of catalyst recycling.

We present here the synthesis and thorough characterisation of immobilised BINAP-Ru and -Rh complexes on a high-density silica. The protected BINAP ligand (as phosphine oxide) has been immobilised in a covalent bidentate manner to the support and subsequently converted to the diphosphine ligand. The immobilised diphosphine ligand has been applied in the rhodium and ruthenium catalysed asymmetric hydrogenation of a number of substrates showing enantioselectivity levels comparable to the parent homogeneous catalysts. The immobilised catalysts have been recycled, showing little loss in enantioselectivity over five cycles.

4.2 Results and Discussion

4.2.1 Synthesis

Scheme 1. Synthesis of immobilised BINAP ruthenium and rhodium complexes.



There are a number of methods for the synthesis of functionalised BINAP ligands. We have chosen one of the more straightforward methods, which is through a facile nitration of BINAP-dioxide that yields 5,5'-dinitro-BINAP-dioxide which is reduced easily to 5,5'-diamino-BINAP-dioxide.^{11b-e} This compound has been reported to be quite unreactive unless in the presence of a highly activated species, *i.e.* an acid chloride or acid anhydride. However, we have coupled it with 3-(triethoxysilyl)propyl-1-isocyanate, and with isocyanate functionalised silica (low porosity, high density^{10,19}) using a large excess of triethylamine in refluxing dichloromethane (DCM) (see scheme 1). Both techniques show complete conversion to the respective di-ureyl compounds. The formed compound **2** was then reacted with a high-density silica yielding silica bound BINAP dioxide **3**. This type of silica was used to ensure the catalyst was immobilised only at easily accessible sites

within the inorganic support material. This ensures no mass transport limitations, or other such adverse effects. The remaining silanol groups on **3** were capped using hexamethyldisilazane yielding **4**, which is also the product of coupling diamino-BINAP-dioxide with isocyanate functionalised silica. Protected diphosphine-dioxide **4** was reduced using trichlorosilane in phenylsilane to yield unprotected, immobilised BINAP ligand **5**. The reasons for immobilisation of the phosphine dioxide are two-fold; firstly it is easier to carry out chemistry on the dioxide, without having to worry about oxidation of the phosphine which will inevitably occur in small quantities; secondly, it has been observed that upon immobilisation of phosphine ligands, using triethoxysilane-type linkers, an ethoxy-phosphonium cation forms quite readily when using silica surfaces.²⁰ Complexation was mediated through various metal precursors ($[\text{RuCl}_2(\text{benzene})]_2$ ²¹ or $[\text{Rh}(\text{COD})_2\text{BF}_4]$) yielding tethered BINAP-Ru and -Rh complexes. The introduction of other heteroligands was also possible (e.g. DPEN). Complexation resulted in stark colour changes of the silica. The material **5** is colourless, however the silica-bound ruthenium and rhodium complexes gave an orange colour in the presence of solvent. Drying of the materials showed less strong colour differences, but there was still a clear indication that the complex has been synthesised on the support. These synthetic procedures have been applied with both (R)- and (S)- enantiomers of diamino-BINAP-dioxide starting materials.

The functionalised systems **2-8** were characterised with both solution and CP-MAS solid-state ^1H , ^{13}C , ^{29}Si and ^{31}P NMR spectroscopy, IR-DRIFT and IR-ATR spectroscopy and elemental content analysis. Both synthetic pathways yielded similar results, and no differences were observed in their spectral data.

4.2.2 Elemental Content Analysis of Catalytic Materials

Elemental content measurements gave us more insight into the effects of chemical modification of the support, and more importantly on the supported ligand/complex. The phosphorous content of the support ligand/complexes remained constant throughout at around 0.20% of the total. Comparing the ratio of elemental loadings allows the characterisation of materials **3-8**. The percentage phosphorous loading compared favourably with the carbon content in material **3** (P:C = 1:12.5), with a ratio that was comparable to that calculated for the unbound compound **2** (1:10). Similarly, comparison of the phosphorous/nitrogen content in material **3** (P:N = 1:0.7) compared favourably with that of compound **2** (1:0.9). These results hold for compounds **3-5**. No significant change in the P and N loadings was observed during any of the synthetic procedures carried out on the immobilised ligands, suggesting the ligand remains bound and chemically unaltered throughout. Complexation reactions yielded materials with the expected ratios of metal to phosphorous loadings. For example in material **7** the expected P:Rh loading ratio is 1:1.7, the observed ratio is 1:1.9. Similarly material **6** showed an expected P:Ru ratio of 1:1.6, and the actual ratio is 1:1.4. Material **8** showed an increased nitrogen and carbon content compared to material **6**, as expected with the introduction of the DPEN ligand. The P:N loading ratio was as expected (1:1.4). Material **8** showed the same P:Ru loading ratio as material **6**. In general these results showed us that little other than the expected reactions are occurring on the functionalised silica surface. The observation that phosphorous/metal elemental content was the expected value

showed us that there is only one site at which the metal is situated on the surface; between the chelating arms of the diphosphine ligand.

4.2.3 Infra-Red Analysis

The ATR-IR spectrum of **2** is shown in figure 1(a).²² The ureyl stretches can be observed at ~ 1660 and 1538 cm^{-1} respectively. The sharp peak at 1438 cm^{-1} is a P-C(aryl) stretch of the BINAP ligand. Using the DRIFT technique we can monitor the difference between the standard silica stretches before and after immobilisation.²³ This method demonstrates that the silanol groups disappear as a result of covalent attachment of the silylpropyl- linker (of **2**) to the support. The spectrum of the starting silica is subtracted from the spectrum of **3** giving an indication of what has been ‘added’ to the silica (figure 1(b)). A trough in the difference spectrum is observed at 3738 cm^{-1} which corresponds to a clear decrease in the intensity of silanol stretches. Subsequent capping of the silanol groups with trimethylsilyl groups (**4**) shows a further decrease in the number of silanol stretches and no apparent effect on the immobilised ligand. Similarly, the immobilisation by coupling between isocyanate functionalised silica and amino-functionalised BINAPO shows a decrease in the intensity of observed isocyanate stretches.

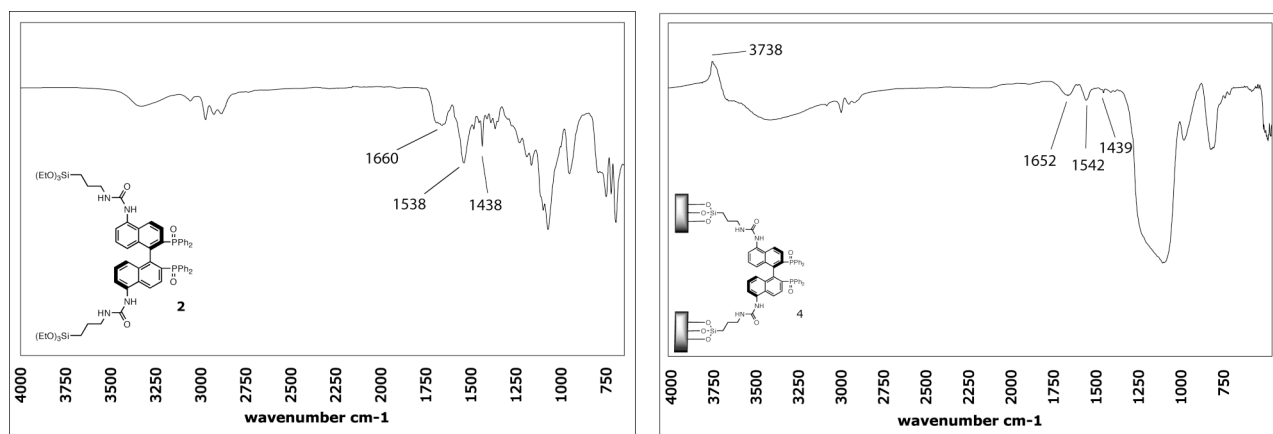


Figure 1. a) ATR-IR of **2**. b) DRIFT-difference spectrum of **4** minus SiO_2 .

The conversion of tethered BINAP dioxide (**4**) to tethered BINAP (**5**) is observed with ease using DRIFT-IR. Figure 2(a) is the difference spectrum between **5** and **4**. Focussing on the P-C(aryl) resonance, there is a clear trough where the $\text{O}=\text{P}-\text{C}(\text{aryl})$ was, 1439 cm^{-1} , and a peak at 1430 cm^{-1} (P-C(aryl)). The final step in the synthesis was to incorporate metal centres in the diphosphine ligand. Monitoring the P-C(aryl) stretch gives similar results, with the immobilised complexes showing a P-C(aryl) vibration of $\sim 1435\text{ cm}^{-1}$. Figure 2(b) depicts the difference spectrum of **6**/ SiO_2 which shows clearly the P-C(aryl) stretch of coordinated BINAP-Ru and also stretches corresponding to ureyl groups and a trough at $\sim 3740\text{ cm}^{-1}$ representing a decrease in the number of silanol stretches.

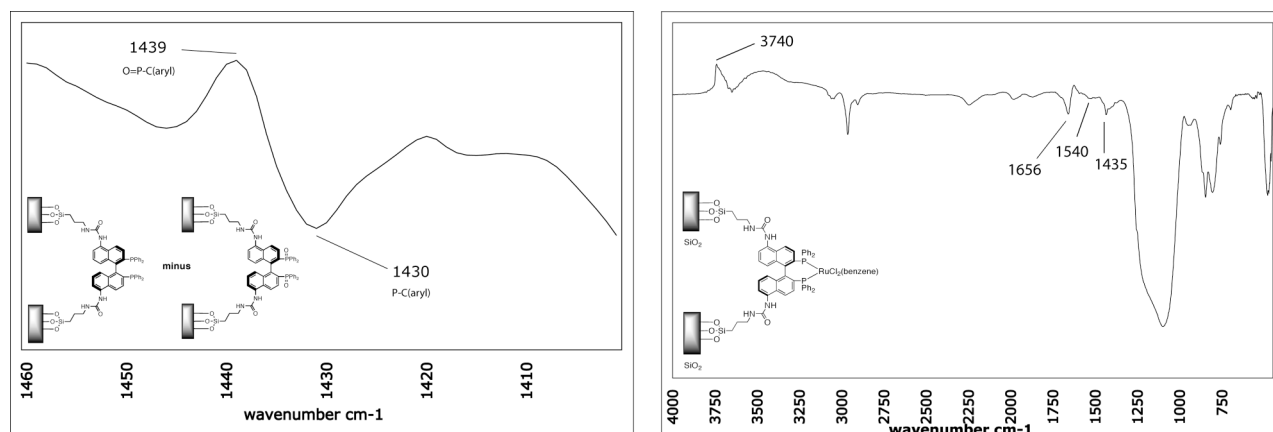


Figure 2. a) Difference spectrum of the DRIFT-spectra of **5** minus **4**. b) DRIFT difference spectrum of **6** minus SiO₂.

4.2.4 NMR Analysis

CP-MAS ²⁹Si NMR of the immobilised ligand (**5**) shows us several peaks that indicate different forms of silicon species (figure 3(a)). Peaks at -102 and -111 ppm are characteristic of *Q*-type (*Si*-(O)₄) silicates, which are in the bulk material. Peaks at -57 and -66 ppm are typical of *T*-type (*R*₁-*Si*-(O)₃) silicates, that is, the silicon bound to the propyl group of **2** at the surface of the support. This is the clearest indication that the ligand is covalently bound to the support. The appearance of two peaks in this region indicates two forms of (*R*₁-*Si*-(O)₃) in the material. This is probably as a result of remnant ethoxide groups that have not reacted with surface silanol groups. Similarly, at the surface, the single peak at 13 ppm is typical of *M*-type (*R*₃-*Si*-(O)-) silicates (where *R* is the methyl group of the trimethylsilyl capped silanol groups). Comparison of the spectra of materials **4-8** shows there is no difference in the silicon species of the material through the various synthetic steps that are carried out. The deprotection of phosphine oxide yielding BINAP and subsequent complexation of BINAP has no effect on the type of silicon species on the silica surface.

³¹P CP-MAS indicates that BINAP has indeed been immobilised on silica. Figure 3(b) shows the NMR spectrum of immobilised ligand **5**. The peak at -15 ppm represents the reduced, unprotected phosphine. There is no sign of any phosphine oxide in the spectrum (~30 ppm). There is a small phosphonium-type species present on the silica surface. This is formed as a result of remnant ethoxide groups of the immobilised silane reacting with the newly formed phosphine yielding a phosphonium ion. This is a common occurrence when immobilising phosphines on silica, however, we believe that as a result of immobilising BINAP-dioxide and then deprotection, the extent of phosphonium formation is greatly reduced. We have ensured this problem is not a hindrance, and most phosphine ligands are available for coordination.

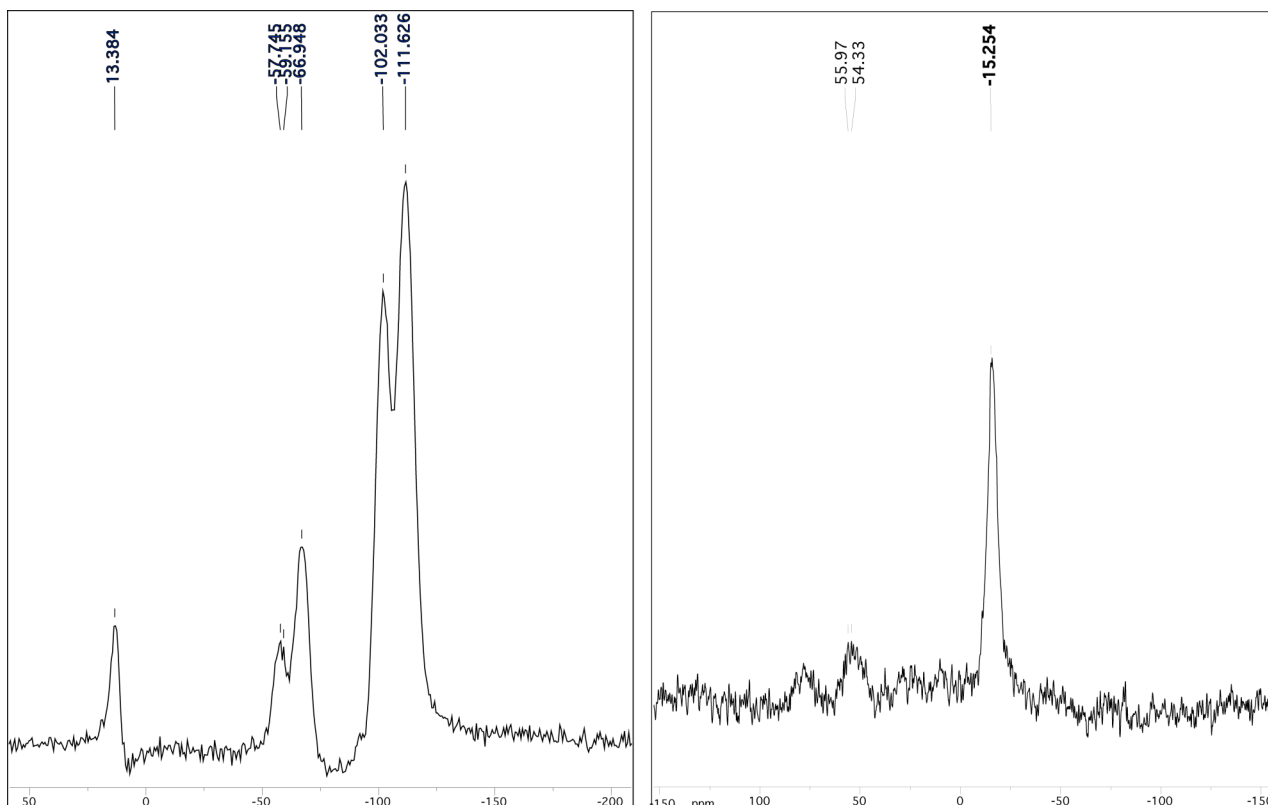


Figure 3. a) ^{29}Si CP-MAS NMR spectrum of **5**. b) ^{31}P CP-MAS NMR spectrum of **5**.

4.2.5 Asymmetric Hydrogenation Catalysis

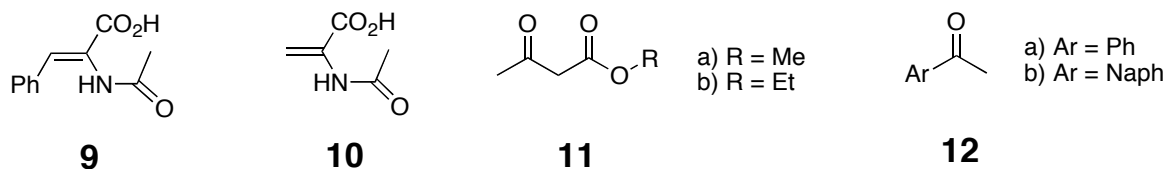


Figure 4. Prochiral substrates for asymmetric hydrogenation.

The ruthenium and rhodium catalytic materials were tested in the asymmetric hydrogenation of several substrates (figures 4 & 5). The use of high density/low porosity silica ensures we are only addressing catalytic sites on the silica's peripheral surface. Thus the support is expected to have little effect on activity and selectivity. Complete conversion of substrate was observed with all catalysts used. In general, the reaction rates were an order of magnitude slower than the homogeneous analogue. This is to be expected, when using heterogenised catalysts because, you are applying catalysts which are not in the substrate phase. A hydrogen uptake curve shows that the heterogenised catalyst **6** shows first order reaction kinetics, as does the homogeneous catalyst. The *R*-isomer of immobilised BINAP has been used throughout this catalytic study.

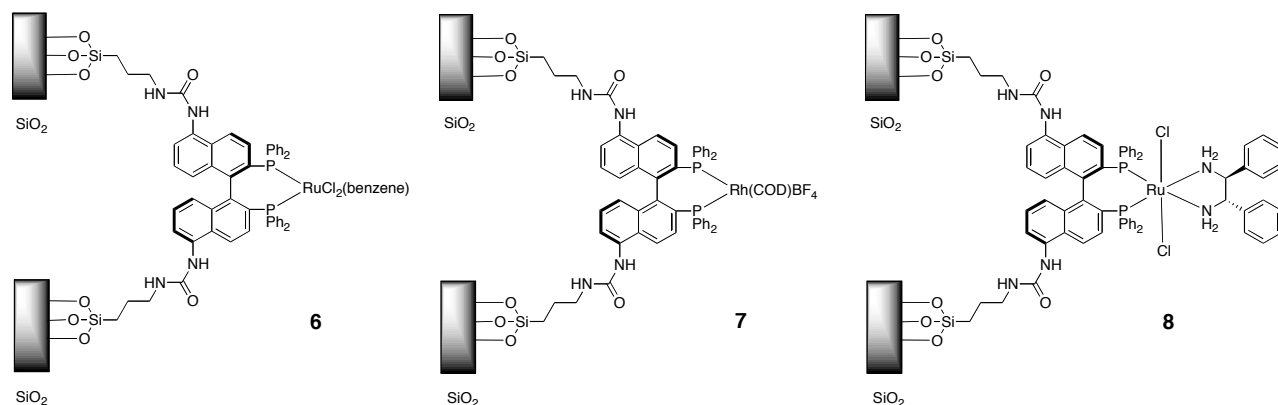


Figure 5. Immobilised BINAP-Ru/Rh catalysts for asymmetric hydrogenation.

Table 1 shows the application of catalyst **6** in the asymmetric hydrogenation of various β -ketoesters²⁴ and enamides²⁵ in the manner of published homogeneous systems. The heterogenised catalyst shows the same, high, enantioselectivity levels of the homogeneous catalyst. 99% enantiomeric excess (*ee*) was observed in the asymmetric hydrogenation of **11a** and **11b**. In the reduction of enamides the immobilised ruthenium complexes gave *ee* values in the 80%'s.

Table 1. Catalytic results from immobilised BINAP-Ru/Rh asymmetric hydrogenation reactions.

Catalyst ^a	Substrate	H ₂ Pressure (bar)	Temperature (C)	Conversion (%) ^b	<i>ee</i> (%) ^c
6	9	2	35	100	85 (86) ^c
	10	2	35	100	72 (76) ^c
	11(a)	40	50	100	>99 (>99) ^c
	11(b)	40	50	100	>99 (>99) ^c
7	9	4	RT	100	85 (84) ^c
	10	40	50	100	60 (67) ^c
8	12(a)	10	30	100	25 (-) ^{d,f}
	12(b)	10	30	100	95 (97) ^d

^aSee refs 24-27 for procedures on catalysis, all catalysis was carried out in a parallel autoclave system AMTEC SPR16 or a Parr 4590 micro reactor. ^bAs determined by ¹H NMR and GC. ^cMeasured by GC. ^dMeasured by HPLC. ^eValues found with homogeneous catalyst in brackets. ^fNo literature value found for this substrate.

Rhodium catalyst **7** was also applied in the asymmetric reduction of enamides.²⁶ It also gave results which were comparable to the homogeneous system in terms of selectivity. This system was, however, not as stable as the ruthenium materials, and catalyst decomposition was observed.

Immobilised BINAP-Ru-diamine material **8** was applied in the asymmetric transfer hydrogenation of aromatic ketones acetophenone and naphthophenone.²⁷ Quantitative conversion of ketone to secondary alcohol was observed in both cases. In the case of acetophenone 25% *ee* was observed. Naphthophenone was also converted to the corresponding secondary alcohol showing the high stereoselectivity values that are expected of these systems.

4.2.6 Catalytic Material Recycling

The catalytic materials were easily separated from the substrate/product solution by either; 1) simple filtration over a glass frit and subsequent washing or; 2) removal of all liquids from the autoclave using applied pressure. The latter was found to be the easier. The autoclave could then be easily recharged with fresh substrate and the reaction could be restarted. This was demonstrated using catalyst **6** for the asymmetric hydrogenation of methylacetoacetate. The post-catalysis solution was forced out of the autoclave after the reaction mixture was allowed to settle, fresh solvent was added to the autoclave with thorough mixing. This batch of solvent was also removed and a fresh batch of substrate solution was added, followed by thorough purging and subsequent application of hydrogen over-pressure. This process could be repeated five times with no significant loss in selectivity, and minimal losses in activity. Furthermore, the post catalysis filtrate, which was colourless, was placed in a catalyst free autoclave and fresh substrate was added. Hydrogen pressure was applied, however no further conversion was observed. The ruthenium content (loading) of the recycled catalytic material was the same as the starting catalytic material suggesting little, if any, ruthenium leaching (P:Ru, 1:1.4). As mentioned previously the rhodium systems showed catalyst decomposition. The rhodium catalytic material was recycled once post hydrogenation of enamide **10**, and showed diminished activity, but moreover, diminished enantioselectivity in the same reaction. We have not got an explanation for this, however, it does show that catalyst stability is essential when immobilising homogeneous catalysts. With rhodium complexes known sensitivity to oxygen, it is likely that some oxygen contamination has occurred resulting in complex decomposition. Furthermore, the process of recycling and subsequent washing could have adverse effects on the complex stability, that is oxidation or mechanical influences.

4.3 Conclusions

In conclusion we have synthesised and immobilised a functionalised BINAP-type ligand with a retention in chirality and in reasonably high yields. We have shown that we can carry out chemistry on the immobilised ligand without having detrimental effects on the support or the functionalised ligand. Several analytical techniques have been used to analyse these immobilised compounds proving conclusively that we have indeed succeeded in covalently immobilising

BINAP-Ru and -Rh complexes on an inorganic support. Catalytic results have shown to be conclusive in the fact that activity is down in comparison with the homogeneous system, however conversion and enantioselectivity levels are as good as if not improved upon, in comparison with the homogeneous catalyst. The catalyst is truly immobilised with the post catalysis solution showing no activity. Furthermore, the catalyst was recycled showing repeated high selectivity levels over at least five cycles.

4.4 Experimental Section

General Information: Standard Schlenk procedures under dinitrogen were utilised throughout. Catalytic experiment preparations were carried out under argon. Reagents were used as supplied from Acros or Sigma-Aldrich. Diamino-BINAP-dioxide was prepared according to a literature procedure.²⁸ Racemic versions of catalytic products were either purchased or prepared using literature procedures.²⁹ Hydrogenation catalysis was carried out simultaneously in the parallel autoclave system AMTEC SPR16, equipped with pressure sensors and a mass-flow controller and suitable for monitoring and recording gas uptakes throughout the reactions, or in a 50ml Parr-4590 micro-reactor. ¹H, ¹³C, and ³¹P solution NMR was carried out on a Varian Inova 300 spectrometer or a Varian Oxford AS400. CP-MAS NMR was carried out using a Bruker AV 750. Elemental analyses were performed by Dornis und Kolbe, Mikroanalytisches Laboratorium, Mülheim a. d. Ruhr, Germany. MS measurements were carried out on an Applied Biosystems Voyager DE-STR MALDI-TOF MS. Infra-Red measurements were carried out on a Perkin-Elmer SpectrumOne FT-IR Spectrometer. GC analyses were performed on a Perkin-Elmer AutosystemXL Gas Chromatograph. HPLC analyses were carried out on a Philips PU1400 liquid chromatograph with an attached PU4120 diode array detector.

Method 1.

5,5'-bis(triethoxysilylpropylureyl)-2,2'-bis(diphenylphosphinooxide)-1,1'-binaphthyl, 2.

5,5'-bis(amino)-2,2'-bis(diphenylphosphinooxide)-1,1'-binaphthyl (0.5261g, 0.77 mmol) was dissolved in dry CH₂Cl₂ (15mL). A solution of NEt₃ (15mL) containing 3-triethoxysilylpropyl-1-isocyanate (0.76g, 3.08 mmol) was added to this, and the resulting solution was heated at reflux for 48h. The resulting brown solution was cooled to room temperature, all solvent was removed, and the title compound was attained by recrystallisation from CH₂Cl₂/hexanes as a light brown powder. Not pristinely pure, some triethylammonium species, which we could not remove. Was used immediately in next step. Yield 60%. IR (ATR); $\nu_{\text{carbamate}}$ 1660 & 1538 cm⁻¹, $\nu_{\text{P-C(aryl)}}$ 1438 cm⁻¹. ³¹P-NMR (162 MHz, CDCl₃) 29.9. M/Z (MALDI-ToF) 1180.38 g/mol (+H).

SiO₂-5,5'-bis(silylpropylureyl)-2,2'-bis(diphenylphosphinooxide)-1,1'-binaphthyl, 3.

5,5'-bis(triethoxysilylpropylureyl)-2,2'-bis(diphenylphosphinooxide)-1,1'-binaphthyl (0.2149g, 0.18mmol) was dissolved in dry toluene (10mL). This solution was added to 1g of silica (BASF/Engelhard, 80m²/g), and the resulting mixture was heated at reflux for 24h. Hot filtration and subsequent washing with CH₂Cl₂, acetone, and finally boiling EtOH yielded a light brown powder. IR (DRIFT, difference); $\nu_{\text{SiO-H}}$ 3738 cm⁻¹ (trough), $\nu_{\text{carbamate}}$ 1652 & 1542 cm⁻¹, $\nu_{\text{P-C(aryl)}}$ 1439 cm⁻¹. ³¹P-NMR (303.6 Mhz) 30 ppm. Elem. anal. found: C 2.49, H 0.82, N 0.14, P 0.20.

Capped SiO₂-5,5'-bis(silylpropylureyl)-2,2'-bis(diphenylphosphinooxide)-1,1'-binaphthyl, 4.

Hexane (30mL) was added to **3** with hexamethyldisilazane (1mL, large excess) and the resulting mixture was heated at reflux for 24h. Hot filtration and subsequent washing with CH₂Cl₂, acetone, and finally boiling EtOH yielded a light yellow powder.

*Method 2:***Capped SiO₂-5,5'-bis(silylpropylureyl)-2,2'-bis(diphenylphosphino)-1,1'-binaphthyl, 4.**

5,5'-bis(amino)-2,2'-bis(diphenylphosphino)-1,1'-binaphthyl (0.5261g, 0.77 mmol) was dissolved in dry CH₂Cl₂ (15mL). This was added to a solution of NEt₃ (3mL) containing capped SiO₂-silyl-3-propyl-1-isocyanate and the resulting solution was heated at reflux for 48h. Hot filtration and subsequent washing with CH₂Cl₂, acetone, and finally boiling EtOH yielded a light yellow powder. IR (DRIFT, difference); $\nu_{\text{SiO-H}}$ 3738 cm⁻¹ (trough), $\nu_{\text{carbamate}}$ 1652 & 1542 cm⁻¹, $\nu_{\text{P-C(aryl)}}$ 1439 cm⁻¹. ³¹P-NMR (303.6 Mhz) 30 ppm. Elem. anal. found: C 4.13, H 1.12, N 0.14, P 0.19.

Capped SiO₂-5,5'-bis(silylpropylureyl)-2,2'-bis(diphenylphosphino)-1,1'-binaphthyl, 5.

Material **4** was placed in phenylsilane (10mL) and the resulting mixture was heated to reflux for 1h. HSiCl₃ (1mL) was added after a further 1, 3, and 16h respectively, with continuous refluxing for a further 8h. Hot filtration and subsequent washing with CH₂Cl₂, acetone, and finally boiling EtOH yielded an off-white powder. IR (DRIFT, difference); $\nu_{\text{SiO-H}}$ 3738 cm⁻¹ (trough), $\nu_{\text{carbamate}}$ 1652 & 1542 cm⁻¹, $\nu_{\text{P-C(aryl)}}$ 1430 cm⁻¹. ³¹P-NMR (303.6 Mhz) -15 ppm. Elem. anal. found: C 4.87, H 1.11, N 0.15, P 0.22.

Capped SiO₂-5,5'-bis(silylpropylureyl)-2,2'-bis(diphenylphosphino)-1,1'-binaphthyl-ruthenium(II) dichloro(benzene), 6.

Material **5** (0.26g) was placed in freshly distilled, degassed EtOH/benzene (10ml (9:1)). To this mixture was added [RuCl₂(benzene)]₂ (0.2g, 0.8mmol, excess) and the resulting mixture was stirred at 60 °C for 24h. Hot filtration and several washings with benzene and CH₂Cl₂ yielded an orange powder. IR (DRIFT, difference); $\nu_{\text{SiO-H}}$ 3740 cm⁻¹ (trough), $\nu_{\text{carbamate}}$ 1656 & 1540 cm⁻¹, $\nu_{\text{P-C(aryl)}}$ 1435 cm⁻¹. Elem. anal. found: C 5.10, H 1.10, N 0.12, P 0.21, Ru 0.20.

Capped SiO₂-5,5'-bis(silylpropylureyl)-2,2'-bis(diphenylphosphino)-1,1'-binaphthyl-rhodium(I) cyclooctadiene-tetrafluoroborate, 7.

Material **5** (0.27g) was placed in freshly distilled, degassed CH₂Cl₂ (10mL). To this was added [Rh(COD)₂BF₄] (0.4g, 0.7mmol, excess). The resulting mixture was stirred at room temperature for 24h. Filtration and several washings with CH₂Cl₂ yielded a yellow powder. IR (DRIFT, difference); $\nu_{\text{SiO-H}}$ 3740 cm⁻¹ (trough), $\nu_{\text{carbamate}}$ 1660 & 1548 cm⁻¹, $\nu_{\text{P-C(aryl)}}$ 1433 cm⁻¹. Elem. anal. found: C 4.90, H 1.18, N 0.15, P 0.22, Rh 0.42.

Capped SiO₂-5,5'-bis(silylpropylureyl)-2,2'-bis(diphenylphosphino)-1,1'-binaphthyl-ruthenium(II) dichloro(diphenylethylenediamine), 8.

Material **5** (0.2g) was placed in freshly distilled, and degassed DMF (10mL). To this was added [RuCl₂(benzene)]₂ (0.2g, 0.8mmol, excess) and the resulting was stirred at 100 °C for 1h. This was subsequently cooled. To the resulting brown mixture DPEN (0.2g, 0.9mmol, excess) was added and the resulting mixture was stirred at room temperature for 24h. Filtration followed by washing with DMF and CH₂Cl₂ yielded a yellow powder. IR (DRIFT, difference); $\nu_{\text{SiO-H}}$ 3740 cm⁻¹ (trough), $\nu_{\text{carbamate}}$ 1660 & 1548 cm⁻¹, $\nu_{\text{P-C(aryl)}}$ 1435 cm⁻¹. Elem. anal. found: C 5.15, H 0.88, N 0.28, P 0.15, Ru 0.17.

Asymmetric hydrogenation of prochiral substrates:

General procedure for the catalysis experiments: Stainless steel autoclaves of the AMTEC SPR16³⁰ were heated to 90°C and flushed with argon (15 bar) four times. The reactors were subsequently cooled to room temperature and flushed with argon (4X). The reactors were charged each with 4 ml of a suspension of the catalyst in the desired solvent as well as 4 ml of the substrate. The atmosphere was further exchanged with hydrogen (gas exchange cycle 1) and the reactors were pressurised with hydrogen (3 bar). After regulating the desired temperature and pressure they

were kept constant throughout the experiment. The spin rate was 1000rpm. The gas uptake of hydrogen was monitored and recorded automatically. The reactors were then cooled to room temperature and the autoclave contents were analysed by means of GC/NMR/HPLC analysis.

Asymmetric hydrogenation of (Z)- α -(acetamido)-cinnamic acid/- α -(acetamido) acrylic acid using catalyst 6.

Catalysis was carried out as for ref. 25. 0.1g of catalytic material (7) was used (2×10^{-6} mol Ru). Product was converted to its methyl ester for ease of separation (MeI, K_2CO_3). GC Lipodex E column (25m*0.25mm), Initial T = 70C, 10 min., then heating 2.5C per min. to 250C. For 10/11.

Asymmetric hydrogenation of β -ketoesters using catalyst 6.

Catalysis was carried out as for ref. 24. 0.1g of catalytic material (7) was used (2×10^{-6} mol Ru). Final products were reacted with acetic anhydride to produce an ester for enantiomer separation. GC Lipodex E column (25m*0.25mm).

Asymmetric hydrogenation of (Z)- α -(acetamido)-cinnamic acid/- α -(acetamido) acrylic acid using catalyst 7.

Catalysis was carried out as for ref. 26. 0.1g of catalytic material (8) was used (4×10^{-6} mol Rh). Product was converted to its methyl ester for ease of separation (MeI, K_2CO_3). GC Lipodex E column (25m*0.25mm), Initial T = 70C, 10 min., then heating 2.5C per min. to 250C. For 9/10.

Asymmetric hydrogenation of Acetophenone/Naphthophenone using catalyst 8.

Catalysis was carried out as for ref. 27. 0.1g of catalytic material (9) was used (2×10^{-6} mol Ru). HPLC; n-hexane/isopropanol 95/5. Chirasil OD. Room temperature for both phenyl and naphthyl products.

4.5 References

- ¹ (a) N. Takaisha, H. Imai, C. A. Bertelo, J. K. Stille, *J. Am. Chem. Soc.*, 1976, **98**, 5401-5402. b) N. Takaishi, H. Imai, C. A. Bertelo, J. K. Stille. *J. Am. Chem. Soc.*, 1978, **100**, 264-265. c) T. Masuda, J. K. Stille, *J. Am. Chem. Soc.*, 1978, **100**, 268-272. (d) S. J. Fritschel, J. J. H. Ackerman, T. Keyser, J. K. Stille. *J. Org. Chem.* 1979, **44**, 18, 3152. (e) W. Dumont, J-C. Poulin, T-P. Dang, H. B. Kagan. *J. Am. Chem. Soc.* 1973, **95**, 8295.
- ² H-U. Blaser. *Chem. Commun.* 2003, 293-296.
- ³ R. Noyori, H. Takaya, *Acc. Chem. Res.* 1990, **23**, 345-350.
- ⁴ (a) D. E. De Vos, I. F. J. Vankelecom, P. A. Jacobs; Chiral Catalyst Immobilisation and Recycling, 2000. *Wiley-VCH*. (b) A. R. McDonald, R. Gossage, G. van Koten, to be submitted, review on Immobilised Homogeneous Catalysts for Asymmetric Hydrogenation.
- ⁵ S. J. Shuttleworth, S. M. Allin, P. K. Sharma. *Synthesis* 1997, 1215. (b) S. J. Shuttleworth, S. M. Allin, R. D. Wilson, D. Nasturica. *Synthesis* 2000, **8**, 1035-1074. (c) D. E. Bergbreiter. *Catal. Today*, 1998, **42**, 389-397. (d) S. Kobayashi, R. Akiyama, *Chem. Commun.*, 2003, 449-460. (e) B. Clapham, T. S. Reger, K. D. Janda, *Tetrahedron* 2001, **57**, 4637-4662. (f) A. Akelah, D. C. Sherrington, *Chem. Rev.* 1981, **81**, 557-587. (g) T. J. Dickerson, N. N. Reed, K. D. Janda, *Chem. Rev.* 2002, **102**, 3325-3344. (h) P. Mastrolilli, C. F. Noble, *Coord. Chem. Rev.* 2004, **248**, 377-395.
- ⁶ C. E. Song, S. Lee, *Chem. Rev.*, 2002, **102**(10); 3495-3524.
- ⁷ G. Pozzi, I. Shepperson, *Coord. Chem. Rev.* 2003, **242**, 115-124.

- ⁸ (a) H. P. Dijkstra, G. P. M. van Klink, G. van Koten. *Acc. Chem. Res.* 2002, **35**, 798-810. (b) R. van Heerbeek, P. C. J. Kamer, P. W. N. M. van Leeuwen, J. N. H. Reek. *Chem. Rev.* 2002, **102**, 3717-3756. (c) H. W. . Peerlings, E. W. Meijer. *Chem. Eur. J.* 1997, **3**, 10, 1563-1570. (d) Y. Riboubouille, G. D. Engel, L. H. Gade, *C.R. Chimie* 2003, **6**, 1087-1096.
- ⁹ (a) M. Berthod, C. Saluzzo, G. Mignani, M. Lemaire, *Tet. Asymm.*, 2004, **15**, 639-645. (b) T. Lamouille, C. Saluzzo, R. ter Halle, F. Le Guyader, M. Lemaire. *Tetrahedron Lett.* 2001, **42**, 663-664. (c) K-T. Wan, M. E. Davis, *Tetrahedron Asym.* 1993, **4**, 12, 2461-2468. (d) K. T. Wan, M. E. Davis, *J. Catal.* 1994, **148**, 1. (e) K. T. Wan, M. E. Davis. *Nature*, 1994, **370**, 449-450. (f) K. T. Wan, M. E. Davis, *J. Catal.* 1995, **152**, 25-30. (g) A. L. Monteiro, F. K. Zinn, R. F. de Souza, J. Dupont. *Tet. Asymm.* 1997, **8**, 2, 177-179.
- ¹⁰ (a) M. Berthod, J-M. Joerger, G. Mignani, M. Vaultier, M. Lemaire, *Tet. Asymm.* 2004, **15**, 2219-2221. (b) H. L. Ngo, A. Hu, W. Lin. *Chem. Commun.*, 2003, 1912-1913. (c) A. Hu, H. L. Ngo, W. Lin, *Angew. Chem. Int. Ed.*, 2004, **43**, 2501-2504. (d) R. A. Brown, P. Pollet, E. McKoon, C. A. Eckert, C. L. Liotta, P. G. Jessop. *J. Am. Chem. Soc.* 2001, **123**, 1254-1255.
- ¹¹ (a) C. Saluzzo, M. Lemaire, *Adv. Synth. Catal.* 2002, **344**, 10,915-927. (b) G-J. Deng, Q-H. Fan, X-M. Chen, G-H. Liu. *J. Mol. Catal. A*, 2003, **193**, 21-25. (c) G-J. Deng, Q-H. Fan, X-M. Chen, D-S. Liu, A. S. C. Chan. *Chem. Commun.* 2002, 1570-1571. (d) Q-H. Fan, Y-M. Chen, X-M. Chen, D-Z. Jiang, F. Xi, A. S. C. Chan. *Chem. Commun.*, 2000, 789-790. (e) G-J. Deng, B. Yi, Y-Y. Huang, W-J. Tang, Y-M. He, Q-H. Fan. *Adv. Synth. Catal.* 2004, **346**, 1440-1444.
- ¹² (a) P. Guerreiro, V. Ratovelomanana-Vidal, J-P. Renet, P. Dellis. *Tet. Lett.* 2001, **42**, 3423-3426. (b) C. Saluzzo, T. Lamouille, F. Le Guyader, M. Lemaire. *Tet. Asymm.* 2002, **13**, 1141-1146. (c) H-B. Yu, Q-S. Hu, L. Pu. *J. Am. Chem. Soc.* 2000, **122**, 6500-6501. (d) H-B. Yu, Q-S. Hu, L. Pu. *Tet. Lett.* 2000, **41**, 1681-1685. (e) W.S. Huang, Q.S. Hu, L. Pu. *J. Org. Chem.* 1999, **64**, 7940. (f) R. ter Halle, B. Colasson, E. Schultz, M. Spagnol, M. Lemaire. *Tet. Lett.* 2000, **41**, 643-646. (g) M. Lemaire, R. ter Halle, E. Schulz, B. Colasson, M. Spagnol; (*Rhodia/CNRS*) *French Patent FR2789992*, 1999, *PCT: WO0049028*, 2000. (h) M. Lemaire, R. ter Halle, E. Schulz, B. Colasson, M. Spagnol, (*Rhodia/CNRS*) *French Patent FR2790477*, 2000. (i) R. ter Halle, E. Schulz, M. Spagnol, M. Lemaire. *Synlett*, 2000, **5**, 680-682. (j) T. Ohkuma, H. Takeno, Y. Honda, R. Noyori. *Adv. Synth. Catal.* 2001, **343**, 4, 369-375. (k) Q-H. Fan, C-Y. Ren, C-H. Yeung, W-H. Hu, A. S. C. Chan. *J. Am. Chem. Soc.* 1999, **121**, 7407-7408. (l) Q. H. Fan, C. H. Yeung, Y.C. Li, A. S. C. Chan. *Abst. Pap. Am. Chem. Soc.* 1997, **213**, 219. (m) Q-H. Fan, G-J. Deng, X-M. Chen, W-C. Xie, D-Z. Jiang, D-S. Liu, A. S. C. Chan. *J. Mol. Catal. A Chem.*, 2000, **159**, 37-43. (n) Q-H. Fan, G-J. Deng, C-C. Lin, A. S. C. Chan. *Tetrahedron Asym.* 2001, **12**, 1241-1247. (o) Q-H. Fan, G-H. Liu, G-J. Deng, X-M. Chen, A. S. C. Chan. *Tet. Lett.* 2001, **42**, 9047-9050.
- ¹³ D. J. Bayston, J. L. Fraser, M. R. Ashton, A. D. Baxter, M. E. C. Polywka, E. Moses. *J. Org. Chem.* 1998, **63**, 3137-3140.
- ¹⁴ (a) I. F. J. Vankelecom, D. Tas, R. F. Parton, V. Van de Vyver, P. A. Jacobs. *Angew. Chem. Int. Ed.* 1996, **35**, 12, 1346-1348. (b) R. F. Parton, I. F. J. Vankelecom, D. Tas, K. B. M. Jansen, P-P. Knops-Gerrits, P. A. Jacobs. *J. Mol. Catal. A: Chem.* 1996, **113**, 283-292. (c) D. Tas, C. Thoelen, I. F. J. Vankelecom, P. A. Jacobs. *Chem. Commun.*, 1997, 2323. (d) I. F. J. Vankelecom, K. A. L. Vercruysse, P. E. Neys, D. W. A. Tas, K. B. M. Janssen, P-P. Knops-Gerrits, P. A. Jacobs. 1998, **5**, 125-132. (e) K. De Smet, A. Pleysier, I. F. J. Vankelecom, P. A. Jacobs, *Chem. Eur. J.* 2003, **9**. (f) A. Kockritz, S. Bischoff, V. Morawsky, U. Prusse, K-D. Vorlop. *J. Mol. Catal. A*, 2002, **180**, 231-243.
- ¹⁵ (a) S. Shimazu, K. Ro, T. Sento, N. Ichikuni, T. Uematsu. *J. Mol. Catal. A*, 1996, **107**, 297-303. (b) T. Sento, S. Shimazu, N. Ichikuni, T. Uematsu. *J. Mol. Catal. A: Chem.*, 1999, **137**, 263-267.
- ¹⁶ (a) F. Gelman, D. Avnir, H. Schumann, J. Blum. *J. Mol. Catal. A*, 1999, **146**, 123-128. (b) J. Blum, D. Avnir, H. Schumann. *ChemTech.* 1999, 32-38. (c) J. Jamis, J. R. Anderson, R. S. Dickson, E. M. Campi, W. R. Jackson. *J. Organometallic Chem.* 2001, **627**, 37-43.
- ¹⁷ (a) A. Hu, H.L. Ngo, W. Lin. *J. Am. Chem. Soc.*, 2003, **125**, 11490-11491. (b) L-X. Dai, *Angew. Chem. Int. Ed.* 2004, **43**, 5726-5729.
- ¹⁸ B. Kesanli, W. Lin, *Chem. Commun.* 2004, 2284-2285.
- ¹⁹ A. R. McDonald, H. P. Dijkstra, B. M. J. M. Suijkerbuijk, M. Lutz, A. L. Spek, G. P. M. van Klink, G. van Koten, **chapter 2** of this thesis, to be submitted for publication.
- ²⁰ J. Sommer, Y. Yang, D. Rambow, J. Blumel, *Inorg. Chem.* 2004, **43**, 7561-7563.
- ²¹ K. Mashima, K-H. Kusano, T. Ohta, R. Noyori, H. Takaya, *J. Chem. Soc. Chem. Commun.* 1989, 1208-1210.
- ²² ATR-IR (attenuated total reflection) is a technique whereby transmission of an IR beam through a sample is measured.

²³ DRIFT-IR (diffuse reflectance fourier transform) is a surface technique which analyses reflected IR beam from the surface/near surface of the material.

²⁴ R. Noyori, T. Ohkuma, M. Kitamura, *J. Am. Chem. Soc.*, 1987, **109**, 5856-5858.

²⁵ H. Kawano, T. Ikariya, Y. Ishii, M. Saburi, S. Yoshikawa, Y. Uchida, H. Kumobayashi, *J. Chem. Soc. Perkin Trans.* 1989, 1571-1575.

²⁶ A. Miyashita, A. Yasuda, H. Takaya, K. Toriumi, T. Ito, T. Souchi, R. Noyori, *J. Am. Chem. Soc.* 1980, **102**, 7932-7934.

²⁷ T. Okhuma, H. Ooka, S. Hashiguchi, T. Ikariya, R. Noyori, *J. Am. Chem. Soc.* 1995, **117**, 2675-2676.

²⁸ US Patent no. 4705895.

²⁹ I. J. B. Lin, H. A. Zahalka, H. Alper, *Tet. Lett.* 1988, **29**, 1759-1762.

³⁰ www.amtec-chemnitz.de

CHAPTER 5

Sequential Compartmentalised Tandem Catalysis; Iridium(III)

Organometallics on Silica for Alkane Activation

Iridium(III) organometallic pincer complexes were immobilised on a high density silica support by synthesis of an alcohol functionalised iridium(III) organometallic and coupling of this with an isocyanate functionalised silica material. The acquired pre-catalytic material was activated *in situ* using ^tBuLi, and applied in the transfer dehydrogenation of several cyclic and linear alkanes, and secondary alcohols. Immobilised Grubbs-II-type catalytic material was also synthesised and applied in both ring closing and ring opening metathesis catalysis. The developed catalytic materials were applied in a sequential manner. This novel technique is described as Sequential Compartmentalised Tandem Catalysis (SCTC), and has been demonstrated for the synthesis of linear, terminal diesters and diketones from unreactive cyclic alkanes by applying the dehydrogenation material in sequence with the metathesis material. Likewise the synthesis of cyclic epoxides from cyclic alkanes was demonstrated using the dehydrogenation material in sequence with a silica bound manganese porphyrin containing material, which catalysed the epoxidation of the formed alkene. Finally the deracemisation of secondary alcohols was demonstrated by application of the dehydrogenation material in sequence with asymmetric hydrogenation material (racemic alcohol - ketone - enantiopure alcohol). The sequential reaction systems were facilitated by simple inter-reactor solution transfer, made possible as a result of catalyst compartmentalisation.

Based on Aidan R. McDonald, Martin Lutz, Gerard P. M. van Klink, Anthony L. Spek, Gerard van Koten to be submitted for publication, and Aidan R. McDonald, Gerard P. M. van Klink, Gerard van Koten, to be submitted for publication

5.1 Introduction

Homogeneous catalyst immobilisation is an important sub-topic in the development of homogeneous catalysts for fine chemical synthesis. The industrial-scale synthesis of widely-used fine chemicals using cheap and/or *reusable* homogeneous catalysts has become an essential goal.¹ Reaction sequences that use less solvent and reduce waste, particularly salts from used organometallic reagents or extensive acid/base cycles, are becoming vitally important. Present trends in this field are moving towards the development of multi-step, one-pot processes where low solvent and salt waste is generated, and energy efficiency is required to produce a cost-effective end-product. However, these one-pot cascade, tandem, or domino catalysed reaction sequences rely on catalyst, substrate and solvent compatibility.² So far very few multi-step procedures have been demonstrated.³ Ideally we would like to mimic nature's ability to compartmentalise catalysts within the cell.⁴ That is, reactions take place at separate sites, in separate 'reaction vessels' to produce sequentially catalysed reactions. In our studies we would like to compartmentalise homogeneous catalysts to allow for reactions to take place under conditions that do not affect earlier or subsequent reactions in a sequence. This would be classified as a Sequential Compartmentalised Tandem Catalysis (SCTC).⁵ A previous report has demonstrated the multi-pot application of immobilised homogeneous catalyst in sequence with an enzyme for the enantioselective synthesis of chiral amino acid from prochiral enamide esters,⁶ however this topic has, to the best of our knowledge, not been investigated in depth.

Standard techniques for the functionalisation/activation of alkanes involve halogenation or oxidation by C-H bond activation. Halogenation of alkanes is often mediated through highly toxic elemental halogens or halogenated inorganic compounds and produces large amounts of corrosive acid side product, or toxic halogen containing inorganic compounds, and is thus environmentally unfavourable. Alkane oxidation has been demonstrated by nature, for example, the conversion of alkanes to alcohols by the monooxygenase family of enzymes, however non-natural examples are rare, and mimetic compounds have shown minimal success. Recently, dehydrogenation of alkanes, resulting in alkenes, which are versatile starting materials for a range of well-known conversions, has become a field of intense interest for the functionalisation of unreactive alkanes. A broad range of reaction-types is available to further functionalise alkenes. Olefin cross metathesis has become a valuable tool for the introduction of functional groups to both terminal and internal alkenes.⁷ Ring opening cross-metathesis demonstrates methods to yield terminally functionalised linear alkyl species.⁸ Several examples of the immobilisation of ruthenium alkylidene N-heterocyclic carbene complexes for metathesis have been demonstrated, the most successful of which have been mediated through tethering of a carbene ligand to a support.⁹

The pincer iridium complexes shown in figure 1 were one of the first homogeneous catalysts to be applied in the transfer dehydrogenation of alkanes.¹⁰ The catalysts have also been demonstrated to selectively transfer dehydrogenate terminal alkane sites with a dihydrogen acceptor.¹¹ Such complexes are also excellent catalysts for transfer dehydrogenation of alcohols and imines.¹² Acceptorless dehydrogenation of alkanes has also been demonstrated and is probably

the most promising result to date for the possible application of these catalysts.¹³ The inherent stability of pincer units with terdentate coordination and a direct carbon-metal σ -bond means these systems have been thoroughly studied and applied. And means they are ideal systems for immobilisation studies.¹⁴

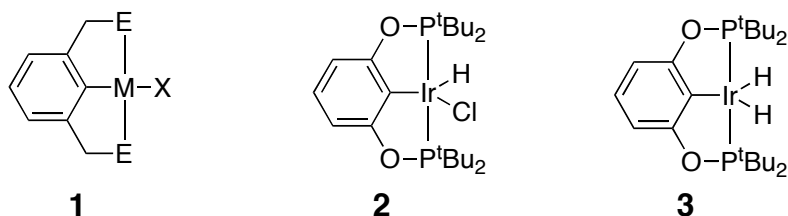


Figure 1. Generic pincer metal complex **1**, and PCP-IrHCl **2**, and PCP-IrH₂ **3**, complexes.

An ECE-pincer organometallic is generally described as a terdentate ligand bound to a metal centre via one sigma and two dative bonds (figure 1, compound **1**).¹⁵ The pincer organometallics have been utilised by our group to demonstrate a range of techniques for catalyst recycling and immobilisation; dendritic,¹⁶ organic polymeric,¹⁷ and inorganic supports¹⁸ have been utilised and the synthesised catalytic materials have been applied in a wide range of catalytic reactions; aldol condensation,¹⁹ double Michael addition,²⁰ Kharasch addition,²¹ transfer hydrogenation,²² and recently allylic stannylation²³ and allylic alkylation reactions.²⁴ The most interesting application of pincer iridium(III) dehydrogenation catalysts has been in tandem catalysed reactions with Schrock-type metathesis catalysts.²⁵ One-pot conversion of lower alkanes to a mixture of higher alkanes was demonstrated. In general ECE pincer organometallics are very stable both towards thermal decomposition and harsh reaction conditions.

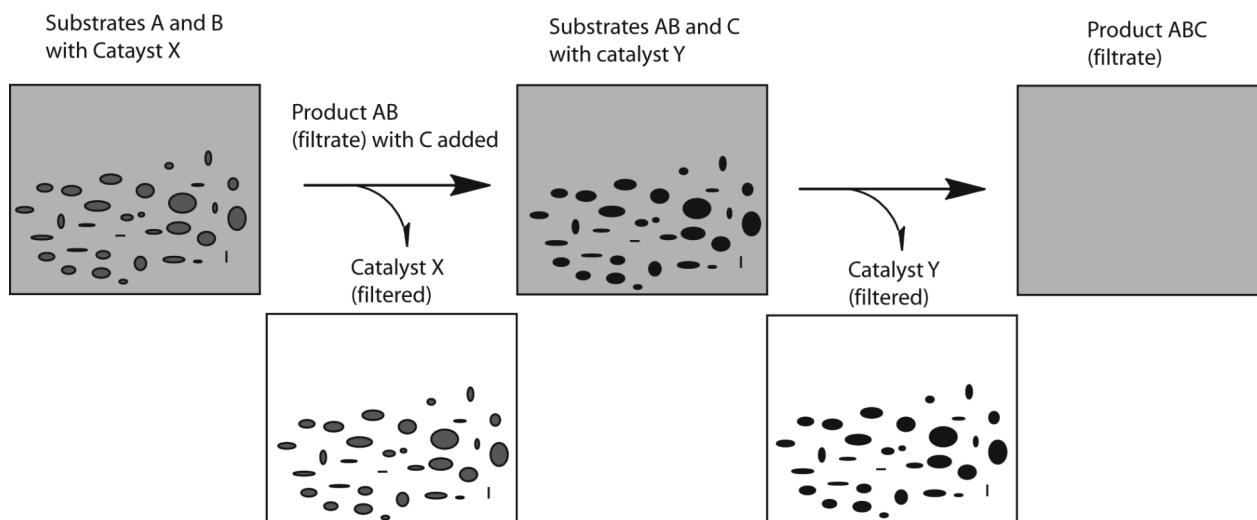
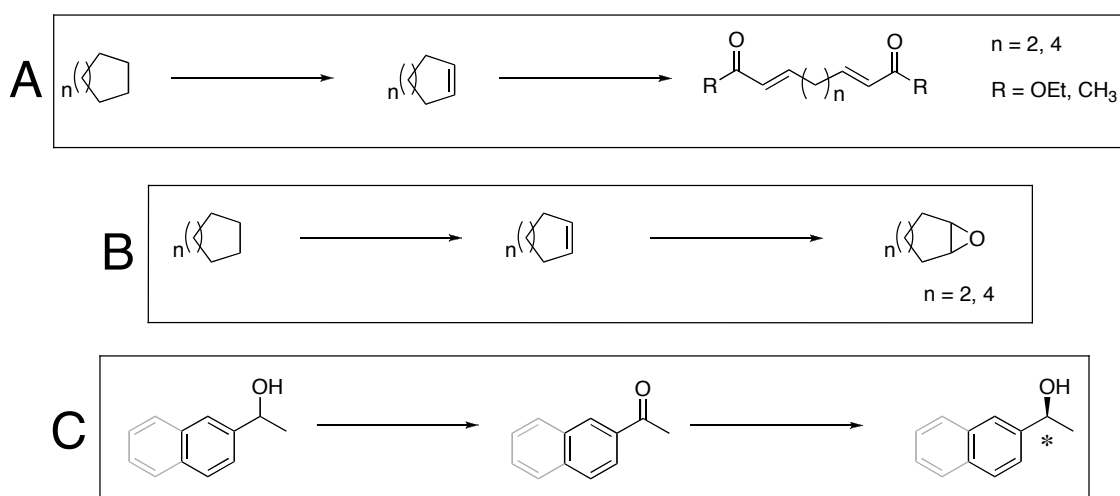


Figure 2. Schematic depiction of sequential multi-pot tandem catalysis, STC.

The SCTC concept is schematically demonstrated in figure 2. Theoretical reactants ‘A’ and ‘B’ can react to yield product ‘AB’ in the presence of catalyst ‘X’. The reaction mixture containing ‘AB’ can then be transferred to a new reaction vessel with the removal of catalyst ‘X’ by simple decantation/filtration. Substrate ‘C’ could be introduced with a different catalyst, ‘Y’, which

catalyses the reaction of ‘AB’ with ‘C’ yielding ‘ABC’, which can be isolated by simple filtration of catalyst ‘Y’. This process is fundamentally green, and obeys several of the principals of green chemistry: waste prevention, atom economy, energy efficiency and catalysis. In this report we applied various different catalytic materials in a sequential manner to demonstrate that simple compartmentalisation of reaction mixtures is an easy, effective principle. We have studied the feasibility of the principle by exploring three reaction sequences (scheme 1): a) cyclic alkane to linear diester/diketone via alkene; b) cyclic alkane to cyclic epoxide via alkene; c) racemic alcohol to enantiopure alcohol via ketone. These reaction sequences are mediated by compartmentalisation of the catalysts, which are mutually sensitive to one another, by catalyst immobilisation (as depicted in figure 2).

Scheme 1. Reaction sequences for application in multi-pot tandem catalysis.



We set out to immobilise the relevant homogeneous catalysts to demonstrate the above-mentioned proof of principle. We present the covalent immobilisation of complex **2** on silica.²⁶ The novel material was applied in the transfer dehydrogenation of cyclooctane (COA), cyclohexane (CHA), *n*-hexane and *n*-octane yielding cyclooctene (COE), cyclohexene (CHE), hexenes, and octenes respectively. The dehydrogenation of racemic 1-aryl-1-ethanols yielding ketones was also performed. We have also investigated the immobilisation of homogeneous catalysts for cross-metathesis (Grubbs II), epoxidation (manganese porphyrin) and asymmetric hydrogenation ([BINAP-RuCl₂-DPEN]).

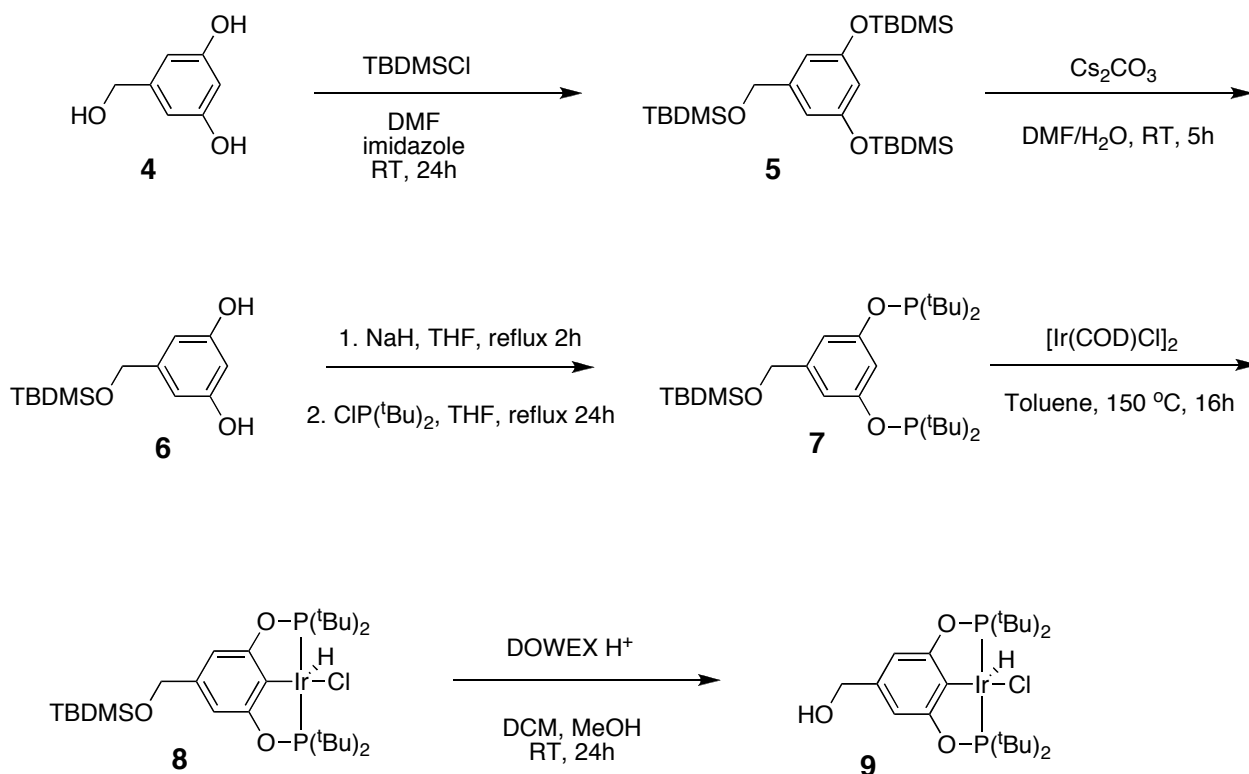
5.2 Results and Discussion

5.2.1 Synthesis of the Catalytic Materials

To tether a pincer metal complex to an inorganic support requires addressing separate ends of a benzene ring; a) to facilitate a functionality for tethering to the support; and b) to synthesise a terdentate-coordinating unit.^{15,27} After several failed attempts with flamenol (5-methoxy-1,3-benzenediol) and phloroglucinol (1,3,5-benzenetriol) we focused our attention on 5-

(hydroxymethyl)-1,3-benzenediol, **4** (scheme 2). Compound **4** was reacted with three equivalents of tert-butyldimethylsilyl-chloride (TBDMSCl) in the presence of an excess of base (imidazole) yielding the tris-silyl ether, **5**. The phenyl-silyl ether groups could be selectively addressed without affecting the benzyl-silyl ether, using Cs_2CO_3 in DMF/water at room temperature.²⁸ This yielded a resorcinol containing a protected benzyl alcohol functionality, **6**. Compound **6** was reacted with bis(tert-butyl)chlorophosphine yielding functionalised ligand **7** which was complexed, using standard techniques, with $[\text{Ir}(\text{COD})\text{Cl}]_2$. It was essential in this reaction, that the $[\text{Ir}(\text{COD})\text{Cl}]_2$ was freshly made and was bright orange in colour,²⁹ otherwise Ir^0 was found in the final product, which is difficult to remove. Deprotection of **8** was mediated through reaction with an acidic ion-exchange resin (the use of other deprotecting reagents, *e.g.* TBAF, resulted in decomposition, and Ir^0 formation). It was discovered in test reactions on **8** and **9** that the use of base caused reaction of the iridium centre resulting in the disappearance of the ^1H hydride resonance in ^1H NMR. Recent reports have shown that Ir(III) hydrochloride species **2** as a precatalyst can easily be activated *in situ* using one equivalent of strong base.³⁰ This alleviates the necessity to use borohydride to synthesise the dihydride **3**, the actual catalyst.³¹ The highly stable **2** can be used with minimal precautions, which would be necessary when using **3** which reacts readily with N_2 in the presence of acceptor alkene, yielding a dimeric dinitrogen complex which is inactive in transfer dehydrogenation catalysis.³² We have chosen to not synthesise materials containing the active catalyst **3** because of the likelihood of catalyst deactivation during the materials synthesis steps. We have chosen to immobilise a complex similar to **2**, because of its relative stability. Finally the bis-*ortho* chelated phosphito complexes of the type **2** and **3** show better activity in transfer dehydrogenation than their phosphine analogue.

Scheme 2. Synthetic pathway to functionalised PCP-IrHCl complex, **9**.



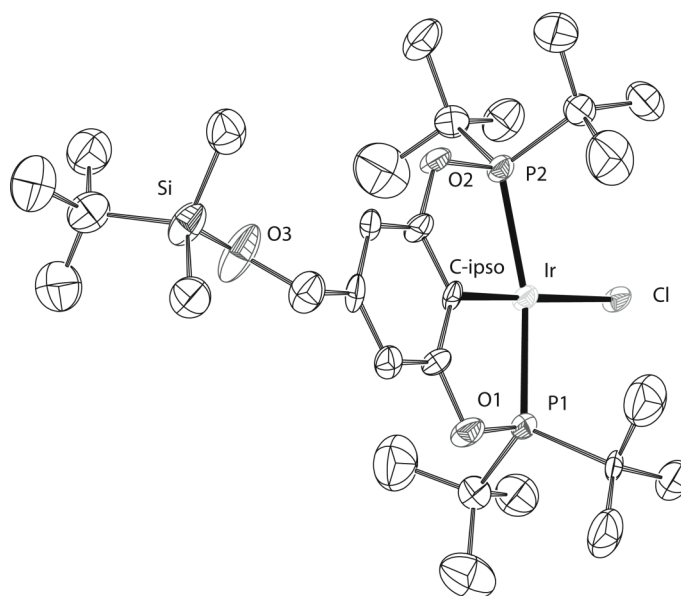


Figure 3. Displacement ellipsoid plot (50% probability level) of **8**. Hydrogen atoms omitted for clarity.

Table 1. Selected bond distances (Å) and angles (°) for **8** and analogous complexes.^a

Complex	Ir-P1	Ir-P2	Ir-C _{ipso}	P1-Ir-P2
8	2.280(3)	2.282(3)	2.060(9)	160.16(11)
	2.2949(16)	2.2889(15)	2.004(5)	159.79(5)
	2.3138(12)	2.3111(12)	2.015(3)	166.80(3)

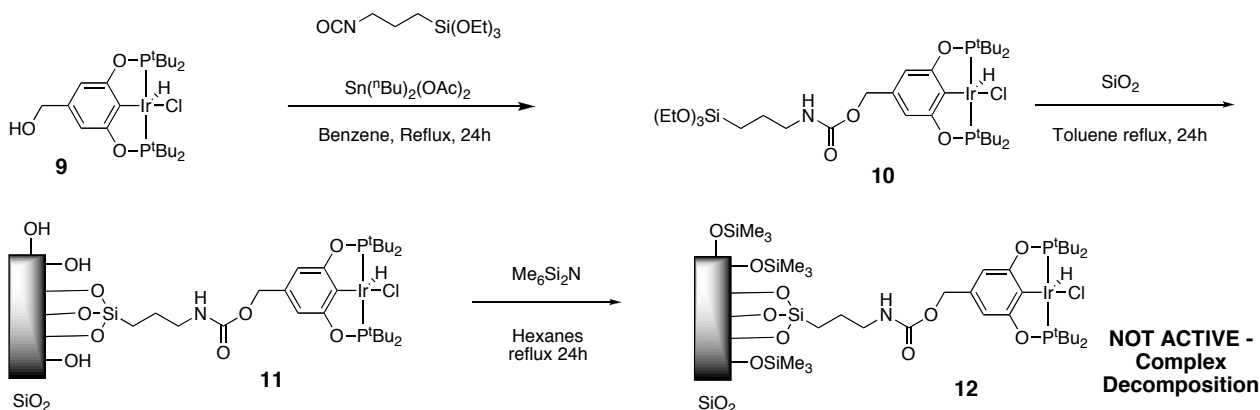
^a*para*-Methoxy results from Brookhart^{33(a)} et al. Para nitro results from Kaska^{33(b)} et al.

Single crystals of **8**, suitable for X-ray diffraction were acquired by slow evaporation of a dichloromethane solution. Figure 3 depicts the ORTEP diagram of the X-ray diffraction pattern. The crystal system was monoclinic with the centric space group P 21/c. It was not possible to observe diffraction for the hydride (hydride resonance in ¹H NMR, $\delta = -41.5$ ppm). All other bond distances are as expected for such complexes (table 1).³³ The ligand is *mer*- η^3 -PCP coordinated in a terdentate manner to the iridium(III) centre. The geometry around iridium is distorted square pyramidal with the hydride expected to be capping the pyramid. The chloride (*trans* to C_{ipso}), phosphorous' and benzene ring are co-planar. The *phosphinite* P-Ir-P bond angle is 160.16⁰, which

is slightly more acute than in analogous *phosphine* complexes, which have a slightly less constrained P-Ir-P bond angle (table 1).

The immobilisation of an organometallic is often mediated through the coupling of a nucleophile-functionalised organometallic with 3-triethoxysilyl-propyl-1-isocyanate in the presence of base. Because the iridium hydrochloride complex is base sensitive, complex **9** was reacted with an excess of 3-triethoxysilyl-propyl-1-isocyanate in benzene at reflux in the presence of a catalytic amount of $\text{Sn}(\text{nBu})_2(\text{OAc})_2$ for 24h (scheme 3). No loss of the hydride signal (^1H NMR spectrum of the reaction mixture) was observed. It was not possible to remove remnant starting complex **9** from **10** by either recrystallisation or column chromatography. Consequently, immobilisation of **10** was carried out without purification by refluxing the mixture of **9** and **10** and a high density silica,³⁴ in toluene for 24h yielding a pinkish silica, **11**. Capping of remnant silanol groups (observed by IR spectroscopy) was carried out by reaction of **11** with hexamethyldisilazane in hexanes at reflux for 24 hours. However, when the final product (**12**, silica with capped silanol groups, and tethered iridium organometallic, scheme 3) was tested as a catalyst in dehydrogenation reactions, the synthesised material showed no catalytic activity. To investigate why the material was inactive, a test reaction of **2** in hexanes with one equivalent of hexamethyldisilazane (the reagent used for capping the remnant silanol groups on the silica support) showed an immediate decolouration from red to dark green, and subsequent Ir^0 formation. This suggests that the process of capping the silanol groups on silica resulted in decomposition of the active organometallic iridium complex bound to the silica surface.

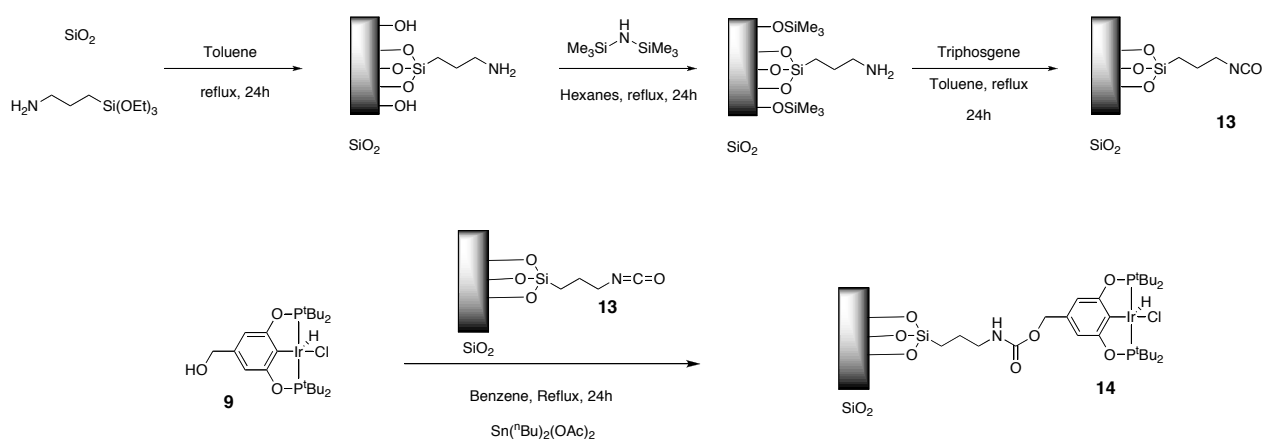
Scheme 3. Immobilisation of **9** by synthesising **10**, led to an inactive catalytic material.



We therefore synthesised material **13**, which is a silica material containing isocyanate functionalities, with all remnant silanol groups capped. Material **13** was synthesised by reaction of 3-aminopropyl-1-triethoxysilane with a high density silica.³⁵ The synthesised amino-functionalised silica was then stirred at reflux in hexane with hexamethyldisilazane, capping any remnant silanol groups. Conversion of the amino groups to isocyanate was mediated through a reaction with triphosgene in refluxing toluene. A large excess of triphosgene was used ensuring all amino groups were converted to isocyanate groups. The benefits of using material **13** lie in the fact that we can easily react functionalised organometallic **9** with **13**, and immediately use the synthesised material in catalysis, without having to perform any further protection, capping, or deprotection steps. Compound **9** was reacted with **13** in benzene at reflux for 24h in the presence of $\text{Sn}(\text{nBu})_2(\text{OAc})_2$

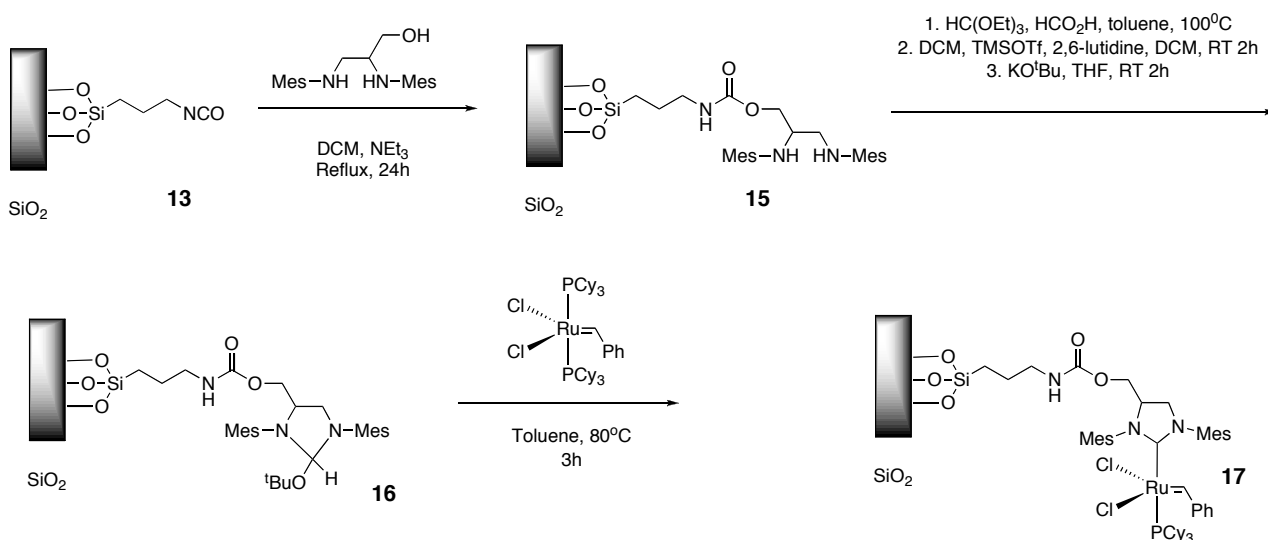
(scheme 4). Hydroxymethylbenzene was added to the solution to ‘cap’ all remnant isocyanate groups. Material **14** was catalytically active.

Scheme 4. Synthetic pathways to material containing immobilised iridium organometallic pre-catalyst **14**.



To immobilise a Grubbs-II-type ruthenium metathesis catalyst on silica we have modified work by Blechert and co-workers.³⁶ In that work an N-heterocyclic carbene ligand is constructed on an organic polymeric support, which has subsequently been reacted with a ruthenium precursor to yield an immobilised Grubbs-II metathesis catalyst. We chose the route shown in scheme 5 which involved the coupling of a carbene precursor (an ethylene diamine³⁷), with material **13** (scheme 5). The tethered amine **15** was then cyclised using formic acid in triethylorthoformate/toluene and subsequently activated yielding a silica bound 2-tert-butoxy-4,5-dihydroimidazoline, **16**. This material was reacted with a ruthenium alkylidene complex at 80°C (high temperature facilitates both carbene formation and complexation) yielding the desired immobilised Grubbs-II complex tethered to silica.

Scheme 5. Synthesis of immobilised Grubbs II, ruthenium carbene alkylidene complex, material **17**.



In previous work carried out in our lab, functionalised 2,2'-bis(diphenylphosphino)-1,1'-binaphthyl (BINAP) ligand has been immobilised on silica by coupling material **13** with a diamino-functionalised BINAP (figure 4).³⁸ We have introduced both ruthenium and rhodium to

immobilised BINAP and applied the formed materials in the asymmetric hydrogenation of various substrates.³⁹ We have also previously developed silica materials containing manganese porphyrin complexes (figure 4).⁴⁰ These materials have been developed by a simple ‘click’ immobilisation technique, and the acquired materials were active catalysts in the epoxidation of a number of alkenyl substrates. This work demonstrates the simple, high yielding tethering of functionalised organometallics on an inorganic support, and allows for the further application of immobilised catalysts in multi-step processes.

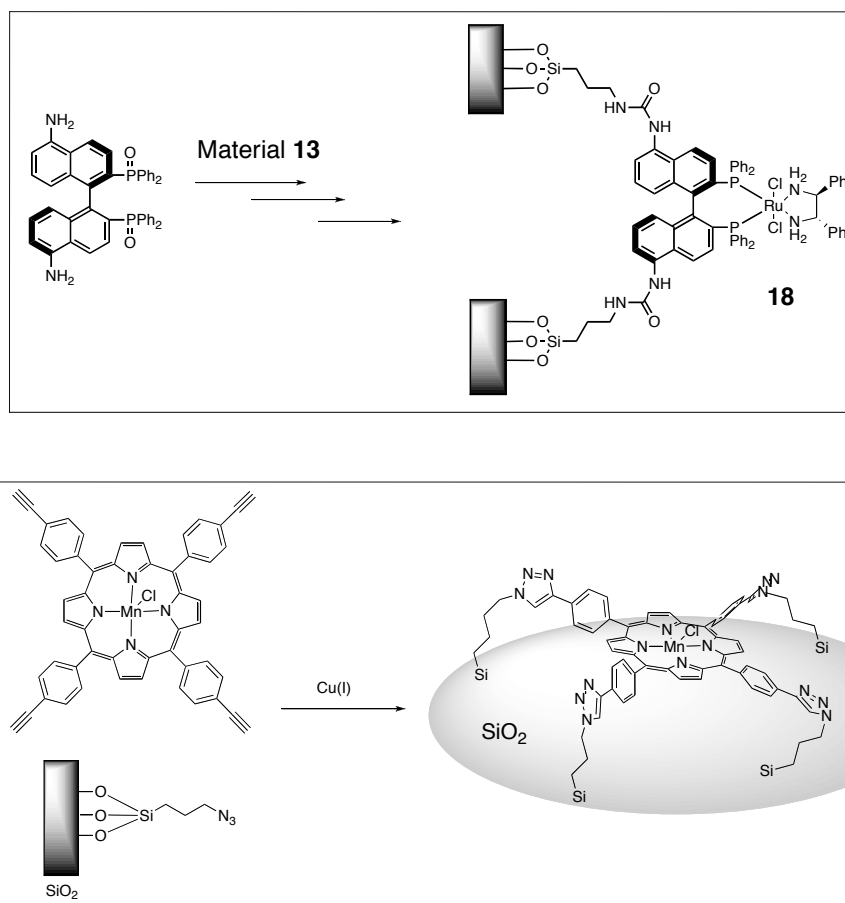


Figure 4. Covalent immobilisation of homogeneous catalysts for asymmetric hydrogenation (**18**) and epoxidation (**19**).

5.2.2 Analysis of Supported Catalytic Materials

5.2.2.1 Elemental Content Analysis

The elemental content analysis of material **9** confirmed that no destruction of ligand or metal had occurred upon immobilisation (table 2). The iridium loading was found to be 0.73% of the total mass, and the phosphorous loading was found to be 0.24% of the total. This approximate ratio of iridium to phosphorous loading content is exactly what is expected. An ideal model compound containing one iridium atom with two phosphorous atoms is calculated as 75.6% iridium and 24.4% phosphorous. Comparing the nitrogen content analysis of materials **13** and **14** shows only a slight difference in the nitrogen loading as would be expected thus confirming that the isocyanate/carbamate remained bound to the support in the immobilisation reaction. The slight

decrease is as a result of extra carbon, iridium, and phosphorous being added to the support, thus reducing the overall fraction of nitrogen present.

Table 2. Elemental content analysis of materials **13**, **14**, and **17**.

Material	Loading ^a	N	P	Ir	Ru	Atomic Ratio ^b
13		1.97	-	-	-	-
14		1.84	0.24	0.73	-	P/Ir = 2:1
17		1.57	0.34	-	1.09	P/Ru = 1:1 N/Ru = 10:1

^aPercentage elemental content. ^bAtom-to-atom equivalents.

Likewise material **17** showed loading values that correspond to the expected P/Ru ratios. The found percentage loading of ruthenium and phosphorous was 1.09% and 0.34% respectively. This corresponds to almost exactly one ruthenium atom for every phosphorous atom (1:1.02 ratio), which is what is expected. The differences in nitrogen loading from carbene precursor material **15** to the carbene complex **17** are almost zero (1.61 cf. 1.57) demonstrating that complexation shows no loss in immobilised ligand. The nitrogen content of material **17** is 1.57%, which corresponds to approximately 10 nitrogen atoms for every one ruthenium atom. This demonstrates that there is an excess of carbene ligands on the silica surface with respect to ruthenium. This is a benefit, because in the event that ruthenium carbene coordination should fail, there are plenty of carbene sites to trap any decoordinated ruthenium.

5.2.2.2 Infra-Red Analysis

ATR⁴¹ and DRIFT⁴² infra-red spectroscopy were used to analyse non-tethered and tethered iridium organometallics. Characterisation with IR spectroscopy was unfortunately limited because the ATR spectrum of **2** shows there are no distinctively intense signals in the spectrum. Figure 5a shows the DRIFT spectrum of material **14** minus the DRIFT spectrum of **13** (a difference spectrum). There is a trough at 2278 cm⁻¹ that corresponds to consumed isocyanate groups. The peaks at 1651 and 1554 cm⁻¹ are carbamate stretching resonances, confirming that the alcohol of **9** has reacted with the isocyanate of **13**. Furthermore, there are subtle peaks between 1440 and 1480 cm⁻¹ that are representative of the characteristic stretches of **2**. Figure 5b shows the DRIFT difference spectrum of **14** minus silica. This inherently shows what has been added and subtracted from the silica surface. The first point of interest is the trough at 3740 cm⁻¹ which is representative of consumed silanol stretches. This means the triethoxysilane which is used to couple the amino tether to the silica surface (for the synthesis of material **13**) has reacted with surface silanol groups. Any remaining groups were capped with trimethylsilyl groups, and hence a substantial trough is observed. The distinct carbamate stretches (1651 and 1551 cm⁻¹) are clearly visible, as mentioned for figure 5a, and the subtle resonances of the iridium organometallic are also visible (1440 and 1480 cm⁻¹). No isocyanate stretch is visible in figure 5b (expected at 2278 cm⁻¹), showing that all isocyanate has been converted to a carbamate. Ruthenium alkylidene complexes tethered to silica

(17) were characterised in the same manner, showing the expected gains and losses in carbamate, isocyanate, and silanol stretches.

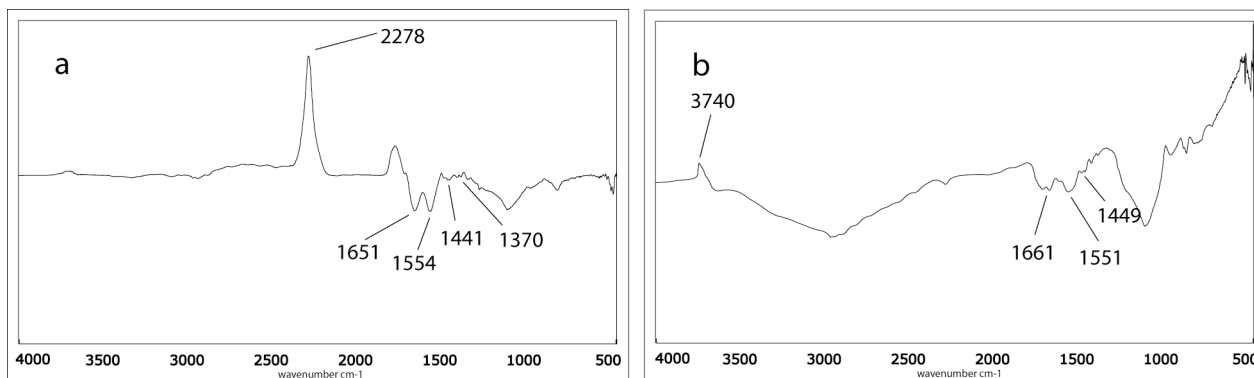


Figure 5 (a and b). IR DRIFT difference spectra of **14** minus **13**, and **14** minus SiO₂.

5.2.2.3 NMR Analysis

It is essential that complex **2** has been bound to silica, and not another species because once activated **2** reacts readily with a large range of organic functionalities, generally resulting in a species that is not catalytically active. ¹H NMR shows us that the hydride (Ir-*H*) remains intact during the deprotection step (**8** to **9**) and also during the reaction of compound **9** with 3-isocyanatopropyl-1-triethoxysilane in solution (**9** to **10**). We therefore assume that no hydride is lost in the reaction of **9** with material **13** (we are unable to take ¹H solid state NMR spectroscopy). Likewise ³¹P NMR solution analysis shows no substantial change in the position or intensity of the resonance for coordinated phosphines during the reaction of **9** to yield **10**.

Solid state ³¹P CP-MAS NMR was used to analyse material **14**. The spectrum is depicted in figure 6(a), which shows a non-symmetrical spectrum centred at 174.7ppm. All other resonances are spinning side bands at 8 kHz. The non-symmetry of the spectrum can be explained as being a result of chemical shift anisotropy (CSA), which is common in ³¹P CP-MAS NMR of solid state samples of phosphine-metal complexes in the solid state.⁴³ We have taken solid state CP-MAS NMR spectra of complex **2** and compared it to the spectrum of material **14**. The spectrum showed the same asymmetric pattern, and disproportionation of peaks. This confirms that the phosphorous iridium coordination remains intact in the immobilisation procedure. The correlation of the solid state results with the homogeneous precursors (³¹P δ = 174.7 ppm cf. 177ppm) demonstrates that the organometallic iridium(III) hydrido chloride complex has been immobilised, and is intact. ²⁹Si CP-MAS NMR was applied to analyse the effects of carrying out organic synthetic procedures on silica in the synthesis of material **14**. Figure 6(b) shows the ²⁹Si spectrum of material **14**. The ²⁹Si CP-MAS NMR of material **17** showed the similar results, and both spectra showed that there was no effect on the morphology/constituents of the silica support after organic synthetic methods were applied to it.³⁵

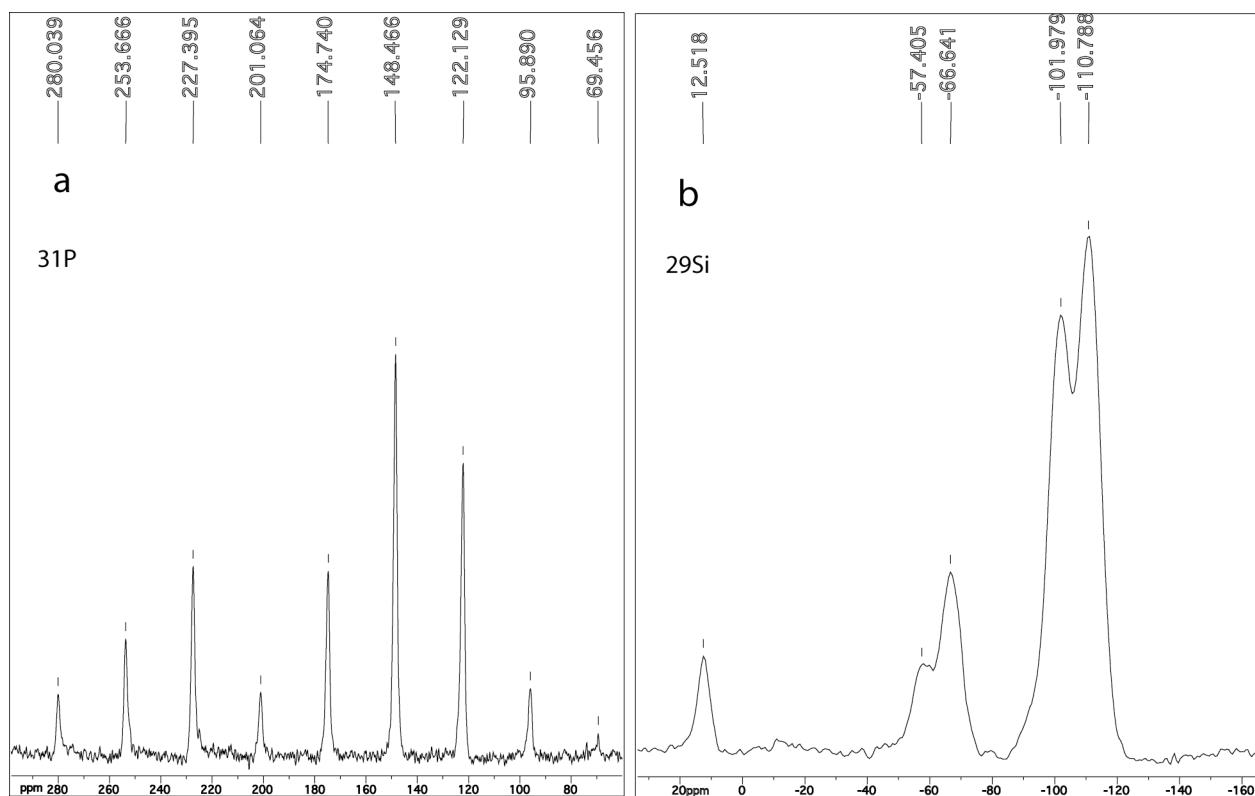


Figure 6 (a and b). ^{31}P (a) and ^{29}Si (b) CP-MAS NMR spectrum of material **14**.

5.2.3 Catalysis

5.2.3.1 ‘Heterogeneous’ Catalysis with Silica Bound Homogeneous Catalysts

To activate the organometallic species in material **14**, to allow it to catalyse transfer dehydrogenation, a base was introduced in the presence of the desired alkane/alcohol and a dihydrogen acceptor, 3,3'-dimethylbut-1-ene (TBE). We have applied the resulting materials in the transfer dehydrogenation of a number of alkanes and alcohols. Our initial attempts to apply material **14** were in the dehydrogenation of cyclooctane (COA), where we used KO^tBu or NaO^tBu as the activating base. The bases were added both in a stoichiometric and excessive amounts, with respect to catalytic sites, however, no catalytic activity was observed. Both bases were poorly soluble in the reaction mixture. To investigate the application of soluble bases for activation of pincer iridium complexes for dehydrogenation catalysis we carried out a number of experiments on untethered organometallics. Very few bases, which show similar pKa values to the butoxide-type bases, are also soluble in alkanes. Alkyl lithium reagents dissolved in pentane have the desired pKa value, so we applied them with the pre-catalyst **2**, as a test system. We found that pre-catalyst **2**, dissolved in the reaction mixture of COA and TBE was activated by the addition of a slight excess of $^t\text{BuLi}$ in pentane (1.5M). Conversion of COA to COE and 1,3-cyclooctadiene (1,3-COD) was observed (1,5-COD was not observed, but is converted to 1,3-COD at high temperatures). The observed turnover number (TON) after 14h of stirring at 200°C was 847 with a COE/COD ratio of approximately 80/20. The TON is slightly lower than previous reports when KO^tBu was used as the activating agent.³⁰ To ensure that functionalisation of the PCP-pincer organometallic does not

affect the catalytic activity of the immobilised iridium complex, functionalised complexes **8** and **9** were also applied in catalysis. Both pre-catalysts showed activity, with **8** comparable to complex **2** in the transfer dehydrogenation of COA. We believe the alcoholic group of **9** reacts yielding an aldehyde that reacts further resulting in deactivation of the catalyst. (table 3).

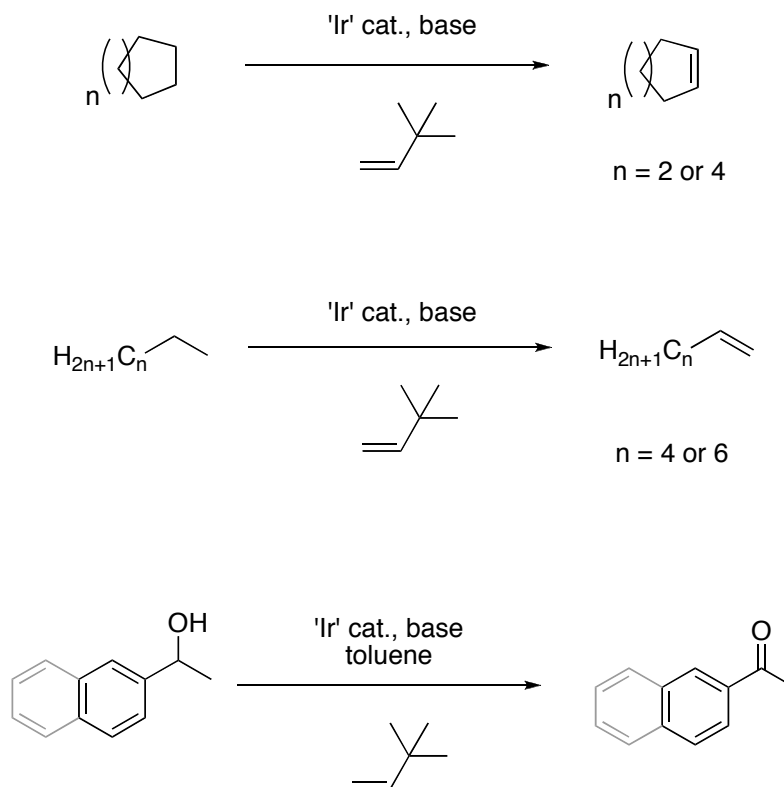


Figure 7. Catalytic transfer dehydrogenation of alkanes using catalytic pincer-iridium complexes in both homogeneous and heterogeneous reaction mixtures.

Table 3. TON of conversion of COA to COE with pre-catalysts **2**, **8** and **9**.

Catalyst	2 ^a	2 ^b	8 ^a	9 ^a
TON ^c (after 14hrs)	~1500 ^d	847	1423	125

^a KO^tBu used as base. ^b 1.5M ^tBuLi in THF used as base. ^c All reactions were carried out at 200^oC with a 1:1 ratio of COA to TBE (0.031mol) for 14 hours. ^dAs reported³⁰.

Material **14** was applied in the transfer dehydrogenation of COA and cyclohexane (CHA) with ^tBuLi as the activating base and showed low activity (figure 7). The TON was found to be 72 after 14 hours, which is an approximate 20-fold decrease in activity compared to pre-catalyst **2**. If the reaction mixture was allowed to stir for 168 hours the TON is found to be 358. The observed TON values are surprising because it is expected that approximately a 1:1 ratio of TBE to COA/COE is formed when an equilibrium has been reached. The low turnover values means less COD is observed, which is to be expected when there is still a large excess of TBE present. Material **14** was also applied in the dehydrogenation of linear alkanes resulting in linear alkenes

(figure 7). Pre-catalyst **2** is known for its selectivity towards terminal sites in alkane dehydrogenation reactions. However, once a certain quantity of terminal alkenes have formed they tend to undergo internal isomerisation in the presence of precatalyst **2**. We applied material **14** in the dehydrogenation of n-hexane and n-octane. We observed that the ratio of terminal to internal alkenes was comparable to the homogeneous precatalyst **2**. Unfortunately, our reactor set-up does not allow for sampling, so we could not do a conclusive study on the rate of terminal alkane dehydrogenation and internal isomerisation of terminal alkenes. However, it can be concluded that material **14** is an active pre-catalyst for the dehydrogenation of linear alkanes. Material **14** was applied in the dehydrogenation of racemic 1-phenyl-1-ethanol and 1-(2-naphthyl)-1-ethanol yielding acetophenone and acetonaphthone, respectively (figure 7). The reactions were carried out in the presence of a large excess of dihydrogen acceptor, and in both cases quantitative yields (100%) of the desired ketone were observed. Again the activity of the immobilised homogeneous catalyst was greatly reduced in comparison with the analogous homogeneous system.

Material **17** was applied in the ring closing metathesis reaction of both diallyl sulphide and diethyl diallyl malonate. In both cases conversion to the desired product in high yields was observed demonstrating that material **17** was an effective metathesis catalyst.

5.2.3.2 Catalytic Material Activity and Stability

In our opinion, the 20-fold decrease in catalyst activity is a greater deactivation than should be expected. The reason for deactivation of immobilised homogeneous catalysts is a rarely touched upon topic in the field, and there remains a lot of ambiguity. One major point is - how heterogeneous is the catalytic site? There is obviously some 'heterogenisation' effect, because there is certainly a diminished rate of interaction between catalytic site and substrate. In relation to the present system, we believe pre-catalytic material **14** is more prone to diminished activity because the catalytic system is a system with three possible phases. The catalytic material is in the solid phase. COA has a boiling point of 151⁰C, and in a sealed reactor at 200⁰C is probably still in the solution phase. TBE, however, has a boiling point of 41⁰C, and thus is most likely in the gas phase in this reaction system. In this proposal, the solubility/quantity of TBE in COA becomes very important. We propose that the rate of TBE entering the COA phase, and then exiting the COA phase to enter the catalyst phase plays a significant role in the reaction kinetics. An extra kinetic parameter has been added to the overall rate kinetics, and that is the rate of TBE entering the heterogeneous phase.

Recycling of catalytic material **14** was mediated by allowing the reactor (COA to COE dehydrogenation) to cool to room temperature and all solid materials to settle post catalysis. The reaction solution was then separated from the catalytic material by filtration. The post-catalysis material was light orange in colour, which is the colour of the active catalyst. The recycled catalytic material showed similar activity to the first catalytic reaction, in a subsequent reaction (COA to COE, TON after 168 hours: 850). It was not necessary to add fresh activating base to the recycled catalytic material. The fluids pumped out of the autoclave were colourless and showed no signs of Ir⁰. Furthermore, the post-catalysis filtrate was charged with extra TBE and placed under the standard reaction conditions. No increase in the quantity of COE was observed demonstrating

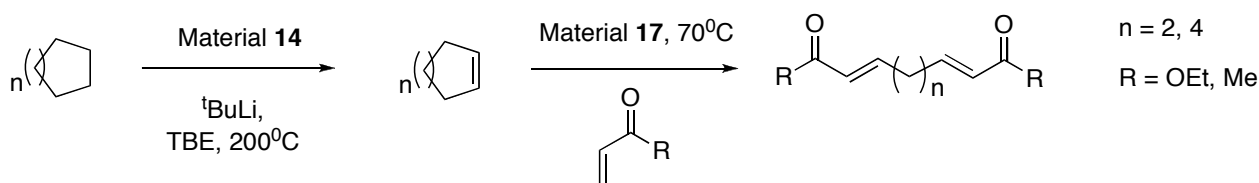
that no active catalyst was present in the reaction solution. The conclusion that the pincer organometallic immobilised on silica is a highly stable complex can be drawn from these results. It can also be concluded that the catalytic organometallic unit remains bound to the silica surface throughout the catalytic process, and is still intact post-catalysis.

5.2.4 Compartmentalised Homogeneous Catalysts: Multi-step Sequential Tandem Catalysis

5.2.4.1 Alkane/Alkene Dehydrogenation/Metathesis Sequences

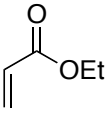
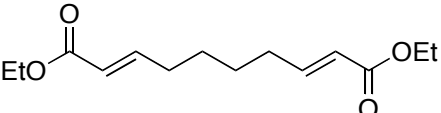
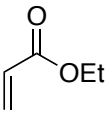
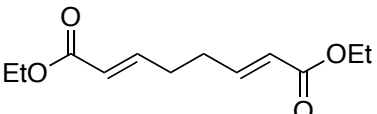
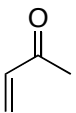
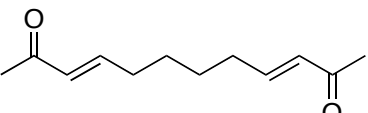
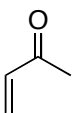
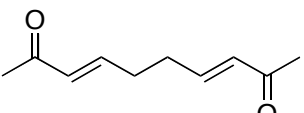
To this point we have shown that a dehydrogenation reaction converts an unreactive alkane to an alkene in the presence of a dihydrogen acceptor. We have shown that the immobilised homogeneous catalytic material **14** can be separated from the alkene containing solution by simple filtration. It must be noted that the TBE (H_2 acceptor) and formed TBA (reduced product) can be removed from the reaction mixture by simply applying vacuum. The resulting solution, when catalyst is removed, is a mixture of starting alkane and desired alkene. We have introduced material **17** to the post-catalysis mixture of COA-COE. We have then introduced ethyl-acrylate to this solution for ring-opening cross-metathesis catalysed by **17**. If applied together in a single batch reactor, complex **2/3** and Grubbs-II ruthenium alkylidene complexes are incompatible, we have found this, and it has been reported elsewhere.²⁵ Furthermore, we have found that Grubbs-II complexes are not active dehydrogenation catalysts and complex **2** is not an active metathesis catalyst. It must also be noted, that the excess COA present in the reaction mixture acts as a solvent.

Scheme 6. Sequential conversion of a cycloalkane to a linear diester/ketone.



The reaction mixture was heated to 70⁰C for 24 hours (see scheme 6). It was observed that all COE was consumed (¹H NMR, and GC analysis), and diester product was observed (yield 87%), along with a small amount of ethyl-acrylate dimerisation product. We also demonstrated this principle using methyl vinyl ketone (MVK, 3-buten-2-one) yielding a linear diketone. The same substrates were also applied with CHA/CHE solutions demonstrating that this principle can be applied for cycloalkanes to yield bis-functionalised products of various linker lengths between functional groups (table 4). The use of the reactant cycloalkane as solvent removes yet another parameter; a separate solvent to dissolve the catalysts/substrates. Post-catalysis, material **17** can be removed from the reaction mixture by simple filtration, and could be reapplied. This sequential dehydrogenation and subsequent ring-opening cross metathesis demonstrates a route to linear diesters/diketones from cycloalkanes without any purification or work-up steps, and little side-product formation.

Table 4. Synthesis of linear bis-functionalised alkenes from sequentially catalysed activation of alkanes.

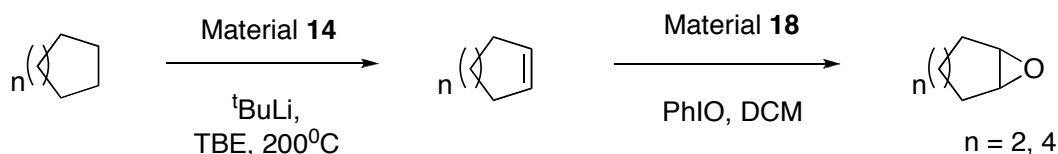
Starting alkane	Functionalised alkene	Product ^a	Yield (%) ^b
COA			87
CHA			48
COA			68
CHA			58

^aFrom sequential multi-pot catalysis; immediate transfer of dehydrogenation solution to metathesis reactor, without work-up/isolation. ^bCalculated using ¹H NMR. Based on alkene formed 'in situ'.

5.2.4.2 Alkane/Alkene Dehydrogenation/Epoxidation Sequences

The same principle was applied with manganese porphyrin containing catalytic epoxidation material **18**. Again, we found the catalysts were not compatible when applied simultaneously in the same reaction vessel, and the conditions used for their separate reactions are detrimental to their respective stabilities. The same COA/COE solution (TBE/TBA removed) was introduced to a reaction vessel containing material **18**, dichloromethane, iodosylbenzene and a catalytic amount of imidazole. The resulting mixture was allowed to stir at room temperature for 24 hours, resulting in complete conversion of all oxidant to epoxide product (cyclooctene oxide, COO). This was also demonstrated for CHA/CHE to cyclohexene oxide, however with much lower yields, due to the lower reactivity of CHE in epoxidation catalysis (scheme 7). This principal demonstrates the conversion of unreactive alkanes to high value, highly reactive epoxides, without work-up, and with relatively high atom efficiency. The observed yields are more dependant on the oxidant added, and less on the conditions used, and thus this system could be optimised further.

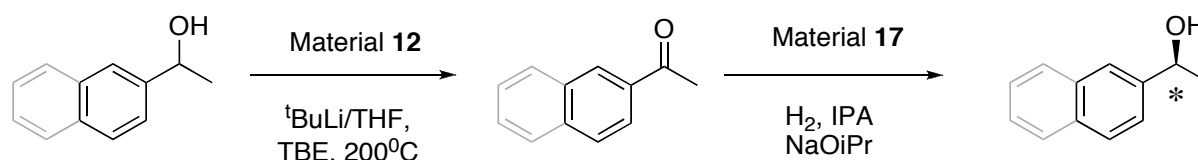
Scheme 7. Sequential work-up free conversion of an unreactive alkane to an epoxide.



5.2.4.3 Alcohol/Ketone Dehydrogenation/Asymmetric Hydrogenation Sequences

We have also found that the sequential compartmentalised catalyst concept can be applied for the chiral resolution of racemic alcohols (scheme 8). In the previous section the dehydrogenation of 1-phenyl-1-ethanol and 1-(2-naphthyl)-1-ethanol yielding acetophenone and naphthophenone was demonstrated. The reaction mixture from these reactions was filtered to remove catalytic material **14**. The filtrate (including solvent-toluene, TBE, TBA) was placed in a separate reaction vessel containing material **19** (a chiral BINAP-Ru-DPEN containing material), NaOⁱPr, and iso-propanol. Dihydrogen pressure was introduced, and the formed ketones were hydrogenated asymmetrically, yielding non-racemic alcohol product. In the case of 1-phenyl-1-ethanol a maximum *ee* of 23% with quantitative conversion of racemic alcohol to non-racemic alcohol was observed. However, with 1-(2-naphthyl)-1-ethanol *ee* levels as high as 97% were observed, again with quantitative conversion levels. This demonstrates an effective, non-natural manner to acquire enantiopure alcohols from racemic mixtures. It also demonstrates that there are minimal inhibition factors, and the catalysts applied can be used repetitively.

Scheme 8. Sequential deracemisation of aryl alcohols.



5.3 Conclusions

A functionalised iridium(III) pincer organometallic has been synthesised and coupled with a novel isocyanate functionalised silica material yielding, for the first time, immobilised homogeneous catalysts for transfer dehydrogenation of unreactive alkanes. A Grubbs-II ruthenium alkylidene complex has also been tethered to silica in a similar manner. The immobilised dehydrogenation catalyst converts both cyclic and linear alkanes to alkenes. The ability to separate the catalyst from the reaction mixture by simple filtration/decantation shows a green approach to catalyst isolation, and is aided by the impressive stability of the immobilised homogeneous catalyst. The stability allows for multiple uses of the catalytic material without loss in reaction rates. Post-dehydrogenation reaction solutions have been applied in subsequent catalysed reaction steps. Multi-step reaction sequences were presented which demonstrate the conversion of said unfunctionalised unreactive precursors to functionalised compounds in two steps, without work-up and minimal interruption of the reaction sequence. Conversion of cyclic alkanes to linear diesters/diketones opens up the field of polyester chemistry from unreactive precursors. Epoxide synthesis from unreactive alkanes is a valuable procedure, which could be further expanded upon by applying epoxide opening catalysts as a third step in the sequence. The standard techniques for the production of the same compounds, would likely produce large amounts of salt, or corrosive halogen containing compounds/waste.

Immobilised sequential catalysis is, we believe, the next step to demonstrating the application of non-natural catalysts in the same way as nature applies natural enzymes. Compartmentalisation of catalysts is essential if we wish to achieve the high selectivity and yields for certain compounds that are observed in the natural world. As has been demonstrated in this report, high catalyst activity is not a prerogative, however, because immobilisation often results in diminished activity, it would be desirable to use the most active catalysts for a certain reaction. Catalyst stability is, however, the key to the further application and development of compartmentalised homogeneous catalysts, because catalyst compartmentalisation is the essence of the concept, and catalysts that readily decoordinate or decompose are of no use. Certainly extended reaction sequences are the desired goal, ultimately allowing for complex molecular syntheses involving no intermediate work-up steps giving high end-product yields.

5.4 Experimental Section

General Information: Standard Schlenk procedures under argon were carried out throughout. Argon was used straight from the cylinder. All reagents were used as supplied from Acros or Sigma-Aldrich, unless otherwise stated. All alkanes were stirred over concentrated H₂SO₄ for 6h before being distilled under vacuum and stored under argon. Before their use in catalysis, all alkanes were subjected to a freeze-pump-thaw cycle (3X) under argon. Likewise 3,3-dimethylbut-1-ene was subjected to a freeze-pump-thaw cycle (3X). An argonated glove-box was not available, so this degassing was essential before every experiment. 1.5M ¹BuLi in THF was transferred via syringe into a Schlenk and subjected to freeze-pump-thaw cycle (3X) under argon immediately before use. All alkenes were vacuum distilled before use and stored under argon. All dehydrogenation catalysis was carried out in a 50ml Parr-4590 micro-reactor. ¹H, ¹³C and ³¹P solution NMR were recorded on a Varian Inova 300 spectrometer or a Varian Oxford AS400. CP-MAS NMR was carried out using a Bruker AV 750. Elemental analyses were performed by Dornis und Kölbe, Mikroanalytisches Laboratorium, Mülheim a. d. Ruhr, Germany. Maldi-ToF MS measurements were carried out on an Applied Biosystems Voyager DE-STR MALDI-TOF MS and IR spectra were recorded on a Perkin-Elmer SpectrumOne FT-IR Spectrometer. GC analyses were performed on a Perkin-Elmer Clarus-500 gas chromatograph. GCMS measurements were measured on a Perkin-Elmer AutosystemXL gas chromatograph with an attached Perkin-Elmer Turbomass Upgrade mass spectrometer.

5-[1,1-(Tert-butyl)dimethylsiloxy-methyl]-1,3-di-[1,1-(tert-butyl)dimethylsiloxy]-benzene, 5.

5-(Hydroxymethyl)-1,3-benzenediol (1.5g, 10.7mmol) was dissolved in dry DMF (30mL). Chloro(1,1-tert-butyl)dimethyl-silane (4.9g, 32.1mmol) and imidazole (2.4g, 35.32mmol) were added and the resulting solution was stirred at room temperature for 24h. DMF was removed *in vacuo*. Water (20mL) was added to the remaining oil and subsequently the solution was extracted with diethylether (2X, 30mL). The combined ether layers were dried over MgSO₄ and evaporated to yield a colourless, viscous oil (83% yield). ¹H NMR (300 MHz, CDCl₃) δ = 0.089 (s, 6H, CH₂OSi(CH₃)₂), 0.187 (s, 12H, OSi(CH₃)₂), 0.942 (s, 9H, CH₂OSi(CH₃)₂C(CH₃)₃), 0.977 (s, 18H, OSi(CH₃)₂C(CH₃)₃), 4.627 (s, 2H, OCH₂), 6.264 (t, 1H, CH), 6.44 (d, 2H, CH's). ¹³C-NMR (75 MHz, CDCl₃) δ = -5.02, -4.18, 18.41, 18.63, 25.90, 26.18, 64.87, 106.30, 110.92, 144.18, 156.83. M/Z (GCMS) 482 g/mol. C₂₅H₅₀O₃Si₃: calcd. C 62.18, H 10.44; found C 61.83, H 10.58.

5-[1,1-(Tert-butyl)dimethylsiloxy-methyl]-1,3-benzenediol, 6.

5-[1,1-(Tert-butyl)dimethylsiloxy-methyl]-1,3-di-[1,1-(tert-butyl)dimethylsiloxy]-benzene (2.61g, 5.42mmol) was dissolved in a water/DMF solution (11mL, 10:1). Cs₂CO₃ (1.18g, 3.61mmol, 2/3 eq.) was added and the resulting was stirred at room temperature for 5h. DMF was removed *in vacuo*. Water (10mL) was added to the remnant sludge,

followed by EtOAc (10mL). The water layer was washed with EtOAc (2X 10mL), and the organic layer was dried over MgSO₄. The product was purified using column chromatography (EtOAc/hexanes, 1:1). White powder (85% yield). ¹H NMR (400 MHz, CDCl₃) δ = 0.091 (s, 6H, OSi(CH₃)₂), 0.923 (s, 9H, OSi(CH₃)₂C(CH₃)₃), 4.60 (s, 2H, OCH₂), 6.202 (s, 1H, CH), 6.37 (s, 2H, CH's), 6.0-6.5 (br s, 2H, OH's). ¹³C-NMR (100 MHz, CDCl₃) δ = -5.07, 18.70, 26.19, 65.05, 101.76, 105.83, 144.29, 157.09. M/Z (GCMS) 253 (-H) g/mol. C₁₃H₂₂O₃Si: calcd. C 61.38, H 8.72; found C 61.46, H 8.65.

5-[1,1-(Tert-butyl)dimethylsiloxy-methyl]-1,3-di[bis(tertbutyl)phosphito]-benzene, 7.

5-[1,1-(Tert-butyl)dimethyl-siloxymethyl]-1,3-benzenediol (0.4g, 1.57mmol) was dissolved in dry degassed THF (20mL). NaH (0.075g, 3.14mmol) was added slowly to this (H₂ evolution!). The resulting mixture was heated at reflux for 2h and cooled to room temperature. Di-1,1-tert-butyl chlorophosphine ((0.66mL, 3.46mmol) was added and the resulting was heated at reflux for 24h. The solvent and excess chlorophosphine was removed in vacuo and diethylether (20mL) was added. The resulting was filtered, under inert conditions, over celite, and the solvent and any remaining chlorophosphine was removed under high vacuum with heating. Colourless oil (90% yield). ¹H NMR (400 MHz, CDCl₃) δ = 0.060 (d, 6H, OSi(CH₃)₂), 0.910 (d, 9H, OSi(CH₃)₂C(CH₃)₃), 1.145 (d, 36H, P(CH₃)₂), 4.63 (s, 2H, OCH₂), 6.73 (s, 2H, CH), 6.79 (s, 2H, CH's). ¹³C-NMR (100 MHz, CDCl₃) δ = -5.03, 18.58, 26.89, 27.67, 35.75, 65.01, 107.41, 109.28, 143.74, 166.80. ³¹P-NMR (162 MHz, CDCl₃) 154.39. M/Z (GCMS) 542 g/mol. C₂₉H₅₆O₃P₂Si: calcd. C 64.17, H 10.40; found C 63.96, H 10.32.

5-[1,1-(Tert-butyl)dimethylsiloxy-methyl]-1,3-di[bis(tertbutyl)phosphito]-2-phenyl-chloro-hydrido-iridium(III), 8.

5-[1,1-(Tert-butyl)dimethylsiloxy-methyl]-1,3-di[bis(tertbutyl)phosphito]-benzene (0.4g, 0.74mmol) was dissolved in dry degassed toluene (3mL). [Ir(COD)Cl]₂ (0.27g, 0.67mmol, essential that this is freshly made. Should be bright orange in colour) was added and the vessel was sealed, and heated to 150°C for 16h. Colour change from bright orange to deep red/purple. The mixture was then cooled and the solvent removed in vacuo yielding a brown sludge. This was dissolved in CH₂Cl₂ and washed over celite. Solvent was removed from the resulting red solution, and the remnant red oil was recrystallised from acetone/water (2X) yielding a red solid which was dissolved in CH₂Cl₂ and dried over MgSO₄. Red powder (82% yield). ¹H NMR (400 MHz, CDCl₃) δ = -41.52 (t, 1H, IrH), 0.067 (s, 6H, OSi(CH₃)₂), 0.944 (d, 9H, OSi(CH₃)₂C(CH₃)₃), 1.357 (t, 36H, P(CH₃)₂), 4.646 (s, 2H, OCH₂), 6.535 (s, 2H, CH). ¹³C-NMR (100 MHz, CDCl₃) δ = -4.97, 18.79, 25.87, 27.78, 27.93, 39.69, 43.28, 65.52, 103.29, 116.60, 139.80, 167.70. ³¹P-NMR (162 MHz, CDCl₃) 176.5. M/Z (MALDI-ToF) 764.23 g/mol (-Cl, + K). C₂₉H₅₆ClIrO₃P₂Si: calcd. C 45.21, H 7.33; found C 45.33, H 7.26.

5-(Hydroxymethyl)-1,3-di[bis(tertbutyl)phosphito]-2-phenyl-chloro-hydrido-iridium(III), 9.

5-[1,1-(Tert-butyl)dimethylsiloxy-methyl]-1,3-di[bis(tertbutyl)phosphito]-2-phenyl-iridium(III)hydrido-chloride (0.448g, 0.58mmol) was dissolved in MeOH/CH₂Cl₂ mixture (12mL, 5:1, dry and degassed). Ion exchange resin (0.5g, DOWEX 50WX8, acidic, thoroughly washed with MeOH and CH₂Cl₂ before use) was added and the resulting mixture was stirred at room temperature for 24h. The solvent was then removed under vacuo and pentane (20mL) was added and the red mixture was placed in a sonication bath. The mixture was then centrifuged. This was repeated twice. Red powder (100% yield). ¹H NMR (400 MHz, CDCl₃) δ = -41.42 (t, 1H, IrH), 1.357 (t, 36H, P(CH₃)₂), 4.585 (s, 2H, OCH₂), 6.596 (s, 2H, CH). ¹³C-NMR (100 MHz, CDCl₃) δ 26.90, 39.74, 43.32, 65.85, 104.10, 116.28, 139.24, 167.61. ³¹P-NMR (162 MHz, CDCl₃) 177.0. M/Z (MALDI-ToF) 621.01 g/mol (-Cl). C₂₃H₄₂ClIrO₃P₂: calcd. C 42.10, H 36.45; found C 42.92, H 6.63.

TMS-capped-3-isocyanatopropyl-1-silica, 13.

TMS-capped-3-aminopropyl-1-silica (5g) was placed in a schlenk with toluene (30mL, dry degassed). Triphosgene (2.03g, 6.8mmol) was added and the resulting mixture was heated at reflux for 24h. The mixture was filtered hot and

then washed with toluene (2X), acetone (2X), CH₂Cl₂ (2X), and pentane (2X), and subsequently dried under vacuum. White powder. IR (DRIFT, difference); ν_{CNO} 2276 cm⁻¹, $\nu_{\text{SiO-H}}$ 3740 cm⁻¹ (trough). Elemental analysis found; C 7.47, H 2.20, N, 1.97.

5-[Silica-1-propyl-3-carbamatomethyl]-1,3-di[bis(tertbutyl)phosphito]-2-phenyl-chloro-hydrido-iridium(III), 14.

5-(Hydroxymethyl)-1,3-di[bis(tertbutyl)phosphito]-2-phenyl-iridium(III)hydrido-chloride (0.1g, 0.15mmol) was dissolved in benzene (10mL). Isocyanate functionalised silica (1g) was added and the resulting was heated at reflux for 40h. The mixture was filtered hot and the resulting red powder was washed with acetone (3X) and CH₂Cl₂ (3X) and dried under vacuum. Red/pink powder. IR (DRIFT, difference); $\nu_{\text{SiO-H}}$ 3740 cm⁻¹ (trough), ν_{CNO} 2276 cm⁻¹ (trough), $\nu_{\text{carbamate}}$ 1661 & 1551 cm⁻¹, ν_{complex} 1441, 1399 cm⁻¹. ³¹P-NMR (303.6 Mhz) 176ppm. Found C 9.08, H 2.38, N 1.84, P 0.24, Ir 0.73.

4-[Silica-1-propyl-3-carbamatomethyl]-[1,3-bis(1-mesityl)-4,5-dihydroimidazo-2-ylidene][benzylidene]-tricyclohexylphosphine-ruthenium(IV) dichloride, 17.

N,N'-dimesityl-2,3-diamino-1-propanol (0.4g, 1.23mmol) was dissolved in dry degassed benzene (20mL) with TMS-capped-3-isocyanatopropyl-1-silica (4g) and stirred at reflux for 24h. The resulting mixture was filtered hot and washed with hot CH₂Cl₂ (20mL, 3X) and boiling EtOH (20mL, 3X) and dried in vacuo. This was subsequently used as is described by Blechert for the analogous polystyrene supported material.³⁶ IR (DRIFT, difference); $\nu_{\text{SiO-H}}$ 3741 cm⁻¹ (trough), ν_{CNO} 2276 cm⁻¹ (trough), $\nu_{\text{carbamate}}$ 1670 & 1560 cm⁻¹, ν_{complex} 1448, 1388, 1260 cm⁻¹. ³¹P-NMR (303.6 Mhz). Elemental analysis found: (immobilised ligand) C 6.73, N 1.61; (immobilised complex) C 7.76, N 1.57, P 0.34, Ru 1.09, Cl 0.47.

Catalysis:

Homogeneous cycloalkane dehydrogenation

Standard experiment: Complex **2** (0.006g, 9.6 x 10⁻⁶ mol) was placed in a flame dry schlenk and evacuated. Cycloalkane (0.03mol) and 3,3-dimethylbut-1-ene (0.03mol, 2.69g, 4.12mL) were added to the schlenk containing the pre-catalyst. ^tBuLi* (10 μ l, 1.5M in THF, 1.5 x 10⁻⁵) was added and the red solution was immediately subjected to two freeze-pump-thaw argon cycles. The solution was allowed to stir for 2h at room temperature and subsequently transferred to a 50ml autoclave (Parr-4590 micro-reactor) and then the reactor was heated to 200^oC for 18h. The reactor was cooled to room temperature and the reaction solution was extracted by applying an overpressure of argon. *KO^tBu can also be used (0.005g, 4.42 x 10⁻⁵ mol). Products analysed with ¹H NMR by comparison of TBE peaks with COE peaks. Based on assumption that TBE is only converted to COE or COD.

Heterogeneous cycloalkane dehydrogenation

Standard experiment: Material **9** (0.1g, 3.8 x 10⁻⁶mol) was placed in a 50ml autoclave (Parr-4590 micro-reactor). The autoclave was evacuated and purged with argon (6X). In a separate flask cycloalkane (0.010mol), 3,3-dimethylbutene (0.010mol, 0.84g, 1.29mL) and ^tBuLi (10 μ l, 1.5M in THF, 1.5 x 10⁻⁵) were combined and subjected to two freeze-pump-thaw argon cycles. This solution was transferred to the autoclave containing the catalyst and the reactor was purged with argon (2X). The mixture was allowed to stir at room temperature for 5h, and then the reactor was heated to 200^oC for 96h. The reactor was cooled to room temperature and the reaction solution was extracted by applying an overpressure of argon. Products analysed with ¹H NMR by comparison of TBE peaks with COE peaks. Based on assumption that TBE is only converted to COE or COD.

Homogeneous aryl-ethanol dehydrogenation

Standard experiment: Complex **2** (0.006g, 9.6×10^{-6} mol) was placed in a flame dry schlenk and evacuated. Toluene (20mL), aryl-1-ethan-1-ol (0.002mol), 3,3-dimethylbut-1-ene (0.01mol, 0.84g, 1.29mL) were added to the schlenk containing the pre-catalyst. $t\text{BuLi}^*$ (10 μl , 1.5M in THF, 1.5×10^{-5}) was added and the red solution was immediately subjected to two freeze-pump-thaw argon cycles. The solution was allowed to stir for 2h at room temperature and subsequently transferred to a 50ml autoclave (Parr-4590 micro-reactor) and then the reactor was heated to 200 $^{\circ}\text{C}$ for 18h. The reactor was cooled to room temperature and the reaction solution was extracted by applying an overpressure of argon. Complete conversion to the desired ketone was observed in both cases. Products analysed with ^1H NMR, yield is isolated yield.

Heterogeneous aryl-ethanol dehydrogenation

Standard experiment: Material **9** (0.1g, 3.8×10^{-6} mol) was placed in a 50ml autoclave (Parr-4590 micro-reactor). The autoclave was evacuated and purged with argon (6X). In a separate flask toluene (20mL), aryl-1-ethan-1-ol (0.002mol), 3,3-dimethylbut-1-ene (0.01mol, 0.84g, 1.29mL) and $t\text{BuLi}$ (10 μl , 1.5M in THF, 1.5×10^{-5}) were combined and subjected to two freeze-pump-thaw argon cycles. The mixture was allowed to stir at room temperature for 5h, and then the reactor was heated to 200 $^{\circ}\text{C}$ for 40h. The reactor was cooled to room temperature and the reaction solution was extracted by applying an overpressure of argon. Complete conversion to the desired ketone was observed in both cases, yield is isolated yield.

Heterogeneous alkane dehydrogenation

Standard experiment: Material **9** (0.1g, 3.8×10^{-6} mol) was placed in a 50ml autoclave (Parr-4590 micro-reactor). The autoclave was evacuated and purged with argon (6X). In a separate flask alkane (10mL), 3,3-dimethylbutene (0.005mol, 0.42g, 0.64mL) and $t\text{BuLi}$ (10 μl , 1.5M in THF, 1.5×10^{-5}) were combined and subjected to two freeze-pump-thaw argon cycles. This solution was transferred to the autoclave containing the catalyst and the reactor was purged with argon (2X). The mixture was allowed to stir at room temperature for 5h, and then the reactor was heated to 200 $^{\circ}\text{C}$ for 96h. The reactor was cooled to room temperature and the reaction solution was extracted by applying an overpressure of argon. Products analysed with ^1H NMR and GC, known concentration of mesitylene added as standard post-catalysis. GC: Alltech, EC-5, 30m x 0.32mm x 0.25 μm . 35 $^{\circ}$ for 5 mins. ramp 5 $^{\circ}$ per min. to 250 $^{\circ}$.

Ring closing metathesis

Material **15** (50mg, mol) was stirred under an inert atmosphere in dichloromethane with allyl sulfide (,) or diethyldiallylmalonate (,) and heated at 45 $^{\circ}\text{C}$ for 24h. Products analysed with ^1H NMR and GCMS. GC: Alltech AT-50HT. 30m x 0.25mm x 0.15 μm .

Ring opening cross metathesis

To cycloalkene (0.13g, 0.0012mol) in cycloalkane (10mL) was added material **15** (50mg). To this was added ethylacrylate or methyl vinyl ketone (0.0024mol) and the resulting was heated at 70 $^{\circ}\text{C}$ for 24h. Products analysed with ^1H NMR and GCMS. ^1H NMR analysis gave yield by comparing COA peak with product alkene peak, and comparing the COA:COE ratio of the starting solution and the final solution. GC: Alltech AT-50HT. 30m x 0.25mm x 0.15 μm . 50 $^{\circ}$ start temp. ramp 20 $^{\circ}$ per min. to 280 $^{\circ}$ hold for 40 min.

Cross Metathesis

To n-alkene (0.13g, 0.0012mol) in n-alkane (10mL) was added material **15** (50mg). The resulting was heated at 50 $^{\circ}\text{C}$ for 24h. Products analysed with GC, known concentration of mesitylene added as standard post-catalysis. GC: Alltech, EC-5, 30m x 0.32mm x 0.25 μm . 35 $^{\circ}$ for 5 mins. ramp 5 $^{\circ}$ per min. to 250 $^{\circ}$.

Asymmetric Hydrogenation

A toluene solution (10mL) containing BINAP-RuCl₂-DPEN immobilised on silica, isopropanol, and NaOⁱPr, and naphthophenone was put under H₂ and stirred at 30⁰C for 24h. Products were analysed using ¹H NMR showing no ketone present. Enantiomeric selectivity was determined using HPLC. Chiralcel OD column. Isopropanol was the mobile phase in n-hexane. (5:95) Separation observed at: 18 and 20 mins. respectively for 1-(2-Naphthyl)-1-ethanol; 17 and 23 min. for 1-phenyl-1-ethanol.

Epoxidation

All experiments were performed at room temperature with magnetic stirring. Catalyst (1 μmol), imidazole (0.02 mmol) and *t*-butylperoxide (0.02 mmol) were stirred in 2 mL dichloromethane. Product formation was checked by taking small aliquots for GC analysis with phenylbromide as internal standard. GC: Alltech, EC-5, 30m x 0.32mm x 0.25μm. 100⁰ for 5 min. ramp 10⁰ per min. to 200⁰ ramp 45⁰ per min to 250⁰.

5.5 References

- ¹ (a) H.-U. Blaser. *Chem. Commun.* **2003**, 293-296. (b) D. E. De Vos, I. F. J. Vankelecom, P. A. Jacobs [Eds. Weinheim]; Chiral Catalyst Immobilization and Recycling, **2000**. Wiley-VCH. (c) D. J. Cole-Hamilton, *Science* **2003**, *299*, 1702-1706.
- ² D. E. Fogg, E. N. dos Santos, *Coord. Chem. Rev.* **2004**, *248*, 2365-2379.
- ³ A. R. McDonald, G. van Koten, Chapter 1 of this thesis.
- ⁴ A. Bruggink, R. Schoevaart, T. Kieboom, *Org. Proc. R. & D.* **2003**, *7*, 622-640.
- ⁵ J.-C. Wasilke, S. J. Obrey, R. T. Baker, G. C. Bazan, *Chem Rev.* **2005**, *105*, 1001-1020.
- ⁶ (a) C. Simons, U. Hanefeld, I. W. C. E. Arends, A. J. Minnaard, T. Maschmeyer, R. A. Sheldon, *Chem. Commun.* **2004**, 2830-2831. (b) C. Simons, U. Hanefeld, I. W. C. E. Arends, T. Mashmeyer, R. A. Sheldon, *Topics in Catal.* **2006**, *40*, 35-44.
- ⁷ S. J. Connon, S. Blechert, *Angew. Chem. Int. Ed.* **2003**, *42*, 1900-1923.
- ⁸ S. Randl, S. J. Connon, S. Blechert, *Chem. Commun.* **2001**, 1796-1797.
- ⁹ (a) S. C. Schurer, S. Gessler, N. Buschmann, S. Blechert, *Angew. Chem. Int. Ed.* **2000**, *39*, 3898-3901. (b) M. Mayr, M. R. Buchmeiser, K. Wurst, *Adv. Synth. Catal.* **2002**, *344*, 712-719.
- ¹⁰ (a) M. Gupta, C. Hagen, R. J. Flesher, W. C. Kaska, C. M. Jensen, *Chem. Commun.* **1996**, 2083-2084. (b) M. Gupta, C. Hagen, W. C. Kaska, R. E. Cramer, C. M. Jensen, *J. Am. Chem. Soc.* **1997**, *119*, 840-841. (c) M. Gupta, W. C. Kaska, C. M. Jensen, *Chem. Commun.* **1997**, 461-462. (d) C. M. Jensen, *Chem. Commun.* **1999**, 2443-2449.
- ¹¹ F. Liu, E. B. Pak, B. Singh, C. M. Jensen, A. S. Goldman, *J. Am. Chem. Soc.* **1999**, *121*, 4086-4087.
- ¹² (a) D. Morales-Morales, R. Redon, Z. Wang, D. W. Lee, C. Yung, K. Magnuson, C. M. Jensen, *Can. J. Chem.* **2001**, *79*, 823-829. (b) X-Q. Gin, W. Chen, D. Morales-Morales, C. M. Jensen, *J. Mol. Catal. A: Chem.* **2002**, *189*, 119-124.
- ¹³ (a) W-W. Xu, G. P. Rosini, M. Gupta, C. M. Jensen, W. C. Kaska, K. Krogh-Jespersen, *Chem. Commun.* **1997**, 2273-2274. (b) F. Liu, A. S. Goldman, *Chem. Commun.* **1999**, 655-656.
- ¹⁴ Other homogeneous catalysts applied in these reactions have shown low stability, and in general lower activity than the pincer-iridium complexes.
- ¹⁵ M. Albrecht, G. van Koten, *Angew. Chem. Int. Ed.* **2001**, *40*, 3750-3781.
- ¹⁶ J. W. J. Knapen, A. W. van der Made, J. C. de Wilde, P. W. N. M. van Leeuwen, P. Wijkens, D. M. Grove, G. van Koten, *Nature* **1994**, *372*, 659

- ¹⁷ a) D. E. Bergbreiter, P. L. Osborn, A. Wilson, E. M. Sink, *J. Am. Chem. Soc.* **2000**, *122*, 9058-9064. b) D. E. Bergbreiter, P. L. Osborn, J. D. Frels, *J. Am. Chem. Soc.* **2001**, *123*, 11105-11106.
- ¹⁸ N. C. Mehendale, C. Bezemer, C. A. van Walree, R. J. M. Klein Gebbink, G. van Koten, *J. Mol. Catal. A: Chemical* **2006**, *257*, 167-175.
- ¹⁹ F. Gorla, A. Togni, L. M. Venanzi, A. Albinati, F. Lianza *Organometallics* **1994**, *13*, 1607-1616.
- ²⁰ H. P. Dijkstra, M. D. Meijer, J. Patel, R. Kreiter, G. P. M. van Klink, M. Lutz, A. J. Canty, G. van Koten, *Organometallics* **2001**, *20*, 3159-3168.
- ²¹ L. A. van de Kuil, H. Luitjes, D. M. Grove, J. W. Zwikker, J. G. M. van der Linden, A. M. Roelofson, L. W. Jenneskens, W. Drenth, G. van Koten, *Organometallics* **1994**, *13*, 468-477.
- ²² Gagliardo, Marcella; Chase, Preston A.; Brouwer, Sander; Van Klink, Gerard P. M.; Van Koten, Gerard. *Organometallics* **2007**, *26*, 2219-2227.
- ²³ a) O. A. Wallner, K. J. Szabo, *Org. Lett.* **2004**, *6*, 1829-1831. b) J. Kjellgren, H. Sunden, K. J. Szabo, *J. Am. Chem. Soc.* **2004**, *126*, 474-475.
- ²⁴ a) N. Solin, J. Kjellgren, K. J. Szabo *Angew. Chem. Int. Ed.* **2003**, *42*, 3656-3658. b) N. Solin, J. Kjellgren, K. Szabo, *J. Am. Chem. Soc.* **2004**, *126*, 7026-7033. c) S. Sebelius, V. J. Olsson, K. J. Szabo, *J. Am. Chem. Soc.* **2005**, *127*, 10478-10479. d) V. J. Olsson, S. Sebelius, N. Selander, K. J. Szabo, *J. Am. Chem. Soc.* **2006**, *128*, 4588-4589.
- ²⁵ A. S. Goldman, A. H. Roy, Z. Huang, R. Ahuja, W. Schinski, M. Brookhart, *Science* **2006**, *314*, 257-261.
- ²⁶ We recently witnessed a lecture by M. Brookhart in which he demonstrated the immobilisation of complexes analogous to **2** using hydrogen bonding interactions. M. Brookhart. *Retirement symposium G. van Koten*, September **2007**.
- ²⁷ M. Q. Slagt, G. Rodriguez, M. M. P. Grutters, R. J. M. Klein Gebbink, W. Klopper, L. W. Jenneskens, M. Lutz, A. L. Spek, G. van Koten, *Chem. Eur. J.* **2004**, *10*, 1331-1344.
- ²⁸ Z-Y. Jiang, Y-G. Wang, *Tet. Lett.* **2003**, *44*, 3850-3861.
- ²⁹ R. Walter, S. Kirchner, R. Franz, *U.S. Patent* **2002**, 6,399,804.
- ³⁰ I. Gottker-Schentmann, P. White, M. Brookhart, *J. Am. Chem. Soc.* **2004**, *126*, 1804-1811
- ³¹ K. B. Renkema, Y. V. Kissin, A. S. Goldman, *J. Am. Chem. Soc.* **2003**, *125*, 7770-7771.
- ³² (a) D. W. Lee, W. C. Kaska, C. M. Jensen, *Organometallics*, **1998**, *17*, 1-3. (b) R. Ghosh, M. Kanzelberger, T. J. Emge, G. S. Hall, A. S. Goodman, *Organometallics* **2006**, *25*, 55668-5671.
- ³³ (a) I. Gottker-Schnetmann, P. White, M. Brookhart, *J. Am. Chem. Soc.* **2004**, *126*, 1804-1811. (b) J. C. Grimm, C. Nachtigal, H.-G. Mack, W. C. Kaska, H. A. Mayer, *Inorg. Chem. Commun.* **2000**, *3*, 511-514.
- ³⁴ Provided by BASF Nederland B.V. Catalysts Division, Process Technologies, Strijkviertel 67, Postbus 19, 3454 ZG DE MEERN. Surface area 220m²/g.
- ³⁵ A. R. McDonald, H. P. Dijkstra, B. M. J. M. Suijkerbuijk, M. Lutz, G. P. van Klink, A. L. Spek, G. van Koten, Chapter 2 of this thesis.
- ³⁶ S. C. Schurer, S. Gessler, N. Buschmann, S. Blechert, *Angew. Chem. Int. Ed.* **2000**, *39*, 3898-3901.
- ³⁷ M. Mayr, M. R. Buchmeiser, K. Wurst, *Adv. Synth. Catal.* **2002**, *344*, 712-719.
- ³⁸ US Patent no. 4705895.
- ³⁹ A. R. McDonald, C. Muller, D. Vogt, G. P. M. van Klink, G. van Koten, Chapter 5 of this thesis.
- ⁴⁰ A. R. McDonald, N. Franssen, G. P. M. van Klink, G. van Koten, Chapter 4 of this thesis.
- ⁴¹ ATR-IR (attenuated total reflection) is a technique whereby transmission of an IR beam through a sample is measured
- ⁴² Diffuse Reflectance Infrared Fourier Transform, a surface technique. Analysis of beam from surface and near surface of a material, thus ideal for species tethered to the surface of an inorganic material.

⁴³ A-C. Carrin, A. V. Ivanov, W. Forsling, O. N. Antzutkin, A. E. Abraham, A. C. de Dios, *J. Am. Chem. Soc.* **2005**, *127*, 2218-2230.

CHAPTER 6

Covalent Immobilisation of a Palladium Picolinate Complex for Hydroxycarbonylation: Silica Supported Synthesis and Catalysis

Picolinic acid (2-pyridine-carboxylic acid) has been immobilised covalently on an inorganic support and has been utilised as a ligand bound to a palladium(II) centre. The palladium picolinate has been reported as one of the best catalysts for the hydroxycarbonylation of 1-(4-isobutylphenyl)ethanol (IBPE). The resulting product, 2-(4-isobutylphenyl)propionic acid (Ibuprofen, IBN) is a widely used anti-inflammatory and for this reason is of particular interest to the pharmaceutical industry. The synthetic route towards immobilised picolinic acid involved the construction of a close analogue of said ligand on a silica support. 3-(4-pyridine)-propan-1-ol was coupled with 3-(triethoxysilyl)propyl-1-isocyanate. The resulting compound was reacted with SiO₂ yielding immobilised pyridine. This was activated and a cyano group was introduced at the 2-position on the pyridine ring. The following step involved the use of an enzyme, nitrilase *rhodococcus rhodochrous*, to hydrolyse the 2-pyridine-carbonitrile moiety bound to the silica surface yielding immobilised 2-pyridine-carboxylate. Palladium was introduced to the immobilised picolinic acid and the immobilised catalyst was tested in the hydroxycarbonylation of IBPE. The catalytic material showed decreased activity with respect to its homogeneous counterpart [Pd(PPh₃)(OTs)(pic)]. A drop in regioselectivity for the desired product Ibuprofen (~95% cf. 99%) was observed. Recycling of the catalyst by simple filtration and then recharging the autoclave with substrates was carried out. However the second use of the catalytic material showed greatly diminished activity. Further study of the material revealed that under the applied catalytic conditions the palladium does not stay bound to the picolinate ligand, and in fact leaches into solution being active but as a homogeneous catalyst different than the previously proposed species [Pd(PPh₃)(OTs)(pic)].

6.1 Introduction

The industrial-scale synthesis of widely-used pharmaceuticals using cheap and/or *reusable* homogeneous catalysts is a subject of great importance to researchers working in homogeneous catalysis.¹ The problems that lie in applied homogeneous catalysis, are as a result of high catalyst cost and low recovery.² The robustness and manageability of heterogeneous catalysts as well as lower costs means they are used in all cases, unless selectivity towards a particular end product is of importance. In those cases, homogeneous catalysts with their high predictability and far greater enantio-, regio-, and chemoselectivity must be used. Simple decantation or filtration techniques are used to separate heterogeneous catalysts from reaction mixtures. Thus, heterogenisation of a homogeneous catalyst is a reasonable proposition in order to combine the advantages of both fields.³ Homogeneous catalyst immobilisation is only interesting when a catalyst can be applied in more than one reaction. It is also essential that a homogeneous catalyst is robust and stable, such that it can be applied on numerous occasions. Present trends in catalysis are directed towards tandem, cascade, or domino processes, where multiple steps are carried out without work-up or solvent exchange. Applying immobilised homogeneous catalysts in multi-step reaction series is our ultimate goal. This relies on high catalyst stability and solvent compatibility.

Inorganic⁴ and organic polymers⁵ are now widely used, as supports for homogeneous catalysts for solid/liquid biphasic catalysis. Similarly liquid/liquid biphasic systems are also widely investigated.⁶ Covalent linkage of a catalyst to an inorganic support gives the best results in terms of recycling of catalyst because the binding of catalyst to support is at its strongest.⁷

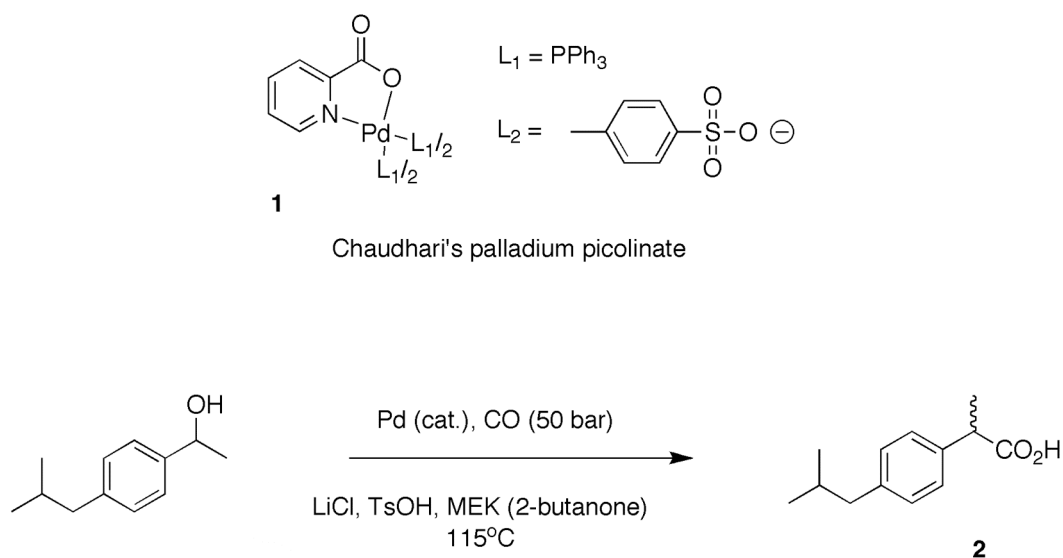


Figure 1. Pd-catalysed hydroxycarbonylation of IBPE.⁹

Hydroformylation is the most widely used transition metal catalysed homogeneous process for the production of aldehydes and alcohols.⁸ Hydroxy- and alkoxy-carbonylations⁹ are widely used for the production of propionic acids/esters and in particular 2-phenylpropionic acids/esters which are an important class of non-steroidal anti-inflammatory drug.¹⁰ A major obstacle when performing hydroxycarbonylation reactions is regioselectivity because the branched product is the

physiologically active isomer. Conversely most carbonylation catalysis is carried out with the sole goal of attaining linear products. Chaudhari and co-workers have produced the only homogeneous catalyst (**1**) which shows regioselectivity results which are worthwhile from an industrial point of view (figure 1).¹¹ With complete conversion, >99% branched product is achieved with a palladium picolinate catalyst in the hydroxycarbonylation of 1-(4-isobutylphenyl)ethanol (IBPE) to yield 2-(4-isobutylphenyl)propionic acid (Ibuprofen, IBN **2**).

Immobilisation of this catalyst was claimed by the same research group.¹² Using propylamine functionalised mesostructured silica's (MCM-41, MCM-48) the homogeneous palladium complex was immobilised. This is proposed as a five coordinate palladium complex, where the amine of the support is coordinating to the palladium as the cap of a square-pyramidal, penta-coordinate, palladium(II) complex (figure 2).

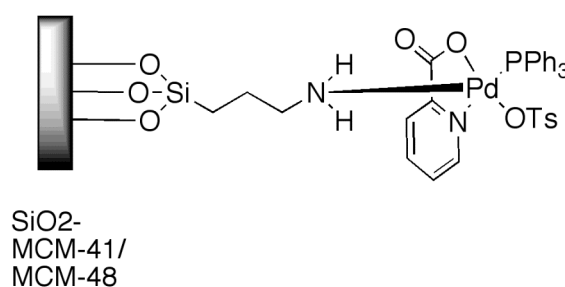


Figure 2. Propylamine functionalised SiO₂ for catalyst immobilisation.¹²

In this report we detail the synthesis and characterisation of covalently immobilised palladium picolinate complexes on silica. We also detail investigative studies on the characteristic properties of the complex on the support. The immobilised catalysts have been tested in the hydroxycarbonylation of IBPE and these results are presented. Furthermore, recycling tests on the immobilised catalyst were carried out. We observed that the immobilised palladium picolinate complex could not be recycled because of almost complete palladium leaching in the first catalytic cycle. Furthermore, it was observed that under catalytic conditions, without the application of CO gas, palladium is cleaved from the surface of the silica.

6.2 Results and Discussion

We set ourselves the task of covalently immobilising Chaudhari's palladium picolinate catalyst (**1**) on an inorganic support. The anchoring point was decided to be via the picolinate ligand, because this is believed to remain bound to the palladium centre throughout the catalytic cycle.¹³ Furthermore, we decided to immobilise the ligand before introduction of the metal, because the acidity of pure silica could have an adverse effect on the palladium picolinate. This was confirmed when stirring **1** in a refluxing toluene solution in the presence of silica (standard conditions for grafting of functionalised species onto silica supports). There was clear formation of palladium black, and also a decolouration in the solution, from bright yellow (species **1**) to brown. By introducing the palladium centre to the supported picolinic acid we hypothesised that we could

initially cap all silanol groups on the surface, so as to decrease the likelihood of them interacting with the palladium upon metallation.

6.2.1 Synthesis of Materials Containing Tethered Palladium Picolinate

Our initial work focussed on using nucleophile-functionalised picolinic acid derivatives seen in figure 3. 3-(hydroxy)-2-pyridine-carboxylate (**3**) is commercially available, and 4-amino-2-pyridine-carboxylate (**4**) was synthesised using a technique developed by Graf.¹⁴ These species are particularly poorly soluble in almost all organic solvents and thus coupling reactions with these systems were in general unsuccessful. Even with acid protecting groups which should enhance solubility, these nucleophilic species showed low solubility and required harsh basic conditions (which often led to deprotection) to achieve any conversion levels. This led us to develop a more soluble, more reactive system to aid us in immobilising picolinic acid. Similar work to that developed by Leclerc et. al. gave the facile synthesis of TBDMS-protected 4-(-hydroxymethyl)-2-pyridine-carbonitrile. 4-(hydroxymethyl)-2-pyridine-carboxylate (**5**) was obtained in 40% overall yield by acidic hydrolysis of the aforementioned carbonitrile.¹⁵

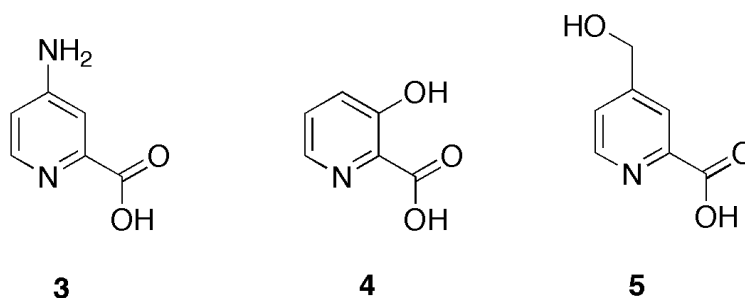


Figure 3. Picolinic acid derivatives.

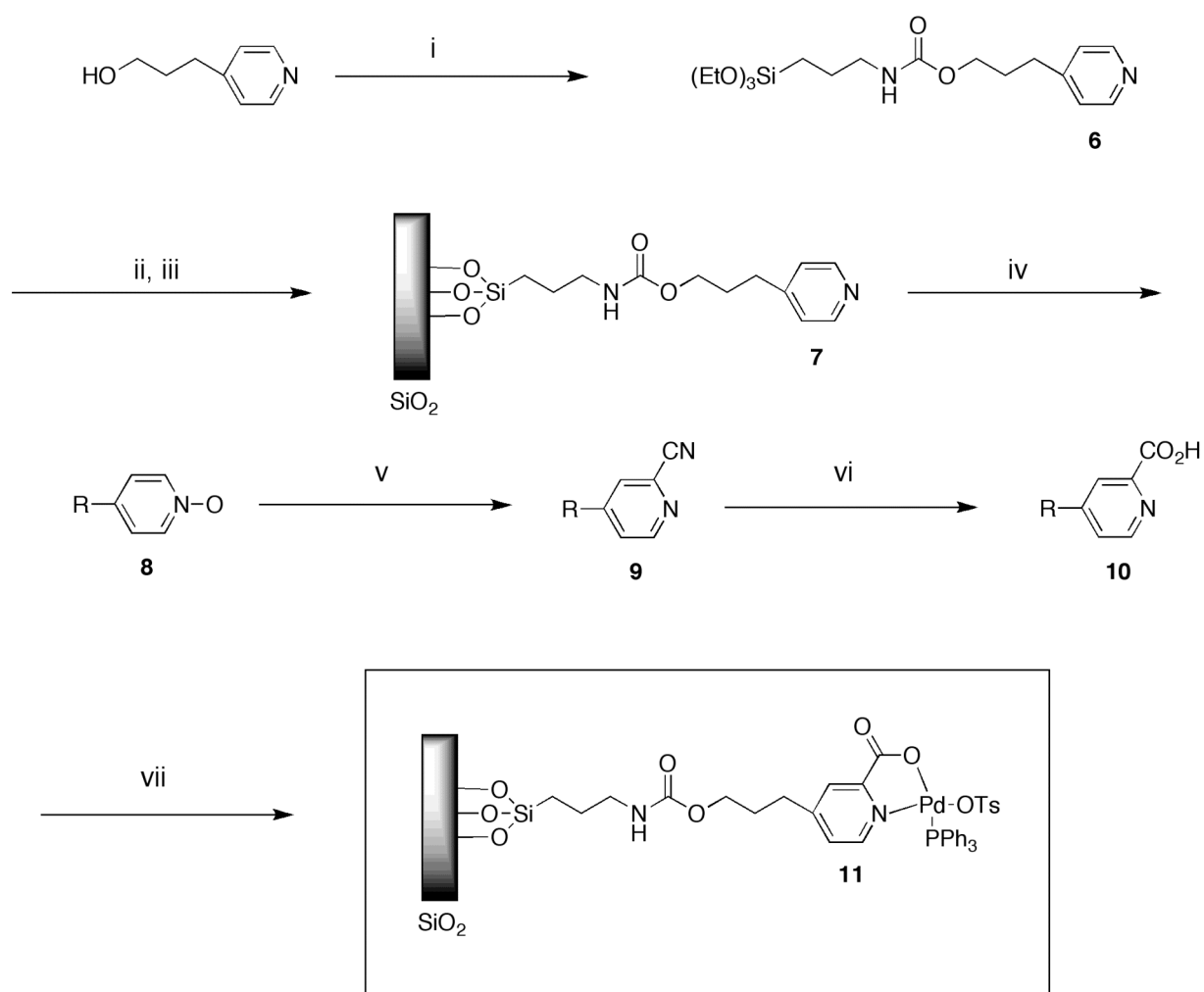
Compound **5** was indeed more soluble in organic solvents. Protection of the carboxylate functionality of **5** was subsequently carried out because the alcoholic functionality is used as a nucleophile to couple with 3-(triethoxysilyl)propyl-1-isocyanate. Obviously the carboxylic acids would react with the isocyanate as well. The morphology of silica is sensitive to aqueous acidic or basic conditions, thus the use of linear alkyl esters as protecting groups was not feasible here, because deprotection would be carried out on the supported, protected ester. We chose to use the trityl- and tert-butyldimethylsilyl- groups as protecting groups. Both of these groups are relatively labile, with tosylic acid (4-toluenesulfonic acid) cleaving them readily. However, in test reactions it became apparent that the silica, which we use as a support, cleaved the protecting groups from the picolinate esters.

As it was not possible to immobilise the protected, functionalised ligand using this work, we decided to construct the catalyst directly on the inorganic support.

The reaction of 3-(4-pyridyl)propan-1-ol with 3-(triethoxysilyl)propyl-1-isocyanate at room temperature in benzene yielded compound **6** in almost quantitative yield (scheme 1). Compound **6** was stirred in toluene at reflux with a high density silica (supplied by BASF Nederland¹⁶) for 24 hours and subsequent capping of the remaining, unreacted silanol groups was carried out by reacting the silica with hexamethyldisilazane yielding functionalised silica **7**. Activation of the

immobilised pyridine was carried out using *meta*-chloroperoxybenzoic acid yielding N-oxide **8**. Reaction of **8** with trimethylsilylcyanide in triethylamine at 90 °C yielded compound **9** which was converted to immobilised picolinic acid **10** using a nitrilase; *rhodococcus rhodochrous*. Nitrilase was used because standard techniques to hydrolyse a pyridine carbonitrile often require aqueous acidic or basic conditions. These types of conditions can be detrimental to the morphology of silica, as previously mentioned. Introduction of palladium was carried out using the same procedure as reported for the homogeneous system, however an excess of palladium to picolinic acid was used (see scheme 1). Characterisation of the silica immobilised picolinate **11** and precursors was done using elemental analysis, infra-red spectroscopy, ¹H and ¹³C solution NMR, and solid state ¹³C, ²⁹Si and ³¹P CP-MAS NMR.

Scheme 1. Synthesis of material **11**, an immobilised form of **1**.



i) 3-(triethoxysilyl)propyl-1-isocyanate, benzene, RT, 16h; ii) SiO_2 , toluene, reflux, 24h; iii) Hexamethyldisilazane, hexanes, reflux, 24h; iv) *m*-CPBA, DCM, RT, 16h; v) trimethylsilylcyanide (v. toxic!), NEt_3 , 70 °C, 18h; vi) *Rhodococcus rhodochrous*, $\text{H}_2\text{O}/\text{MeOH}$ (9:1), 4 days; vii) $\text{Pd}(\text{OAc})_2$, PPh_3 , TsOH, CHCl_3 , RT, 8h.

6.2.2 Elemental Analysis

Micro-analysis for carbon, nitrogen, phosphorous and palladium content was used as a tool to analyse all intermediates and the final product in the synthesis of a silica bound palladium

picolinate complex. Nitrogen content is of particular interest when converting **8** to **10** over two steps. The cyanation of **8** led to a noted increase in nitrogen content as would be expected of introduction of a cyanide group to pyridine. More importantly, the hydrolysis of pyridine carbonitrile **9** with nitrilase in the solid state led to a decrease in nitrogen content. Palladium loading was calculated to be approximately 0.5%. Palladium to phosphorous atom-to-atom ratios were calculated to be almost exactly 1:2. This is a surprising result because the Chaudhari work reported monodentate coordination of tosylate counterion, bidentate N,O- coordination of picolinate and a single triphenylphosphine bound to the palladium centre. The above results suggest that picolinic acid has been immobilised on silica and a palladium picolinate species has been synthesised.

6.2.3 Infra-Red Spectroscopy

We have chosen to use a high density silica thus ensuring that almost all catalytic sites are at the surface and fully accessible. DRIFT (Diffuse Reflectance Infra-red Fourier Transform) spectroscopy was used to analyse the surface of the various silica materials. The technique is a surface technique which analyses reflected beam from the surface/near surface of a solid. Figure 4 shows an ATR-IR spectrum of unsupported **6**, while figure 5 shows a DRIFT *difference* spectrum of supported **7**. The spectrum of SiO₂ was subtracted from that of **7** to get an indication of what had been added to the SiO₂. The similarities between the spectra (figures 4 and 5) are obvious. Furthermore, the trough at 3740 cm⁻¹ (figure 5) corresponds to the point at which the OH stretch of silanol groups is normally located. This trough implies a substantial loss of silanol stretches indicating that the surface silanol groups have reacted with the triethoxysilane functionality of **6**. This is conclusive proof that the precursor of the immobilised catalyst is covalently bound to the silica support. The carbamate functionality has characteristic stretches in the region ~1705 cm⁻¹. Aromatic C-N stretches (from pyridine) are also clearly visible at ~1610 cm⁻¹.

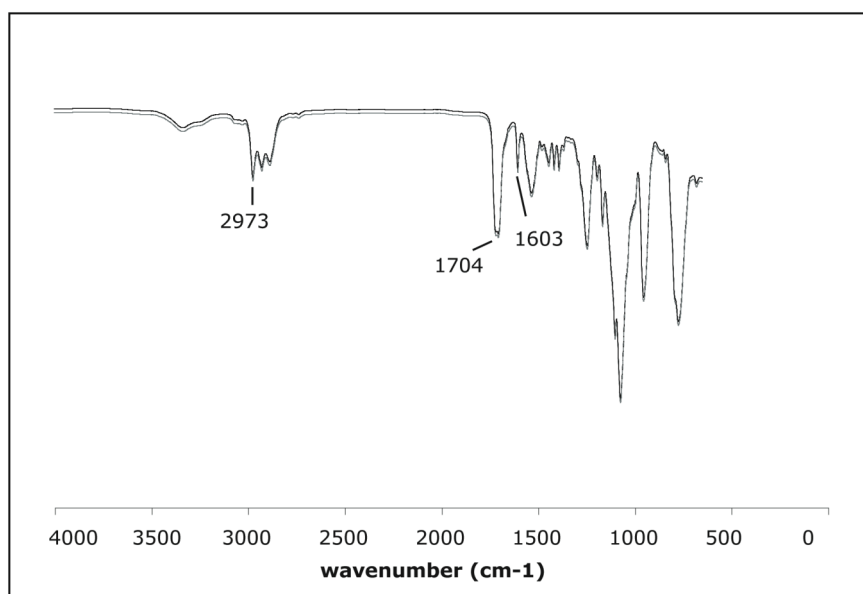


Figure 4. ATR-FT-IR spectrum of **6**.

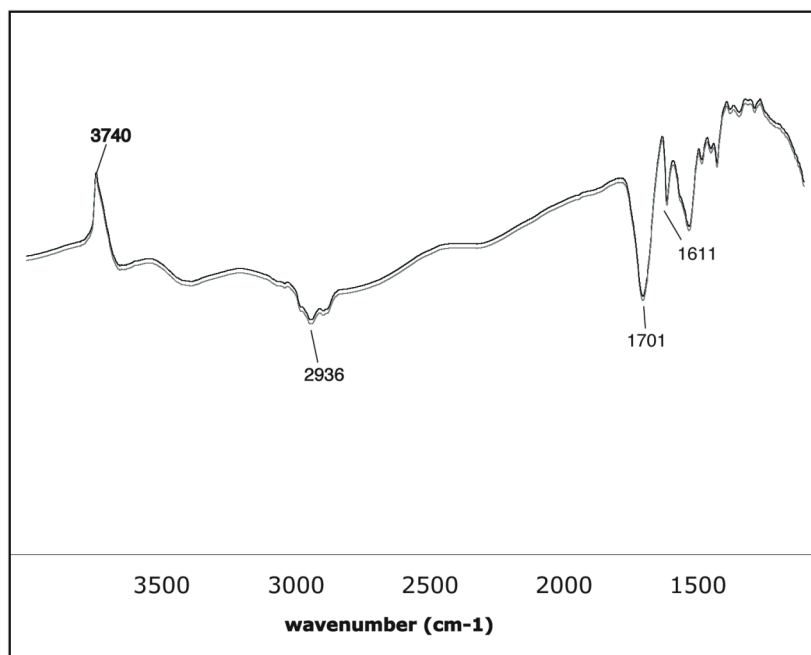


Figure 5. DRIFT difference spectrum of 7 minus SiO₂.

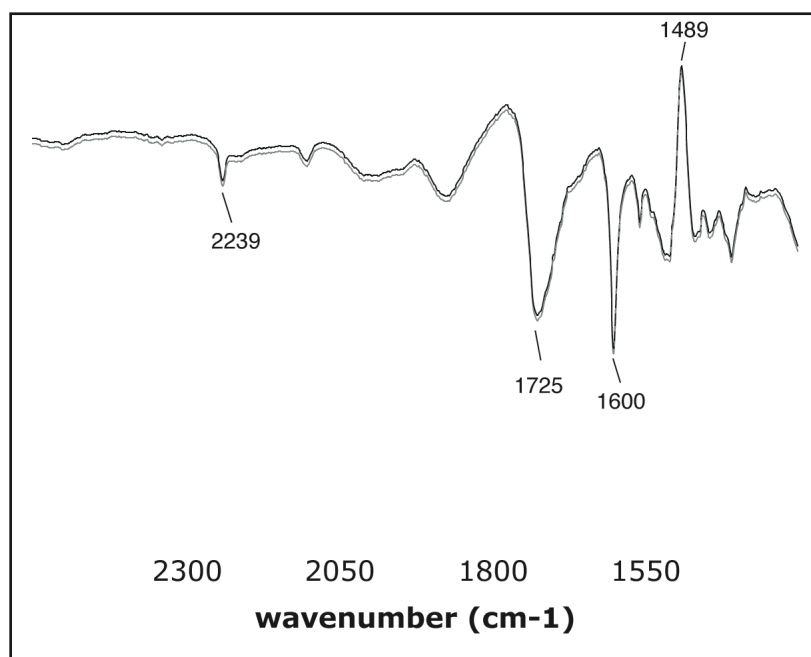


Figure 6. 9 minus 8 DRIFT difference spectrum.

The subsequent synthetic steps towards the construction of **11** showed similar peak gains and losses. We will focus on the discussion of only one of these, which shows the clear hydrolysis, using nitrilase, of pyridine carbonitrile **9** to picolinic acid **10**. Figure 6 shows the DRIFT **9** minus **8** - difference spectrum. ν_{CN} is clearly visible at 2239 cm⁻¹. Furthermore, all N-oxide (aromatic C-N trough, 1489 cm⁻¹) had been converted to 2-pyridine cyanide (aromatic C-N peak, 1600 cm⁻¹). In the DRIFT difference spectrum of **10** minus **9**, a clear trough is observed at 2239 cm⁻¹ indicating loss (hydrolysis) of the cyano group. Unfortunately, the carboxylate of the resulting supported picolinic acid gives a less diagnostic peak. It is in a region which is overlapping with the carbamate

stretching frequency. An obvious broadening of the peak in the $\nu_{\text{C=O}}$ region ($1650\text{--}1720\text{ cm}^{-1}$), however gives an indication of the carboxylic acid forming.

The DRIFT difference spectrum of **11** minus SiO_2 , the immobilised catalyst (figure 7), shows a number of peaks corresponding to the carbamate, picolinate, pyridine ring, tosylate and finally the triphenylphosphine co-ligand. The clearest indication that the catalyst itself has been immobilised is the $\text{P-C}_{(\text{aryl})}$ stretch of coordinated triphenylphosphine which lies at 1438 cm^{-1} . A Pd-N vibration at 568 cm^{-1} is also observed.

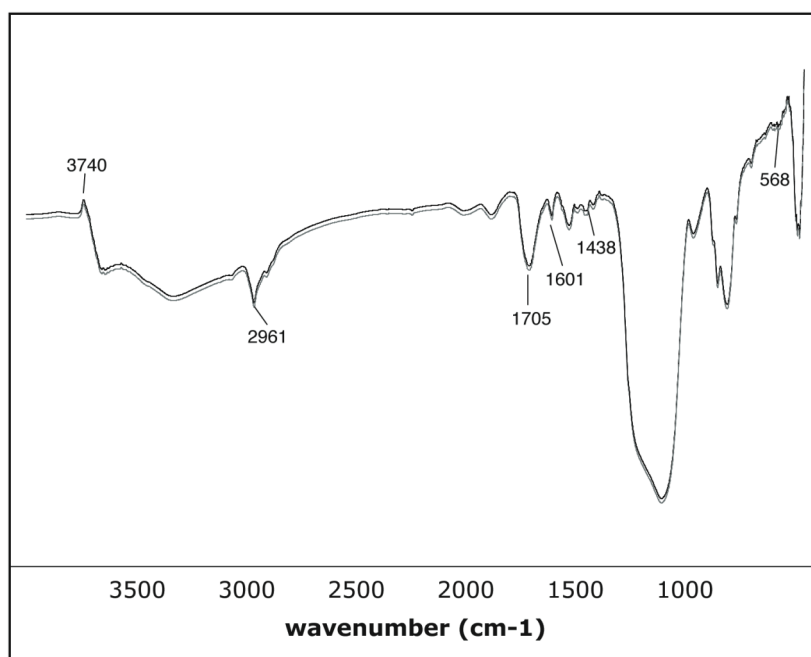


Figure 7. DRIFT difference spectrum of **11** minus SiO_2 .

6.2.4 NMR Spectroscopy

^{13}C CP-MAS NMR was used to characterise some of the intermediates in the construction of the catalyst on the silica support. Unfortunately, unlike the DRIFT technique we were not able to differentiate between compounds **10** and **9** using this technique. However, ^{13}C -NMR of **10** did show that an asymmetric pyridine (five aromatic C peaks) with tether (six alkyl C peaks, along with some ethoxide signals) was present in the material (figure 8).

CP-MAS ^{29}Si NMR of the immobilised catalyst (**11**) shows us several peaks that indicate different forms of silicon species (figure 9). Peaks at -101 and -111 ppm are characteristic of Q type ($\text{Si}(\text{O})_4$) silicates, which are in the bulk material. Peaks at -57 and -65 ppm are typical of T-type ($\text{R}_1\text{-Si}(\text{O})_3$) silicates, that is, the silicon bound to the propyl group of **11** at the surface of the support. This is the clearest indication that the catalyst is covalently bound to the support. The presence of double peaks in the -60 ppm region indicates that not all ethoxy groups of **6** have reacted in the grafting process. Similarly, the single peak at 13 ppm is typical of M-type ($\text{R}_3\text{-Si}(\text{O})$) silicates (where R is the methyl groups of the trimethylsilyl capped silanol groups at the silica surface).

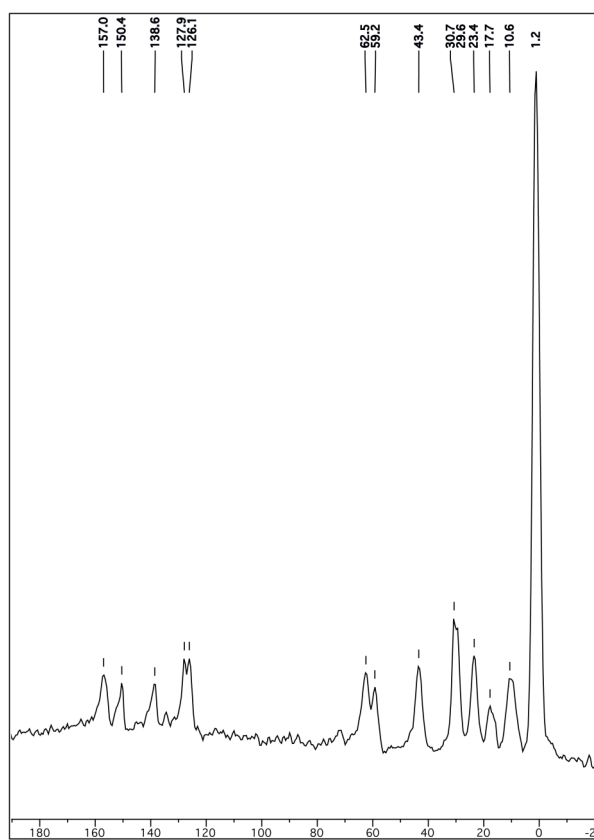


Figure 8. CP-MAS ^{13}C NMR of **10**.

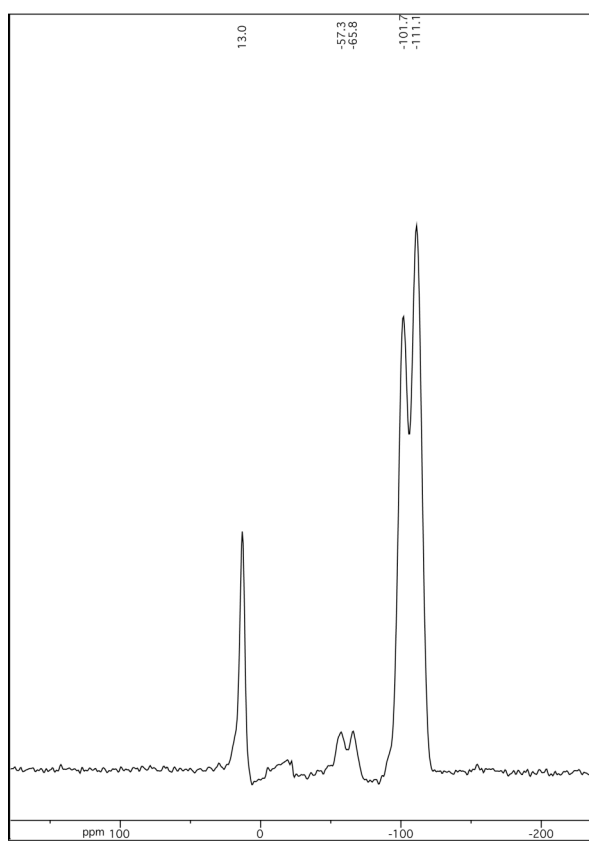


Figure 9. CP-MAS ^{29}Si NMR of **11**.

Figure 10 shows the CP-MAS ^{31}P NMR spectrum of immobilised complex **11**. The broad peak at 29 ppm is that of coordinated triphenylphosphine. The other peaks all correspond to spinning side bands at a frequency of approximately 8000 Hz. The peak is quite broad indicating that in the solid state a mixture of isomers is possibly present (PPh_3 *trans* or *cis* to pyridine-N) as reported by Chaudhari previously. The same researchers have reported a ^{31}P CP-MAS NMR of catalyst **1** showing very similar results to those observed with the immobilised catalyst **11**. Conversely, the previously reported immobilised catalyst in figure 2, gives a sharp peaked CP-MAS ^{31}P NMR. Apparently the introduction of SiO_2 -propylamine reduced the possibility of ligand association/dissociation. It is possible that the propylamine has reacted with the picolinic acid yielding an amide and released a palladium species stabilised by phosphine ligands.

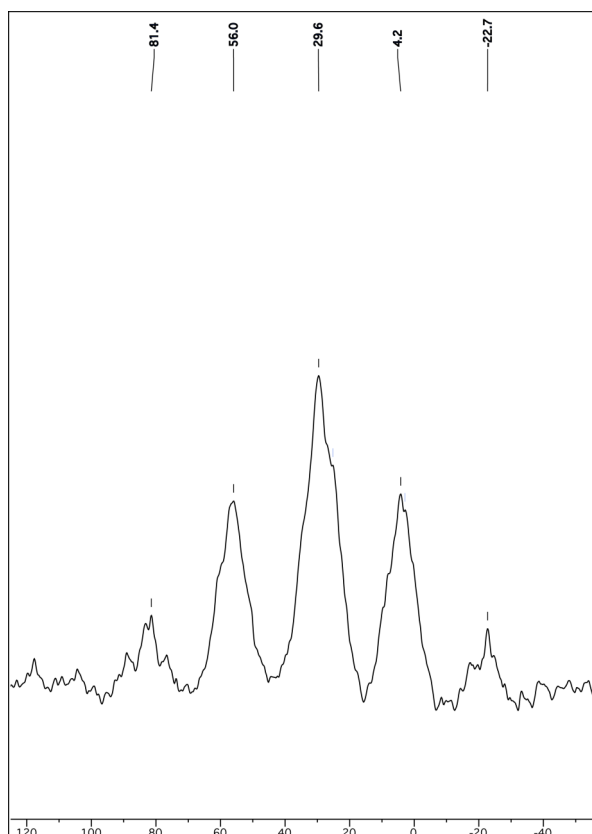


Figure 10. CP-MAS ^{31}P NMR of **11**.

6.2.5 Hydroxycarbonylation Catalysis

Hydroxycarbonylation of IBPE to IBN was carried out using **11** (figure 1). LiCl and tosylic acid were used as promoters, in excess with respect to the catalyst, as was the case with the homogeneous catalyst. IBPE was completely consumed in the reaction. The regioselectivity of the immobilised catalyst was less than that of the homogeneous catalyst, with around ~95% branched product (IBN) observed. This is less than what was observed when using **1** (99%⁹).

Analysis of the post-catalysis solution led to some interesting observations. The pre-catalysis solution was colourless before the addition of **11**. However, the post catalytic solution had a bright yellow colour. DRIFT-IR analysis of the silica support, isolated by simple filtration and washing with water and dichloromethane, suggested that coordinated triphenylphosphine from the

catalyst had been removed from the surface (no P-C_(aryl) IR stretch). Furthermore no Pd-N stretch was observed. Furthermore, elemental analysis of the recycled material showed a dramatic decrease in the palladium loading. Less than 0.1% palladium was measured in the recycled material. Post catalysis **11** had lost its light yellow colour, and was colourless. Recycled **11** was reused in a following catalytic run. No conversion of IBPE to IBN was observed. The post catalysis solution was recharged with substrate and promoters and tested in a catalytic run. It showed conversion of IBPE to IBN, showing similar activity to the first run and selectivity of ~95% for the branched product.

Tests on the effects of the substrates on the supported catalyst were carried out. It was observed that a butan-2-one ‘solution’ of **11** remained colourless until tosylic acid was added (no change when IBPE, LiCl, or H₂O added). A light yellow solution was observed after the addition of tosylic acid. This solution was tested in the hydroxycarbonylation of IBPE to IBN and showed similar activity to the first test with **11** and selectivity of ~95% of the branched product. A CDCl₃ solution containing **11** was analysed step-wise using ³¹P NMR spectroscopy. When butanone, water, LiCl, IPBE were added, *no* ³¹P signal was observed. When tosylic acid was added to the mixture a peak at 29ppm appeared immediately. This is a clear signal of a phosphorous coordinated palladium species which has detached from the supported ligand.

Table 1. Hydroxycarbonylation of IBPE with various derivatives of **1**.

Catalyst	1	11	Recycled 11 ^[b]	Pre-cat. Filtrate 11 ^[c]	Post-cat. Filtrate 11 ^[d]
IBN (%) ^[a]	99	~95	-	~95	~95

[a] GC yield, [b] filtration of inorganic material and reapplication with fresh substrate and promoters, [c] insoluble inorganic filtered off prior to application of CO gas, [d] insoluble inorganic filtered off, new substrate and promoters added to filtrate.

We have carried out a number of analytical investigations on the homogeneous catalyst **1**. We carefully followed the synthesis of **1** as published. Initially we closely analysed the ¹H and ³¹P NMR spectra of the complex in CDCl₃. The aromatic region of the ¹H NMR spectrum showed a number of broad peaks for the picolinate and triphenylphosphine ligands. The alkyl CH region showed one distinct peak. H-H correlation spectroscopy showed that this peak corresponded to two doublets in the aromatic region, and thus corresponded to a single tosylate-type compound. This disagrees with the reports of Chaudhari which proposed triphenylphosphine and tosylate ligands rapidly exchanging on the palladium centre. The ³¹P NMR shows two broad major peaks at 36 and 34 ppm respectively, as published. However, they do not report two signals for the tosylate CH₃ ¹H signals, which would be expected. We also observed minor peaks at 33 and 32 ppm, respectively. We have found that the introduction of propyl amine to complex **1** in CDCl₃ (mimicking the immobilisation on propylamine functionalised silicates, figure 2) showed a sharpening of the ³¹P signals of coordinated phosphine, and only a single peak at 29.8 ppm, and the formation of free triphenylphosphine (δ³¹P = 3ppm). The aromatic ¹H NMR signals of the same solution, show a

dramatic sharpening as well. The spectrum indicates that only one palladium picolinate species is present.

We have also carried out MALDI-TOF mass analysis of complex **1**. The mass spectrum of **1** showed major peaks at 801.27 [(PPh₃)₂Pd(tos)], 752.26 [(PPh₃)₂Pd(pic)], and 629.24 [(PPh₃)₂Pd]. No observed mass corresponded to complex **1** or derivatives thereof. No peaks corresponding to a palladium complex with only one triphenylphosphine coordinated were observed.

Previous reports by the Chaudhari group have shown [PdCl₂(PPh₃)₂] to be a highly active and regioselective catalyst for the hydroxycarbonylation of phenylethanol derivatives.¹⁷ In this system the active catalyst is believed to be a [(PPh₃)₂Pd(0)] species which is formed in situ in the presence of tosylic acid. TOF and yields are similar, however, this system shows one difference to catalyst **1**. The regioselectivity achieved with **1** is 99%, and with [PdCl₂(PPh₃)₂] 97%.

From all of the above results, it is clear that the reported palladium picolinate is not the active catalyst in the hydroxycarbonylation of IBPE. However, from the regioselectivity results, it is also clear that the picolinic acid has an effect on the selectivity. Indeed, it is a bit circumspect to debate differences of 3-4% in selectivity (**1** = 99%, **11** = ~95%), however these catalytic results are consistent and show the same results repeatedly. It is also apparent that a [Pd(PPh₃)(OTs)(pic)] (**1**) species may not exist at all. Most of the results point to the likelihood that whatever type palladium species is present it contains two bound triphenylphosphine ligands.

6.3 Conclusions

Chaudhari's complex **1** was covalently immobilised on a high density, low porosity silica support by step-wise construction of the catalyst on the support. Enzymatic hydrolysis was used in the construction of the ligand on the support. DRIFT-IR and multinuclear CP-MAS solid state NMR spectroscopy were used to analyse intermediates and characterise the immobilised catalyst. The immobilised catalyst was used in the hydroxycarbonylation of 1-(4-isobutylphenyl)ethanol yielding the commercially attractive non-steroidal anti-inflammatory drug Ibuprofen. Post-catalytic analysis showed that the palladium picolinate, which was initially proposed as the active species during catalysis, is probably not the active catalyst. It was shown that catalytic promoters induce the decomplexation of palladium picolinate. It was also shown that the newly formed palladium species was active in the hydroxycarbonylation reaction. This newly formed palladium species shows lower selectivity in the hydroxycarbonylation of IBPE.

6.4 Experimental Section

General Information: All reagents were used as supplied from Acros or Sigma-Aldrich, unless otherwise stated. butan-2-one was distilled over molecular sieves. 1-(4-isobutylphenyl)ethanol (IBPE) was synthesised by a literature procedure,¹⁸ and was distilled twice over molecular sieves. ¹H, ¹³C and ³¹P solution NMR were recorded on a Varian Inova 300 spectrometer or a Varian Oxford AS400. CP-MAS NMR was carried out using a Bruker AV 750. Elemental analyses were performed by Dornis und Kolbe, Mikroanalytisches Laboratorium, Müllheim a. d. Ruhr, Germany. MS

measurements were carried out on an Applied Biosystems Voyager DE-STR MALDI-TOF MS and IR spectra were recorded on a Perkin-Elmer SpectrumOne FT-IR Spectrometer. GC analyses were performed on a Perkin-Elmer AutosystemXL Gas Chromatograph.

Synthesis of 3-(4-pyridyl)-propyl-1-(3-(triethoxysilyl)propyl-1-carbamate), 6:

3-(4-Pyridyl)-propan-1-ol (9.85g, 0.0718mol) was stirred at room temperature with 3-(triethoxysilyl)propyl-1-isocyanate (20 mL, 0.0808mol, 1.1 equivalents) in benzene for 24 hrs. All solvent was subsequently removed yielding a mixture of product and starting isocyanate. Separation of these was carried using column chromatography with pure ethanol as eluent yielding the product with 95% yield as a colourless oil. ¹H NMR (300 MHz, CDCl₃) δ = 0.61 (t, 2H, CH₂), 1.20 (t, 9H, OCH₂CH₃), 1.61, (m, 2H, CH₂), 1.93 (m, 2H, CH₂), 2.66 (t, 2H, CH₂), 3.15 (t, 2H, CH₂), 3.80 (q, 6H, OCH₂CH₃), 4.06 (t, 2H, CH₂), 5.00 (broad, 1H, NH), 7.10 (d, 2H, pyridine CH), 8.46 (d, 2H, pyridine CH). ¹³C-NMR (75 MHz, CDCl₃) 7.85, 18.50, 23.49, 29.84, 31.77, 43.59, 58.66, 63.83, 124.04, 149.99, 150.62, 156.73. IR (KBr) 1710 & 1704 cm⁻¹ (ν_{C=O}), 1603 cm⁻¹ (ν_{C-N (arom)}) m/z found 384.2262. C₁₈H₃₂O₅N₂Si (384.5467): calcd. C 56.11, H 8.39, N 7.28; found C 55.90, H 8.45, N 7.43.

Synthesis of 3-(4-pyridyl)-propyl-1-(3-(silica)propyl-1-carbamate), 7:

3-(4-pyridyl)-propyl-1-(3-(triethoxysilyl)propyl-1-carbamate) (0.92g, 0.239mmol) was placed in a round bottom flask with Engelhard silica (4 g, C500-383) with dry toluene (50 mL) and heated at reflux for 24 hours using mechanical stirring. After cooling to room temperature the silica was filtered and washed twice with hot toluene and then three times with boiling ethanol. Soxhlet purification was carried out using ethanol. Pure white powder. IR (KBr) 1705cm⁻¹ (ν_{C=O}), 1605 cm⁻¹ (ν_{C-N (arom)}). Elemental analysis found; C 4.39, H 0.73, N 0.72.

Synthesis of trimethylsilyl-capped-3-(4-pyridyl)-propyl-1-(3-(silica)propyl-1-carbamate), 7:

3-(4-pyridyl)-propyl-1-(3-(silica)propyl-1-carbamate) (1 g) was placed in a round bottom flask with dry hexanes (50 mL) and hexamethyldisilazane (5 mL, large excess) and heated at reflux for 24 hours using mechanical stirring. After cooling to room temperature the silica was filtered and washed twice with hot dichloromethane and then three times with boiling ethanol. Soxhlet purification was carried out using ethanol. Pure white powder. IR (KBr) 1705cm⁻¹ (ν_{C=O}), 1605 cm⁻¹ (ν_{C-N (arom)}). Elemental analysis found; C 5.86, H 0.91, N 0.73.

Synthesis of of trimethylsilyl-capped-3-(4-pyridyl-N-oxide)-propyl-1-(3-(silica)propyl-1-carbamate), 8:

Trimethylsilyl-capped-3-(4-pyridyl)-propyl-1-(3-(silica)propyl-1-carbamate) (1 g) was placed in dry dichloromethane (50 mL) with *meta*-chloroperoxybenzoic acid (1 g) and stirred at room temperature for 24 hrs. After this the silica was filtered and washed twice with hot dichloromethane and then three times with boiling ethanol. Soxhlet purification was carried out using ethanol. Pure white powder. IR (KBr) 1705cm⁻¹ (ν_{C=O}), 1489 cm⁻¹ (ν_{C-N-O (arom)}). Elemental analysis found; C 5.78, H 0.94, N 0.73.

Synthesis of trimethylsilyl-capped-3-(4-pyridyl-2-carbonitrile)-propyl-1-(3-(silica)propyl-1-carbamate), 9:

Trimethylsilyl-capped-3-(4-pyridyl-N-oxide)-propyl-1-(3-(silica)propyl-1-carbamate) (1 g) was placed in freshly distilled, dry triethylamine (50 mL) and trimethylsilylcyanide (1.2mL, HIGHLY TOXIC). The resulting mixture was heated at 90°C for 24 hours with mechanical stirring. After this the mixture was filtered hot and washed with boiling dichloromethane twice and boiling ethanol three times. Yellowish powder. IR (KBr) 2239cm⁻¹ (ν_{C-N (cyanide)}), 1705cm⁻¹ (ν_{C=O}), 1600 cm⁻¹ (ν_{C-N (arom)}). Elemental analysis found; C 6.68, H 1.12, N 1.09.

Synthesis of trimethylsilyl-capped-3-(4-pyridyl-carboxylate)-propyl-1-(3-(silica)propyl-1-carbamate), **10**:

Trimethylsilyl-capped-3-(4-pyridyl-2-carbonitrile)-propyl-1-(3-(silica)propyl-1-carbamate) (1 g) was placed in ethanol (1 mL) and then added to deionised water (9 mL). 10 ml of a solution (100 ml water and 50 mg of 10U per gram) of nitrilase rhodococcus rhodochrous was then added to this and the resulting mixture was stirred in the presence of tris buffer (pH = 8) for 4 days. After which the solid was filtered and washed with deionised water and methanol and finally with boiling ethanol. Off-white powder. IR (KBr) broad 1709cm^{-1} ($\nu_{\text{C=O}}$), 1600cm^{-1} ($\nu_{\text{C-N (arom.)}}$). Elemental analysis found; C 6.02, H 1.20, N 0.75.

Synthesis of trimethylsilyl-capped-3-(4-pyridyl-carboxylato)-(triphenylphosphino)-(tosylato)-(palladium(II))-propyl-1-(3-(silica)propyl-1-carbamate), **11**:

Trimethylsilyl-capped-3-(4-pyridyl-carboxylate)-propyl-1-(3-(silica)propyl-1-carbamate) (1 g) was placed in dry chloroform (20 mL) with $\text{Pd}(\text{OAc})_2$ (0.2 g, 0.89mmol) and triphenylphosphine (0.46 g, 1.78mmol) and 4-toluenesulfonic acid (0.34 g, 1.78mmol). The resulting mixture was stirred vigorously for 2 hours at room temperature. Filtration and then washing with chloroform and dichloromethane (at room temperature) yielded the final product as a yellowish powder. IR (KBr) broad 1705cm^{-1} ($\nu_{\text{C=O}}$), 1601cm^{-1} ($\nu_{\text{C-N (arom.)}}$), 1438cm^{-1} ($\nu_{\text{P-C(aryl)}}$), 568cm^{-1} ($\nu_{\text{Pd-N}}$). Elemental analysis found; C 6.51, H 1.07, N 0.77, P 0.26, Pd 0.42.

Hydroxycarbonylation catalysis; standard procedure⁹:

1-(4-isobutylphenyl)ethanol (5 g, 28.1mmol) was placed in a 100 ml autoclave. To this was added catalyst **11** (1.32 g, approximately 0.05 mmol) lithium chloride (0.24 g, 5.6 mmol), 4-toluenesulfonic acid (0.96 g, 5.6 mmol) and deionised water (0.1189 g, 6.6 mmol). Freshly distilled butan-2-one (25 mL) was then added thereto, and the resulting mixture was stirred vigorously. The autoclave was sealed and purged twice with argon, and subsequently twice with CO. The autoclave was put under 50 bar of CO pressure and heated to 115°C .

6.5 References

- ¹ (a) H.-U. Blaser, *Chem. Commun.* **2003**, 293-296. (b) D. E. De Vos, I. F. J. Vankelecom, P. A. Jacobs, [Eds. Weinheim]; Chiral Catalyst Immobilization and Recycling, **2000**. Wiley-VCH.
- ² D. J. Cole-Hamilton, *Science* **2003**, *299*, 1702-1706.
- ³ Q.-H. Fan, Y.-M. Li, A. S. C. Chan, *Chem. Rev.* **2002**, *102*, 3385-3466.
- ⁴ C. E. Song, S. Lee, *Chem. Rev.* **2002**, *102*, 3495-3524.
- ⁵ (a) S. J. Shuttleworth, S. M. Allin, P. K. Sharma, *Synthesis* **1997**, 1217-1239. (b) Y. Ribourbouille, G. D. Engel, L. H. Gade, *C.R. Chimie* **2003**, *6*, 1087-1096.
- ⁶ (a) G. Pozzi, I. Shepperson, *Coord. Chem. Rev.* **2003**, *242*, 115-124. (b) W. A. Herrmann, C. W. Kohlpaintner, *Angew. Chem. Int. Ed. Engl.* **1993**, *32*, 1524-1544.
- ⁷ U. Schubert, *New J. Chem.* **1994**, *18*, 1049-1058.
- ⁸ I. del Rio, C. Claver, P. W. N. M. van Leeuwen, *Eur. J. Inorg. Chem.* **2001**, 2719-2738.
- ⁹ (a) A. Seayad, S. Jayasree, R. V. Chaudhari, *Org. Lett.* **1999**, *1*, 459-461. (b) A. Seayad, S. Jayasree, R. V. Chaudhari, *J. Mol. Catal. A: Chemical* **2001**, *172*, 151-164.
- ¹⁰ J.-P. Rieu, A. Boucherle, H. Cousse, G. Mouzin, *Tetrahedron* **1-956**, *42*, 15, 4095-4131.
- ¹¹ S. Jayasree, A. Seayad, R. V. Chaudhari, *Org. Lett.* **2000**, *2*, 203-206.

- ¹² K. Mukhopadhyay, B. R. Sarkar, R. V. Chaudhari, *J. Am. Chem. Soc.* **2002**, *124*, 9692-9693.
- ¹³ S. Jayasree, A. Seayad, B. R. Sarkar, R. V. Chaudhari, *J. Mol. Catal. A: Chemical* **2002**, *181*, 221-235.
- ¹⁴ H. Meyer, R. Graf, *Chem. Ber.* **1928**, *61*, 2202-2215.
- ¹⁵ L. S. von Chrzanowski, M. Lutz, A. L. Spek, A. R. McDonald, G. P. M. van Klink, G. van Koten. *Acta Cryst.* **2007**, *E63*, o1121–o1122.
- ¹⁶ BASF Nederland B.V. Catalysts Division, Process Technologies, Strijkviertel 67, Postbus 19, 3454 ZG DE MEERN
- ¹⁷ A. Seayad, S. Jayasree, R. V. Chaudhari, *Catal. Lett.* **1999**, *61*, 99-103.
- ¹⁸ G. Parrinello, J. K. Stille, *J. Am. Chem. Soc.* **1957**, *109*, 7122-7127.

Probing the *mer-* to *fac-* Isomerisation of Tris-Cyclometallated Homo and Heteroleptic (C,N)₃ Iridium(III) Complexes

Abstract. We have developed techniques to covalently tether, via a ‘hetero-’ cyclometallating ligand, heteroleptic tris-cyclometallated iridium(III) complexes to polymeric supports (for application in LED technologies, tethered materials are basis of another report). This involved the synthesis and thorough characterisation of heteroleptic $[\text{Ir}(\text{C},\text{N})_2(\text{C}',\text{N}')]$ tris-cyclometallated iridium(III) complexes. Furthermore, the synthesis and characterisation of heteroleptic $[\text{Ir}(\text{C},\text{N})_2\text{OR}]$ complexes is presented. Under standard thermal conditions for the synthesis of the *facial* (*fac*) isomer of tris-cyclometallated complexes it was not possible to synthesise pure heteroleptic complexes of the form $[\text{Ir}(\text{C},\text{N})_2(\text{C}',\text{N}')]$. Instead a mixture of homo- and heteroleptic complexes was acquired. It was found that a step-wise procedure involving the synthesis of pure *meridional* (*mer*) isomer followed by photochemical isomerisation of this *mer-* to the *fac-* isomer was necessary to synthesise pure *fac*- $[\text{Ir}(\text{C},\text{N})_2(\text{C}',\text{N}')]$ complexes. Furthermore, under thermal isomerisation conditions the conversion of *mer*- $[\text{Ir}(\text{C},\text{N})_2(\text{C}',\text{N}')]$ to *fac*- $[\text{Ir}(\text{C},\text{N})_2(\text{C}',\text{N}')]$ was also not a clean reaction, with again a mixture of homo- and heteroleptic complexes acquired. An investigation into the thermal *mer-* to *fac-* isomerisation of both homo- and heteroleptic tris-cyclometallated complexes is presented. It was found that the process is an alcohol catalysed reaction with the formation of an iridium alkoxide $[\text{Ir}(\text{C},\text{N})_2\text{OR}]$ intermediate in the isomerisation process. We have synthesised analogous complexes and have shown that they do indeed react so as to give *fac*-tris-cyclometallated products. A detailed explanation of the intermediates (and all their stereoisomers) formed in the *mer-* to *fac-* isomerisation process is presented, including how the formed intermediates react further, and the stereoisomeric products they yield.

7.1 Introduction

Since the initial discovery by Watts and co-workers that *facial*-tris[2-pyridinyl- κ N-phenyl- κ C²]iridium (*fac*- $[\text{Ir}(\text{ppy})_3]$) complexes display emission quantum yields as high as 0.4, tremendous effort has been invested into developing similar compounds for use in organic light emitting diodes (OLED's).¹ The photophysical properties of bis- and tris-cyclometallated iridium(III) complexes are very interesting for several applications. The most impressive of these is their application in combination with phosphorescent dopants which leads to even higher quantum efficiencies with electrophosphorescence.² Other applications include chemiluminescent devices,³ molecular oxygen sensors,⁴ and as templates in oxalate-based chiral magnets.⁵

Present work in this field has been directed towards augmenting ligand electronics so as to adjust energy levels in tris-*C,N*-cyclometallated iridium(III) ($[\text{Ir}(\text{C},\text{N})_3]$) complexes and thus to improve quantum efficiencies and cover the whole spectrum of colour. This has resulted in a huge range of aromatic cyclometallating ligands being tested and used in homoligated complexes.⁶ Tris-cyclometallated iridium complexes tend to show higher quantum yields and internal quantum efficiencies than their bis-cyclometallated analogues. However, bis-cyclometallated complexes are still very valuable photochemically and thus a huge range of charged heteroleptic $[\text{Ir}(\text{C},\text{N})_2\text{L}][\text{X}]$ complexes where L is a neutral chelating diamine or diphosphine ligand, have also been developed.⁷ Neutral heteroleptic $[\text{Ir}(\text{C},\text{N})_2(\text{E},\text{E}')]$ complexes exist with the heteroligand (E,E') as a monoanionic acetate (O,O') or picolinate (N,O).⁸ Very few reports have shown the synthesis of heteroleptic $[\text{Ir}(\text{C},\text{N})_2(\text{C}',\text{N}')]$ complexes.⁹

$[\text{Ir}(\text{C},\text{N})_3]$ -type complexes have two stereochemical forms; meridional (*mer*-) and facial (*fac*-). The *mer*-isomers possess three nitrogen's around the equator of the molecule with two nitrogen's *trans* to each other and the third nitrogen *trans* to an aromatic carbon. The *fac*-isomer has three nitrogen atoms capping a face of an octahedron around the iridium centre, the carbon atoms do likewise on the opposite face. All nitrogen atoms are *trans* to a carbon atom. Previous work has shown the differences between the photophysical¹⁰ and stereochemical¹¹ properties of the *mer*- and *fac*-isomeric forms of the complexes. Generally the *fac*-isomer has an order of magnitude longer emission lifetime (τ) than the *mer*-. Similarly, the quantum yield of emission (Φ) in the *fac*- tends to be an order of magnitude greater than that of the *mer*-isomer. Conversion of *mer*- to *fac*-isomers is possible using both thermal and photochemical techniques.

We are interested in developing heteroleptic $[\text{Ir}(\text{C},\text{N})_2(\text{C}',\text{N}')]$ complexes, because this can provide an entry to tris-cyclometallated Ir(III) complexes tethered to dendritic and polymeric supports. Eventually we would like to develop OLED devices based on supported iridium complexes. Binding of cyclometallated Ir(III) complexes to dendritic,¹² linear polymeric,¹³ and biochemical supports¹⁴ has shown some very promising results for the future development of photochemical devices.

In this report we present our initial results towards the synthesis of heteroleptic $[\text{Ir}(\text{C},\text{N})_2(\text{C}',\text{N}')]$ complexes.¹⁵ The synthesis of these complexes has thrown up some stumbling

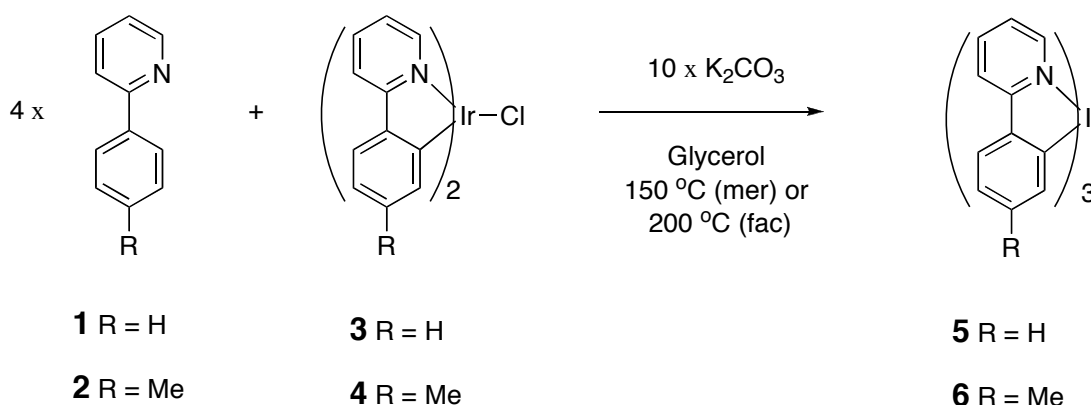
blocks. It was found that using standard thermal techniques it is not possible to synthesise pure *fac*-heteroleptic complexes, due to ligand scrambling. We devised a stepwise procedure which involves the reaction of $[\text{Ir}(\text{ppy})_2\text{Cl}]$ with a hetero-arene ligand, 4-methylphenyl-2-pyridine (Htolpy), yielding a heteroleptic *mer*-isomer, followed by conversion of this *mer*- to the corresponding *fac*-isomer using photochemical techniques. Furthermore we also applied this technique to synthesise mixed ligand functionalised species for immobilisation on polymeric supports.¹⁶ This has allowed us to analyse the photophysical effects of the support on the complex.¹⁷ We also investigated why using standard thermal *mer*- to *fac*-isomerisation techniques, a clean reaction is not observed. The mechanism involved in the thermodynamic *mer*- to *fac*-isomerisation of tris-cyclometallated iridium complexes was studied, and a number of analogues of possible intermediates was synthesised. From these investigations we have developed novel methods to synthesise both homo and heteroleptic tris-cyclometallated *fac*-type complexes, including at lower temperatures.¹⁸ This report contains a detailed discussion on the various stereochemical forms of heteroleptic tris-cyclometallated iridium complexes.

7.2 Results and Discussion

7.2.1 Synthesis and Characterisation of Heteroleptic Complexes $[\text{Ir}(\text{C},\text{N})_2(\text{C}',\text{N}')]_3$; *mer*-Isomers of **7** and **8**.

All experiments in the following section were carried out in the absence of light. The synthesis of $[\text{Ir}(\text{C},\text{N})_2\text{Cl}]$ complexes **3** and **4** was carried out according to literature procedures.^{1(c,d)} Tris-cyclometallated complexes **5** and **6** were synthesised using reaction techniques developed by Thompson.¹¹ The *fac*-isomer of **5** (from **1** and **3**) and **6** (from **2** and **4**) was synthesised when temperatures above 200°C were used. At temperatures of approximately 150°C the *mer*-isomer was formed (scheme 1).

Scheme 1. The Thompson method for the synthesis of homoleptic tris-cyclometallated iridium(III) complexes.¹¹



The reaction of **2** with **3** (and likewise **1** with **4**) using Thompson conditions for the synthesis of *fac*-isomers, did not proceed cleanly (figure 1). ¹H NMR of the isolated products showed the presence of a mixture of several similar complexes. UV-vis absorption spectroscopy

suggested that these were *fac*-type products. MALDI-TOF mass analysis, however, showed that scrambling of ligands had occurred and in fact a mixture of four different complexes (*fac*-**5-8**) had been synthesised (figure 1). Separation of the individual complexes from this *fac*-**5-8** mixture was attempted, but in our hands was not possible.

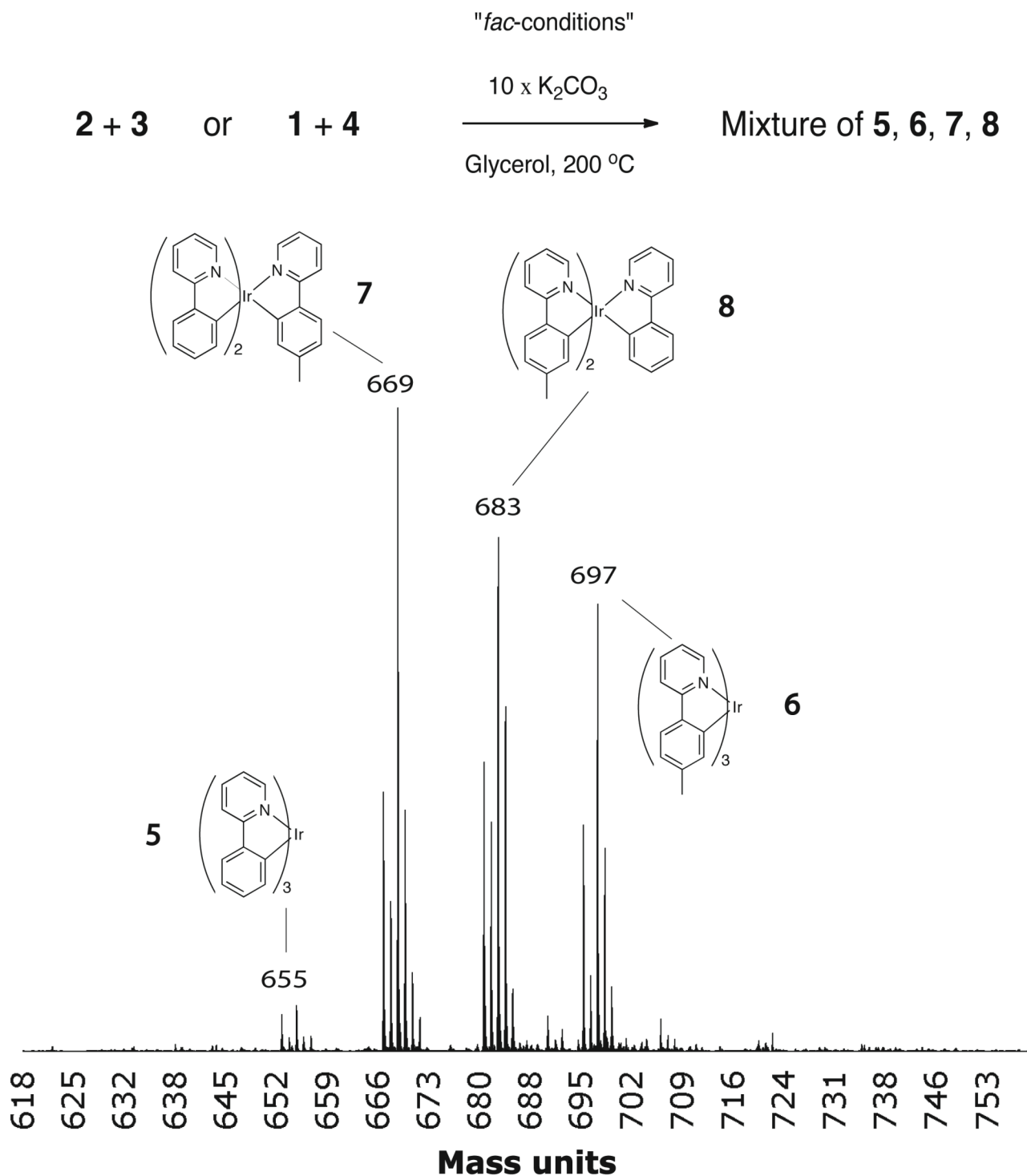
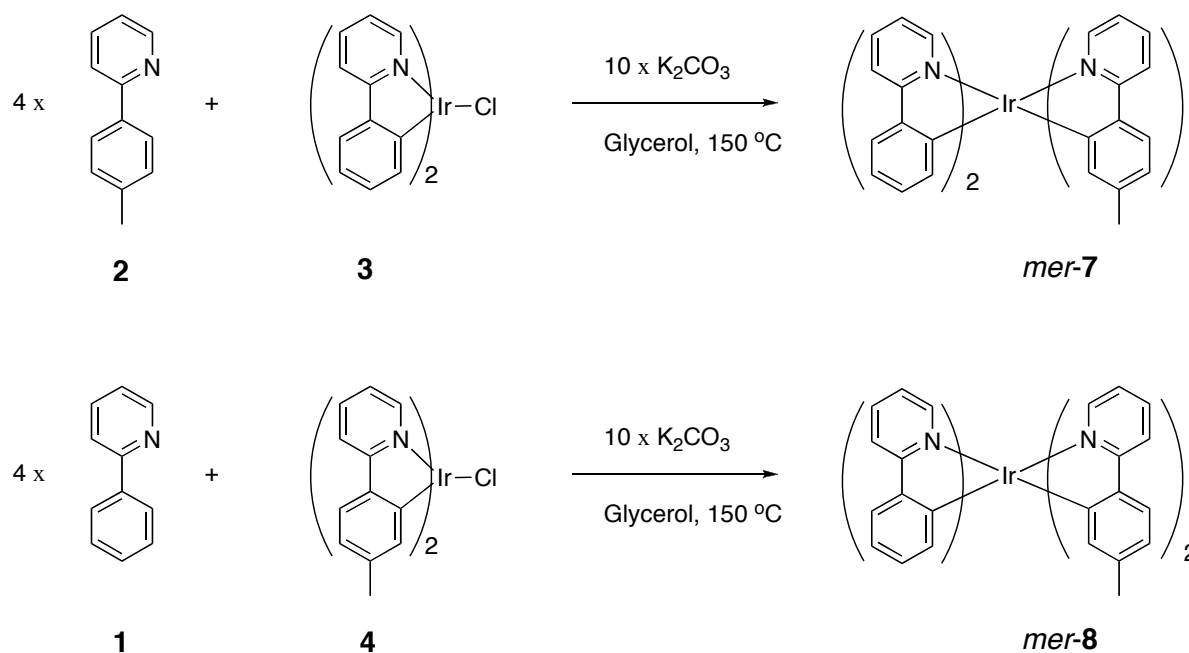


Figure 1. Attempted synthesis of heteroleptic *fac*-complexes **7** (from **2** and **3**) and **8** (from **1** and **4**) respectively. MALDI-TOF mass spectrum from reaction of **2** with **3** at 200°C.

Reaction of **2** with **3** (and likewise **1** with **4**) using the Thompson reaction conditions for the synthesis of *mer*-isomers, gave only one product, a *mer*-isomer of **7** and **8**, respectively (scheme 2). ^1H NMR of the acquired *mer-7* showed a single peak at 2.12 ppm corresponding to the methyl group, and 23 proton resonances in the aromatic region. ^{13}C NMR showed a single peak for the methyl group and 33 aromatic resonances. ^1H NMR of the acquired *mer-8* showed two peaks at 2.02 and 2.04 ppm corresponding to the methyl groups, and 22 proton resonances in the aromatic region. ^{13}C NMR showed two peaks for the methyl groups and 33 aromatic peaks. UV-vis absorption spectroscopy results corroborated that a *mer*-isomer had indeed been synthesised and was isolated as a pure product (figure 7c). In homo-ligated complexes ($[\text{Ir}(\text{C},\text{N})_3]$ **5** and **6**) the *mer*- and *fac*-isomer have dissimilar UV-vis absorption spectra, with the *mer*-isomer showing one significant absorption at 272nm (figure 7a) whereas the *fac*-isomer shows three strong absorptions at 245, 283 and 376nm (figure 7b). The synthesised heteroligated *mer*-isomers, *mer-7* and *mer-8* have a UV-vis absorption spectrum distinctly similar to those observed for the *mer*-isomer of **5** and **6**.

Scheme 2. Heteroleptic *mer*-complex synthesis.



7.2.2 Molecular Geometries of Acquired *mer-7* and *mer-8* in the Solid State.

Single crystals of *mer-7*, suitable for X-ray diffraction structure determination, were acquired from slow evaporation of a dichloromethane solution. The crystal system was monoclinic with the centrosymmetric space group $C2/c$ and two independent molecules in the asymmetric unit.¹⁹ The molecular structure of both independent molecules confirmed that a *mer*-isomer had indeed been isolated (figure 2). The three cyclometallating ligands are aligned in an octahedral configuration around the iridium centre. The C-C and C-N bond lengths and angles are within normal ranges expected for *mer*-tris-cyclometallated iridium(III) complexes.²⁰ The monoanionic heteroligand, 2-(4-methylphenyl)pyridine (tolpy), has longer Ir-N bond distances (2.142(5) and

2.136(3) Å, respectively) compared to those of the homoligands (2-(phenyl)pyridine, ppy) which have their nitrogen's aligned *trans* to each other (2.047(3) and 2.032(3) Å, respectively, table 1). This can be explained by the different *trans* influence both on carbon and nitrogen. However, subtle effects, for example the role of the tolyl-CH₃ group, could also be influencing the Ir-N or Ir-C bond distances.

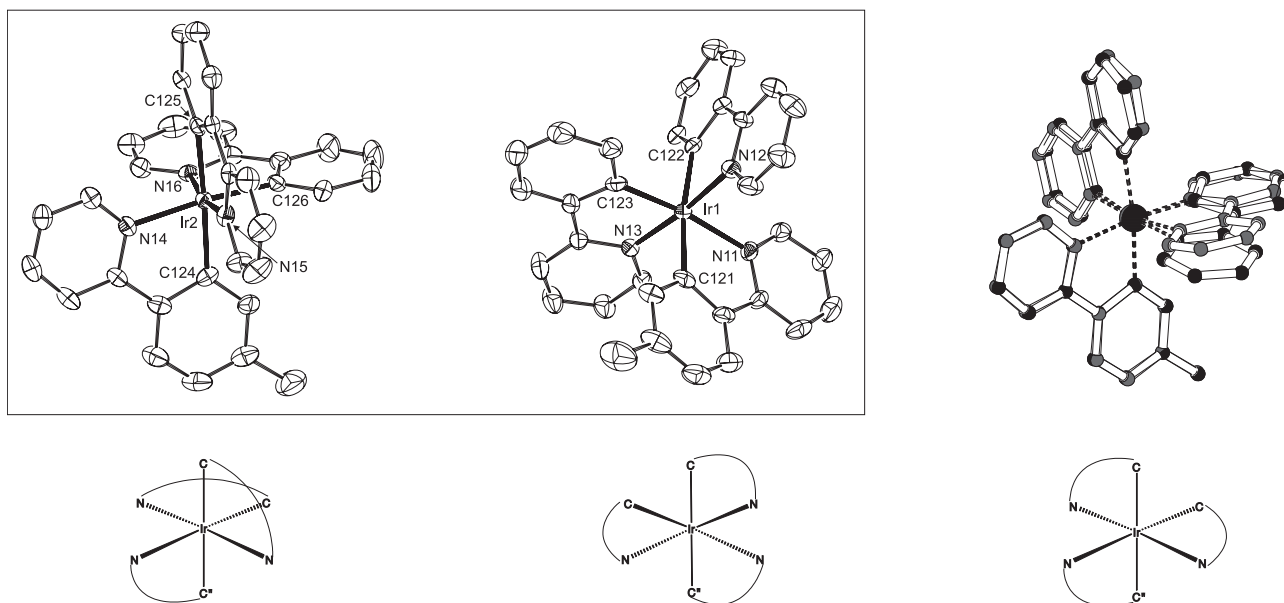


Figure 2. (left) Displacement ellipsoid plot (50% probability level) of the two independent molecules of *mer-7-homo-N-trans* in the crystal structure. View along the crystallographic *a,c*-diagonal. Hydrogen atoms and disordered solvent molecules have been omitted for clarity. (right) Quaternion fit overlay plot of residue 1 and the inverted residue 2.

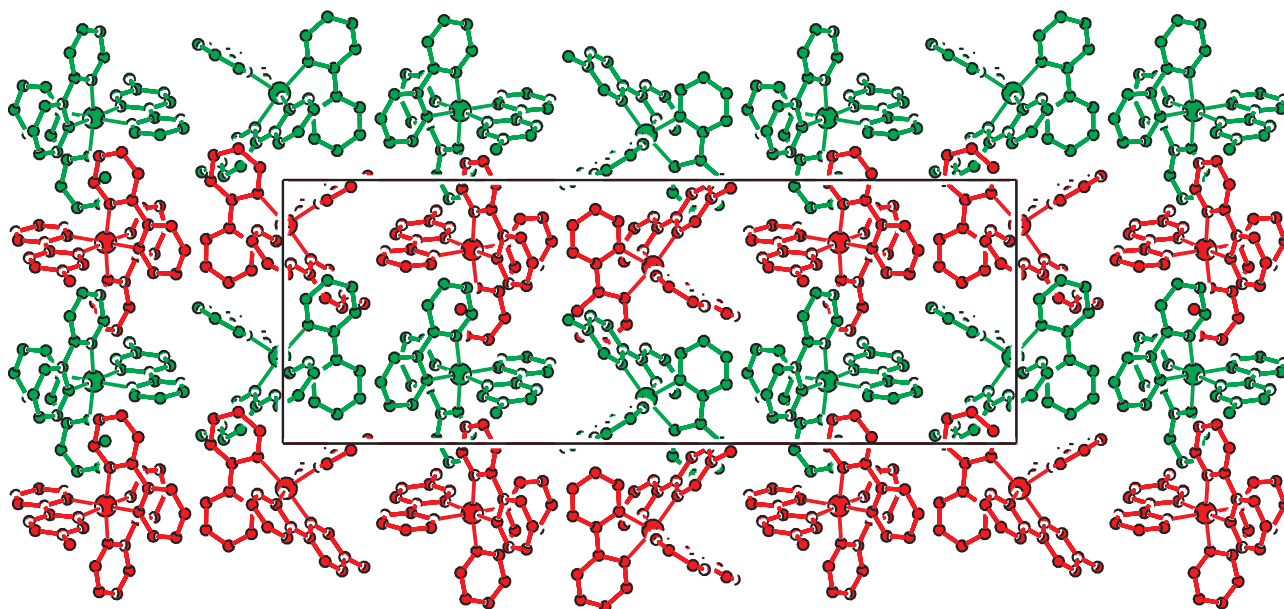


Figure 3. Packing of *mer-7-homo-N-trans*. The Δ enantiomer is light grey and Λ enantiomer is dark grey. View along the crystallographic *a* axis. The differences between residues 7.1 and 7.2 have been ignored for the sake of this diagram. Hydrogen atoms are omitted for clarity.

It is also noteworthy that the homoligands have retained their position relative to each other. The C_2 -*trans*(*N*) (the molecule is C_2 symmetrical with N's lying *trans* to each other) configured octahedral dimeric starting material **3** has two ppy ligands with nitrogen's aligned *trans* to each other while the *ortho* carbons lie mutually *cis* to each other and *trans* to the bridging halides.²¹ In the acquired *mer-7* the carbons of the homoligands bound to iridium are now *trans* to the heteroligand. The N's of the homoligands lie *trans* to one another. Therefore we call it *mer-7-homo-N-trans*¹⁵ (there are two other geometrical isomers of *mer-7*, this is discussed in the following section). Due to the centrosymmetry of the space group the crystal is a racemic mixture of both Λ and Δ stereoisomers. It should be noted that 15% of the unit cell is filled with disordered solvent molecules (see experimental section). The small differences in the residues can be clearly seen in the fit diagram in figure 2. Figure 3 depicts the crystal packing present in the crystal structure of *mer-7-homo-N-trans*. Alternating layers of Δ and Λ enantiomers are observed. Despite the centrosymmetry of the racemic crystal structure, a partial resolution of the Δ and Λ enantiomers has occurred.²²

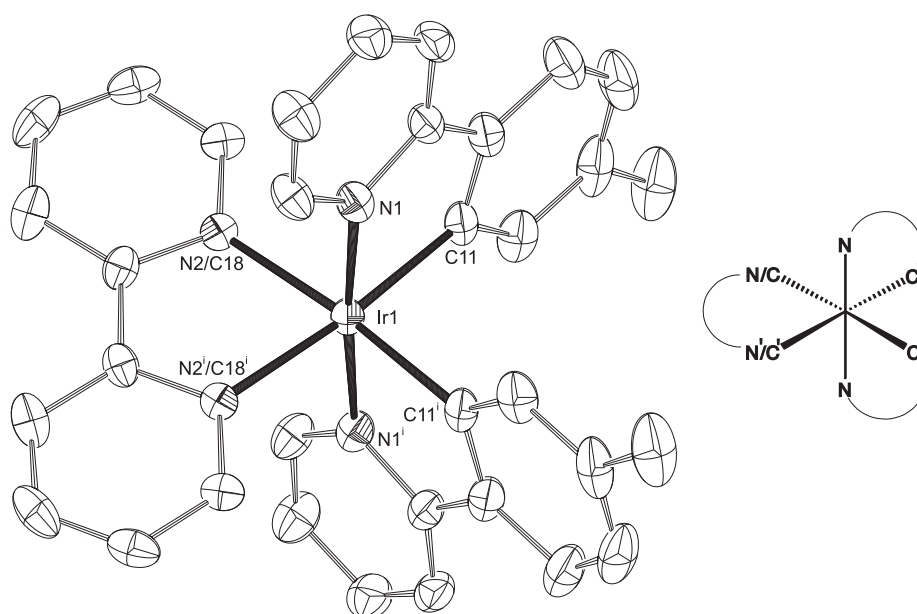


Figure 4. Displacement ellipsoid plot (50% probability level) of the *mer-8-homo-N-trans* isomer in the crystal. Hydrogen atoms and disordered solvent molecules have been omitted for clarity. Symmetry operation *i*: $1/3+x-y$, $2/3-y$, $1/6-z$.

Single crystals suitable for X-ray analysis of *mer-8* were acquired by slow evaporation of an ethanol/dichloromethane solution. The system was trigonal with space group $R\bar{3}c$.²³ The molecule is located on a crystallographic twofold axis which is bisecting the heteroligand (ppy) and the iridium centre. Due to this symmetry, a differentiation between carbon and nitrogen on the heteroligand is not possible. In the refinement this was handled as occupational disorder between nitrogen N2/N2' and carbon C18/C18'. The molecular structure confirmed that a *mer*-isomer had indeed been isolated (figure 4, homo-ligand N's *trans* to each other). The three cyclometallating ligands are aligned in an octahedral configuration around the iridium centre. As with the previous crystal structure, the C-C and C-N bond lengths and angles are within normal ranges expected for

mer-tris-cyclometallated iridium(III) complexes. The complex is assigned the name *mer-8-homo-N-trans* because the nitrogen atoms of the homoligands (tolpy) are arranged *trans* to each other. The orientation of the ppy ligand (N2/C18 *trans* to C11 or C11ⁱ) will only govern whether a Λ or Δ enantiomer/helimer has formed. As a consequence of the centrosymmetry of the space group the whole crystal is racemic.

Table 1. Bond length (Å) information about *mer-7*- and *mer-8-homo-N-trans* compared to *mer-6*. Symmetry operation i: 1/3+x-y, 2/3-y, 1/6-z.

mer-6 ^{20(a)}		mer-7.1		mer-7.2		mer-8	
Ir-N1	2.151(9)	Ir1-N11	2.142(3)	Ir2-N14	2.136(3)	Ir1-N2/C18	2.119(3)
Ir-N2	2.044(8)	Ir1-N12	2.047(3)	Ir2-N15	2.048(3)	Ir1-N1 ⁱ	2.041(2)
Ir-N3	2.065(8)	Ir1-N13	2.032(3)	Ir2-N16	2.034(3)	Ir1-N1	2.041(2)
Ir-C1	2.076(10)	Ir1-C121	2.076(4)	Ir2-C124	2.071(4)	Ir1-N2 ⁱ /C18 ⁱ	2.119(3)
Ir-C2	2.086(12)	Ir1-C122	2.073(4)	Ir2-C125	2.074(4)	Ir1-C11	2.041(3)
Ir-C3	2.020(8)	Ir1-C123	2.018(4)	Ir2-C126	2.001(4)	Ir1-C11 ⁱ	2.041(3)

7.2.3 Stereochemical aspects of heteroleptic [Ir(C,N)₂(C',N')] complexes.

The complexes *mer-7*- and *mer-8-homo-N-trans* are geometrical isomers. There are three possible geometrical isomers of both *mer-7* and *mer-8* which are depicted in figure 5. The *homo-N-trans* isomer is the acquired product from the reaction of *C*₂-*trans* starting material **3**. The *homo-C-trans* isomer shows the cyclometallated carbons of the homo ligands lying *trans* to each other. The *homo-cis* isomer shows cyclometallated carbons, and coordinating nitrogen's of the homoligands lying *cis* to one another. Each of the depicted geometrical isomers also has two enantiomers/helimers, Λ and Δ . We have found no reports commenting on any other isomer than *homo-N-trans*-type isomers in bis-cyclometallated (C,N) iridium(III) complexes. This report is the first to deal with tris-cyclometallated isomers in detail. The attained *mer-7*- and *mer-8-homo-N-trans* are racemic mixtures. The entering heteroligand does not show preference for one enantiomer over another.

It is timely at this point to discuss why the formation of only the *mer-homo-N-trans* isomers is observed in the synthesis of *mer-7* and *mer-8*. A close look at starting materials **3** and **4** gives us some clues. Complexes of the type **3** or **4** are believed to be dimeric octahedral *C*₂-*trans-N* isomers (figure 6). We attained crystals suitable for X-ray diffraction measurements of **3**. The refined crystal structure showed severe disorder at the ligand sites. However, a 4-centred-4-electron IrCl₂Ir core was observed, with no disorder. The molecular geometry of **4** in the solid state was previously reported showing a dimeric complex with *C*₂-*trans-N* geometry.²¹ We have observed that in coordinating solvents a non-symmetrical system is formed, *i.e.* ¹H NMR in CD₂Cl₂ showed **3** to

have eight peaks in the aromatic region, whereas for **3** dissolved in d_6 -DMSO 16 peaks in the aromatic region were observed. Previous reports point towards the likelihood that the dimer is in equilibrium with a monomer in non-coordinating solution.²⁴ All of these observation points to only *N-trans* type compounds, and absolutely no isomerisation to a *C-trans* or other isomers is observed.

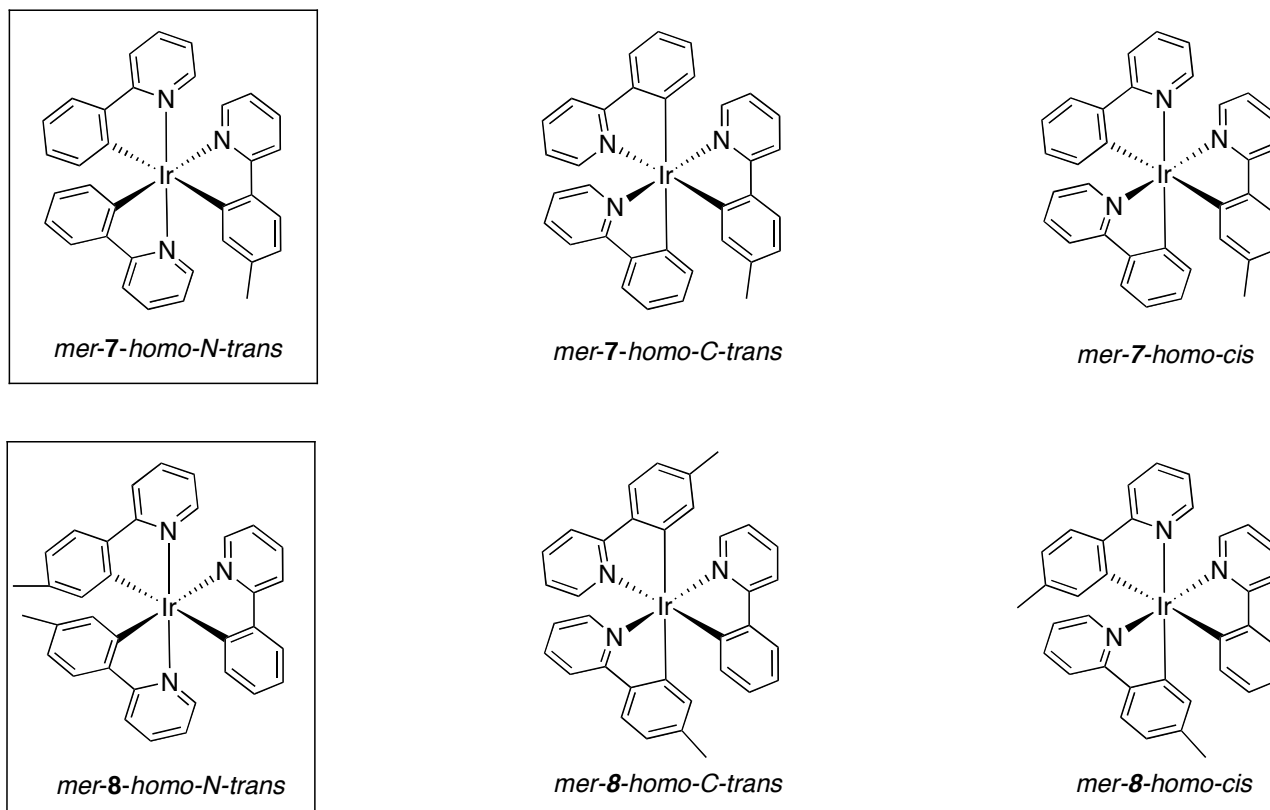


Figure 5. Geometrical isomers of *mer-7* and *mer-8* (the highlighted compounds are the synthesised species).

The *trans-N* configuration of **3** forms as a result of the reaction of $[\text{IrCl}_3 \cdot 3\text{H}_2\text{O}]$ with cyclometallating ligand. A previous report has stated that Hppy reacts with $[\text{Ir}(\text{acac})_3]$ to yield pure *fac*- $[\text{Ir}(\text{ppy})_3]$.^{1(b)} The mechanism is debated in the report and the authors state that when intermediate $[\text{Ir}(\text{ppy})_2(\text{acac})]$ is formed from $[\text{Ir}(\text{ppy})(\text{acac})_2]$, the *trans*-effect predicts that an incoming nitrogen ligand will attack *trans* to an aryl carbon in preference to an acac or pyridine ligand, this would result in an intermediate $[\text{Ir}(\text{ppy})_2(\text{acac})]$ C_1 isomer. So far, no proof of the formation of this isomer was presented and no such analogous C_1 complexes have previously been reported. Furthermore, this reaction was carried out in refluxing glycerol, which is an ideal condition for *mer*- to *fac*- isomerisation. Therefore, no proof that a C_2 -*trans-N* $[\text{Ir}(\text{ppy})_2(\text{acac})]$ had formed and further reacted to give *mer*- $[\text{Ir}(\text{ppy})_3]$ which eventually isomerised to *fac*- $[\text{Ir}(\text{ppy})_3]$, was given.

According to the authors $[\text{IrCl}_3]$ would be expected to react with Hppy in a similar manner to $[\text{Ir}(\text{acac})_3]$, but does not. The authors explain that because chloride is a monodentate ligand, the intermediate “ $[\text{Ir}(\text{ppy})\text{Cl}_2]$ ” complex forms a pentacoordinate dimeric complex which leads to the formation of the C_2 -*trans-N* $[\text{Ir}(\text{ppy})_2\text{Cl}]$ complex (the observed product). In the synthesis of **3** from $[\text{IrCl}_3 \cdot 3\text{H}_2\text{O}]$ with excess Hppy, ~10% *fac-5* ($[\text{Ir}(\text{ppy})_3]$) is always observed. This is probably

as a result of the intermediate “[Ir(ppy)Cl₂]” reacting with Hppy to yield a C_1 -[Ir(ppy)₂Cl] which requires less energy to react further to yield *fac*-**5** than the C_2 -*trans-N*-[Ir(ppy)₂Cl] requires to yield *mer*-**5**. No traces of *mer*-**5** are observed in the reaction. A C_1 isomer of analogous systems has never been reported (one N *trans* to a C, one N *cis* to a C, and one N and one C *trans* to ‘free’ sites, no symmetry). It is also possible that in solution these systems have a *tbp-trans-N* or *sp-trans-N-trans-C* or *sp-cis-N-cis-C* geometry (figure 6).

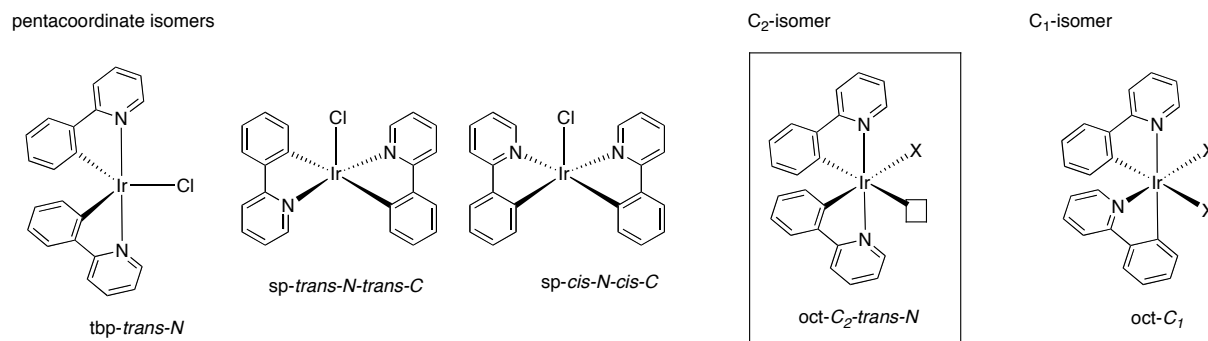


Figure 6. Possible geometrical isomers of monomeric $[\text{Ir}(\text{C},\text{N})_2\text{X}]$ complexes. The highlighted structure is the observed structure in the solid state.

We have attempted isomerisations of **3** at extreme conditions, and *never* have we observed isomerisation of **3**. The *trans-N* configuration of **3** holds when other ligands, either monodentate or bidentate monoanionic ones, are substituted for the halide, for example cyanide^{7(c)} and *acac*^{24(a)} complexes. We have also observed that *no* C_2 -*trans-N* to C_1 or C_2 -*trans-C* (likewise *tbp-trans-N* to *tbp-cis* or *tbp-trans-C*) isomerisation of these complexes occurs even under relatively extreme conditions.²⁵

In the reaction of **2** with **3**, *mer-7-homo-N-trans* is the observed product. The reaction is believed to be an electrophilic substitution reaction by electrophilic attack of the metal on the *ortho* carbon of the ligand.^{1(d)} If we consider how Hppy reacts with the possible forms of **3** we can draw some conclusions (figure 6). No ligand scrambling or the formation of non-*homo-N-trans* products was observed in the synthesis of *mer-7-homo-N-trans*, suggesting that homoligands remain bound, in the *trans-N* fashion, to the iridium centre, throughout the reaction.²⁵ This makes the *sp* geometries highly unlikely; if the attacking ligand were to coordinate at the free site of either *sp* isomers the electrophilic attack on the *ortho*-carbon would likely result in the decoordination of one of the cyclometallating pyridyl ligands. This would inevitably result in the formation of *fac*-products or *mer-homo-cis* or *mer-homo-C-trans* products (see figure 6).

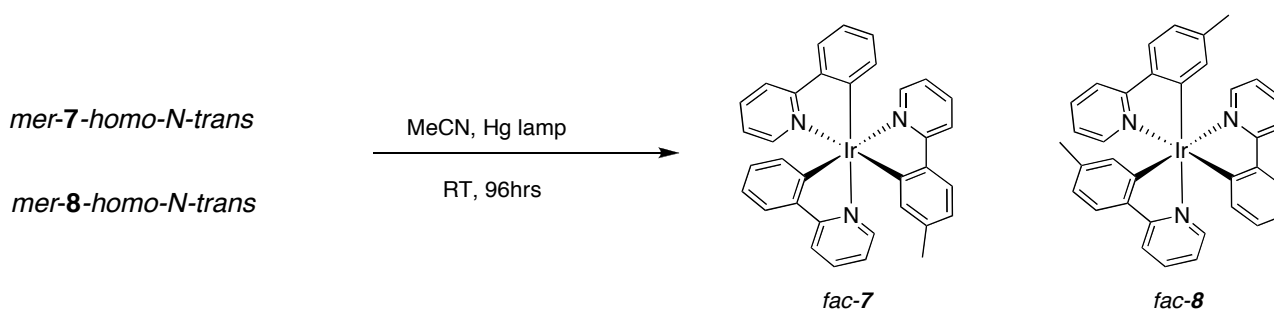
In the case of *tbp* the site at which Hppy reacts only enforces the helicity of *mer-7-homo-N-trans* (*i.e.*, Λ or Δ) if the attacking pyridine coordination is at the point along Cl-Ir-C plane. Attack *trans* to the Cl ligand (C-Ir-C plane) would yield non-*homo-N-trans* products, and is thus unlikely. This is also the case with C_2 -*trans-N*. Because the homoligands remain *trans-N* in the synthesis of *mer-7-homo-N-trans* we assume they play no role in the reaction, and their geometry never changes with respect to each other during the cyclometallation reaction. If there were any geometrical positional ligand exchange, different geometrical isomers would definitely be

expected.²⁶ A *mer-homo-N-cis* heteroleptic complex has previously been reported, via an unusual synthetic procedure, however how it formed was not discussed.^{4(a)}

7.2.4 Synthesis and Characterisation of Heteroleptic Complexes [Ir(C,N)₂(C',N')]; *fac*-Isomers of **7** and **8** Obtained by *mer*- to *fac*- Isomerisation

All experiments in the following section were carried out in the absence of natural light. The acquired complexes *mer-7-* and *mer-8-homo-N-trans* could be quantitatively converted to *fac-7* and *fac-8* photochemically, without scrambling of ligands, by stirring the complexes in deoxygenated acetonitrile at room temperature over 4 days in the presence of a medium pressure 150W Hg UV lamp (scheme 3). Similar synthetic techniques with analogous systems were published during the time this work was carried out.²⁷ The ¹H and ¹³C NMR spectra of *fac-7* and **-8** showed a slight shift in the resonance ppm's of all aromatic and tolyl CH's in comparison with *mer-7-* and *mer-8-homo-N-trans*. UV absorption spectra showed three distinct absorptions at 245/247nm, 285/286nm, and 376/376nm respectively (figure 7d), similar to that of *fac-5/6*. *Fac-7* and **-8** have only one geometrical isomer. They both have two enantiomers/helimers, Λ and Δ. The attained *fac-7* and **-8** are racemic mixtures. Crystals suitable for X-ray diffraction of *fac-8* were acquired. However, the CH₃ groups could not be localised on a specific ligand. Partially populated tolyl-CH₃ positions of all three ligands were observed.

Scheme 3. Photochemical conversion of *mer-7-* and *mer-8-homo-N-trans* to *fac-7* and *fac-8*.



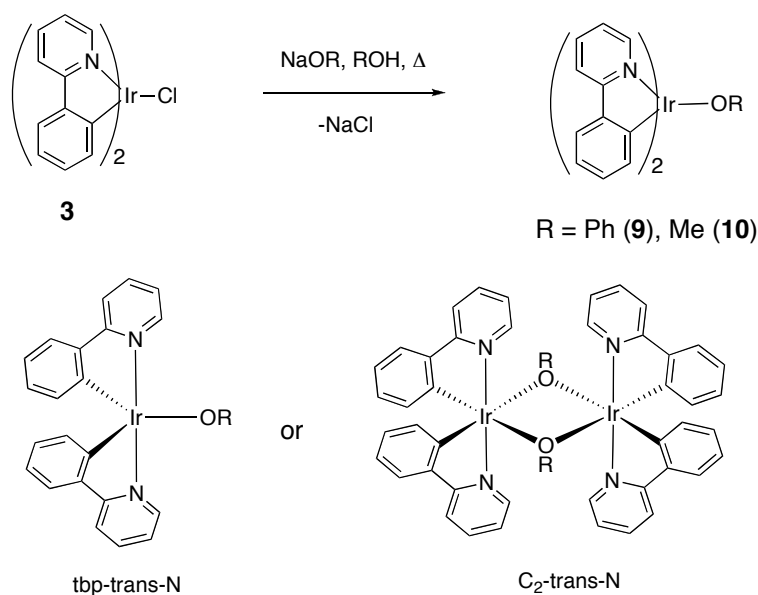
7.2.5 Synthesis and Characterisation of Heteroleptic [Ir(C,N)₂(alkoxide)] Complexes

All experiments in the following section were carried out in the absence of light. We believe iridium alkoxide complexes to be intermediates in the thermal *mer*- to *fac*-isomerisation. To this date, all reports on the isomerisation (also see later in this report) have been carried out in alcoholic solvents. We have therefore synthesised iridium alkoxide [Ir(C,N)₂OR] complexes and studied their reaction with cyclometallating ligands. Complex **3** was added to a solution of NaOPh in large excess. A colour change was observed after heating, from yellow to dark orange. A single isomer of **9** was isolated after 24h which was identified using ¹H and ¹³C NMR spectroscopy and elemental analysis. We observed a symmetrical ¹H NMR spectrum (scheme 4). Two isomers are possible for **9**; either a dimeric structure comprising octahedral hexacoordinate iridium centres in a *C₂-trans-N* configuration; or a monomeric structure with a five-coordinate iridium centre with both nitrogen's *trans* to each other in the case of an ideal *tbp-trans-N* (see scheme 4). In

both structures a symmetrical ^1H NMR spectrum is expected (11 aromatic H resonances, 8 ppy, 3 phenolate) which indeed has been observed for **9**. The alternative dimeric asymmetrical C_1 complex would show a non-symmetrical ^1H NMR spectrum which is obviously not the case. Only the dimeric C_2 -*cis* complex would also show a symmetrical ^1H NMR spectrum. However, we believe it unlikely that the C_2 -*trans-N* complex **3** would yield a C_2 -*cis* complex without any signs of a C_1 complex. Moreover, previous reports of the synthesis of the analogous hydroxyl and solvento- complexes stated that the complex was a dimeric C_2 -*trans-N* isomer.^{20(a)}

Complex **10** was synthesised in a similar manner, however it showed very low solubility in all organic solvents, and thus was not characterised using NMR techniques.

Scheme 4. Synthesis of iridium(III) alkoxide complexes and possible isomers thereof.



Heating of complex **9** in phenolic solution at reflux showed no change in the constitution of the complex, the complex stayed in the C_2 -*trans-N*/*tbp-trans-N* configuration. To study whether complexes **9** and **10** could be the starting point for the synthesis of tris-cyclometallated $[\text{Ir}(\text{C},\text{N})_3]$ complexes they were separately dissolved in 1,2-dichlorobenzene (*mer-fac* isomerisation does not occur in this solvent, b.p. 180°C) with one equivalent of Hppy and heated to reflux (in darkness). After 24 hrs the reactions were stopped. With both complexes **9** and **10** ^1H NMR and UV-vis spectroscopy both showed the presence of [tris(2-pyridinyl- κN)phenyl- κC^2]iridium(III) complex **5**. In the case of **9** more than 50% was *fac-5*. Similarly complexes **9** and **10** were reacted with Htolpy. The formation of tris-cyclometallated products was also observed, however *with* scrambling of ligands. These are the only examples of non-photochemical *fac-* product formation in hydroxyl-free solvents. Obviously one equivalent of ROH is released during this reaction, which could then promote *mer-* to *fac-* isomerisation of any formed *mer-* species (see later in this report).

7.2.6 Photophysical Aspects of the $[\text{Ir}(\text{C},\text{N})_2(\text{C}',\text{N}')] (7 \text{ and } 8)$ and $[\text{Ir}(\text{C},\text{N})_2\text{OR}] (9 \text{ and } 10)$ Complexes

As stated above *mer-7* and *-8-homo-N-trans*, and *fac-7* and *-8* show similar photophysical properties to the homoleptic complexes **5** and **6**. Table 2 shows a summary of all absorption and emission results. As is common in trisarylpyridine iridium complexes intense absorption bands are observed between 240nm and 300nm. These are assigned to spin-allowed ($\pi\text{-}\pi^*$ transitions) of the ligand. Peaks above 350nm are assigned to both spin allowed and spin forbidden MLCT transitions.

In the range of isolated *fac*-isomers of complexes **5,6,7**, and **8**, the position of the band at approximately 245nm increases from *fac-5* through *fac-8*. Similarly the band at ~285nm is bathochromically shifted. The band of the *mer*-isomers **5,6,7**, and **8** at ~276nm shows similar bathochromic shift along the series. In the *fac*-complexes the relative intensity of the bands decreases along the series. The absorption at ~245nm becomes gradually less intense relative to the absorption at ~285nm when going from complexes *fac-5* to *fac-8*. The red-shifting of the bands with increased tolyl substitution is indicative of a decrease in energy of the π^* orbital or an increase in the energy of the π orbital. This would correspond to a decreased energy required to excite the complex. This is believed to be as a result of energy donation from the CH_3 group to the HOMO. The position of the CH_3 group is in fact very important in this aspect, and a thorough study on this particular topic has been reported.^{6(c)}

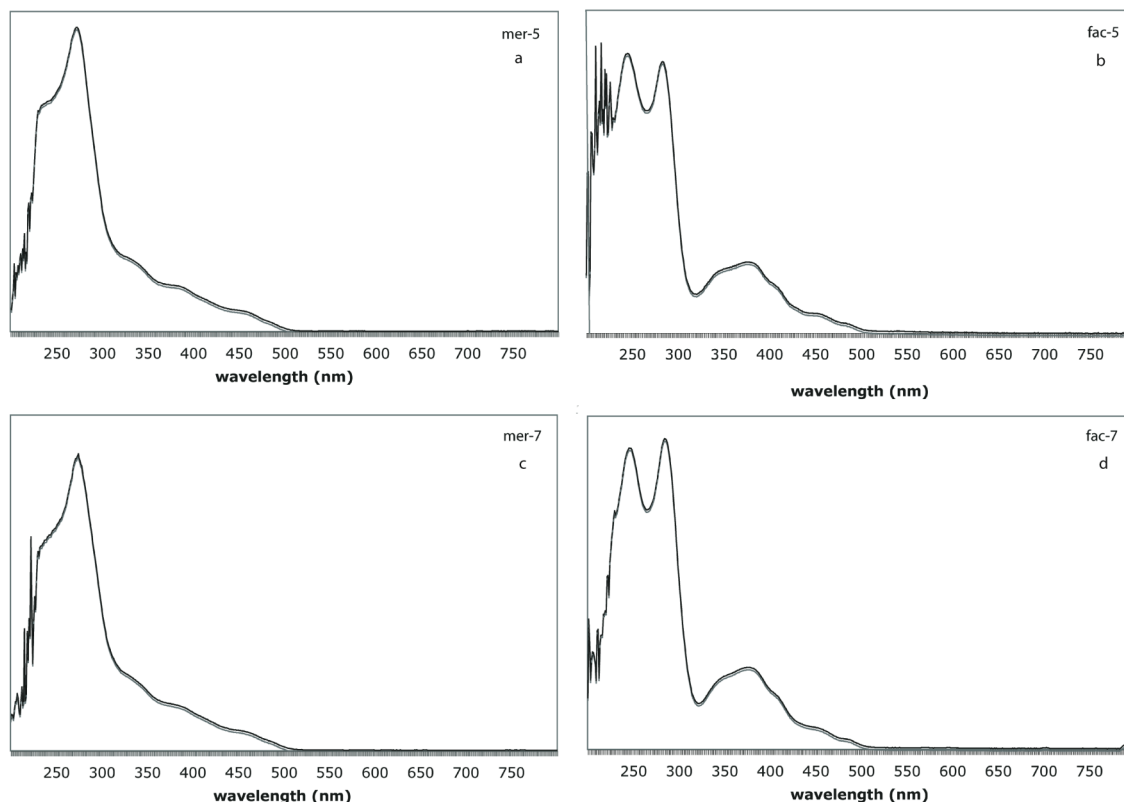


Figure 7(a-d). UV-vis absorption spectra of a) *mer-5*, b) *fac-5*, c) *mer-7-homo-N-trans*, d) *fac-7*.

Both the acquired *mer-homo-N-trans* and *fac*-isomers of both **7** and **8** are luminescent at room temperature, with the *fac*-isomer showing intense luminescence at ~ 513nm. The luminescence of the *mer*-isomers is red-shifted (577nm) and its efficiency is an order of magnitude lower than that of the *fac*-isomer.

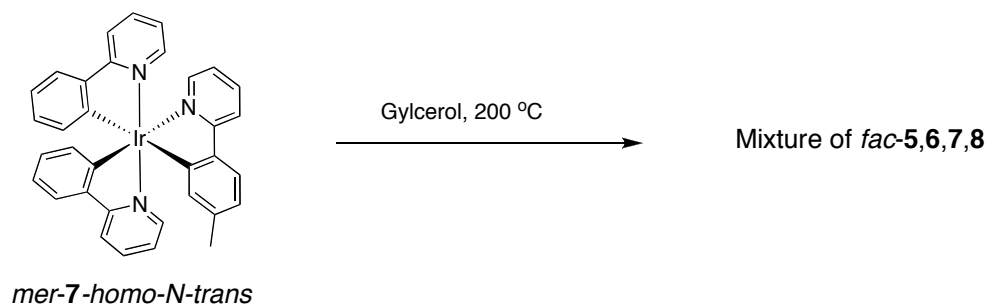
The [Ir(C,N)₂OR] complexes **9** and **10** show absorption spectra similar to that of the *mer*-type trisphenylpyridine iridium complexes. A strong absorption at around ~ 266nm (spin allowed π - π^* transition) is observed with weaker absorptions seen at ~ 400, 450, and 500nm (spin forbidden MLCT). The emission spectra of **9** and **10** show bands between 530 and 600nm, showing better quantum efficiencies than the *mer*-complexes **5-8**. In fact **10** shows a quantum yield two times greater than that of *fac*-complexes **5-8**.

Table 2. photophysical and electrochemical properties of complexes **5-10**.²⁸

Complex	Absorption λ (nm), { ϵ , 10 ³ L mol ⁻¹ cm ⁻¹ }	Emission 298K(nm) (RT MeTHF)	Φ (RT MeTHF)	Redox (V)
<i>Mer-5</i>	276 (51.0), 339 (9.2), 382 (10.7), 457 (3.4)	512	0.036	0.25
<i>Fac-5</i>	244 (45.5), 283 (44.8), 377 (12.0)	510	0.40	0.31
<i>Mer-6</i>	276 (53.3), 336 (12.4), 383 (8.4), 456 (0.9)	550	0.051	0.18
<i>Fac-6</i>	248 (41.4), 287 (44.7), 374 (11.8)	510	0.50	0.30
<i>Mer-7-homo-N-trans</i>	272 (53.1), 332 (12.9), 381 (8.3), 455 (2.9)	561	0.10	0.25
<i>Fac-7</i>	245 (47.6), 285 (48.3), 376 (12.9)	513	0.36	0.30
<i>Mer-8-homo-N-trans</i>	276 (52.2), 335 (13.0), 387 (7.3), 455 (2.9)	569	0.10	0.21
<i>Fac-8</i>	247 (40.4), 286 (43.1), 376 (11.3)	513	0.54	0.29
9	264(59.0), 383 (8.7), 417 (6.2), 468 (2.3), 499 (1.4)	534	0.18	0.63
10	266 (33.4), 399 (5.1), 464 (1.7), 505 (1.2)	596	0.83	0.50

7.2.7 Investigation of Thermal *mer*- to *fac*- Isomerisation

All experiments in the following section were carried out in the absence of light. Earlier studies have shown that heating of *mer*-[Ir(ppy)₃] in glycerol at 200^oC for 24 hours yields *fac*-[Ir(ppy)₃].¹¹ Heating of either *mer-7*- or *-8-homo-N-trans* in glycerol at 200^oC for 24 hours did not yield pure *fac-7* or *-8*, respectively, but instead a mixture of complexes **5-8** (scheme 5). UV-vis absorption suggested that *fac*-type isomers were present. MALDI-TOF mass analysis showed a similar pattern of the *fac-5-8* mixture as is depicted in figure 1. This would indicate that scrambling of ligands has occurred during isomerisation.

Scheme 5. Attempted thermodynamic conversion of *mer-7-homo-N-trans* to *fac-7*.

A number of conditions of the thermodynamic *mer-* to *fac-* isomerisation were investigated;

a) To investigate intermolecular interactions, isomerisations under thermal conditions were carried out, while varying the dilution of *mer-7-homo-N-trans* in glycerol. At every dilution *mer-* to *fac-* isomerisation was observed with ligand scrambling. By ^1H NMR/MALDI-TOF there was no observable difference in the intensity of the various peaks corresponding to compounds **5-8** when using different dilutions. Therefore the process of ligand scrambling is *not* concentration dependent.

b) Upon gradual heating of a solution of *mer-7-homo-N-trans* in glycerol, from 150 $^{\circ}\text{C}$ to 200 $^{\circ}\text{C}$, no *mer-* to *fac-* isomerisation occurred below 191 $^{\circ}\text{C}$. Furthermore, ligand scrambling products **5**, **6**, or **8** were not observed below 191 $^{\circ}\text{C}$.

c) *Mer-* to *fac-* isomerisation was a faster process in the absence of base. When base (K_2CO_3) was present the process was an order of magnitude slower. In both cases ligand scrambling was observed.

d) From experiments involving the heating of *fac-7* for 24 hours in glycerol at 150 $^{\circ}\text{C}$ or at 200 $^{\circ}\text{C}$ (with and without K_2CO_3 present) pure *fac-7* was recovered quantitatively. Neither *mer-* products nor ligand scrambling products were observed in this set of experiments.

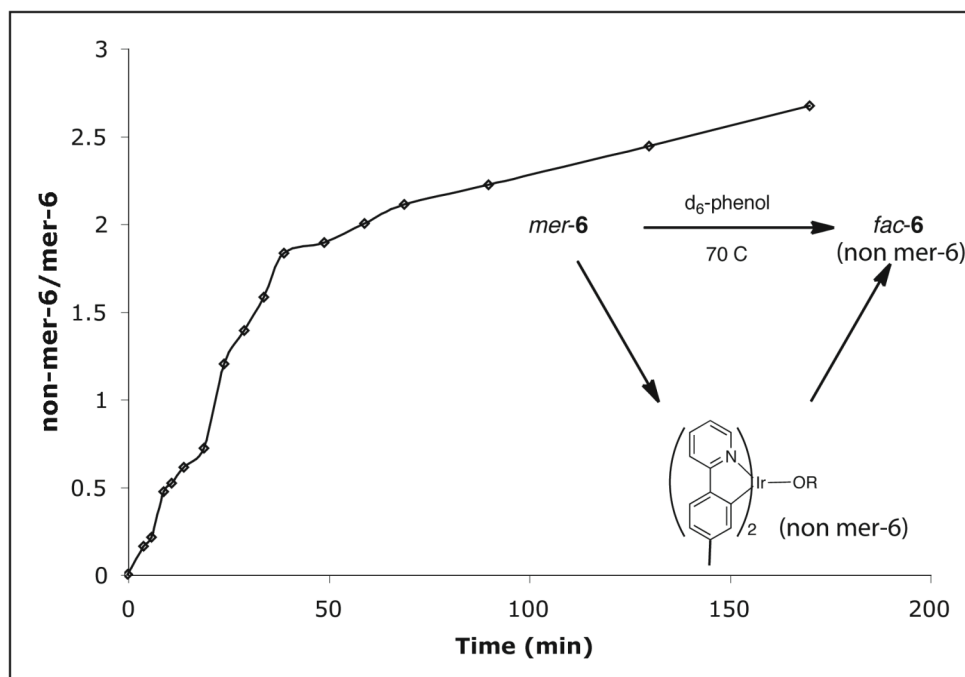
e) A range of solvents was then tested. In refluxing decane (174 $^{\circ}\text{C}$) *mer-7-homo-N-trans* did not dissolve or isomerise to *fac-* product(s), nor was ligand scrambling observed. Moreover, with *mer-7-homo-N-trans* dissolved in refluxing 1,2-dichlorobenzene (180 $^{\circ}\text{C}$) or benzonitrile (191 $^{\circ}\text{C}$), respectively, *no* isomerisation or ligand scrambling was observed and the starting material was recovered (likewise, when *mer-5* is used in these experiments, no isomerisation was observed). However, when glycerol (in excess) was added to the refluxing decane solution, isomerisation with scrambling was observed. In neat 1-decanol at 200 $^{\circ}\text{C}$, *mer-7-homo-N-trans*, was converted to the *fac-5,6,7,8* mixture while decomposition was also observed. In refluxing phenol (184 $^{\circ}\text{C}$) complete conversion to *fac-* isomers, with ligand scrambling, was observed. Subsequently it was found that in non-crystalline (50 $^{\circ}\text{C}$) phenol *mer-7-homo-N-trans* was converted to the *fac-5,6,7,8* mixture, however, over a substantially longer time period (compared to the reaction done in refluxing phenol). This is a very important point because it was often believed that a temperature above 150 $^{\circ}\text{C}$ was necessary to facilitate isomerisation. In fact, a refluxing solution of 1,2-dichlorobenzene with *mer-5* and 10mol% phenol (compared to *mer-5*), showed 40% *mer-* to *fac-* conversion in

24hrs. Water, when added to a glycerolic or phenolic solution of *mer-7-homo-N-trans* and heated to reflux, had *no* effect on the rate of isomerisation or on the extent of scrambling.

From the observations made with these solvent tests we can deduce that under thermal conditions, isomerisation of *mer-* compounds to *fac-* compounds is an alcohol catalysed reaction.

It was noted that similar quantities of scrambling products were observed throughout. That is, the amounts of individual *fac*-isomers in the *fac-5, 6, 7, 8* mixture did not vary considerably in all experiments that were performed. Figure 1 shows an average distribution pattern of the thermal reaction of *mer-7-homo-N-trans* to a *fac-5, 6, 7, 8* mixture. Complex **7** was the most abundant while only minute amounts of **5** were observed (max. 5%). This indicates that conditions did not affect the extent of ligand scrambling and scrambling was a statistical phenomenon.²⁹

For real time analysis of the thermal isomerisation process of homoleptic complexes, complex **6** was used because it was the easiest to monitor using 1H NMR.³⁰ An NMR tube at $70^\circ C$ was loaded with *mer-6* and d_6 -phenol and spectra were taken at certain time increments. Graph 1 represents the disappearance of *mer-6* complex vs. formation of non-*mer-6* compounds.³¹



Graph 1. Conversion of *mer-6* over time at $70^\circ C$ in d_6 -phenol.

The conversion of *mer-6* (all CH_3 's non-equivalent) did not show a simple disappearance of its three tolyl peaks and a concomitant appearance of one tolyl peak for *fac-6* (all CH_3 's equivalent). In fact, several new and overlapping peaks were observed in the tolyl CH_3 region of the 1H NMR spectrum during the course of the reaction (figure 8). Two of the new peaks can be assigned as free Htolyl (2.34ppm) and *fac-6* (2.26ppm). Two other non-equivalent peaks at 2.10 and 2.08ppm (upfield of all other peaks) are unidentifiable. The peak at 2.10ppm appears rapidly upon introduction of *mer-6* to the d_6 -phenol solution. It then increases in intensity at a similar rate to the consumption of *mer-6* aromatic signals.

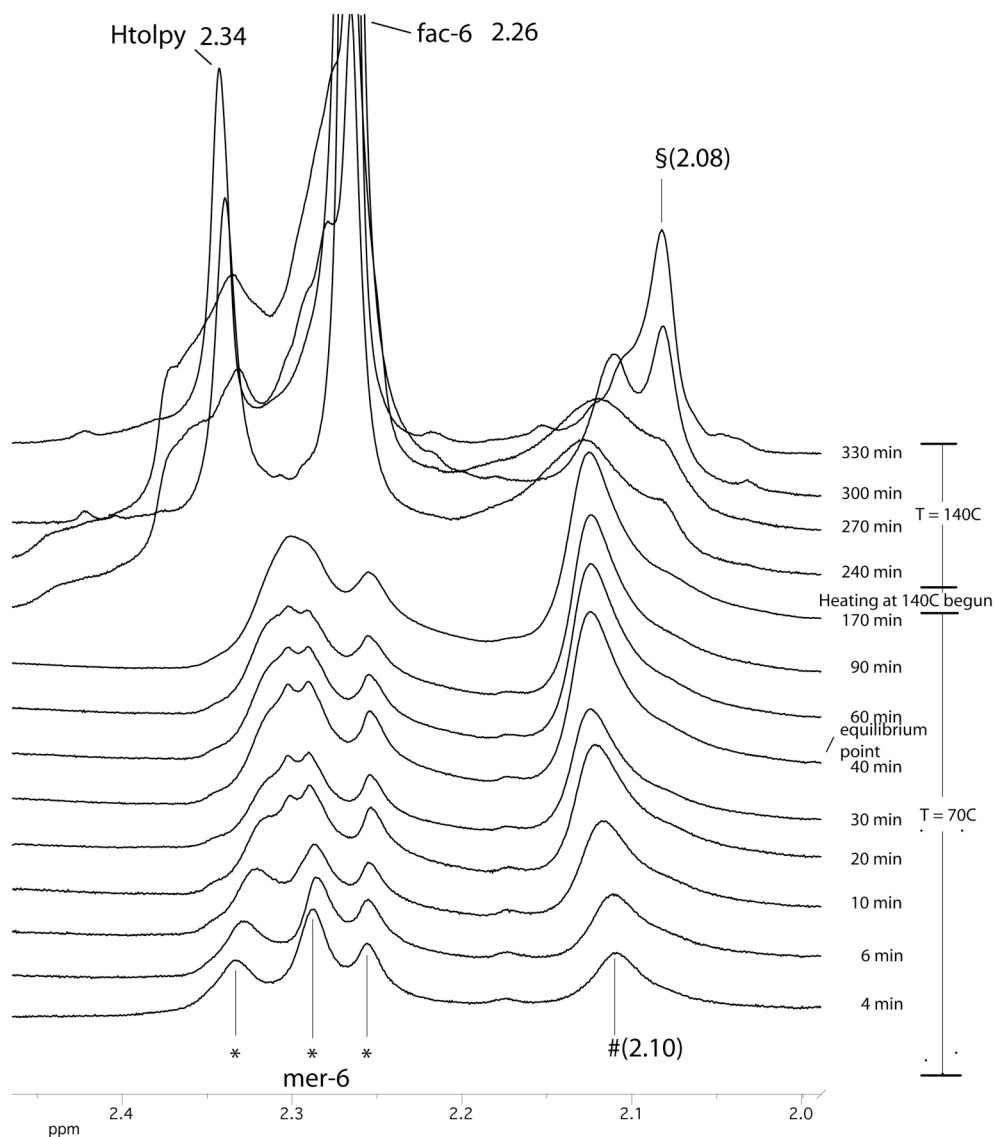


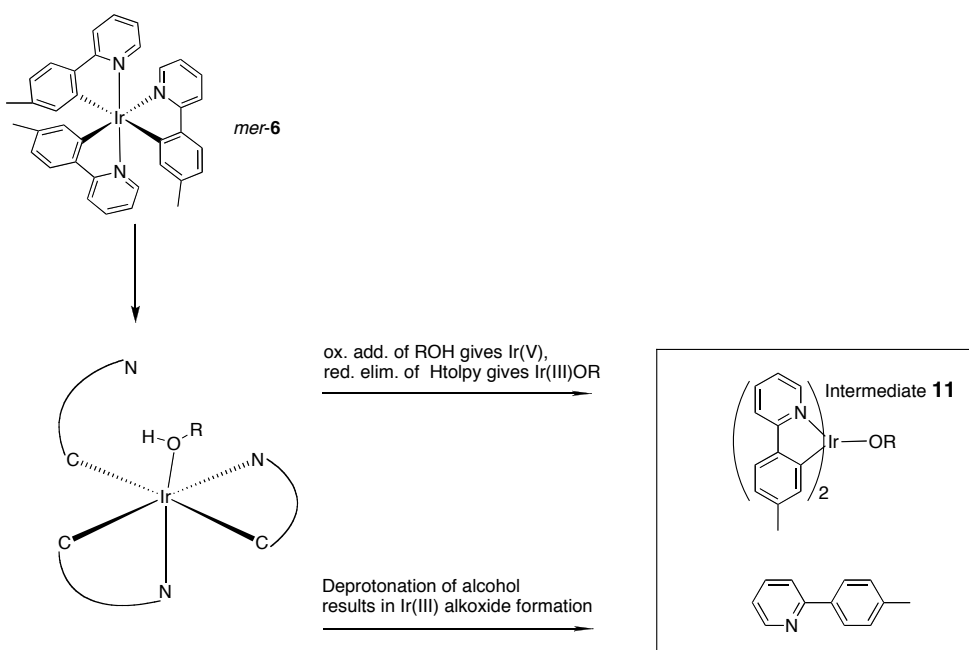
Figure 8. Toluyl CH_3 region of 1H NMR of conversion of *mer-6* to non-*mer-6*/*fac-6* in d_6 -phenol at $70^\circ C$.

After approximately 40 mins., the slope of the plot changes, suggesting a change in rate determining process. When the reaction is complete, thus when all *mer-6* has been consumed, there are three signals observable in the d_6 -phenol solution 1H NMR spectrum. These belong to *fac-6* (2.26ppm) and a small quantity of free Htolpy (2.34ppm). We have been unable to identify the peak at 2.08ppm, however we believe it may be unreacted intermediate(s). The presence of Htolpy suggests the loss of a ligand in the isomerisation process and the formation of an $[Ir(C,N)_2X]$ intermediate possibly represented by the peaks at 2.08ppm or 2.10ppm. The conversion of *mer-6* is rapid until approximately 66% of it has been consumed (~40 mins.). After that there is a slower disappearance of *mer-6* until it is completely consumed. This would suggest that there is an equilibrium between *mer-6* and an intermediate complex which is not *fac-6*. *Fac-6* is then formed from the intermediate, and does not convert back. In fact, no report of a back conversion, of any similar *fac*-complexes, has ever been made. We believe the change in slope of the plot is when

mer-6 and the intermediate(s) are in equilibrium. Extra heat allows the reaction rate to increase substantially.

Because ligand scrambling is observed in heteroleptic systems, we assume an iridium-carbon bond breakage. We propose that exchange of an N-donor pyridine ligand by alkoxide can occur by either dissociative or associative pathways (scheme 6). We also propose that all Ir-C bonds remain intact during this exchange. Ligand substitution can now occur in one of two ways; 1) nucleophilic attack on the Ir(III) centre, of the hydroxyl resulting in loss of Htolpy, and formation of an iridium(III) alkoxide species (**11**); 2) oxidative addition of the coordinated alcohol yielding an Ir(V) species. This species could then reductively eliminate Htolpy and result in an iridium(III) alkoxide species (**11**). The formation of an intermediate is substantiated by the fact that an equilibrium between *mer-6* and another complex(es) was observed. The observance of free ligand further supports this theory. The subsequent reaction of the intermediate **11** with released Htolpy can either yield tris-cyclometallated *mer*-type complexes or yield thermodynamically stable *fac*-type complexes. We therefore observe a change in the reaction kinetic profile once the equilibrium has been reached.

Scheme 6. Intermediate formation from *mer-6* during thermal isomerisation in d_6 -phenol.



If we closely examine how *mer-6* loses Htolpy we can clarify the kinetic measurements further. When considering how the *mer-* to *fac*-isomerisation proceeds, which of the tolyl moieties of *mer-6* becomes substituted by -OR at the iridium centre, to yield intermediate **11**, is important. *Mer-6*, which has no geometrical isomers, can form different alkoxide intermediates **11(a-c)**. Either a *trans-N*, *trans-C*, or a *cis* isomer can form (figure 9, depicted as *tbp* for clarity, most likely octahedral alkoxide bridged dimers). This observation explains why we see more than one newly formed peak in the tolyl CH_3 region of the 1H NMR kinetic measurements. There are three possible isomers, which would all give contrasting 1H NMR signals. We cannot explain why excess Htolpy

and an unidentified compound (peak at 2.08ppm) are present at the end of the isomerisation reaction.

In the following discussion the monodentate alkoxide intermediate complexes **11(a-c)**, when reacting with the formed Htolpy, are believed to behave the same as the monodentate chloride complex **3** in the synthesis of *mer-7-homo-N-trans*. That is, the remaining cyclometallated Ir-bound ligands of **11(a-c)** do not lose their configuration relative to each other (the *trans-N*, *trans-C*, or *cis* configuration is held) in the subsequent reaction. When **3** is reacted with Htolpy the ppy ligands bound to the iridium *never* lose their configuration relative to each other. That is believed to be as a result of a high energetic barrier to Berry pseudo rotation. Compared to rhodium(III), pentacoordinate iridium(III) complexes have an increased effective nuclear charge, and thus M-L sigma interactions are strengthened, and thus bond breakage and subsequent rotation is unlikely.³² In this case we believe, as a result of experimental evidence, that Berry pseudo rotation does not occur in these complexes. As stated previously complexes **3** and **9** were heated separately under high temperature in glycerol and phenol respectively, and there was no change in the *trans-N* configuration. As is the case with **3**, we believe the *sp* form of **11** is not favoured with these intermediate complexes.

In the reaction of **11(a-c)** with released Htolpy only **11a** can give *fac-6*. Intermediates **11b** and **11c** will always revert to *mer-6*. The reaction of **11a** with Htolpy would yield either *mer-6* or *fac-6*. If the incoming Htolpy reacts with N *trans* to N (of metal bound ligand), then *mer-6* will form. If Htolpy reacts with N *trans* to C (of metal bound ligand), then *fac-6* will form. The reaction of **11b** with Htolpy will yield either Λ or Δ enantiomers/helimers of *mer-6*, nothing else. Likewise the reaction of **11c** with Htolpy will yield either Δ or Λ enantiomers/helimers of *mer-6*, nothing else. It must be noted that phenoxide and methoxide are monodentate ligands.³³

From the observations we have made to this point, the photochemical *mer-* to *fac-* isomerisation is completely unrelated to the thermal isomerisation. In the photochemical isomerisation no ligand dissociation is believed to occur, and the isomerisation is mediated through an excited state.³⁴ *It must, once again, be noted, that all experiments in the above section were carried out in the absence of light.*

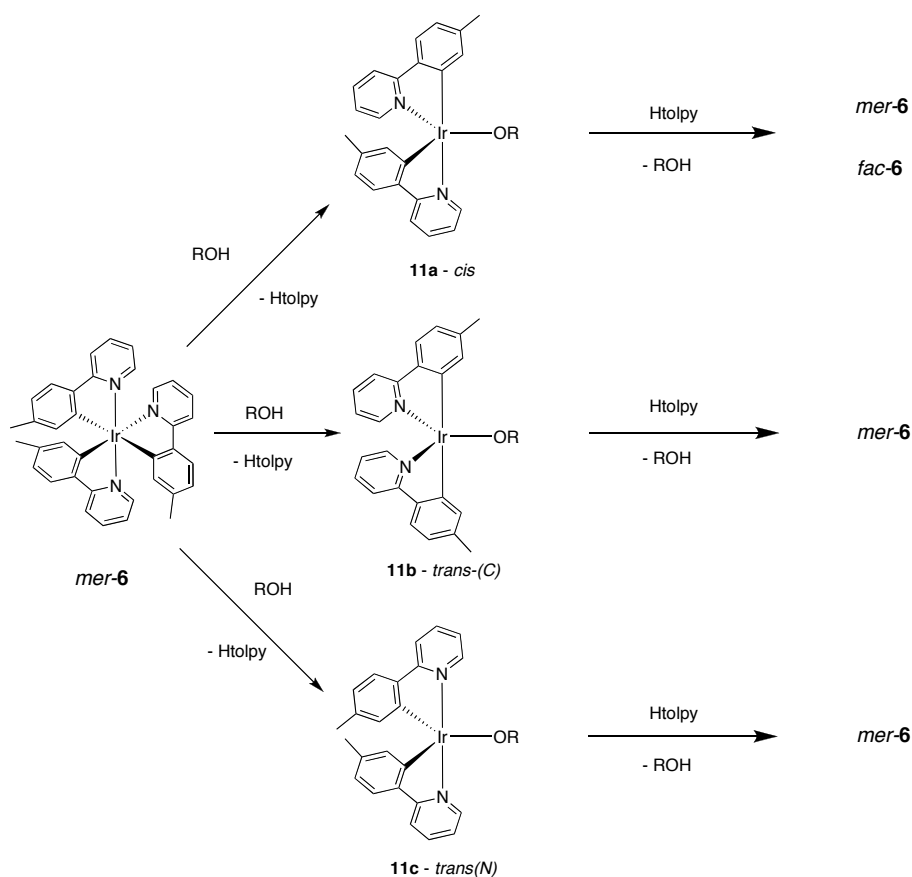


Figure 9. Ligand substitution on *mer-6* yielding alkoxide intermediates **11(a-c)** and their subsequent reaction with released Htolpy.

7.2.8 Mechanism of Thermal *mer-* to *fac-* Isomerisation of Heteroleptic $[\text{Ir}(\text{C},\text{N})_2(\text{C}',\text{N}')]]$ Complexes.

When converting *mer-7-homo-N-trans* to *fac-7* under thermal conditions, it was noted that scrambling of the ligands occurred. When the reaction was carried out photochemically *no* scrambling of ligands was observed as mentioned in the synthesis of pure *fac-7* and **-8**. If we now treat heteroleptic complexes *mer-7-* and **-8-homo-N-trans** as we have *mer-6* in the previous section, and focus on ligand substitution reactions and subsequent reaction of the formed alkoxide intermediates with released ligand we get a clear explanation for ligand scrambling. In both homo- and heteroleptic complexes ligand substitution can be approached in two ways; 1) there is a higher probability for one of the ligands over the other two ligands to be substituted or 2) any of the three ligands can be substituted and further react with the formed intermediates. In the previous section we saw that the formation of only one of the intermediates (the *Cis* isomer **11a**) resulted in the formation of the final product *fac-6*.

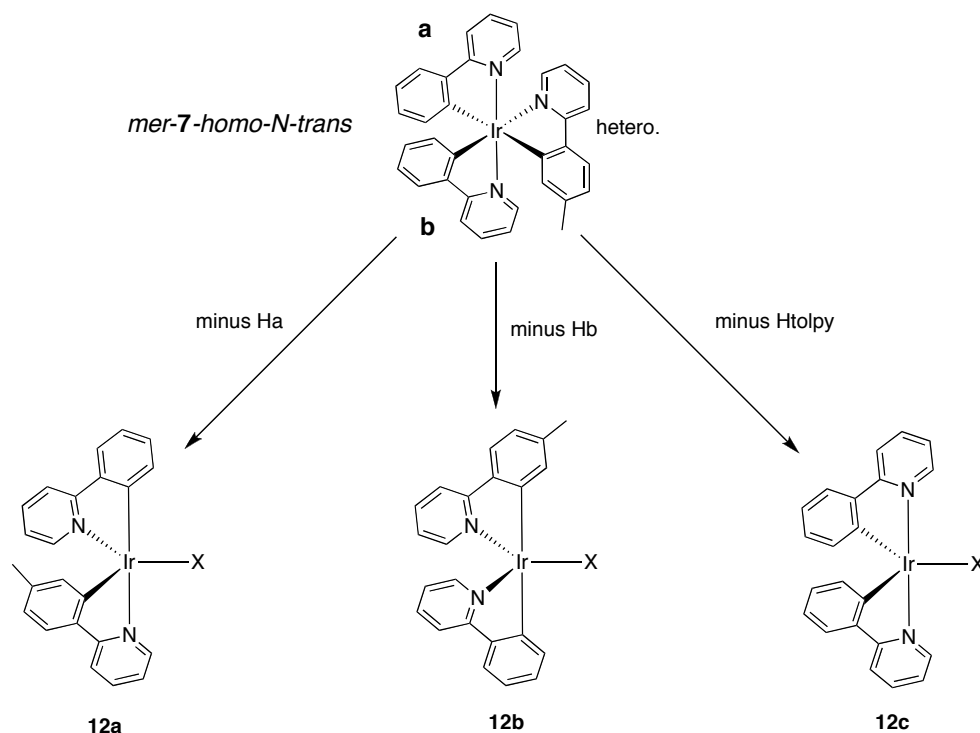


Figure 10. Substitution of ligand of *mer-7-homo-N-trans* and intermediates.

In *mer-7-homo-N-trans* each ligand must be treated separately, because they are all bound differently to the iridium centre. Ligand **a** has N *trans* to N and C *trans* to C. Ligand **b** has N *trans* to N, and C *trans* to N, and the heteroligand is a different ligand altogether (figure 10).

Figure 10 depicts the isomers (**12 a-c**) that can form as a result of substitution of ligands *only* in *mer-7-homo-N-trans*. If ligand **a** is substituted, an intermediate, *cis* configured complex, will be formed. If only ligand **a** was substituted then the only products possible, as a result of reaction of **12a** with only **a** (Hppy), would be *mer-7-homo-N-trans* and *fac-7*. If **b** dissociates a *trans-C* intermediate is formed. If only ligand **b** was substituted and **12b** had to re-react with only **b** (Hppy), *mer-7-homo-N-cis* or *-trans* would be formed. If the tolpy (heteroligand) were substituted by an alkoxide a *trans-N* isomer would be formed (**9**). Hypothesising that only the Htolpy ligand could re-react with **12c** would lead to only different enantiomers/helimers of *mer-7-homo-N-trans*. Because ligand scrambling was observed, this suggests that not one single ligand is substituted, and that all ligands can be substituted and react further. It could be that there is a preference for one ligand to be substituted easier than another, however, we cannot prove this experimentally.

We can now explain why we see *fac*-complexes **5-8** after the reaction of *mer-7*- and *mer-8-homo-N-trans* under thermal isomerisation conditions. Figure 11 only shows half of the possible complexes that can form. The newly formed *mer-8-homo-N-trans*, *mer-7-homo-cis*, *mer-8-homo-cis* and *mer-5* can all react further to give a range of *mer*- and *fac*- isomers of **5-8**. Once a *fac*- has formed it will not re-react.

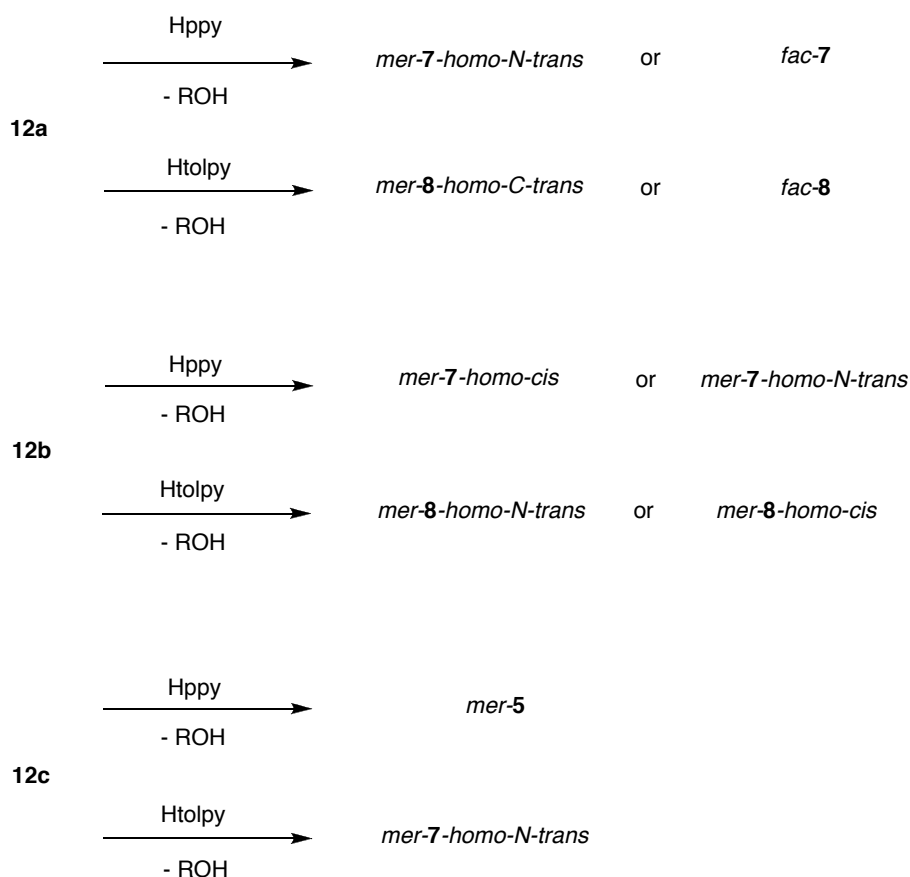


Figure 11. Products from the reaction of Hppy and Htolpy with intermediates **12(a-c)**.

A very recent report has claimed the low temperature synthesis of both *mer*- and *fac*- tris-cyclometallated homoleptic Ir(III) complexes.³⁵ The report demonstrates the synthesis of a charged C_2 -*trans-N* bis acetonitrile analogue of **3**. This is reacted with excess Hppy in 1,2-dichlorobenzene yielding only pure *fac-5*. This is claimed to be the first low temperature, protic solvent free, synthesis of such compounds. The authors also demonstrate the reaction of the analogous hydroxo compound with Hppy under the same conditions. However only pure *mer-5* is observed. The authors put this down to base inhibition of the *fac* forming reaction, and that in the absence of base (-OH group) the *fac* product would form, as is observed when the bis-acetonitrile complex is used. We disagree with this point and believe the answer is much more likely to be that the *mer* product has formed initially in both reactions, however, in the presence of acetonitrile *and light* the *mer* isomer has been converted to the *fac* isomer. This does not occur with the hydroxo system because the formed water, is probably in it's own phase not the chlorinated solvent phase. Previous reports have stated complete photochemical *mer* to *fac* isomerisation occurs in NMR tubes, containing pure *mer* compounds, left on the lab-bench for a number of days. All reactions in this report were carried out over 120 hours (5 days!). Furthermore, protic solvents show slower *mer* to *fac* photochemical isomerisation. Importantly, it is *not* stated whether all experiments were carried out in the dark or not, which is essential if searching for low-temperature, thermal isomerisation procedures.

A mechanistic proposal is given to rationalise the selection for the *fac* product over the *mer* product. This proposal depicts the formation of *fac* product by iridium(III) C-H activation of an incoming ligand, with its pyridine group coordinated, and an acetonitrile group intact. The incoming C forces the decoordination of a chelating ppy ligand preferentially to the monodentate acetonitrile. This is mediated, it is claimed, by proton transfer between the incoming ligand C-H, and the coordinated, 'departing' pyridine.

7.3 Conclusions

A number of heteroleptic tris-cyclometallated iridium(III) $[\text{Ir}(\text{C},\text{N})_2(\text{C}',\text{N}')]]$ complexes have been synthesised and fully characterised using a range of techniques. The *mer-homo-N-trans* isomer of heteroleptic complexes **7** and **8** was synthesised and converted to the *fac*-isomer using photochemical techniques. The synthesised *mer*- and *fac*- **7** and **-8** have been fully characterised and a discussion on the mechanism of their formation has been presented. The synthesis of *mer*-heteroleptic isomers followed by conversion to their *fac* isomer demonstrates a high yielding, simple protocol for the synthesis of tethered tris-cyclometallated iridium(III) complexes. This is essential for materials science, which requires covalent linkage of lumiphore materials (iridium organometallics) to hole transport and electron transport layers in LED's.

Under thermal reaction conditions the conversion of the *mer-homo-N-trans* isomers to the *fac*- complexes led to ligand scrambling. This thermal isomerisation was thoroughly investigated and it was found that it was an alcohol catalysed process. Phenol was found to be an ideal solvent to facilitate thermal *mer*- to *fac*-isomerisation. It was found that under conditions where isomerisation does not occur, the addition of 10mol% of phenol facilitated *mer*- to *fac*-isomerisation. Bis-cyclometallated iridium(III) alkoxides are proposed intermediates in the *mer*- to *fac*- isomerisation of $[\text{Ir}(\text{ppy})_3]$ -type systems. Analogous *trans-N* configured bis-cyclometallated iridium(III) alkoxide complexes were synthesised and characterised. Furthermore, the reaction of these complexes with Hppy yielding complex **5** shows that Ir(III) alkoxide species are viable intermediates.

A proposed mechanism of the thermodynamic isomerisation reaction was presented, which gives an explanation as to why ligand scrambling is observed. Kinetic examination of the *mer*- to *fac*- isomerisation of homoleptic trisphenylpyridine iridium(III) complexes supports the proposed mechanism. The kinetic analysis supported the theory that an iridium(III) alkoxide intermediate is formed. A detailed discussion on possible geometrical isomers of intermediates in both the homo- and heteroleptic systems is presented.

This report is essential to the field of OLED devices for three reasons. Firstly it demonstrates the synthesis of heteroleptic $[\text{Ir}(\text{C},\text{N})_2(\text{C}',\text{N}')]]$ complexes which are desired for the covalent tethering of these organometallics to polymeric supports. This tethering is the basis of another report which is presently being completed. Secondly, the synthesis of heteroleptic $[\text{Ir}(\text{C},\text{N})_3]$ complexes opens up the field of electronic fine tuning of ligands for mixed ligand species. To this point all complexes developed were tris-cyclometallated homoleptic species and

thus relatively subtle changes in electron densities around the iridium(III) centre were not possible. With heteroleptic [Ir(C,N)₃] systems subtle electronic changes can be introduced to provide, for example, emission colour changes on demand, while retaining the high quantum yield values these complexes are renowned for. Thirdly, and most importantly, it is the first thorough investigation of *mer*- and *fac*- heteroleptic octahedral organometallic species. It gives essential insights into how *fac*- tris-cyclometallated iridium(III) species can be synthesised, and the energetic barriers to their synthesis. Furthermore, it gives a clear explanation of the properties of solvents/materials required for the synthesis of cyclometallated iridium(III) species, and also suggestions so as to synthesise these complexes at lower temperatures.

7.4 Experimental

General Information: Standard Schlenk procedures under N₂ were carried out throughout. Reactions were carried out in the absence of light, unless otherwise stated. Reagents were used as supplied from Acros BV or Sigma-Aldrich, unless otherwise stated. The synthesis of **3** and **4** was carried out according to literature procedures.^{1(c,d)} The synthesis of **5** and **6** was carried out according to the Thompson method.¹¹ ¹H and ¹³C solution NMR was carried out on a Varian Inova 300 spectrometer or a Varian Oxford AS400. Elemental analyses were performed by Dornis und Kölbe, Mikroanalytisches Laboratorium, Mülheim a. d. Ruhr, Germany. MS measurements were carried out on an Applied Biosystems Voyager DE-STR MALDI-TOF MS.

Photophysics:

UV-vis absorption analysis was performed on a Varian CARY 50 Scan UV-visible spectrophotometer in CH₂Cl₂. Emission measurements were carried out on a SPEX FLUOROLOG 1680 0.22m Spectrometer in acetonitrile. *fac*-[Ir(ppy)₃] in 2-MeTHF was used as a reference ($\Phi = 0.4$).

Electrochemistry:

CV measurements were carried out on an EG&G Princeton Applied Research Potentiostat Model 263A. Experiments were carried out at room temperature (20 °C). A platinum disc working electrode was polished with alumina on felt before use. A platinum wire was used as counter electrode. A silver wire was used as a pseudo-/quasi-reference electrode. Tetrabutylammonium hexafluorophosphate (0.1M) in CH₃CN was used as electrolyte. The scan rate was 0.1 V/s. The silver reference electrode was calibrated using ferrocene/ferrocenium (Fc/Fc⁺) redox couple as an internal standard. The oxidation potential of Fc/Fc⁺ was found to be 0.51V against the silver reference electrode.

***mer*-Ir(tpy)(ppy)₂:** *Mer*-[mono(4-methyl-(2-pyridinyl-κN)phenyl-κC²)-bis(2-pyridinyl-κN)phenyl-κC²)]iridium(III), *mer*-7-homo-*N*-*trans*.

Bis(2-pyridinyl-κN)phenyl-κC)iridium(III) chloride (0.2045g, 0.381mmol) was placed in glycerol (2 mL). To this was added K₂CO₃ (0.525g, 10 equivalents, 3.8mmol), and 4-methylphenyl-2-pyridine (0.25mL, 4 equivalents, 1.5mmol). The resulting suspension was heated, under inert conditions, in an oil bath, to 150°C for 40h. This resulted in a dark brown solution. After cooling to room temperature, de-ionised water was added and the mixture was vigorously mixed until a dark precipitate was observed. The dark precipitate was filtered and washed with water twice and subsequently with ethanol twice. The precipitate was then purified using column chromatography with dichloromethane as eluent (yield 84%). The final product was bright orange in colour and was a fine powder. ¹H NMR (300 MHz, d₆-dmsO) δ = 2.00 (s, 3H, CH₃), 6.44 (d, 1H, CH), 6.59 (d, 1H, CH), 6.71 (s, 1H, CH), 6.75-7.05 (m, 8H, CH's), 7.50-7.75 (m, 7H, CH's), 7.87 (2x d, 2H, CH's), 7.91 (2x d, 2H, CH's), 8.15 (d, 1H, CH). ¹³C-NMR (75 MHz, d₆-dmsO) δ = 22.29, 119.2,

119.4, 119.8, 119.9, 121.5, 122.7, 123.1, 123.2, 123.3, 124.8, 125.0, 125.2, 129.8, 130.2, 130.7, 132.7, 135.5, 137.2, 138.1, 138.5, 138.8, 143.0, 143.4, 145.4, 148.1, 150.8, 153.0, 160.0, 167.7, 168.3, 170.4, 175.5, 177.7. M/Z 669.03 g/mol. C₃₄H₂₆IrN₃: calcd. C 61.06, H 3.92, N 6.28; found C 61.11, H 3.96, N 6.11

fac-Ir(tpy)(ppy)₂: *Fac-[mono(4-methyl-(2-pyridinyl-κN)phenyl-κC²)-bis(2-pyridinyl-κN)phenyl-κC²]iridium(III), fac-7.*

Mer-[Ir(tpy)(ppy)₂] (0.2g, 0.3mmol) was dissolved in spectrometric grade CH₃CN (500mL). The solution was stirred in the presence of a medium pressure 150W mercury lamp for 4 days. Column chromatography, using dichloromethane as eluent, yielded the desired product in quantitative yield as a bright yellow powder. ¹H NMR (300 MHz, d₆-dmsO) δ = 1.97 (s, 3H, CH₃), 6.48 (s, 1H, CH), 6.60 (d, 1H, CH), 6.67-6.70 (m, 4H, CH's) 6.75-6.80 (m, 2H, CH's), 7.02-7.11 (m, 3H, CH's), 7.40-7.47 (m, 3H, CH's), 7.61 (d, 1H, CH), 7.70-7.80 (m, 5H, CH's), 8.04 (d, 1H, CH), 8.10 (2x d, 2H, CH's). ¹³C-NMR (75 MHz, d₆-dmsO) δ = 21.491, 118.7, 119.0, 119.1, 119.4, 119.5, 120.6, 120.7, 122.1, 122.1, 122.7, 122.9, 124.1, 124.2, 129.0, 129.0, 136.2, 136.3, 136.7, 136.8, 136.9, 137.9, 141.3, 143.7, 143.8, 146.6, 146.7, 146.8, 160.8, 160.85, 160.9, 165.58, 165.6, 165.61. M/Z 669.03 g/mol. C₃₄H₂₆IrN₃: calcd. C 61.06, H 3.92, N 6.28; found C 60.98, H 4.06, N 6.20.

mer-Ir(tpy)₂(ppy): *Mer-[bis(4-methyl-(2-pyridinyl-κN)phenyl-κC²)-mono(2-pyridinyl-κN)phenyl-κC²]iridium(III), mer-8-homo-N-trans.*

Bis(4-methyl-(2-pyridinyl-κN)phenyl-κC²)iridium(III) chloride (0.405g, 0.718 mmol) was placed in glycerol (10 mL). To this was added K₂CO₃ (1.0g, 10 equivalents, 7.18 mmol), and 2-phenylpyridine (0.45mL, 4 equivalents, 2.87 mmol). The resulting suspension was heated, under inert conditions, in an oil bath, to 150°C for 24h. This resulted in a dark brown solution. After cooling to room temperature, de-ionised water was added and the mixture was vigorously mixed until a dark precipitate was observed. The dark precipitate was filtered and washed with water twice and subsequently with ethanol twice. The precipitate was then purified using column chromatography with dichloromethane as eluent (yield 46%). The final product was bright orange in colour and was a fine powder. ¹H NMR (300 MHz, d₆-dmsO) δ = 2.02 (s, 3H, CH₃), 2.04 (s, 3H, CH₃), 6.08 (s, 1H, CH), 6.23 (s, 1H, CH), 6.62 (d, 1H, CH), 6.71 (2x d, 2H, CH's), 6.80-6.90 (m, 4H, CH's), 7.10 (t, 1H, CH), 7.48 (d, 1H, CH), 7.60-7.70 (m, 4H, CH's), 7.77-7.84 (m, 3H, CH's) 7.91-7.99 (m, 3H, CH's) 8.14 (d, 1H, CH). ¹³C-NMR (75 MHz, d₆-dmsO) δ = 21.7, 118.2, 118.6, 119.3, 120.2, 121.0, 121.4, 121.75, 122.2, 122.5, 124.1, 124.3, 124.5, 129.9, 131.3, 133.7, 134.3, 135.7, 136.7, 137.8, 139.6, 139.9, 140.0, 142.5, 145.7, 147.9, 151.4, 153.1, 159.9, 167.9, 168.5, 170.6, 175.4, 177.8. M/Z 683.19g/mol. Elem. Anal. C₃₅H₂₈IrN₃: calcd. C 61.56, H 4.13, N 6.15; found C 61.51, H 4.12, N 6.10.

fac-Ir(tpy)₂(ppy): *Fac-[bis(4-methyl-(2-pyridinyl-κN)phenyl-κC²)-mono(2-pyridinyl-κN)phenyl-κC²]iridium(III), fac-8.*

Mer-[Ir(tpy)₂(ppy)] (0.1038g, 0.15mmol) was dissolved in spectrometric grade CH₃CN (600mL). The solution was stirred in the presence of a medium pressure 150W mercury lamp for 4 days. Column chromatography, using dichloromethane as eluent, yielded the desired product in quantitative yield as a bright yellow powder. ¹H NMR (300 MHz, d₆-dmsO) δ = 1.95 (s, 3H, CH₃), 1.96 (s, 3H, CH₃), 6.45 (s, 1H, CH), 6.49 (s, 1H, CH), 6.59 (2x d, 2H, CH's), 6.67 (2x d, 2H, CH's), 6.77 (m, 1H, CH), 7.02 (m, 2H, CH's), 7.07 (t, 1H, CH), 7.35-7.40 (m, 3H, CH's), 7.60 (2x d, 2H, CH's) 7.74 (m, 4H, CH's) 8.02 (t, 2H, CH) 8.08 (d, 1H, CH). ¹³C-NMR (75 MHz, d₆-dmsO) δ = 22.2, 22.4, 119.2, 119.3, 119.4, 119.7, 120.2, 121.5, 121.6, 122.8, 123.4, 124.7, 124.8, 124.9, 129.8, 137.0, 137.4 137.52, 137.55, 137.58, 137.60, 137.7, 138.5, 138.55, 138.60, 141.90, 141.93, 144.4, 147.2, 147.3, 147.4, 161.7, 161.8, 166.3, 166.4. M/Z 683.19g/mol. Elem. Anal. C₃₅H₂₈IrN₃: calcd. C 61.56, H 4.13, N 6.15; found C 61.47, H 4.15, N 6.11.

C₂-trans-N-Ir(ppy)₂OPh: *Mer-[bis(2-pyridinyl-κN)phenyl-κC²)-monophenoxy]iridium(III), 9.*

Freshly distilled, degassed phenol (0.8532g, 0.009 mol) was added to a thoroughly degassed THF (20mL) solution with lump Na (0.2g, 0.009mol). This was stirred at room temperature until all Na had reacted (H₂ evolution!). The

system was kept under N_2 and bis(2-pyridinyl- κN)phenyl- κC^2 iridium(III) chloride (0.2g, 0.0004mol) was added with continuous stirring. The resulting yellow solution was stirred at the same temperature for 24h after which it had become red. The solution was filtered to remove Na salts. The solvent was removed from the filtrate and EtOH was added precipitating a dark orange powder. Yield 48%. 1H NMR (300 MHz, d_6 -dmsO) δ = 5.22 (d, 2H, CH), 5.64, (d, 2H, CH), 6.01 (t, 1H, *OPh*CH), 6.17 (t, 2H, CH), 6.28 (t, 2H, CH), 6.64 (t, 2H, CH), 6.83 (t, 2H, CH), 7.68 (d, 2H, CH), 7.84 (t, 2H, CH), 8.23 (d, 2H, CH), 8.77 (d, 2H, CH). ^{13}C -NMR (75 MHz, d_6 -dmsO) δ = 113.0, 119.8, 120.7, 122.7, 123.1, 123.5, 124.4, 125.3, 127.6, 128.4, 129.3, 129.4, 138.0, 143.5, 145.3. Elem. Anal. $C_{28}H_{21}IrON_2$: calcd. C 56.65, H 3.57, N 4.72; found C 56.79, H 3.69, N 4.75.

***C*₂-*trans-N*-Ir(ppy)₂OMe: *Mer*-[bis(2-pyridinyl- κN)phenyl- κC^2]-monomethoxo]iridium(III), **10**.**

Lump Na (0.23g, 10mmol) was added to dry, deoxygenated methanol (40mL) and dry degassed THF (10mL). Once all Na had dissolved, bis(2-pyridinyl- κN)phenyl- κC^2 iridium(III) chloride (0.38g, 0.71mmol) was added to the solution. The resulting mixture was stirred at reflux for 2 hours showing a colour change from yellow to bright orange. After cooling the precipitated bright red powder was filtered and recrystallised using a large volume of dichloromethane and hexanes. The final compound was highly insoluble in all organic solvents.

X-ray crystal structure determinations.

Reflections were measured on a Nonius Kappa CCD diffractometer with rotating anode (graphite monochromator, λ = 0.71073 Å) up to a resolution of $(\sin \theta/\lambda)_{\max} = 0.65 \text{ \AA}^{-1}$. The structures were solved with Direct Methods (SIR-97³⁶) and refined with SHELXL-97³⁷ against F^2 of all reflections. Non-hydrogen atoms were refined with anisotropic displacement parameters. All hydrogen atoms were introduced in calculated positions and refined with a riding model. Geometry calculations and checking for higher symmetry was performed with the PLATON program.³⁸

mer-7-homo-N-trans $C_{34}H_{26}IrN_3$ + disordered solvent, Fw = 668.78^[*], yellow block, 0.12 x 0.09 x 0.06 mm³, monoclinic, C2/c (no. 15), a = 25.0705(1), b = 35.7759(2), c = 17.6973(1) Å, β = 133.3535(2)^o, V = 11541.81(11) Å³, Z = 16, D_x = 1.539 g/cm³ ^[*], μ = 4.653 mm⁻¹ ^[*]. 122103 Reflections were measured at a temperature of 150 K. An absorption correction based on multiple measured reflections was applied (0.65-0.75 correction range). 13252 Reflections were unique (R_{int} = 0.0735). The crystal structure contains large voids (1756 Å³ / unit cell) filled with disordered solvent molecules. Their contribution to the structure factors was secured by back-Fourier transformation using the SQUEEZE routine of the program PLATON³⁸, resulting in 590 electrons / unit cell. 685 Parameters were refined with no restraints. R1/wR2 [$I > 2\sigma(I)$]: 0.0296/0.0685. R1/wR2 [all refl.]: 0.0453/0.0732. S = 1.050. Residual electron density between -1.47 and 2.12 e/Å³.

mer-8-homo-N-trans $C_{35}H_{28}IrN_3$ + disordered solvent, Fw = 682.80^[*], yellow block, 0.45 x 0.24 x 0.21 mm³, trigonal, $\overline{R} 3 c$ (no. 167), a = b = 20.02588(1), c = 36.14264(2) Å, V = 12552.593(11) Å³, Z = 18, D_x = 1.626 g/cm³ ^[*], μ = 4.815 mm⁻¹ ^[*]. 51277 Reflections were measured at a temperature of 110 K. An absorption correction based on multiple measured reflections was applied (0.07-0.37 correction range). 3176 Reflections were unique (R_{int} = 0.0633). The crystal structure contains large voids (708 Å³ / unit cell) filled with disordered solvent molecules. Their contribution to the structure factors was secured by back-Fourier transformation using the SQUEEZE routine of the program PLATON³⁸, resulting in 163 electrons / unit cell. Atoms N2/N2ⁱ and C18/C18ⁱ were constrained to the same coordinates and displacement parameters (occupancy 0.5). 178 Parameters were refined with no restraints. R1/wR2 [$I > 2\sigma(I)$]: 0.0229/0.0496. R1/wR2 [all refl.]: 0.0299/0.0514. S = 1.088. Residual electron density between -0.77 and 1.62 e/Å³.

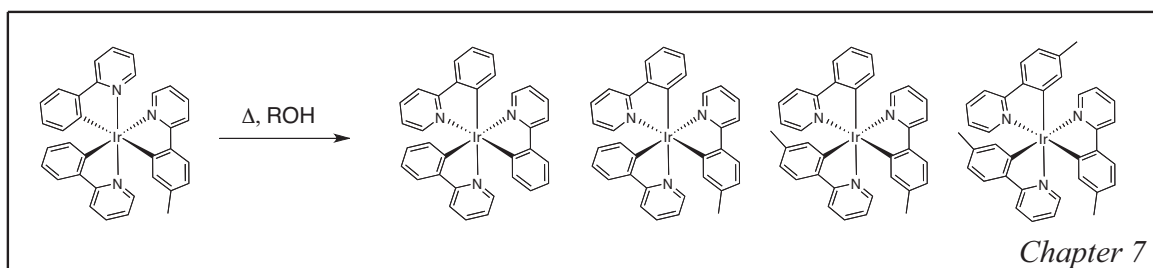
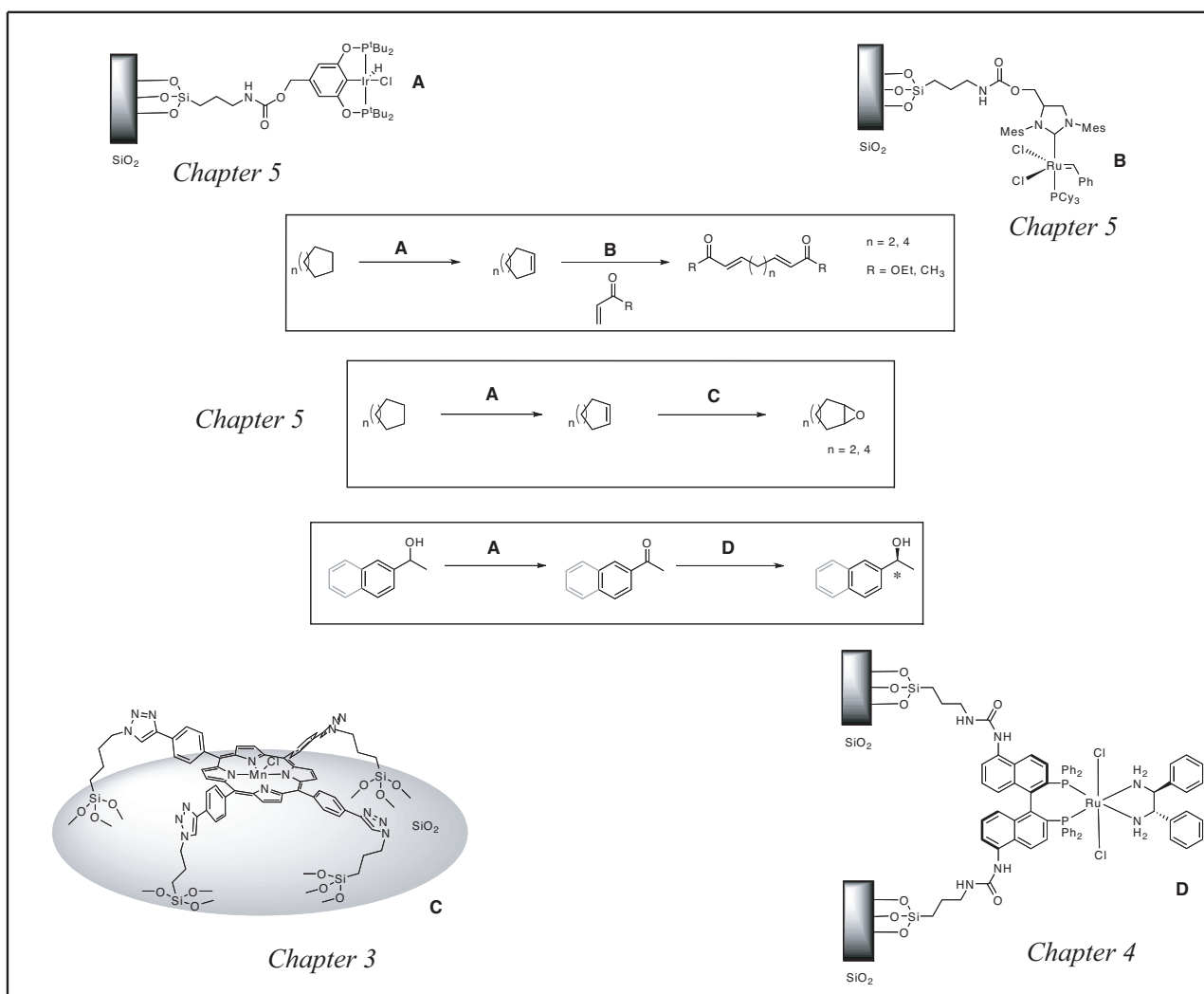
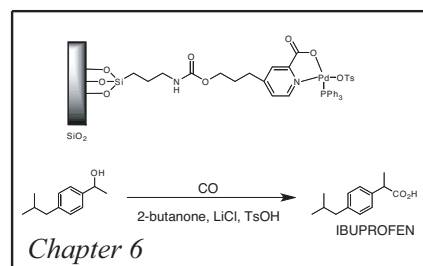
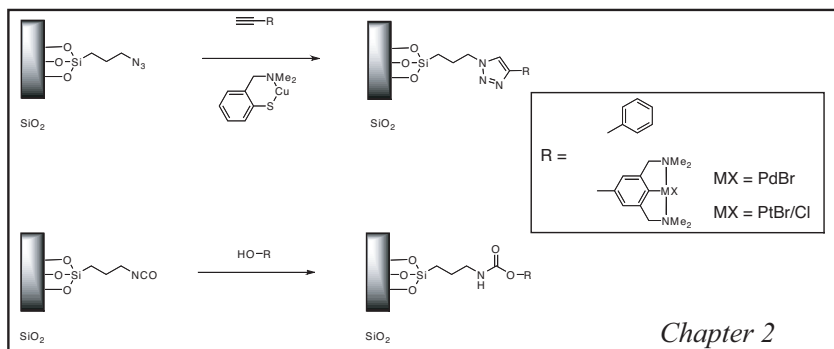
[*] Derived parameters do not contain the contribution of the disordered solvent.

7.5 References

- ¹ (a) King, K. A.; Spellane, P. J.; Watts, R. J. *J. Am. Chem. Soc.* **1985**, *107*, 1431-1432. (b) Dedeian, K.; Djurovich, P. I.; Garces, F. O.; Carlson, G.; Watts, R. J. *Inorg. Chem.* **1991**, *30*, 1685-1688. (c) Garces, F. O.; King, K. A.; Watts, R. J. *Inorg. Chem.* **1988**, *27*, 3464-3471. (d) Sprouse, S.; King, K. A.; Spellane, P. J.; Watts, R. J. *J. Am. Chem. Soc.* **1984**, *106*, 6647-6653. (e) Ohsawa, Y.; Sprouse, S.; King, K. A.; DeArmond, M. K.; Hanck, K. W.; Watts, R. J. *J. Phys. Chem.* **1987**, *91*, 1047-1054
- ² (a) Baldo, M. A.; O'Brien, D. F.; You, Y.; Shoustikov, A.; Sibley, S.; Thompson, M. E.; Forrest, S. R. *Nature* **1998**, *395*, 151-154. (b) Baldo, M. A.; Lamansky, S.; Burrows, P. E.; Thompson, M. E.; Forrest, S. R. *Appl. Phys. Lett.* **1999**, *75*, 4-6. (c) Adachi, C.; Baldo, M. A.; Forrest, S. R.; Thompson, M. E. *Appl. Phys. Lett.* **2000**, *77*, 904-906.
- ³ Kim, J. I.; Shin, I.-S.; Kim, H.; Lee, J.-K. *J. Am. Chem. Soc.* **2005**, *127*, 1614-1615.
- ⁴ (a) DeRosa, M. C.; Hodgson, D. J.; Enright, G. D.; Dawson, B.; Evans, C. E. B.; Crutchley, R. J. *J. Am. Chem. Soc.* **2004**, *126*, 7619-7626. (b) Gao, R.; Ho, D. G.; Hernandez, B.; Selke, M.; Murphy, D.; Djurovich, P. I.; Thompson, M. E. *J. Am. Chem. Soc.* **2002**, *124*, 14828-14829.
- ⁵ Clemente-León, M.; Coronado, E.; Gomez-Garcia, C. J.; Soriano-Portillo, A. *Inorg. Chem.* **2006**, *45*, 5653-5660.
- ⁶ (a) Huo, S.; Deaton, J. C.; Rajeswaran, M.; Lenhart, W. C.; *Inorg. Chem.* **2006**, *45*, 3155-3157. (b) Sajoto, T.; Djurovich, P. I.; Tamayo, A.; Yousufuddin, M.; Bau, R.; Thompson, M. E.; Holmes, R. J.; Forrest, S. R. *Inorg. Chem.* **2005**, *44*, 7992-8003. (c) Jung, S.; Kang, Y.; Kim, H.-S.; Kim, Y.-H.; Lee, C.-L.; Kim, J.-J.; Lee, S.-K.; Kwon, S.-K. *Eur. J. Inorg. Chem.* **2004**, 3415-3423. (d) Okada, S.; Okinaka, K.; Iwawaki, H.; Furugori, M.; Hashimoto, M.; Mukaide, T.; Kamatani, J.; Ogawa, S.; Tsuboyama, A.; Tagiguchi, T.; Ueno, K. *Dalton Trans.* **2005**, 1583-1590. (e) Su, Y.-J.; Huang, H.-L.; Li, C.-L.; Chien, C.-H.; Tao, Y.-T.; Chou, P.-T.; Datta, S.; Liu R.-S. *Adv. Mater.* **2003**, *15*, 884-888. (f) Grushin, V. V.; Herron, N.; LeCloux, D. D.; Marshall, W. J.; Petrov, V. A.; Wang, Y. *Chem. Commun.* **2001**, 1494-1495.
- ⁷ (a) Li, J.; Djurovich, P. I.; Alleyne, B. D.; Yousufuddin, M.; Ho, N. N.; Thomas, J. C.; Peters, J. C.; Bau, R.; Thompson, M. E. *Inorg. Chem.* **2005**, *44*, 1713-1727. (b) Nazeeruddin, M. K.; Humphry-Baker, R.; Berner, D.; Rivier, S.; Zuppiroli, L.; Graetzel, M. *J. Am. Chem. Soc.* **2003**, *125*, 8790-8797. (c) Ionkin, A. S.; Marshall, W. J.; Fish, B. M. *Organometallics* **2006**, *25*, 1461-1471. (d) Tamayo, A. B.; Garon, S.; Sajoto, T.; Djurovich, P. I.; Tsyba, I. M.; Bau, R.; Thompson, M. E. *Inorg. Chem.* **2005**, *44*, 8723-8732. (e) Yang, C.-H.; Li, S.-W.; Chi, Y.; Cheng, Y.-M.; Yeh, Y.-S.; Chou, P.-T.; Lee, G.-H.; Wang, C.-H.; Shu, C.-F. *Inorg. Chem.* **2005**, *44*, 7770-7780.
- ⁸ (a) You, Y.; Park, S. Y. *J. Am. Chem. Soc.* **2005**, *127*, 12438-12439. (b) Kwon, T.-H.; Cho, H. S.; Kim, M. K.; Kim, J.-W.; Kim, J.-J.; Lee, K. H.; Park, S. J.; Shin, I.-S.; Kim, H.; Shin, D. M.; Chung, Y. K.; Hong, J.-I. *Organometallics* **2005**, *24*, 1578-1585
- ⁹ (a) Böttcher, H.-C.; Graf, M.; Krüger, H.; Wagner, C.; *Inorg. Chem. Commun.* **2005**, *8*, 278-280. (b) Tsuboyama, A.; Takiguchi, T.; Okada, S.; Osawa, M.; Hoshino, M.; Ueno, K. *Dalton Trans.* **2004**, 1115-1116.
- ¹⁰ Karatsu, T.; Nakamura, T.; Yagai, S.; Kitamura, A.; Yamaguchi, K.; Matsushima, Y.; Iwata, T.; Hori, Y.; Hagiwara, T. *Chem. Lett.* **2003**, *32*, 886-887.
- ¹¹ Tamayo, A. B.; Alleyne, B. D.; Djurovich, P. I.; Lamansky, S.; Tsyba, I.; Ho, N. N.; Bau, R.; Thompson, M. E. *J. Am. Chem. Soc.* **2003**, *125*, 7377-7387.
- ¹² Lo, S.-C.; Namdas, E. B.; Burn, P. L.; Samuels, I. D. W. *Macromolecules* **2003**, *36*, 9721-9730.
- ¹³ (a) Furuta, P. T.; Deng, L.; Garona, S.; Thompson, M. E.; Frechet, J. M. J. *J. Am. Chem. Soc.* **2004**, *126*, 15388-15389. (b) Sandee, A. J.; Williams, C. K.; Evans, N. R.; Davies, J. E.; Boothby, C. E.; Kohler, A.; Friend, R. H.; Holmes, A. B. *J. Am. Chem. Soc.* **2004**, *126*, 7041-7048.
- ¹⁴ Lo, K. K.-W.; Li, C.-K.; Lau, J. S.-Y. *Organometallics* **2005**, *24*, 4594-4601.
- ¹⁵ We have searched the literature to find reports on the stereochemistry of octahedral $[M(ab)_2(a'b')]_2$ complexes. There is very little reported on such compounds, and we have therefore altered nomenclature derived from $[M(ab)_2(a'a')]_2$ systems. Please note; throughout the following discussion helicity of the various complexes is negated. Any implied helicity in diagrams should be ignored. To the best of our knowledge and understanding, the complexes are in racemic mixtures. Any implied helicity is present to help with the understanding of the geometrical isomer of a complex, unless otherwise stated.

- ¹⁶ McDonald, A. R.; van Klink, G. P. M.; van Koten, G. Unpublished work.
- ¹⁷ The properties of the polymer supported complexes can be easily altered, by both tethering to a support, and secondly by altering the phobicity of the co-polymer/co-dendron.
- ¹⁸ McDonald, A. R.; van Klink, G. P. M.; van Koten, G. Unpublished work.
- ¹⁹ See experimental section.
- ²⁰ (a) Garces, F. O.; Dedeian, K.; Keder, N. L.; Watts, R. J. *Acta. Cryst.* **1993**, *C49*, 1117-1120. (b) See ref. 11.
- ²¹ (a) Schmid, B.; Garces, F. O.; Watts, R. J. *Inorg. Chem.* **1994**, *33*, 9-14. (b) Douglas, B. E.; Saito, Y. *ACS Symposium Series*, **1980**, *119*, 338.
- ²² Muller, G.; Lutz, M.; *Z. Naturforsch* **2001**, *56b*, 871.
- ²³ See experimental section.
- ²⁴ (a) Lamansky, S.; Djurovich, P.; Murphy, D.; Abdel-Razzaq, F.; Kwong, R.; Tsyba, I.; Bortz, M.; Mui, B.; Bau, R.; Thompson, M. E. *Inorg. Chem.* **2001**, *40*, 1704-1711. (b) See ref. 1(c).
- ²⁵ This is related to the slow rate of isomerisation of Ir(III), and the disfavour of such systems to undergo Berry-pseudo rotation. Deeming, A. J.; Proud, P. J.; Dawes, H. M.; Hursthouse, M. B.; *J. Chem. Soc. Dalton Trans.* **1986**, 2545-2549.
- ²⁶ Springer, C. S. *J. Am. Chem. Soc.* **1973**, *95*, 1459-1467.
- ²⁷ Dedeian, K.; Shi, J.; Shepherd, N.; Forsythe, E.; Morton, D. C.; *Inorg. Chem.* **2005**, *44*, 4445-4447.
- ²⁸ See experimental section for details of how analyses were carried out.
- ²⁹ Crude tests were done on complexes **5-8** to test their response to the MALDI-TOF apparatus. All 4 complexes had very similar response factors.
- ³⁰ We have attempted a wide range of experiments to elucidate the reaction rate and carry out some kinetic tests on the thermodynamic conversion of *mer-7* to *fac-5*, **6**, **7**, **8**. ¹H or ¹³C NMR spectroscopy was not possible due to overlapping of the marker signals (tolyl CH₃) of *fac-6,7* and **8** and *mer-7*. UV-vis is not feasible here because all products have almost exactly the same absorption spectra. When it was attempted no isobestic points were observed, but this is due to slight differences in the molar absorptivities of the complexes. The products are not separable by GC or HPLC.
- ³¹ The disappearance of *mer-6* was measured by integrating an aromatic peak belonging to *mer-6* and comparing it to the integration of all tolyl- signals. This relies on the assumption that all *mer-6* is eventually converted to *fac-6*.
- ³² Green, M.; Parker, G. J.; *J. Chem. Soc.; Dalton Trans.* **1974**, 333-343.
- ³³ All solvents or activating ligands previously used in the synthesis of *fac*-[Ir(ppy)₃] have been bidentate; glycerol, 2-ethoxyethanol, acac. We believe that a monodentate intermediate state must exist at some stage during the reaction of intermediates of the type **11**. We believe the bidentate solvents form intermediate complexes in a similar binding manner to acac. This leads to another variable as to where the attacking arylpyridine will bind in intermediate **11**, *trans* to a carbon or *trans* to a nitrogen. This could lead to preferences towards certain *fac*- or *mer*- products over others.
- ³⁴ (a) See ref. 10 (b) Karatsu, T.; Ito, E.; Yagai, S.; Kitamura, A. *Chem. Phys. Lett.* **2006**, *424*, 353-357.
- ³⁵ McGee, K. A.; Mann, K. R.; *Inorg. Chem.* **2007**, *46*, 7800-7809.
- ³⁶ Altomare, A.; Burla, M. C.; Camalli, M.; Cascarano, G. L.; Giacovazzo, C.; Guagliardi, A.; Moliterni, A. G. G.; Polidori, G.; Spagna, R.; *J. Appl. Cryst.* **1999**, *32*, 115-119.
- ³⁷ Sheldrick, G. M. (1997). SHELXL-97. Program for crystal structure refinement. University of Göttingen, Germany.
- ³⁸ Spek, A.L.; *J. Appl. Cryst.* **2003**, *36*, 7-13.

GRAPHICAL ABSTRACT





SUMMARY

The work described in this thesis has demonstrated the application of heterogenised homogeneous catalysts. We have shown that by coupling a homogeneous catalyst to a heterogeneous support we could combine the benefits of two major fields of catalysis: *retain the high selectivity of homogeneous catalysts with the ease of separation and cost-efficiency of heterogeneous catalysts*. A number of techniques both for the functionalisation of organometallic complexes, and the functionalisation of inorganic support materials have been demonstrated and applied. These techniques are a breakthrough because they demonstrate simple, highly efficient procedures for the desired products. Furthermore, they demonstrate a very simple ‘from lab shelf to reaction vessel’ concept for the immobilisation of homogeneous catalysts and application of such catalytic materials.

It was further demonstrated that by compartmentalising heterogenised homogeneous catalysts we could mimic nature’s ability to carry out highly selective multi-step reaction sequences without work-up or intermediate isolation steps. This achievement is a simple, but highly important and distinguished achievement because it brings the field of multi-step catalysis a step closer to being truly efficient, and more importantly, environmentally benign.

Chapter 1 of this thesis gives a general introduction to the two fields of importance to this study; *catalyst immobilisation* and *multi-step catalysis*. The heterogenisation of homogeneous catalysts is a tremendously broad field, and thus a review of the literature has been focussed on the areas of asymmetric hydrogenation and C-C bond forming reactions. Industrially these reactions are widely applied for the synthesis of fine chemicals, and are the cornerstone to many synthetic pathways. A broad overview of the various support media for the heterogenisation of homogeneous catalysts was given, which showed that inorganic polymeric, organic polymeric (including ordered, i.e. dendritic, and non-ordered supports) and solubility functionalities have been used to heterogenise homogeneous catalysts. The general conclusion drawn from this was that heterogenisation on an inorganic support gives the best results in terms of recycling, and the least effects on the selectivity of a heterogenised homogeneous catalyst. Catalyst activation/deactivation was also discussed, because, in some cases it has been observed that heterogenisation of homogeneous catalysts leads to increases/decreases in catalyst activity and selectivity. Furthermore, insights into the true catalytic species have been given, as a result of heterogenisation of homogeneous catalysts, with some reports demonstrating that the believed catalyst is in fact a pre-catalyst to a completely different catalytically active species.

Multi-step sequential catalysis using transition metal complexes was discussed with a general overview of the field. The general conclusions that were drawn from this were that catalysts/substrate incompatibility has hindered this field. Best results were often observed when intermediate substrates/reactants were introduced after an initial reaction in a sequence had

occurred. Almost no work had shown the application of immobilised homogeneous catalysts in sequential multi-step catalysis. It was concluded that another manner to alleviate the problem of incompatibility would be to compartmentalise catalysts as is depicted below (figure 1).

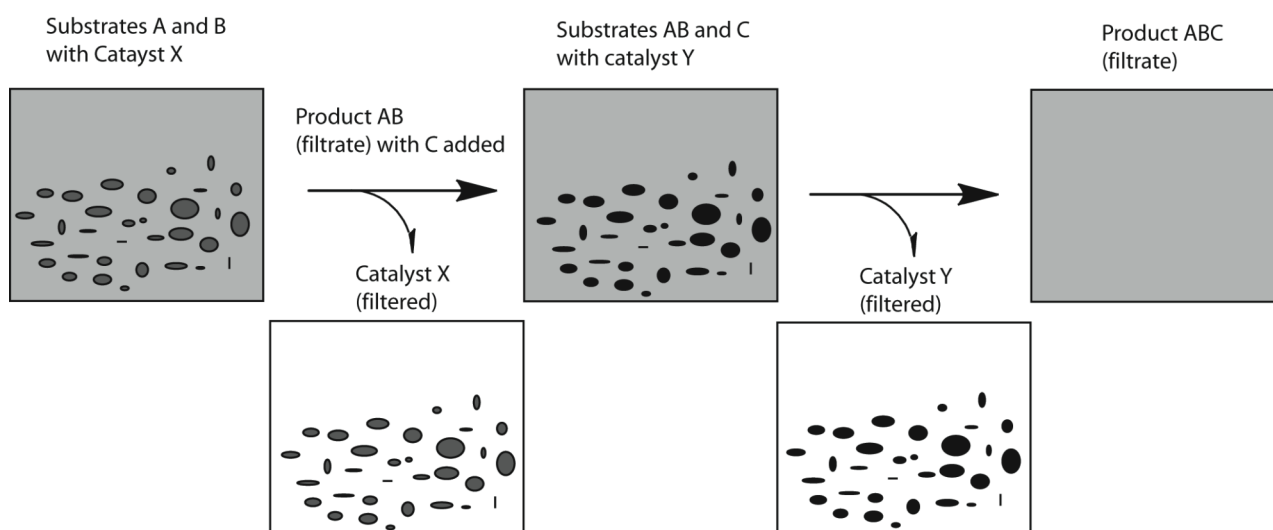


Figure 1. Homogeneous catalyst compartmentalisation by immobilisation for multi-step sequential reactions.

In **chapter 2** two synthetic protocols for the simple, high yielding, efficient immobilisations of homogeneous catalysts were demonstrated. The synthesis of novel materials for so-called ‘click’ immobilisation was presented. The synthesis of azide and isocyanate functionalised high-density silica materials was presented. These materials reacted readily with ethynyl and alcoholic functionalities, respectively. Palladium(II) and platinum(II) organometallic compounds with ethynyl and alcoholic functionalities were immobilised on silica using the ‘click’ technique (figure 2). Palladium containing materials were applied as Lewis acid catalysts in the double Michael addition and were found to be highly active catalysts. The material was tested for recyclability and showed no reduction in reactivity (activity or selectivity) over 3 cycles. The palladium containing materials were also applied in an allylic stannylation reaction, and were found to be active catalysts, approximately three times slower than the homogeneous catalysts when measured on a per-palladium site basis. These materials could also be recycled when applied in the allylic stannylation reaction showing no decrease in activity over three cycles.

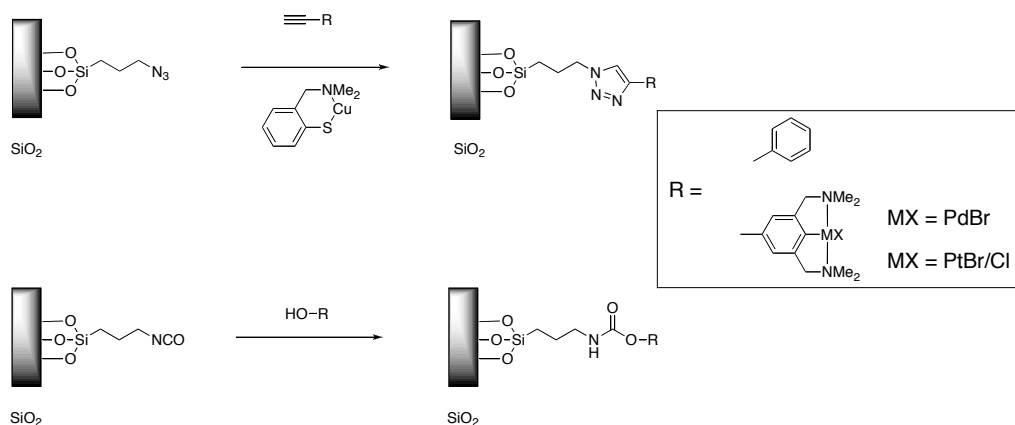


Figure 2. Functionalised support materials for ‘click’ immobilisation of organometallics.

In **chapter 3** ‘click’ immobilisation techniques were used to tether porphyrin complexes to an inorganic support. Ethynyl functionalised porphyrin ligands were synthesised and reacted with both manganese and zinc precursors to yield ethynyl functionalised metallo-porphyrin complexes. These functionalised complexes were coupled with azide functionalised silica (from chapter 2) to tether the porphyrin complexes to the insoluble inorganic support. The developed manganese containing materials were applied as catalysts in the epoxidation of several alkene substrates, showing activity that is diminished relative to the homogeneous catalyst, and also diminished epoxide yields. The catalytic materials were recycled and reapplied in catalysis and showed constant decreases in activity over several cycles until the catalytic material was completely deactivated. The rate of deactivation of the heterogenised catalysts was greater than that observed for the homogeneous catalysts, which decompose as a result of intermolecular oxidation of metalloporphyrin species. Some possible reasons for the catalytic material deactivation were proposed, the most likely of which is the accumulation of side products (as a result of reaction of oxidant with itself) on the inorganic support. The formed side-product blocks access to the catalytic site, and thus results in lower catalytic activity upon recycling.

Chapter 4 demonstrates the synthesis and immobilisation of a functionalised protected BINAP ligand (protected as the phosphine oxide) on a silica support. It was shown that deprotection chemistry (silane mediated reduction) could be carried out on the immobilised phosphine oxide without having detrimental effects on the support or the functionalised ligand. Metal introduction (Ru and Rh) to the immobilised BINAP ligand was demonstrated with all phosphine sites coordinated to a metal centre. Catalytic results (with Ru and Rh) showed that activity is down in comparison with the homogeneous system, however conversion and enantioselectivity levels are as good as if not improved upon, in comparison with the homogeneous catalyst. This was demonstrated for a wide range of substrates. The catalyst is truly immobilised with the post catalysis solution showing no activity. Furthermore, the catalyst was recycled showing repeated high selectivity levels over at least five cycles.

The synthesis of functionalised iridium(III) organometallics for immobilisation was demonstrated in **chapter 5**. A benzyl-alcohol functionalised iridium(III) pincer organometallic has been synthesised and coupled (‘click’) with isocyanate functionalised silica material. The pre-catalytic materials and their precursors have been thoroughly characterised showing that the iridium(III) -hydride and -chloride bonds remain intact throughout the immobilisation procedure. A Grubbs-II ruthenium alkylidene complex has also been tethered to silica.

The immobilised dehydrogenation catalytic material was applied sequentially with other heterogenised homogeneous catalysts (figure 3). Multi-step reaction sequences were presented which demonstrate the conversion of non-functionalised, unreactive precursors to functionalised compounds in two steps, without work-up and minimal interruption of the reaction sequence. The dehydrogenation of a basic cyclic alkane yielding a cyclic alkene in sequence with ring opening cross-metathesis of the formed alkene was demonstrated. This is mediated by simple reaction solution transfer between reaction vessels, while filtering the heterogenised dehydrogenation catalyst away from the reaction mixture. We have demonstrated the ring-opening cross coupling of cyclic alkenes with ethyl acrylate and methyl vinyl ketone yielding bis-alkyl esters and ketones,

respectively. Subsequently, post-metathesis, which was quantitative for the alkene, the metathesis catalyst was filtered off and the final reaction mixture could be simply worked-up. In a second example, a similar sequence was demonstrated for the epoxidation of the aforementioned cyclic alkenes. A material containing immobilised manganese porphyrin catalysts was applied in the sequence after the dehydrogenation step. Finally, it was demonstrated that in two steps racemic alcohols could be deracemised with dehydrogenation catalytic materials in sequence with immobilised asymmetric hydrogenation materials.

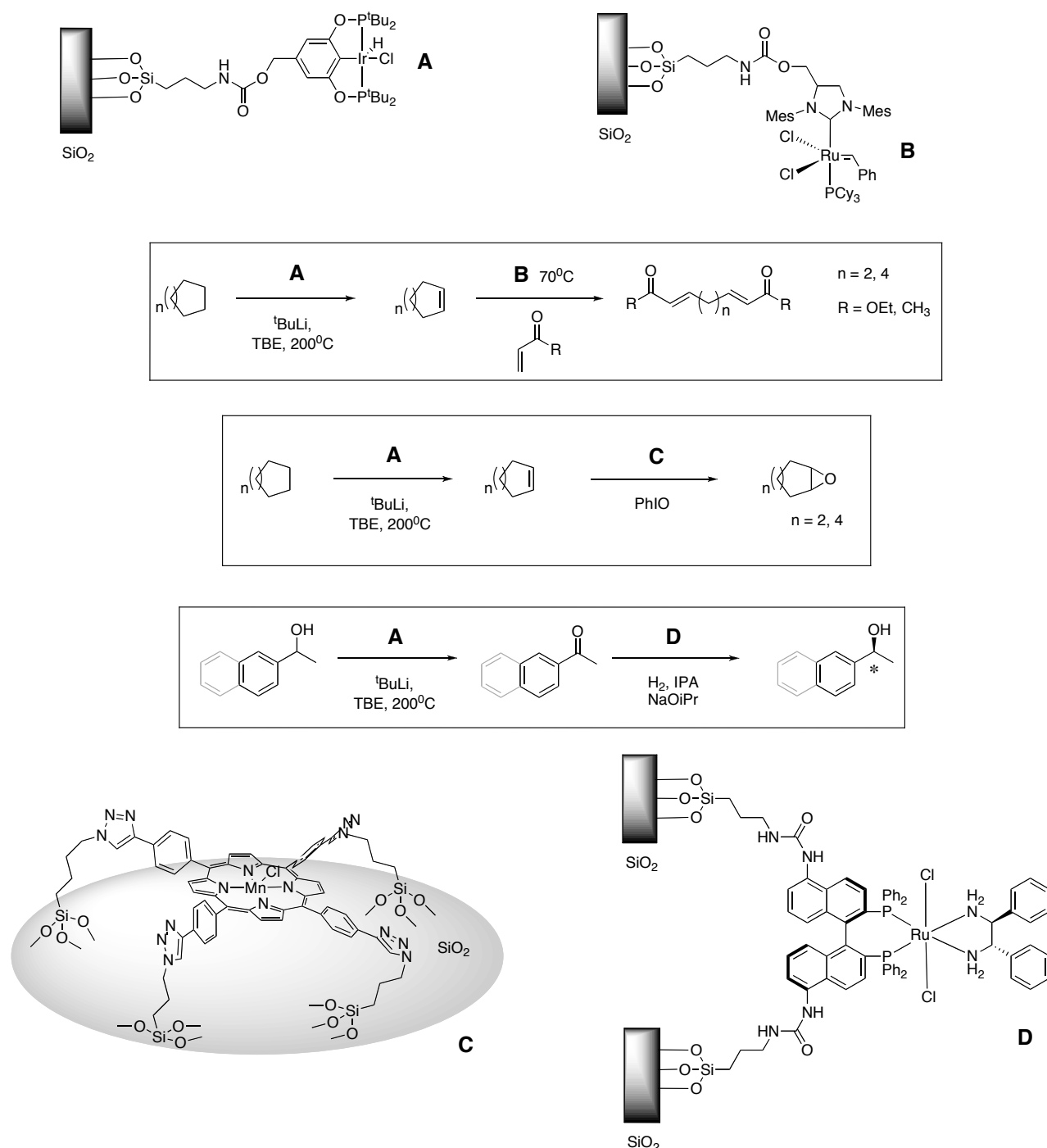


Figure 3. Immobilised homogeneous catalysts for sequential fine chemical synthesis.

In **chapter 6** a palladium picolinate was covalently immobilised on a high-density silica support by step-wise construction of the catalyst on the support. Enzymatic hydrolysis was used in the construction of the ligand on the support. DRIFT-IR and multinuclear CP-MAS solid state NMR spectroscopy were used to analyse intermediates and characterise the immobilised catalyst, proving that palladium picolinate had been tethered to the inorganic support. The immobilised catalyst was used in the hydroxycarbonylation of 1-(4-isobutylphenyl)ethanol (IBPE) yielding the commercially attractive non-steroidal anti-inflammatory drug *Ibuprofen* (IBN, see figure 4). Post-catalytic analysis showed that the palladium picolinate, which was initially proposed by another group of researchers as the active species during catalysis, is probably not the active catalyst. It was shown that catalytic promoters used in the catalytic reaction induce the decomplexation of palladium picolinate. It was also shown that the newly formed palladium species was active in the hydroxycarbonylation reaction. This newly formed palladium species shows lower regioselectivity in the hydroxycarbonylation of IBPE.

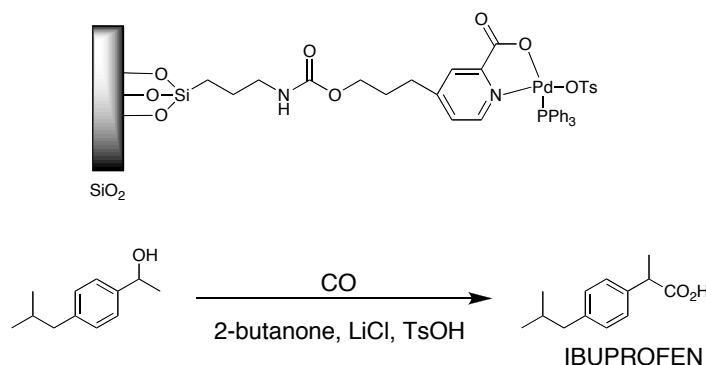


Figure 4. Palladium picolinate complex bound to silica for hydroxycarbonylation.

General Conclusions and Outlook for Sequential Immobilised Catalysis.

The immobilisation of homogeneous catalysts is often a challenging synthetic project, reliant both on the durability and neutrality of a support material, *and* on the sensitivity and stability of an organometallic complex. We have demonstrated mild, efficient procedures for the covalent immobilisation of a wide range of organic and organometallic moieties on inorganic supports. We have also demonstrated a wide range of organic synthetic techniques to introduce functionalities to organic/organometallic compounds to facilitate tethering to both inorganic and organic polymeric support materials. However, all of these procedures rely heavily on high organometallic catalyst stability. As we have demonstrated the pincer-metal compounds are ideal compounds to demonstrate immobilisation techniques (chapters 2 and 5). The reasons for this are essentially due to the high thermal stability of the complexes. Furthermore, the pincer organometallics are highly flexible in the range of catalytic reactions they can be applied in. With ligands and complexes that do not contain the high stability of the pincer metal complexes we have found that relatively long-winded organic synthetic protocols are required to immobilise the organometallic catalyst (chapters 4 and 6).

The developed catalytic materials, all of which are insoluble in common organic solvents and water, could be applied as ‘heterogeneous’ catalysts in a wide range of catalytic reactions:

hydrogenations, dehydrogenations, oxidations, and C-C couplings. In most cases, the catalytic materials could be easily recycled without loss in activity or selectivity. In the cases where recycling of the catalysts showed adverse results, we have investigated as to why this is so. Catalyst stability to the reaction conditions is the reason, in this thesis, why immobilised homogeneous catalysts become deactivated upon recycling. We have found that a deep understanding of the mechanistic flow of a catalytic reaction should be present before attempts are made at immobilising a homogeneous catalyst (chapter 6). Furthermore, immobilisation can give insights into catalytic mechanisms that were previously not possible (chapters 1 and 6). The nature of catalytic reactants is also of importance, as has been observed in chapters 2 and 3. In both chapters the support material/linkers to the support have facilitated either an increase or decrease in catalytic activity.

The developed catalytic materials were also applied in a sequential manner, demonstrating multi-step reaction sequences which have no work-up steps, and are high yielding and highly selective. This is where the future lies in homogeneous catalysis. The present desire is to have flexible catalytic systems that are generally applicable. It is also desired to carry out multiple reactions in a single reaction vessel, thus alleviating the necessity to isolate intermediates, which results in large amounts of by-product and solvent waste. This thesis has demonstrated the first step on the road to mimicking nature's compartmentalisation of catalysts, however we have done it with non-natural catalysts. The next step is to extend the reaction sequences to three, four or five step procedures. For example, in the system described in chapter 5, where an epoxide or di-alkenyl diester is formed, ring opening of the epoxide or reduction of the alkene, respectively, can be easily carried out, in the same reaction mixture using an enzyme or heterogeneous catalyst.

The important future application of the concepts introduced in this thesis lie in expansion to other catalysed reactions, and the development of extended multi-step systems where processes can work both in tandem and in sequence. Single reaction vessel compartmentalisation is also an important goal. This would involve having catalytic sites separated by membranes that are solvent and substrate porous, however the catalysts remain compartmentalised/immobilised to one area within the vessel. According to the principles of green chemistry, catalysis is ultimately a green process, however we can make it 'greener' by developing systems such as those demonstrated in this thesis.

OLED Investigation Section

A number of heteroleptic tris-cyclometallated iridium(III) $[\text{Ir}(\text{C},\text{N})_2(\text{C}',\text{N}')]_3$ complexes were synthesised and fully characterised using a range of techniques in **chapter 7**. The *mer-homo-N-trans* isomer of heteroleptic complexes was synthesised and converted to the *fac*-isomer using photochemical techniques demonstrating a high yielding, simple protocol for the synthesis of tethered tris-cyclometallated iridium(III) complexes. Under thermal reaction conditions the conversion of the *mer-homo-N-trans* isomers to the *fac*- complexes led to ligand scrambling (figure 5). This thermal isomerisation was thoroughly investigated and it was found to be an alcohol catalysed process. Bis-cyclometallated iridium(III) alkoxides are proposed intermediates in the alcohol catalysed thermal *mer*- to *fac*- isomerisation of $[\text{Ir}(\text{ppy})_3]$ -type systems. Analogous *trans-N*

configured bis-cyclometallated iridium(III) alkoxide complexes were synthesised and characterised and were found to be likely intermediates by examining their reaction with cyclometallating ligands.

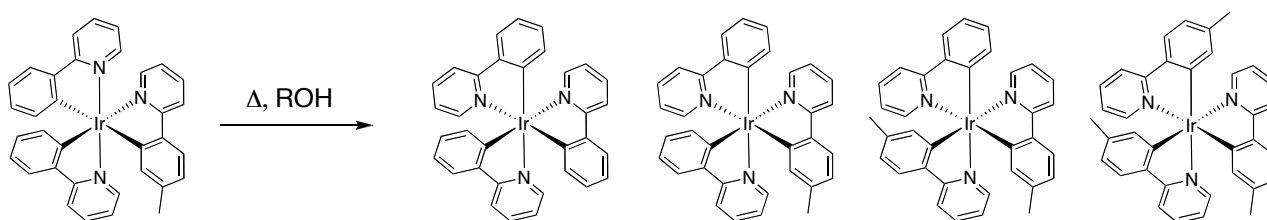


Figure 5. Thermal isomerisation of heteroleptic *mer* isomer yields mixtures of four *fac* isomers.

A proposed mechanism of the thermodynamic isomerisation reaction was presented, which gives an explanation as to why ligand scrambling is observed. Ligand substitution of one of the cyclometallating ligands by an alkoxide ligand occurs yielding an intermediate bis-cyclometallated iridium(III) alkoxide complex. This Ir(III) alkoxide then reacts with the ‘free’ cyclometallating ligand resulting in a tris-cyclometallated complex. This formed complex can either be a *mer*- or *fac*- isomer. The *fac*- isomer is a thermodynamic end-product, and does not react further, while the *mer*- isomer will re-react until all *mer* has been converted to *fac*. Kinetic examination of the *mer*- to *fac*- isomerisation of homoleptic trisphenylpyridine iridium(III) complexes supports the proposed mechanism. A detailed discussion on possible geometrical isomers of intermediates in both the homo- and heteroleptic systems was presented. This report is essential to the field of OLED devices for three reasons; 1) it demonstrates the synthesis of heteroleptic $[\text{Ir}(\text{C},\text{N})_2(\text{C}',\text{N}')]_3$ complexes which are desired for the covalent tethering of these organometallics to polymeric supports; 2) the synthesis of heteroleptic $[\text{Ir}(\text{C},\text{N})_3]$ complexes opens up the field of electronic fine tuning of ligands for mixed ligand species; 3) and most importantly, it is the first thorough investigation of *mer*- and *fac*- heteroleptic octahedral $[\text{M}(\text{a},\text{b})_2(\text{c},\text{d})]$ organometallic species, and thus a thorough structural and nomenclature discussion was presented. It gives essential insights into how *fac*- tris-cyclometallated iridium(III) species can be synthesised, and the energetic barriers to their synthesis.

General Conclusions from OLED Investigations

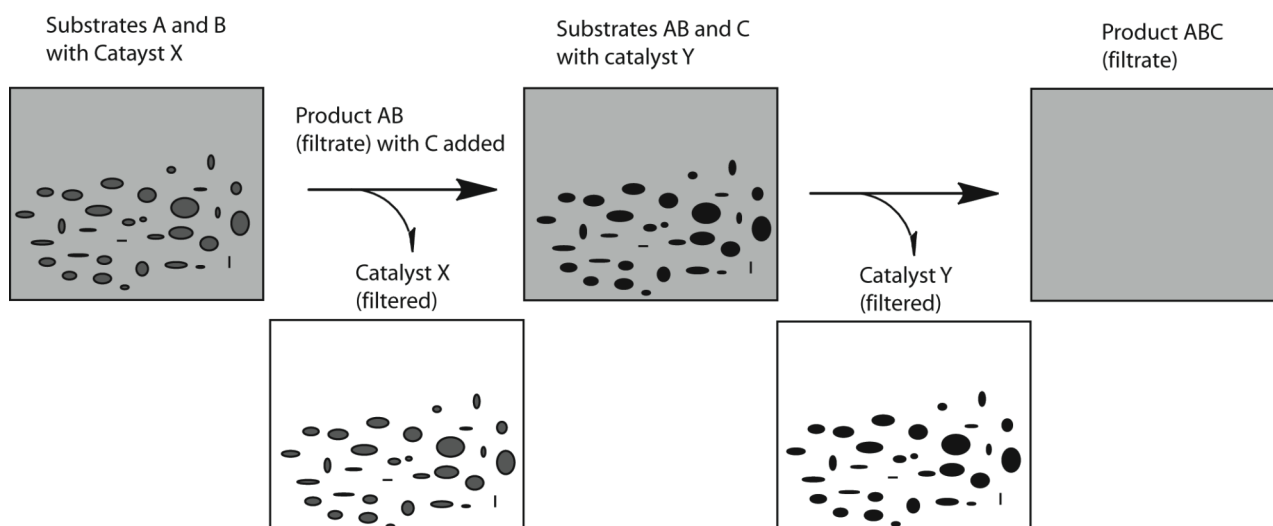
The ultimate goal of this study was to demonstrate the tethering of organometallic phosphors to polymeric supports. This goal was achieved, with a fundamental study carried out to facilitate the tethering. Complexes of the generic formula $[\text{Ir}(\text{C},\text{N})_3]$ were studied because they show the highest quantum yield values when applied in OLED devices. The tethering of these systems has never been demonstrated because the synthesis of analogous heteroleptic complexes is particularly challenging. In this thesis we have demonstrated techniques to overcome these challenges, and have furthermore studied the reaction pathways. These discoveries are key to the future of OLED technologies, because controlling interactions between hole transport and electron transport layers (both widely available organic polymers) and the phosphorescent layers (Ir(III) organometallic) is essential to reach high quantum efficiency levels, and ultimately reliable OLED devices.

SAMENVATTING

Het in dit proefschrift beschreven onderzoek toont de toepassing aan van geheterogeniseerde homogene katalysatoren. Door de koppeling van een homogene katalysator aan een heterogene drager konden de voordelen worden gecombineerd van twee belangrijke deelgebieden van de katalyse: *behoud van de hoge selectiviteit van homogene katalysatoren met het scheidingsgemak en de kostefficiëntie van heterogene katalysatoren*. Een aantal technieken, zowel voor het functionaliseren van organometaalcomplexen alsmede van anorganische dragermaterialen, werden gedemonstreerd en toegepast. Deze technieken zijn een doorbraak aangezien zij eenvoudige, efficiënte procedures voor de gewenste producten impliceren. Bovendien, tonen zij een zeer eenvoudig “van chemicaliënkast tot reactievat” concept aan voor het verankeren van homogene katalysatoren en de toepassing van de daaruit voortkomende katalysematerialen.

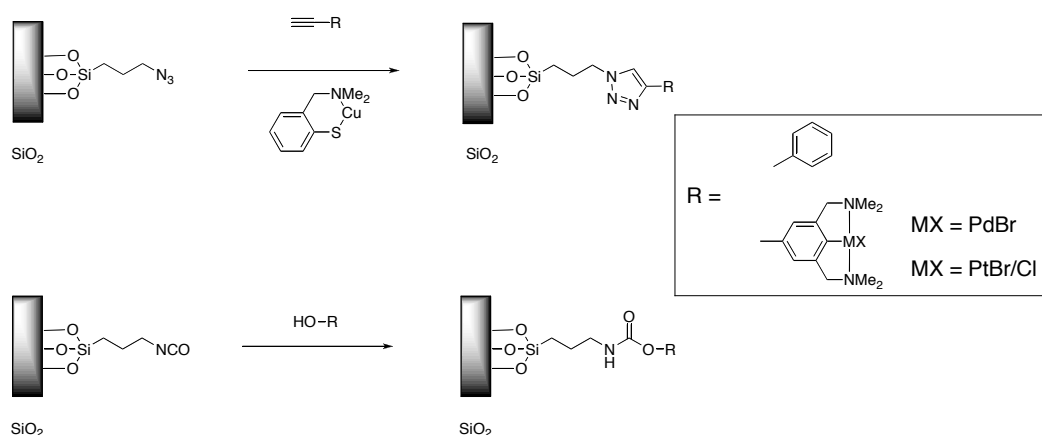
Door het in ruimte scheiden van geheterogeniseerde homogene katalysatoren werd tevens aangetoond dat het vermogen van de Natuur kon worden nagebootst om hoogselectieve meerstapsreactiereeksen uit te voeren zonder opwerking of tussentijdse isolering van de intermediären. Dit wapenfeit is een simpel, maar zeer belangrijk en kentekenend resultaat omdat het een grote stap is in de richting van de meerstapskatalyse die werkelijk efficiënt en nog belangrijker, milieuvriendelijk is.

Hoofdstuk 1 geeft een algemene inleiding in de twee belangrijke onderzoeksgebieden beschreven in dit proefschrift; het *verankeren van katalysatoren* en de *meerstapskatalyse*. Het heterogeniseren van homogene katalysatoren is een enorm groot en gevarieerd gebied en daarom is het overzicht beperkt tot de asymmetrische hydrogenering en C–C bindingvormingsreacties. Deze reacties worden industrieel veelvuldig toegepast voor de synthese van fijn-chemicaliën en zijn de hoeksteen voor verscheidene syntheseroutes. Er werd een breed overzicht gegeven van de verschillende dragermaterialen voor het heterogeniseren van homogene katalysatoren waarbij ondermeer gebruik werd gemaakt van anorganische polymeren, organische polymeren (inclusief geordende, dendritische, en niet-geordende dragers) en oplosbaarheideigenschappen om dit doel te bereiken. De algemene conclusie was dat het heterogeniseren op een anorganische drager het beste resultaat gaf met betrekking tot hergebruik en het geringste effect had op de selectiviteit van de geheterogeniseerde homogene katalysator. Het activeren/deactiveren van de katalysator werd ook besproken omdat, in een aantal gevallen, werd waargenomen dat het heterogeniseren van homogene katalysatoren leidt tot een toe- of afname in activiteit en selectiviteit van de katalysator. Daarbij werd, vanwege het heterogeniseren van homogene katalysatoren, een inzicht gegeven op het werkelijke katalytisch actieve deeltje; een aantal publicaties toonden aan dat de vermeende katalysator in feite een prekatalysator is voor een totaal verschillend katalytisch actief deeltje.



Figuur 1. Gescheiden, verankerde homogene katalysatoren voor meerstapsreactiereeksen.

Meerstapskatalyse gebruikmakend van overgangsmetaalcomplexen werd besproken aan de hand van een algemeen overzicht van dit onderzoeksgebied. De algemene conclusie hieruit was dat de verenigbaarheid tussen katalysator en substraat de grootste beperking gaf. De beste resultaten werden doorgaans verkregen als het introduceren van de intermediaire substraten/reactanten gebeurde nadat een initiële reactie in een reactiereeks al had plaats gevonden. De toepassing van verankerde homogene katalysatoren in gekatalyseerde meerstapsreactiereeksen was vrijwel onvermeld in literatuur. Om het probleem van de verenigbaarheid op te lossen werd geconcludeerd dat een manier hiervoor het scheiden van de katalysatoren zou kunnen zijn zoals in figuur 1 weergegeven.



Figuur 2. Gefunctionaliseerde materialen voor ‘klik’-verankering van organometaalverbindingen.

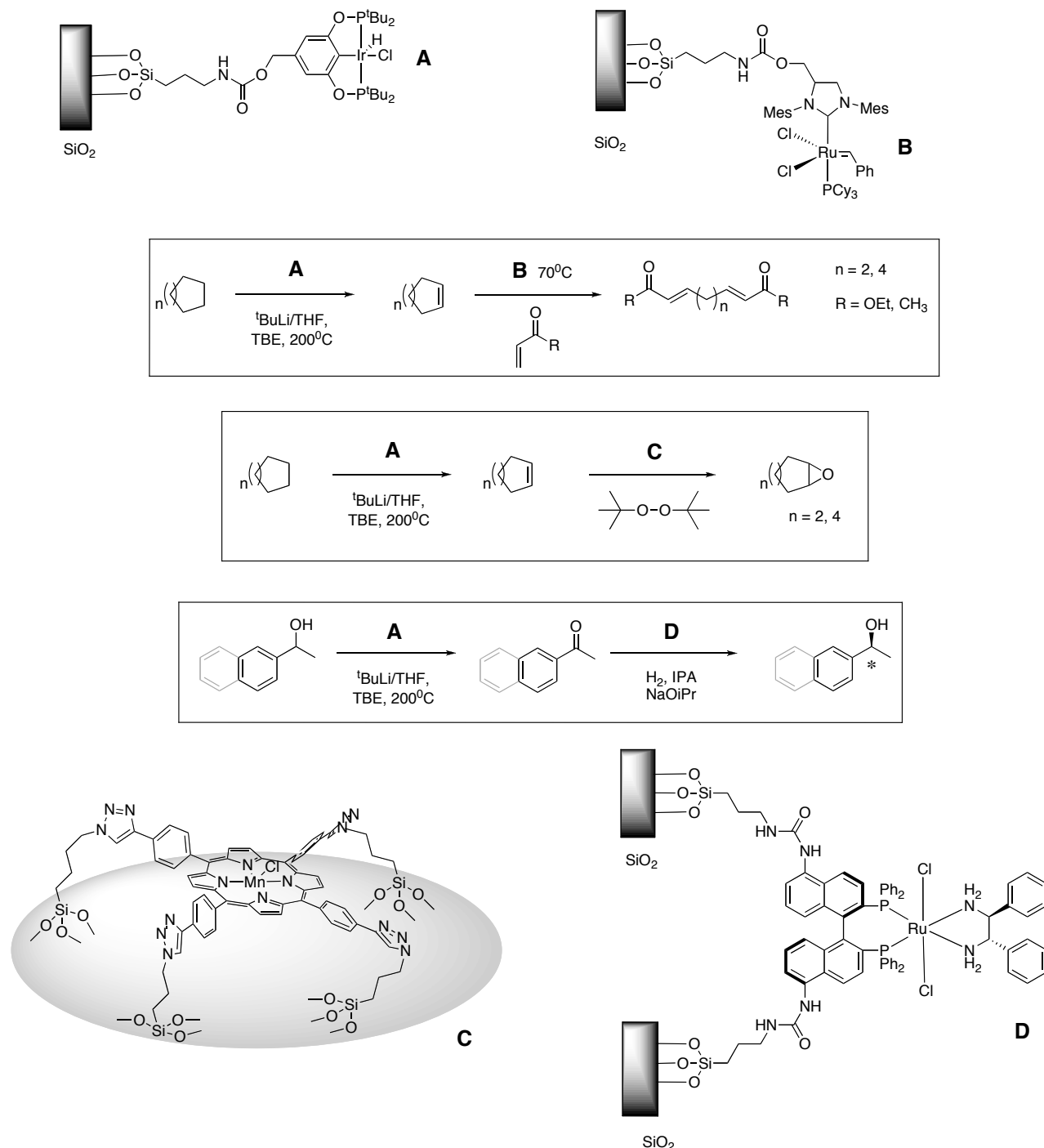
In **Hoofdstuk 2** worden twee syntheseprotocolen gegeven voor eenvoudige, kwantitatieve, efficiënte verankering van homogene katalysatoren. De syntheses van nieuwe verbindingen voor de zogenoemde ‘klik’ immobilisatie werden gepresenteerd. De synthese van nieuwe verbindingen voor de zogenoemde ‘klik’ immobilisatie werden gepresenteerd. De synthese van azide- en isocyanat-gefunctionaliseerde silicamaterialen met een hoge dichtheid werd gerapporteerd. Deze materialen reageerden gemakkelijk met respectievelijk ethyn- en hydroxylfragmenten. Palladium(II) and platina(II) organometaalverbindingen werden verankerd op de aldus verkregen azide- en isocyanato-gefunctionaliseerde silicamaterialen door gebruik te maken van de ‘klik’-techniek

(figuur 2). De gepalladeerde materialen werden toegepast als Lewiszuurkatalysator in de dubbele Michael additie en bleken hoogactieve katalysatoren. Het materiaal werd getest op herwinning en hergebruik en vertoonde geen vermindering in reactiviteit (activiteit en selectiviteit) gedurende 3 cycli. De gepalladeerde materialen werden ook toegepast in de allylische stannylering en bleken actieve katalysatoren; ongeveer drie keer langzamer dan de homogene katalysatoren uitgaande van gelijke hoeveelheden palladium. Ook in de allylische stannyleringsreactie konden deze materialen hergebruikt worden zonder verlies in activiteit gedurende drie cycli.

In **Hoofdstuk 3** werden ‘klik’ verankeringsstechnieken gebruikt om porfyrienecomplexen te bevestigen aan een anorganische drager. Ethynyl-gefunctionaliseerde porfyrineliganden werden gesynthetiseerd en gereageerd met zowel mangaan- als zinkzouten hetgeen resulteerde in ethynylgefunctionaliseerde metaal-porfyrienecomplexen. Deze gefunctionaliseerde complexen werden gekoppeld aan azidegefunctionaliseerd silica (hoofdstuk 2) om zodoende de porfyrienecomplexen aan de onoplosbare, anorganische drager te koppelen. Het verkregen mangaan bevattende materialen werd toegepast als katalysator in de epoxidatie van verschillende alkeensubstraten en gaf een verminderde activiteit en opbrengst te zien in vergelijking met de homogene katalysator. De katalysematerialen werden herwonnen en opnieuw gebruikt in katalysereacties en vertoonden over verschillende cycli een constante afname in activiteit totdat het materiaal volledig gedeactiveerd was. Een aantal mogelijke redenen voor deze deactivering werden geponeerd waarvan de waarschijnlijkste is de opeenhoping van nevenproducten (het reactieresultaat van de oxidant met zichzelf) op de anorganische drager is. De gevormde nevenproducten blokkeren de toegankelijkheid van de katalytisch-actieve metaalcentra, resulterend in een lagere katalytische activiteit.

Hoofdstuk 4 demonstreert de synthese en verankering van een gefunctionaliseerd BINAP-ligand (beschermd als fosfineoxide) op een silicadrager. Er werd aangetoond dat de ontscherming (silaan gerelateerde) van het verankerde fosfineoxide ligand kon worden uitgevoerd zonder nadelige effecten op dragermateriaal of ligand. Het introduceren van het metaal (Ru en Rh) in het BINAP-ligand werd aangetoond waarbij alle fosforatomen coördineerden aan een metaalcentrum. De katalytische resultaten (met Ru en Rh) gaven aan dat de activiteit enigszins verlaagd is vergeleken met het homogene systeem maar dat omzetting en enantioselectiviteit vergelijkbaar zijn met zo niet beter zijn dan de overeenkomstige homogene katalysator. Dit werd aangetoond voor een groot aantal substraten. Een verder bewijs voor de daadwerkelijke verankering werd verkregen na de katalytische reactie: de oplossing na filtratie veroonde die zelf geen katalytische activiteit. Bovendien kon de katalysator gedurende vijf cycli herwonnen en opnieuw gebruikt worden met telkens hoge selectiviteit.

De synthese van gefunctionaliseerde iridium(III) organometaalcomplexen voor verankering werd beschreven in **Hoofdstuk 5**. Een tang-iridium(III)-verbinding gefunctionaliseerd met een benzylic alcohol werd gesynthetiseerd en gekoppeld (‘geklikt’) met een isocyanaatgefunctionaliseerd silicamateriaal. De prekatalytische materialen en hun uitgangstoffen werden grondig gekarakteriseerd hetgeen aantoonde dat de iridium(III)-waterstof en halogenidebindingen intact bleven gedurende de verankeringsprocedure. Een Grubbs-II rutheniumalkylidencomplex werd ook op silica verankerd.

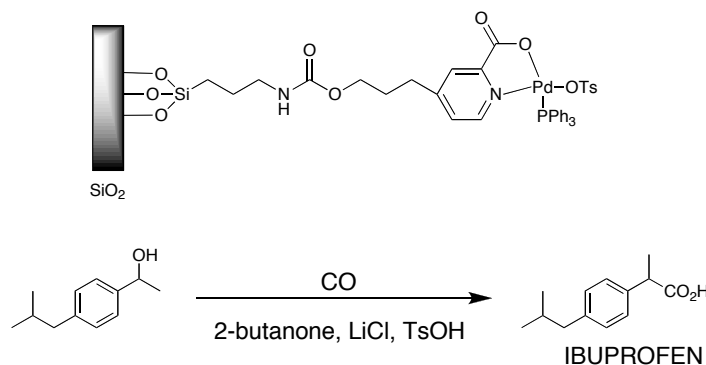


Figuur 3. Verankerde homogene katalysatoren voor de meerstapsynthese van fijn-chemicaliën.

De verankerde dehydrogeneringskatalysatoren werden in serie toegepast met andere verankerde homogene katalysatoren (Figuur 3). Meerstapsreactiereeksen werden gerapporteerd die in twee stappen de omzetting aantoonen van niet-gefunctionaliseerde, niet-reactieve substraten tot gefunctionaliseerde verbindingen, zonder opwerking en minimale verstoring van de reactiereeks. De dehydrogenering van een eenvoudig cyclisch alkaan tot een cyclisch alkeen in serie met een ringopeningsmetathesereactie van het gevormde alkeen werd angetoond. Dit werd mogelijk gemaakt door een eenvoudige overbrenging van het reactiemengsel tussen verschillende reactievaten waarbij de verankerde dehydrogeneringskatalysator uit het reactiemengsel werd

gefilterd. Tevens werd de ringopenings-kruiskoppeling tussen een cyclisch alkeen met ethylacrylaat en but-1-en-3-on uitgevoerd hetgeen respectievelijk di(alkyl)esters en ketonen opleverden. Vervolgens werd na de metathesereactie de metathesekatalysator afgefilterd en kon het uiteindelijke reactiemengsel eenvoudig worden opgewerkt. Een soortgelijke reactiereeks werd aangetoond voor de epoxidatie van een cyclisch alkeen. Een materiaal met daarop verankerd porfyriene-mangaankatalysatoren werd in een reactiereeks toegepast na de dehydrogeneringsstap. Tenslotte werd een voorbeeld gegeven waarbij in twee stappen racemische alcoholen gederacemiseerd konden worden door een dehydrogeneringskatalysator in serie met een verankerde, asymmetrische hydrogeneringskatalysator.

In **Hoofdstuk 6** werd een palladium-picolinaatverbinding covalent verankerd op een silicadrager met hoge dichtheid door stapsgewijze opbouw van de katalysator op de drager. Voor de vervaardiging van het ligand op de drager werd ondermeer gebruik gemaakt van een enzymatische hydrolyse. DRIFT-IR and multikern CP-MAS vaste stof NMR-spectroscopie werden gebruikt voor de analyse van de intermediären en karakterisering van de verankerde katalysator waarbij bewezen werd dat het palladium-picolinaat bevestigd was aan de anorganische drager. De verankerde katalysator werd gebruikt in de hydroxycarbonyleringsreactie van 1-(4-isobutylfenyl)ethanol (IBFE), resulterend in de commercieel aantrekkelijke, niet-steroïde ontstekingsremmer *Ibuprofen* (IBN, zie Figuur 4). Analyse na de katalyse toonde aan dat het palladium-picolinaat, dat eerder door een andere groep onderzoekers als het katalytisch actieve deeltje was geponeerd, hoogstwaarschijnlijk niet de daadwerkelijk actieve katalysator is. Voorts werd aangetoond dat katalysepromotoren een decomplexering bewerkstelligde van het palladium-picolinaat. Bovendien bleek de nieuwgevormde palladiumverbinding actief te zijn in de hydroxycarbonyleringsreactie van IBFE weliswaar met een lagere regioselectiviteit.



Figuur 4. Palladium-picolinaatverbinding verankerd aan silica voor hydroxycarbonylering.

Algemene conclusies en toekomstperspectief voor verankerde katalysatoren

Het verankeren van homogene katalysatoren is vaak een uitdagend synthese-project dat vertrouwt op zowel de duurzaamheid en neutrale staat van het dragermateriaal *alsmede* op de gevoeligheid en stabiliteit van het organometaalcomplex. Er werden milde, efficiënte procedures opgesteld voor het covalent verankeren van een verscheidenheid aan organische en organometaalfragmenten op anorganische dragers. Verder werden diverse organische synthesetechnieken voor het introduceren van organische- en organometaalverbindingen

gedemonstreerd die de verankering aan zowel anorganische als organische polymeerdragers vergemakkelijken. Echter, al deze procedures leunen sterk op een hoge stabiliteit van de organometaal-katalysator. Zoals al aangetoond, zijn tang-metaalverbindingen ideale materialen om verankeringsstechnieken aan te tonen (hoofdstukken 2 en 5). De grondslag hiervoor is de hoge thermische stabiliteit van deze complexen. Bovendien zijn de pincer-metaalverbindingen zeer flexibel toepasbaar in een diversiteit aan katalysereacties. Met liganden en complexen die de inherent hoge stabiliteit van tang-metaalcomplexen niet bezitten, bleken relatief langdurige synthese protocollen nodig te zijn om de organometaal-katalysatoren te verankeren (hoofdstukken 4 en 6).

De ontwikkelde materialen, welke allen onoplosbaar zijn in de gebruikelijke organische oplosmiddelen en water, konden worden toegepast als “heterogene” katalysator in een brede variatie aan katalytische reacties: hydrogeneringen, dehydrogeneringen, oxidaties en C–C koppelingsreacties. Bovendien kon in de meeste gevallen de katalytische materialen gemakkelijk herwonnen en opnieuw gebruikt worden zonder een merkbare achteruitgang in activiteit en selectiviteit. In die gevallen waarbij het herwinnen en hergebruik van de katalysatoren leidde tot tegengestelde resultaten, werd onderzocht waarom dit was en werden uit de waarnemingen belangrijke conclusies getrokken. Een grondige kennis van het mechanisme van een gekatalyseerde reactie is nodig voordat pogingen worden ondernomen om een homogene katalysator te verankeren (hoofdstuk 6). Bovendien geeft verankering soms nieuwe inzichten in het reactiemechanisme die voorheen onopgemerkt bleven (hoofdstukken 1 en 6). De aard van het katalytische materiaal is ook van belang zoals in hoofdstukken 2 en 3 werd ondervonden. In beide hoofdstukken bewerkstelligen zowel de drager als de linker een toe- dan wel afname in katalytische activiteit.

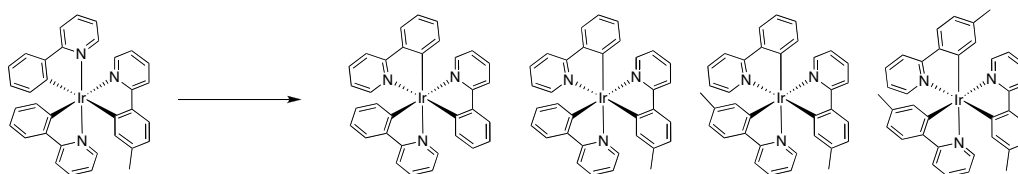
De ontworpen materialen werden ook toegepast in een serie van syntheses waarmee meerstapsreactiereeksen werden aangetoond die geen tussentijdse opwerking behoeften en een hoge opbrengst en selectiviteit vertoonden. Dit wordt beschouwd als de toekomst voor de homogene katalyse. De huidige trend is om flexibele katalytische systemen te ontwikkelen die breed toepasbaar zijn. Een andere trend is om meerstapsreacties uit te voeren in één reactievat zonder de noodzaak om intermediëren te isoleren hetgeen gewoonlijk grote hoeveelheden nevenproducten en verspilling van oplosmiddelen tot gevolg heeft. Dit proefschrift toont de eerste aanzet tot nabootsing van de Natuur aan waarbij wordt gestreefd naar ruimtelijke scheiding van gebruikte kunstmatige katalysatoren. De volgende stap is de uitbreiding van de reactiereeksen tot drie, vier of vijf stappen. In Hoofdstuk 5 bijvoorbeeld, waar een epoxide of een dialkenylester werden gevormd, kon respectievelijk ringopening van het epoxide of reductie van het alkeen makkelijk worden uitgevoerd in hetzelfde reactiemengsel gebruikmakend van een enzym of een heterogene katalysator.

De belangrijke toekomstige toepassingen van de concepten die in dit proefschrift geïntroduceerd zijn, liggen in de uitbreiding naar andere katalytische reacties en de ontwikkeling van grotere meerstapssystemen die zowel in gezamenlijk als in serie kunnen opereren. Toepassing in een enkel reactievat is tevens een belangrijk doel. Dit zou scheiding inhouden van de katalyseplekken door membranen die doorlaatbaar zijn voor oplosmiddelen en substraten maar bij de katalysatoren verblijven in één specifiek compartiment van het reactievat. Volgens de ‘Groene

Chemie' principes is katalyse een ultiem groen proces maar kan het nog groener gemaakt worden door de ontwikkeling van systemen zoals degene beschreven in dit proefschrift.

OLED onderzoeksgedeelte

Een aantal heteroleptische, drievoudig ringgemetaleerde $[\text{Ir}(\text{C},\text{N})_2(\text{C}',\text{N}')]_{\text{Iridium(III)}$ complexen werden gesynthetiseerd en volledig gekarakteriseerd middels verschillende technieken in **Hoofdstuk 7**. De *mer-homo-N-trans* isomeer van heteroleptische complexen werd gesynthetiseerd en omgezet naar het *fac*-isomeer met behulp van fotochemische technieken. Dit leverde een simpel protocol met een hoge opbrengst op voor de synthese van verankerde drievoudig ringgemetaleerde iridium(III) complexen. Onder thermische omstandigheden vond tijdens de omzetting van de *mer-homo-N-trans* isomeren naar de *fac*- complexen liganduitwisseling plaats (figuur 5). Deze thermische isomerisatie werd grondig bestudeerd en bleek een alcoholgekatalyseerd proces te zijn. Tweevoudig ringgemetaleerde iridium(III)alkoxides werden voorgesteld als de intermediaren in de *mer*- tot *fac*-isomerisatie van $[\text{Ir}(\text{ppy})_3]$ -type systemen. Analoge *trans-N* geconfigureerd tweevoudig ringgemetaleerde iridium(III) alkoxidecomplexen werden gesynthetiseerd en gekarakteriseerd en werden na reactie met ringgemetaleerde liganden beschouwd als de meest waarschijnlijke intermediaren.



Figuur 5. Thermische isomerisatie van heteroleptisch *mer*-isomeer leidend tot mengsels van vier *fac*-isomeren.

Er werd een mechanisme gepresenteerd voor de thermodynamische isomerisatiereactie dat de waargenomen liganduitwisseling kon verklaren. Liganduitwisseling van één van de ringgemetaleerde liganden door een alkoxideligand resulteert in een tweevoudig ringgemetaleerd iridium(III)-alkoxidecomplex. Dit iridium(III)alkoxide reageert vervolgens met een 'vrij' ringmetalerend ligand resulterend in een drievoudig ringgemetaleerd complex. Het gevormde complex kan zowel een *mer*- als een *fac*-isomeer zijn. Het *fac*-isomeer is een thermodynamisch eindproduct en reageert niet verder, terwijl het *mer*-isomeer net zolang kan reageren totdat alle *mer*-isomeren omgezet zijn naar *fac*-isomeren. Kinetische beschouwing van de *mer*- tot *fac*-isomerisatie van homoleptische trifenylpyridine iridium(III)complexen ondersteunen het voorgestelde mechanisme. Een diepgaande bespreking van de mogelijke geometrische isomeerintermediaren van zowel de homo- alsmede de heteroleptische systemen werd gepresenteerd. Deze rapportage is essentieel voor het gebied van OLEDs vanwege drie redenen. Ten eerste demonstreert het voor de synthese van heteroleptische $[\text{Ir}(\text{C},\text{N})_2(\text{C}',\text{N}')]_{\text{Iridium(III)}$ complexen die gewild zijn voor covalente verankering aan polymere dragermaterialen. Ten tweede de synthese van heteroleptische $[\text{Ir}(\text{C},\text{N})_3]_{\text{Iridium(III)}}$ complexen opent de mogelijkheid tot elektronische fijnafstemming van de liganden voor ligandgemengde complexen. Ten derde, en het belangrijkste, het is het eerste grondige onderzoek aan *mer*- en *fac*-heteroleptische octahedrale $[\text{M}(\text{a},\text{b})_2(\text{c},\text{d})]_{\text{Iridium(III)}}$ organometaalcomplexen en werd daarom voorzien van een gedetailleerde structuur- en

naamgevingdiscussie. Het onderzoek geeft waardevol inzicht in hoe de drievoudig ringgemetaleerde *fac*-iridium(III) complexen gesynthetiseerd kunnen worden alsmede de energiebarrières die overwonnen moeten worden voor hun synthese.

Algemene conclusies van OLEDs onderzoek

Het uiteindelijke doel van dit onderzoek was het aantonen van het verankeren van organometaalfosforescente centra aan polymere dragers. Door middel van een fundamentele studie die werd ondernomen om het verankeren te vergemakkelijken werd dit doel bereikt. Complexen met de algemene formule $[\text{Ir}(\text{C}_3\text{N})_3]$ werden bestudeerd omdat zij de hoogste kwantumopbrengsten vertoonden bij toepassing in OLEDs. Het verankeren van deze systemen was nooit eerder aangetoond vanwege de uitdagende synthese van analoge heteroleptische complexen. In dit proefschrift worden technieken beschreven om deze uitdagingen te overwinnen alsmede studies betreffende het reactiemechanisme. Deze ontdekking is vitaal voor toekomstige OLED-technologieën omdat het controleren van de interacties tussen holte- en elektrontransportlagen (beide ruim beschikbare organische polymeren) en de fosforescente lagen (Ir(III)-organometaalverbinding) essentieel is voor het bereiken van hoge kwantumefficiëntieniveaus en uiteindelijk betrouwbare OLEDs.

ACKNOWLEDGEMENTS

The research detailed in this book would not have been completed without the help of a number of people, and I would not have enjoyed the last four years in Utrecht without the help and encouragement of both academic and social acquaintances.

First and foremost I would like to thank Prof. Gerard van Koten for inviting me to come and carry out my Ph.D. in Utrecht back in 2001, and eventually I showed up in 2003. Dear Gerard, you took me on as a relatively naïve chemist and allowed me to develop along lines that I chose, while guiding me to the eventual goal of a thesis on tandem catalysis. I thoroughly enjoyed the work you introduced me to on Iridium organometallics for OLED devices, and enjoyed every meeting we had (however few and short they were). You never failed to inspire me to delve deeper into my work, and thoroughly investigate every discovery I made. I wish you every success with your new positions in Wales, Switzerland and The Netherlands, and I look forward to many future chemistry discussions with you.

Secondly I would like to thank Dr. Gerard van Klink for the contribution he has made to this thesis, and my four years in Utrecht. Dear Gerard (I will not use any of your nicknames here, this is a respectable publication!), thank you for the time and effort you put into many STW meetings, work group discussions, poster and lecture presentations. Also thank you for the time you put into correcting the work in this thesis, and your help with the Dutch summary, all of which were beyond what would be expected of you after how things have gone in the last two years. Your door was always welcome to the Irishman, and you never failed to entertain me at the coffee table. Seeing as the written word is fact and thus can *never* be argued again; the heaviest bird to ever fly is, in fact, the mute swan (an adult may weigh as much as 18kg (40 lb)); and, the most folds of a piece of paper was 12. Thanks Gerard.

I would also like to thank the other permanent members of staff at the VOS (Henk Kleijn, Johann Jastrzebski, Bert Klein Gebbink) for the time they always had to discuss chemistry with me, or to help with experimental problems. Henk, oude lul, thank you very much for everything you have done for me, you manage to keep the entire lab running and functional, while still doing your own research. In the meantime you manage to make all of us laugh on a daily basis at the coffee table. In memory of you and Johann I will eat cookies every Thursday afternoon for the rest of my life. Johann, thank you for all of the chemistry problems you could solve for me, and also all of the computer problems (resolved or not!). Your door was always open to me to ask the most irrelevant of questions. Bert, thank you for your input at work discussions, and in the corridor, some of your suggestions have become important details in the research described in this thesis. Also thank you to Peter Wijkens for his help in the lab in the first year I was in Utrecht.

I will be forever indebted to the Pruiksma sisters, without whom I would not have filled in any official documents in Utrecht, or had much of a social life. Margo, Hester, thank you so much for everything you have done. Without you I would not have survived here, and you have both consistently helped me without complaint, and really gone out of your way to help me, for the last four years. I will miss the lunches, dinners and nights in Micks/Stairway/Filemon.

Several members of the permanent staff at the FOC have also helped. Dr. Cees van Walree, thank you for all of your help on the photophysical aspects of the OLED work. We had quite a few (heated) discussions about photochemistry, and I learned a great deal from you. Thank you also for the help with solid state NMR. Ed Vliestra, thank you for helping with several technical problems with both IR and UV-vis spectroscopy, all the best in retirement.

The X-ray crystallography facility in Utrecht is a fantastic institution, and I think we forget how lucky we are to be able to walk around the corner and ask Dr. Martin Lutz to have a look at the latest amorphous junk we have produced. I am an expert in producing the worst possible crystals, but Martin still managed to produce some nice results, some of which are included in this thesis. Thank you Martin for your time and patience with me. Also thank you to Prof. A. Spek and Dr. Lars von Chrzanowski for their contributions to work I have carried out.

Thank you also to Dr. Harry Bitter at the department of Inorganic Chemistry and Catalysis for his help with surface area measurements, which were carried out very much as a last minute thing, and I am very grateful for the speed and quality of the results. I am very grateful to the members of the glass-blowing department, who were always prepared to make any piece that was required, and were always ready for a chat and a laugh. They have produced some fantastic pieces of art-work for the various promos we have requested in the last years, and were always very friendly to me. Hans Heesen at the technical service was wonderfully helpful to me throughout the four years, and always helped with any problems I had with the autoclaves and with building some filtration set-ups. Thank you very much!

I have carried out work in collaboration with several groups in the Netherlands, all of whom I am very grateful to for their help. Firstly, Prof. Jacob Moulijn, Prof. Freek Kapiteijn, and Dr. Nakul Thakar thank you for your involvement in the STW project, and even though the end result was not a success, the collaboration was fruitful. Thank you also to Dr. Jim Brandts and Dr. Annemarie Beers of BASF Nederland for the advice and help in relation to the STW guidance committee. In particular thanks Jim, for the interest you showed in my work, and your readiness to help at any stage. At the Technical University of Eindhoven, I am grateful to Dr. Christian Müller and Prof. Dieter Vogt for their help with chapter 4. I enjoyed my trips to Eindhoven, and using the AMTEC reactor set-up, also, Christian your enthusiasm for chemistry was contagious, thank you. Dr. Marjo Mittelmeijer at the UvA was very helpful with carbonylation catalysis, thank you your help! Dr. Johan Hollander, thank you for all of the solid-state measurements you did for me, even with all of my forgetfulness, you were always welcoming and very helpful in Leiden. Dr. Roger Pretot of CIBA speciality chemicals, thank you for all of the information and enthusiasm you brought to the OLED project. I really enjoyed the investigations we carried out. Also thank you to

Dr. Paul van der Schaaf at CIBA, and Dr. Jeroen de Pater and Niels Meis, who helped initiate the project.

Working in the lab is my favourite thing to do, and I enjoyed the atmosphere on the eighth floor of the Kruyt. The atmosphere in the lab was mostly fun, sometimes fractious, and sometimes a talkative Italian woman and a stubborn Dutch woman would shout at each other for 8 hours. Thank you to everyone who was in the SOC for the last four years: Guido, Preston, Sylvestre, Marianne, Alessandro, Nesibe, Erwin, Anne, Sipke, Nilesh, Morgane, Peter, Marcella, Kamil, Pieter, Ilenia, Sylvia, Ilenia, Marcel, Henk, Catelyne, Dennis, Kees, Niels, Rob K, Rob C, Bart, Patrick, Birgit, Jeroen, Jerome, Thomas, Monika, Irene, Judith, Harm, Alexey, Paul, Elena, Maaïke. Also thank you to the FOCcers Jacco, Jan and Layo. A big thank you goes out to the Filemon crew. I will never forget those Friday evenings which would involve a sober dinner, a half sober Micks, a drunk hard rock Stairway, and a throwing shapes Filemon, all the ingredients necessary for laughing until you fall over, thanks Sara, Koentje, Bart, Pieter, Sylvia, Margo, Hester, Catelyne, Keesie, Elena, Guido, and Marcella (I haven't used my remote control since you left). Thank you also to students that made life in and out of the lab a lot of fun: Koen (promoveren?), Sarita (we miss you every time you leave), Guido K., Maria, and of course who could forget Thomas and Kimberley. I was also given the opportunity to work with some great bachelors and masters students: Jolke, Johann, Dinesh, Guido K., Davide and Nicole thank you, you have all made contributions to this thesis, and in particular work by Davide and Nicole have developed into full papers, I wish you both every success as Ph.D. students. Thanks to Rob Gossage for the nice collaboration in the pub and the lab!

If we were not in the filemon on a Friday, we were there on a Tuesday. Some people made my first few years in Utrecht a lot of fun and I miss them since they left. Preston, you loud, hairy Canadian moose, thanks for the fun and unabashed enthusiasm for *everything*, and thanks for drinking the beers that we bought you, even though you were supposed to be at home. Alex, thanks for making me laugh at Preston, thanks for sleeping at the church, thanks for smelling all of the girls' feet. Elena, ciao mates, you are great, and always made me think of things other than chemistry, you also have the sickest mind of any female on the planet. Koentje, thanks for cycling your bike around in circles until you fell over, I will miss all you guys a lot when I'm gone.

Outside the lab I played cricket, and didn't do much else. Kampong cricket club is fantastic, and I will never forget Sunday evenings at the cricket 'pavilion' having a beer and chatting about the day's results. I enjoyed all the teams I played for, but you cant beat running in to bowl on a Sunday morning, on another gem of a Cantrell wicket, sun shining, Devo and Jonno screaming to knock'em over, and getting pucked for six into the slot. I absolutely loved summer Sundays in Utrecht, thanks everyone at Kampong. In particular thanks to Debbo (easy tiger), Adrian, Jochen, Jonno, Pete (Maaarshy), Q., Marcel, and Pete C., and all the boys on Heren 1 and 2.

Thanks to all my friends in Dublin who made coming home fun: Mount Temple posse; Mullins, Jimmy, Amy, Ciara and the rest of the gang. The Trinnerns group; Gary, Liz, Mary, Dave, Ciara B. and all the gang. Colm and Louise thanks for coming to visit, and always being around for a chat when I was in Dublin (and Joan and Des for all of the encouragement you always gave me).

Thanks to the Cummings', Boersmas, O'Tooles, Smeatons, and O'Neills for all of the encouragement you all gave me, and for putting me up when I visited. Grandma, Grandpa, Gran and Granda thank you for always looking out for me and supporting me. Mam, Dad, Claire and Cathy, thank you for putting up with me, and always, unflinchingly, encouraging me to achieve my best, and always supporting me. It is difficult to put down in words how grateful I am to you all, and you would probably tell me to f-off if I did, this book is a testament to you and the time you guys gave to me, THANK YOU.

Aidan

CURRICULUM VITAE

The Author of this thesis was born in Dublin, Ireland on the 30th of May 1980. He took the Leaving Certificate examination in June 1998 achieving 7 honours in Irish, English, Maths, German, Geography, Chemistry and Physics. The author carried out his undergraduate studies at the University of Dublin, Trinity College, where he graduated as a gold medallist, with a first class honours degree in Chemistry, in June 2002. During his undergraduate studies he carried out an Erasmus/Socrates sponsored research internship at the Department of Metal Mediated Synthesis on *para*-Functionalised Pincer Palladium Complexes under the guidance of Prof. Gerard van Koten, at Utrecht University.

From September 2003 to September 2007 the author of this thesis carried out his Ph.D. studies in the department of Organic Chemistry and Catalysis, at Utrecht University, under the guidance of Prof. Gerard van Koten. The research was sponsored by the Dutch Technology Foundation (Stichting Technologische Wetenschap, STW) and involved the immobilisation of homogeneous catalysts on insoluble inorganic supports for sequential tandem catalysis. The work described in this thesis has been presented at both national and international conferences as both poster and lecture presentations: The Netherlands Catalysis and Chemistry Conference (NCCC, Noordwijkerhout 2003-07, posters and lecture), 6th International Conference on Catalysis in Membrane Reactors (Lahnstein, 2004, poster), OMCOS 13 (Geneva 2005, poster), Pacificchem (Honolulu 2005, lecture), 3rd International Conference on Green and Sustainable Chemistry (Delft 2007, lecture), European Symposium on Organic Chemistry (Dublin 2007, poster).

LIST OF PUBLICATIONS

para-Functionalized NCN-Pincer Palladium(II) Complexes: Synthesis, Catalysis and DFT Calculations

H. P. Dijkstra, M. Q. Slagt, A. R. McDonald, C. A. Kruithof, R. Kreiter, A. M. Mills, M. Lutz, A. L. Spek, W. Klopper, G. P. M. van Klink, G. van Koten; *Eur. J. Inorg. Chem.* **2003**, 830-838.

Self-Assembly of p-Nitro NCN-Pincer Palladium Complexes into Dimers through Electron Donor-Acceptor Interactions

M. Q. Slagt, H. P. Dijkstra, A. R. McDonald, R. J. M. Klein Gebbink, M. Lutz, D. D. Ellis, A. M. Mills, A. L. Spek, G. van Koten, *Organometallics* **2003**, 22, 27-29.

2-Carboxy-4-(hydroxymethyl)pyridinium chloride hemihydrate

Lars S. von Chrzanowski, Martin Lutz, Anthony L. Spek, Aidan R. McDonald, Gerard P. M. van Klink and Gerard van Koten *Acta Cryst.* **2007**, E63, o1121-o1122;

Immobilised Homogeneous Catalysts for Asymmetric Hydrogenation

Aidan R. McDonald, Robert Gossage, Gerard P. M. van Klink, Gerard van Koten, to be submitted for publication.

BINAP-Ru and Rh Catalysts Covalently Immobilised on Silica and their Repeated Application in Asymmetric Hydrogenation Catalysis

Aidan R. McDonald, Christian Müller, Dieter Vogt, Gerard P. M. van Klink, Gerard van Koten, accepted by *Green Chemistry*.

Covalent Immobilisation of a Palladium Picolinate Complex for Hydroxycarbonylation: Silica Supported Synthesis and Catalysis

Aidan R. McDonald, Gerard P. M. van Klink, Gerard van Koten, submitted for publication.

Probing the mer- to fac- Isomerisation of Tris-Cyclometallated Homo and Heteroleptic (C,N)₃ Iridium(III) Complexes

Aidan R. McDonald, Martin Lutz, Lars S. von Chrzanowski, Gerard P. M. van Klink, Anthony L. Spek, Gerard van Koten, submitted for publication

'Click' Immobilisation of Organometallic Catalysts for C-C Coupling Reactions

Aidan R. McDonald, Harm P. Dijkstra, Bart M. J. M. Suijkerbuijk, Martin Lutz, Anthony L. Spek, Gerard P. M. van Klink, Gerard van Koten, submitted for publication.

Supramolecular Dendri-LED's: Anionic Organometallic Phosphors Embedded in Polycationic Dendritic Species

Aidan R. McDonald, Davide Mores, Celso de Mello Donegá, Cornelis A. van Walree, Robertus J. M. Klein Gebbink, Martin Lutz, Anthony L. Spek, A. Meijerink, Gerard P. M. van Klink, Gerard van Koten, to be submitted for publication

Anionic Organometallic Phosphors Embedded in Polycationic Dendritic Species

Aidan R. McDonald, Gerard van Koten, patent application in progress.

Sequential Compartmentalised Homogeneous Tandem Catalysis

Aidan R. McDonald, Gerard P. M. van Klink, Gerard van Koten, to be submitted for publication

Sequential Compartmentalised Tandem Catalysis; Iridium(III) Organometallics on Silica for Alkane Activation

Aidan R. McDonald, Martin Lutz, Gerard P. M. van Klink, Anthony L. Spek, Gerard van Koten to be submitted for publication.

Immobilised Pincer Complexes Applied in Catalysis, Book chapter.

Aidan R. McDonald, Harm P. Dijkstra. Pincer Organometallics, expected **2008**, editors G. van Koten, P. A. Chase

'Click' Silica Immobilisation of Metallo-Porphyrin Complexes and their Application in Epoxidation Catalysis

Aidan R. McDonald, Nicole M. G. Franssen, Gerard P. M. van Klink, Gerard van Koten, to be submitted for publication.